University of Alberta

Polyyne Natural Products and Materials:
Synthetic Methodology and Physical Characterization

By Thanh Luu ©

A thesis submitted to the Faculty of Graduate Studies and Research in partial
fulfillment of the requirements of the degree of Doctor of Philosophy

Department of Chemistry

Edmonton, Alberta

Fall, 2007

Library and
Archives Canada

Published Heritage
Branch

395 Wellington Street
Ottawa ON K1A 0N4
Canada

Bibliothèque et
Archives Canada

Direction du
Patrimoine de l'édition

395, rue Wellington
Ottawa ON K1A 0N4
Canada

Your file Votre référence
ISBN: 978-0-494-33022-7
Our file Notre référence
ISBN: 978-0-494-33022-7

NOTICE:
The author has granted a non-exclusive license allowing Library and Archives Canada to reproduce, publish, archive, preserve, conserve, communicate to the public by telecommunication or on the Internet, loan, distribute and sell theses worldwide, for commercial or non-commercial purposes, in microform, paper, electronic and/or any other formats.

The author retains copyright ownership and moral rights in this thesis. Neither the thesis nor substantial extracts from it may be printed or otherwise reproduced without the author's permission.

AVIS:
L'auteur a accordé une licence non exclusive permettant à la Bibliothèque et Archives Canada de reproduire, publier, archiver, sauvegarder, conserver, transmettre au public par télécommunication ou par l'Internet, prêter, distribuer et vendre des thèses partout dans le monde, à des fins commerciales ou autres, sur support microforme, papier, électronique et/ou autres formats.

L'auteur conserve la propriété du droit d'auteur et des droits moraux qui protège cette thèse. Ni la thèse ni des extraits substantiels de celle-ci ne doivent être imprimés ou autrement reproduits sans son autorisation.

In compliance with the Canadian Privacy Act some supporting forms may have been removed from this thesis.

While these forms may be included in the document page count, their removal does not represent any loss of content from the thesis.

Conformément à la loi canadienne sur la protection de la vie privée, quelques formulaires secondaires ont été enlevés de cette thèse.

Bien que ces formulaires aient inclus dans la pagination, il n'y aura aucun contenu manquant.

Canada

Abstract

A new synthesis of triynol natural products was initially pursued. Using a carbenoid rearrangement starting from a dibromoolefin precursor, nine triynols, including six natural products and three analogues, have been synthesized in good yield. This study has shown that the stability of triynols increases via either the addition of terminal substituents or addition of methylene units.

A new method was developed to trap kinetic instability of terminal di–, tri–, and tetraynes with benzyl azide to form stable triazole products in reasonable to good yield. The primary results from ^{1}H/^{13}C NMR spectroscopy and X–ray crystallographic analysis for a wide range of derivatives show that this protocol is successful with terminal di–, tri–, and tetraynes; results only in formation of 1,4–triazole products; does not give multiple addition products; and can be used to trap naturally occurring terminal polyynes.

The synthesis of triynols has led to the development of a one–pot reaction sequence. In this study, a one–pot protocol has been developed for the construction and derivatization of di– and triynes. This method allows for the formation of a lithium–acetylide intermediate via a tandem Fritsch–Buttenberg–Wiechell rearrangement and deprotonation step. This intermediate can either be trapped directly with electrophiles to provide di– and triynols, or undergo transmetallation with zinc, copper, tin, or platinum to generate different conjugated polyynes or ynones.

A series of α,ω–diraylpolyynes with up to 16 consecutive sp–hybridized carbon atoms has been synthesized via Fritsch–Buttenberg–Wiechell rearrangement as the key transformation step. These findings have shown that as a function of increasing number

of alkynes, (a) the maximum absorption in their UV–vis spectra shifts to a lower energy and (b) the ^{13}C chemical shifts of the internal carbons shift upfield and approach ca. 63 ppm (in $CDCl_3$).

Four tetraynes have been synthesized and studied. The 4–NO_2 aryl tetrayne was chosen for an in depth polymerization study, and was analyzed by solid–state UV–vis, IR, and ^{13}C NMR spectroscopies. Initial findings show that this compound can undergo a 1,6–polymerization in the solid state.

Acknowledgements

My Ph.D. journey has covered rather an interesting spectrum, ranging from happy to glum days. During five years, I have discovered my potential and I have been blessed by being surrounded with good supervisors, lab mates, and friends. Without them, I would not be sitting here compiling this thesis.

First of all, I would like to acknowledge my supervisor and former supervisors. I thank my long–term supervisor, Professor Rik R. Tykwinski, for his support and guidance through five years. He has taught me how to make a poster, oral presentation; how to write articles; particularly he allowed me to explore my idea and transfer it to a reaction. For my former supervisor, Professor Frederick G. West, I thank him for letting me attending his group meetings and working for him. From him I learnt how to design a new reaction and how to reason organic mechanisms. I would also like to acknowledge my Japanese former supervisor, Professor Yoshito Tobe who gave me an opportunity to work in a big research group and to learn about a Japanese culture.

Secondly, I would like to thank my friends who have helped my writing or making my days go smoother. My coffee partner, Andreea Spanculescu and Guy Bernard; my lunch partners, John Lo, Mai Pham, and Nina Vo. In these leisure times, we learnt things related to chemistry as well as those related to society.

I thank my collaborators who took my projects beyond my limit and taught me more than just theory. My undergraduate students: Tu Lam, Nina Cunningham, Tyler Taerum, Edward Ha, Danielle Vallee; Wei Shi in the Lowary group, Dr. Guy Bernard in the Wasylishen group, Aarron Slepkov in the Hegmann group.

I would like to acknowledge Dr. Guy Bernard, Dr. Hayley Wan, Amber Sadowy, Danielle Vallee, Dan Lehnherr and Erin Graham for spending their time to proof read some sections of thesis.

I would also like to thank my past and present group members for their motivation and support: Andreea, Amber, Dan, Mojtaba, Wes, Shar, Yanqing, Andrew, B. J., Erin, Khalid, etc.

Finally, I would like to acknowledge my mom Mrs. Muoi, sisters Emily Ha and Shirly Tang and my best friend K. J. Brown for their financial support and encouragement.

Financial support was provided by NSERC and the University of Alberta.

Table of Contents

Chapter 1. A Brief Historical Review of Polyynes[1] 1

1.1 Before the 1900s 1

1.2 1900s to 1970s 2

1.3 1970s to 1990s 7

1.4 1990s to Present 9

1.5 References and Notes 19

Chapter 2. Synthesis and Stability of a Homologous Series of Triynol Natural Products and Their Analogues 23

2.1 Introduction 23

2.2 Results and Discussion 26

2.3 Further Elaboration 34

2.4 Conclusions 35

2.5 References and Notes 35

Chapter 3. 1,2,3–Triazole Formation: Trapping Terminal Di–, Tri–, and Tetraynes with Benzyl Azide 40

3.1 Introduction 40

3.2 Results and Discussion **42**

3.2.1 Mechanistic Study *42*

3.2.2 Synthesis *47*

3.2.3 Physical Properties *55*

3.2.4 X–ray Crystallographic Analysis *58*

*3.2.5 Trapping Diynone **318p'** from Chrysanthemum coronarium* *65*

3.3 Conclusions **67**

3.4 References and Notes **68**

Chapter 4. Synthesis and Physical Properties of α,ω–diarylpolyynes **72**

4.1 Introduction **72**

4.2 Results and Discussion **75**

4.2.1 Synthesis *75*

4.2.2 Physical Properties *82*

4.2.3 ^{13}C NMR Spectroscopy *89*

4.2.4 Electronic Properties *95*

4.2.5 X–ray Crystallography *104*

4.3 Conclusions **108**

4.4 References and Notes **109**

Chapter 5. A One–Pot Synthesis and Functionalization of Di– and Triynes Based on the Fritsch–Buttenberg–Wiechell Rearrangement **112**

5.1 Introduction **112**

5.2 Result and Discussions **115**

5.2.1 Formation of Diynes and Triynes by Trapping Li–Acetylides with Electrophiles *117*

5.2.2 Formation of Di–, Tri–, and Tetraynes from the Negishi Coupling *123*

5.2.3 Formation of Tetra– and Hexaynes *126*

5.2.4 Formation of Di– and Triynones *127*

5.2.5 Formation of Pt–Complexes *129*

5.2.6 Synthesis of cis Pt–complexes *130*

5.3 Toward Optically Active Polyynols **131**

5.4 Conclusions **134**

5.5 References and Notes **135**

Chapter 6. Synthesis and Structural Analysis of Tetraynes **142**

6.1 Introduction **142**

6.2 Results and Discussion **144**

6.2.1 Synthesis *144*

6.2.2 Physical Properties *145*

6.2.3 X–ray Crystallographic Analysis *149*

6.2.4 Electronic Properties *153*

*6.2.5 Synthesis of Compound **604** ^{13}C–enriched at a Specific Position* *161*

6.2.6 *Solid–State ^{13}C NMR Spectroscopy of **604*** *162*

6.3 Conclusions 165

6.4 References and Notes 166

Chapter 7. Conclusions and Future Plans 168

Chapter 8. Experimental Section 171

8.1 General Details 171

8.2 General Experimental Procedures 173

8.3 Experimental Procedures 180

8.3.1 Chapter 2 .... *180*

8.3.2 Chapter 3 .... *209*

8.3.3 Chapter 4 .... *242*

8.3.4 Chapter 5 .... *261*

8.3.5 Chapter 6 .... *288*

8.4 References and Notes 293

Appendix A Selective $^1H/^{13}C$ NMR Spectra 291

List of Tables

Table 3.1 Conditions and results for the formation of **307** 45

Table 3.2 Formation of ethynyl triazoles **317a–r** 50

Table 3.2 (continued) Formation of ethynyl triazoles **317a–r** 51

Table 3.3 Formation of butadiynyl triazoles **324a–f** 54

Table 3.4 Chemical shift of compounds **315a–d, 317a–r, 324a–f, 326a,b** 57

Table 3.5 Dihedral angles and selected bond lengths of compounds **317c,e,g,j,l, 324c,e,** and **326b** 64

Table 3.6 Alkynyl bond angles of compounds **317c,e,g,j,l,p, 324c,e,** and **326b** 65

Table 4.1 Melting points and DSC data of polyynes **403–412d,** and **413** 83

Table 4.2 Melting points of triynes **424a–c** 89

Table 4.3 Summary of alkyne chemical shifts for polyynes **407–412a,** and **413** 91

Table 4.4 Summary data for IR and EIMS for **408–413** 96

Table 4.5 UV–vis data for the λ_{max} in both regions in THF for **407–412a** and **413** 98

Table 4.6 UV–vis data for symmetrical hexaynes **412a–d** in THF 102

Table 4.7 UV–vis spectra data for unsymmetrical triynes **424a–c** in THF. 103

Table 5.1 Effect of solvent and conditions on the FBW–deprotonation reaction. 117

Table 5.2 One pot formation of di– and triynes through trapping with carbon based electrophiles. 119

Table 5.3 Acetylide addition to epoxides 122

Table 5.4 One–pot formation and Negishi coupling of di– and triynes 124

Table 5.5 One–pot formation and oxidative homocoupling of di– and triynes 127

Table 5.6 One–pot formation, stannylation, and Stille coupling of diynes. 128

Table 5.7 Pt–acetylide formation from di– and triynes. 130

Table 6.1 IR, mass, and ^{13}C NMR spectroscopic data for compounds **601a–d** 146

Table 6.2 Observed melting points and DSC data of tetraynes **601a–d** 147

Table 6.3 Maximum absorbance of tetraynes **601a–d**, measured in THF 154

Table 6.4 UV–vis absorption of compound **601d** in the solid state on a quartz 156

Table 6.5 Solvent systems and results obtained for crystallization of compound **601d**. 159

List of Figures

Figure 1.1 Polyynes **146, 147,** and carbyne **148** 14

Figure 1.2 Acetylenosaccharide **149** 14

Figure 1.3 Dehydrobenzoannulene **150** 15

Figure 1.4 Bicyclic compound **151** 16

Figure 1.5 Macrocycle **152** 17

Figure 1.6 Pyridine macrocycle **153** 18

Figure 2.1 Naturally occurring polyynols **201a,b, 202** and **203** 24

Figure 2.2 Targeted triynols **207a–c, 208a,b, 204,** and **209a–c** 25

Figure 2.3 Possible reaction pathways of carbenoid **211** or alkylidene carbene **212** rearrangement 26

Figure 2.4 Acetylated and glycosylated triynols **235a-d** 35

Figure 3.1 Naturally occurring tri–, tetra–, and pentaynes 41

Figure 3.2 ^{1}H NMR spectra of compound **307** (arrow denotes the triazole proton) 46

Figure 3.3 ORTEP drawing (20% probability level, hydrogen atoms are omitted for clarity) of compound **315a** 59

Figure 3.4 ORTEP drawing (20% probability level) of compound **317c**. 59

Figure 3.5 ORTEP drawing (20% probability level) of compound **317e**. 60

Figure 3.6 ORTEP drawing (20% probability level) of compound **317g** 60

Figure 3.7 ORTEP drawing (20% probability level) of compound **317j**. 61

Figure 3.8 ORTEP drawing (20% probability level, selected hydrogen atoms are omitted for clarity) of compound **317l** 61

Figure 3.9 ORTEP drawing (20% probability level) of compound **317p** 62

Figure 3.10 ORTEP drawing (20% probability level) of compound **324c** 62

Figure 3.11 ORTEP drawing (20% probability level) of compound **324e** 63

Figure 3.12 ORTEP drawing (20% probability level) of compound **326b** 63

Figure 3.13 ^{1}H NMR spectrum of a solution containing fractions from a trapping experiment involving the extract of *Chrysanthemum coronarium* and benzyl azide. 67

Figure 4.1 Polyynes **401–406** 73

Figure 4.2 A series of conjugated polyynes **407–413** 74

Figure 4.3 DSC trace of tetrayne **410** 84

Figure 4.4 DSC trace of pentayne **411** 85

Figure 4.5 DSC trace of hexayne **412a** 86

Figure 4.6 DSC trace of hexayne **412b** 86

Figure 4.7 DSC trace of hexayne **412c** 87

Figure 4.8 DSC trace of hexayne **412d** 87

Figure 4.9 DSC trace of octayne **413** 88

Figure 4.10 ^{13}C NMR spectra of diphenyl polyynes **407–412a** and **413** 93

Figure 4.11 UV–vis spectra of polyynes **407–412a** and **413**. Up arrows denote λ_{max} for Region 1 and down arrows λ_{max} for Region 2 97

Figure 4.12 Plot of λ_{max} of lowest energy absorption versus the reciprocal of the number of triple bonds for compounds **407–409** 99

Figure 4.13 Plot of the energy gap vs the number of repeat alkyne units in the diphenyl polyyne series. 100

Figure 4.14 UV–vis spectra of polyynes **412a–d**. 102

Figure 4.15 UV–vis absorption spectra for triynes **424a–c** 104

Figure 4.16 ORTEP drawing of compound **410** showing several parallel–oriented molecules 105

Figure 4.17 ORTEP drawing of diphenyl hexayne **412a**. 106

Figure 4.18 ORTEP drawing of *t*-butyl derivative **412d**. 107

Figure 5.1 ORTEP drawing of **509a** (20% probability level). 121

Figure 6.1 Optimal geometry and parameters for topochemical polymerization. a) 1,4–polymerization. b) 1,6–polymerization. c) 1,8–polymerization. 143

Figure 6.2 DSC plots of the tetraynes **601a–d** 148

Figure 6.3 TGA plot for compound **601d** scanned from 20 to 700 °C at a rate of 10 °C/min. 149

Figure 6.4 ORTEP drawing of compound **601a** (20% probability level) and packing diagram as viewed along the crystallographic *b*-axis. 150

Figure 6.5 ORTEP drawing of compound **601c** (20% probability level) and packing diagram as viewed along the crystallographic *a*-axis. 151

Figure 6.6 ORTEP drawing of compound **601d** (20% probability level) and packing diagram as viewed along the crystallographic *a*-axis. 152

Figure 6.7 UV–vis absorption spectra of tetraynes **601a–d** 153

Figure 6.8 Solid–state UV–vis spectra for compound **601d** 155

Figure 6.9 Reflection IR spectra of solid–state compound **601d** on gold. 157

Figure 6.10 a) Inner–outer chambers. b) Upper–lower layers. 158

Figure 6.11 Solid–state ^{13}C NMR spectra of compound **601d** at 75 MHz.................... 161

Figure 6.12 Solid–state ^{13}C NMR spectra for compound **604**. a) Before Heating. b) After Heating. Spectra were acquired at 11.75 T (125 MHz for ^{13}C) 164

Figure A.1 ^{1}H and ^{13}C NMR spectra of **229a** 298

Figure A.2 ^{1}H and ^{13}C NMR spectra of **230a** 299

Figure A.3 ^{1}H and ^{13}C NMR spectra of **231a** 300

Figure A.4 ^{1}H and ^{13}C NMR spectra of **231b** 301

Figure A.5 ^{1}H and ^{13}C NMR spectra of **231c** 302

Figure A.6 ^{1}H and ^{13}C NMR spectra of **209a** 303

Figure A.7 ^{1}H and ^{13}C NMR spectra of **209b** 304

Figure A.8 ^{1}H and ^{13}C NMR spectra of **209c** 305

Figure A.9 ^{1}H and ^{13}C NMR spectra of **317f** 306

Figure A.10 ^{1}H and ^{13}C NMR spectra of **317p** 307

Figure A.11 ^{1}H and ^{13}C NMR spectra of **317q** 308

Figure A.12 ^{1}H and ^{13}C NMR spectra of **325b** 309

Figure A.13 ^{1}H and ^{13}C NMR spectra of **325b'** 310

Figure A.14 ^{1}H and ^{13}C NMR spectra of **326b** 311

Figure A.15 ^{1}H and ^{13}C NMR spectra of **412b** 312

Figure A.16 ^{1}H and ^{13}C NMR spectra of **412c** 313

Figure A.17 ^{1}H and ^{13}C NMR spectra of **412d** 314

Figure A.18 ^{1}H and ^{13}C NMR spectra of **435** 315

Figure A.19 ^{1}H and ^{13}C NMR spectra of **431** 315

Figure A.20 ^{1}H and ^{13}C NMR spectra of **438a** 316

Figure A.21 ^{1}H and ^{13}C NMR spectra of **438b** 316

Figure A.22 ^{1}H and ^{13}C NMR spectra of **432** 317

Figure A.23 ^{1}H and ^{13}C NMR spectra of **433** 317

Figure A.24 ^{1}H and ^{13}C NMR spectra of **506e** 318

Figure A.25 ^{1}H and ^{13}C NMR spectra of **506f** 319

Figure A.26 ^{1}H and ^{13}C NMR spectra of **506g** 320

Figure A.27 ^{1}H and ^{13}C NMR spectra of **508i** 321

Figure A.28 ^{1}H and ^{13}C NMR spectra of **508j** 322

Figure A.29 ^{1}H and ^{13}C NMR spectra of mixtures of **508j/508k** 323

Figure A.30 ^{1}H and ^{13}C NMR spectra of **509h** 324

Figure A.31 ^{1}H and ^{13}C NMR spectra of **515d** 325

Figure A.32 ^{1}H and ^{13}C NMR spectra of **516b** 326

Figure A.33 ^{1}H and ^{13}C NMR spectra of **526b** 327

List of Schemes

Scheme 1.1 The Glaser coupling of compound **104**........1

Scheme 1.2 Unsymmetrical coupling for the formation of diyne **106**........2

Scheme 1.3 Synthesis of 1,3–pentadiyne **107** and triyne **108**........3

Scheme 1.4 Synthesis of diynes **117**........4

Scheme 1.5 Eglinton and Galbraith coupling to form cyclic diyne **119**........5

Scheme 1.6 Hay coupling reaction for the formation of diyne **121**........5

Scheme 1.7 Heterocoupling between a terminal alkyne **122** and a bromoalkyne **123**......6

Scheme 1.8 1,4– and 1,6–topochemical polymerizations........8

Scheme 1.9 A modified Sonogashira reaction for diyne **130**........10

Scheme 1.10 A modified Negishi coupling for triyne **133**........11

Scheme 1.11 A modified Stille reaction........11

Scheme 1.12 Formation of triyne **139** by SS–FVP........12

Scheme 1.13 Formation of diyne **141** from cobalt deprotection........12

Scheme 1.14 Formation of triyne **139** from vinylidene rearrangement........13

Scheme 1.15 Formation of triyne **144** from photolysis........13

Scheme 2.1 Formation of compound **204** via Cadiot–Chodkiewicz coupling........25

Scheme 2.2 Attempted synthesis of dibromoolefin **216**........27

Scheme 2.3 Synthesis of triyne **221** and byproduct **222**........28

Scheme 2.4 Formation of aldehydes **223a** and **223b** by two different methods........29

Scheme 2.5 Formation of terminal alcohols **207a–c**........31

Scheme 2.6 Formation of methyl endcapped alcohols 208a,b, and 204 33

Scheme 2.7 Formation of phenyl endcapped alcohols **209a–c** 34

Scheme 3.1 Proposed mechanism for the formation of triazole **307** 44

Scheme 3.2 Formation of bis–trizoles **315a–d** 48

Scheme 3.3 Formation of bis–triazoles **319** and **320** 52

Scheme 3.4 Formation of triazoles **326a,b** 55

Scheme 4.1 Synthesis of unsymmetrical polyynes **409** and **411** 76

Scheme 4.2 Syntheses of symmetrical polyynes **410, 412a** and **413** 78

Scheme 4.3 Syntheses of symmetrical hexaynes **412a–d** 79

Scheme 4.4 Synthesis of triynes **424a–c** 80

Scheme 4.5 Synthesis of labeled polyynes **431–433** 81

Scheme 5.1 Formation of metal acetylides **501** 113

Scheme 5.2 General Scheme for the divergent route for the formation and substitution. 114

Scheme 5.3 Desilylation of compounds **517a–g** 115

Scheme 5.4 Formation of tetrayne **521** 125

Scheme 5.5 Synthesis of **525** 126

Scheme 5.6 Transformation of *trans*–acetylides **516a–c** to *cis*–acetylides **526a–c** 131

Scheme 5.7 Conversion of the propargylic alcohols to Mosher ester using *R*–Mosher acid chloride 133

Scheme 6.1 Synthesis of tetraynes **601a–d** 145

Scheme 6.2 Synthesis of labeled tetrayne **604** 162

Scheme 6.3 Predicted 1,6–topochemical polymerization of labeled 604. a) Before heating. b) After heating. 163

List of Abbreviations

Ac	acetyl
Aq	aqueous
Bn	benzyl
Bu	*n*-butyl
cm	centimeter
d	doublet
dec	decomposition
DMF	*N,N*–dimethylformamide
DOKE	differential optical Kerr effect
dppe	bis(diphenylphosphino)ethylene
dppp	bis(diphenylphosphino)propane
DSC	differential scanning calorimetry
Eg	energy gap
EI	electron ionization
Et	ethyl
ESI	electrospray ionization
g	gram(s)
h	hour(s)
hex	hexyl
HOMO	highest occupied molecular orbital

HRMS	high resolution mass spectrometry
Hz	hertz
i	*iso*
IR	infrared
LUMO	lowest unoccupied molecular orbital
m	multiplet
M	Molar
MALDI	matrix-assisted laser desorption ionization
Me	methyl
MHz	megahertz
mL	milliter
mmol	millimole
Mp	melting point
MS	mass spectrometry
NLO	nonlinear optics
nm	nanometer
NMR	nuclear magnetic resonance
oct	octyl
ORTEP	Oak Ridge thermal ellipsoid plot
Ph	phenyl
ppm	parts per million
Pr	propyl
q	quartet

quint	quintet
rt	room temperature
t	triplet
TBAF	tetrabutylammonium fluoride
t-Bu	tertiary-butyl
TGA	thermal gravity analysis
THF	tetrahydrofuran
TLC	thin layer chromatography
TMEDA	*N,N,N',N'*–tetramethylethylenediamine
TOF	time of flight
UV-vis	ultraviolet–visible

List of Symbols

Å	angstrom
δ	chemical shift
γ	molecular second hyperpolarizability
λ_{max}	maximum wavelength

Chapter 1. A Brief Historical Review of Polyynes[1]

Compounds containing conjugated alkynes have been known for almost two centuries. The evolution of polyyne chemistry has ranged from natural product isolation to materials applications. The discovery and study of polyynes can be roughly divided into four periods.

1.1 Before the 1900s

In this time frame, many fundamental polyyne compounds and methods were discovered, even though many basic concepts of organic chemistry had yet to be discovered.

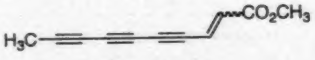

101

The first polyyne natural product was discovered in 1826. Crystals of triyne **101** were isolated from a Japanese essential oil obtained from a species of *Artemisia*.[2] The structure of this compound was not, however, determined until the late 1950s.

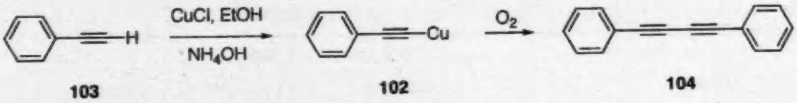

Scheme 1.1 The Glaser coupling of compound **104**

The oldest reported acetylenic reaction dates back to 1869.[3] Carl Glaser reported the generation and isolation of Cu(I) phenylacetylide **102** from phenylacetylene **103** in the presence of CuCl, in EtOH, and under an O_2 atmosphere, **102** reacted to produce diphenyldiacetylene **104** (Scheme 1.1). This reaction later was named after him and has become know as the Glaser coupling. Unfortunately, a serious problem was associated with this reaction: isolation of the explosive Cu(I) phenylacetylide **102**.

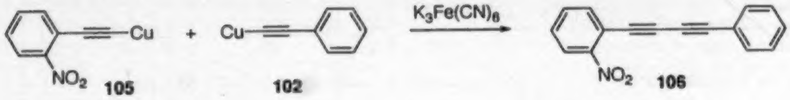

Scheme 1.2 Unsymmetrical coupling for the formation of diyne **106**

Approximately ten years later in 1882, Baeyer reported an unsymmetrical coupling between Cu(I) *o*–nitrophenylacetylide **105** and Cu(I) phenylacetylide **102** in the presence of aqueous $K_3Fe(CN)_6$ to produce compound **106** (Scheme 1.2).[4] This reaction gave a better yield when ethanol was used as solvent. During this period, scientists were limited to identifying the structures of polyynes by comparing elemental analysis and/or hydrogenation data to that of the known compounds.

1.2 1900s to 1970s

The discovery of polyynes based both on synthesis and isolation from natural products in the late 1800s was a stepping–stone for the next century. In 1911, Stobbe and Ebert reported, for the first time, the use of UV–vis spectroscopy to study diphenyldiacetylene. Unfortunately no discussion about the chromophore of this compound was provided.[5] Five years later, MacBeth and Stewart published the article entitled "The Absorption Spectra of Substances Containing Conjugated and Unconjugated Systems of Triple Bonds".[6] The authors compared the UV–vis spectral data of 2,4–hexadiyne and 1,3,5–hexatriene. They reported different shapes in the absorbance bands due to the different chromophores present in the molecules.

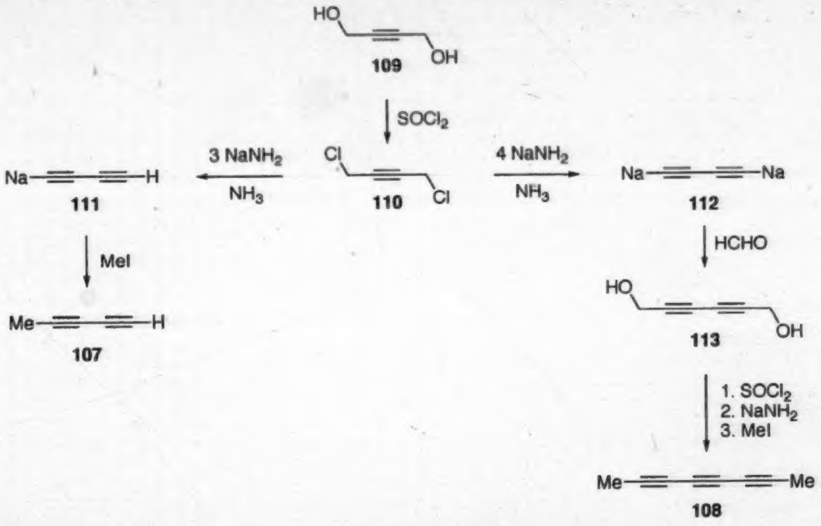

Scheme 1.3 Synthesis of 1,3–pentadiyne **107** and triyne **108**

During this time, polyynes continued to be formed using the copper coupling reaction discovered by Glaser, although new procedures were being developed. In 1950, Jones presented a series of lectures at the University of Notre Dame. He showed that the synthesis of terminal diyne **107**, triyne **108** and even a pentayne could be synthesized starting from the elimination of 2–butyn–1,4–diol **109** (Scheme 1.3). Diol **109** was converted to dichloride **110** with thionyl chloride. The dehydrohalogenation of compound **110** with sodium amide produced compound **111** or **112** depending on the stoichiometry of sodium amide used. Compound **111** was reacted with methyl iodide to produce *in situ* 1,3–pentadiyne **107**, while the dianionic diyne was reacted with formaldehyde to form diol **113**, which was then converted to a dichloride with thionyl chloride. Dehydrohalogenation then formed a dianionic triyne intermediate that was trapped with methyl iodide to form 2,4,6–octatriyne **108**. This triyne could not be handled at room temperature and pale yellow crystals turned black within a few minutes. However, in solution triyne **108** was reasonably stable. Furthermore, Jones also reported the absorption λ_{max} values of the methyl endcapped polyyne **108** in ethanol.[7]

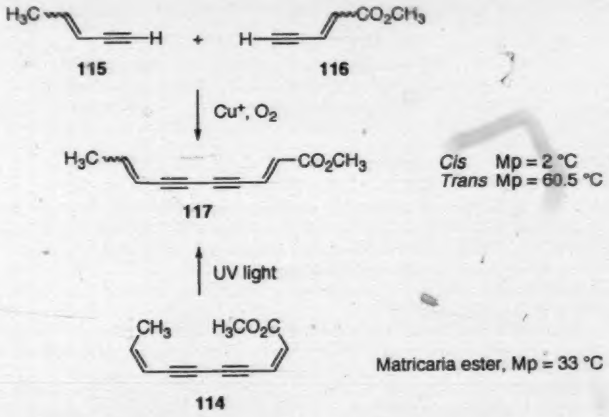

Scheme 1.4 Synthesis of diynes **117**

In the same year, 1950, Sorensen and coworkers synthesized matricaria ester **114**,[8] which had been isolated in 1941 from the essential oil of *Matricaria inodora* (Scheme 1.4).[9] The synthesis derived from enyne **115** and methyl pentenynoate **116**, via reaction in the presence of cuprous salts and O_2. As expected, only a small quantity of the desired diyne **117** was formed as a result of coupling the two different coupling partners. Diyne **117** was produced as a mixture of the two stereoisomers and both had different melting points compared to that of the natural ester **114**, but the UV–vis absorption spectra were identical. By irradiating matricaria ester with UV light, however, the *cis*–isomer **114** could be isomerized to the mixture of *cis*– and *trans*–**117**.[7]

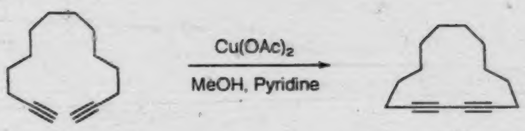

118

119

Scheme 1.5 Eglinton and Galbraith coupling to form cyclic diyne **119**

Only a few coupling reactions had developed before 1950, most of which are still commonly employed today. The most widely used reaction in the 1900s was the original Glaser oxidative coupling; however, its application for the homocoupling of terminal acetylenes was compromised by the explosive nature of the isolated copper acetylide salt. Eglinton and Galbraith subsequently reported a modified and safer homocoupling reaction.[10] The authors showed that two terminal alkynes tethered by a long alkyl chain (**118**) could be coupled in the presence of excess $Cu(OAc)_2$, MeOH, and pyridine to produce macrocyclic diyne **119** (Scheme 1.5). The reaction was proposed to proceed via a radical pathway in which a terminal alkyne anion is oxidized by Cu(II) to a terminal radical alkyne. The two radicals terminate to form a diyne. The beauty of this method is that the explosive Cu–acetylide is not isolated, making it widely used today.

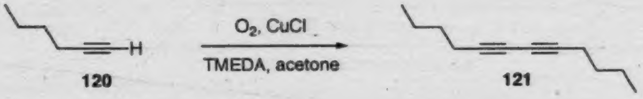

120

121

Scheme 1.6 Hay coupling reaction for the formation of diyne **121**

Hay modified the Eglinton and Galbraith reaction by using a Cu(I) TMEDA complex to improve the solubility of the Cu(I) acetylide (Scheme 1.6).[11,12] 1–Hexyne **120** was reacted in the presence of excess O_2, a catalytic amount of CuCl, and TMEDA to produce diyne **121**. This method is widely used currently for the oxidative coupling between terminal conjugated alkynes to produce polyynes.

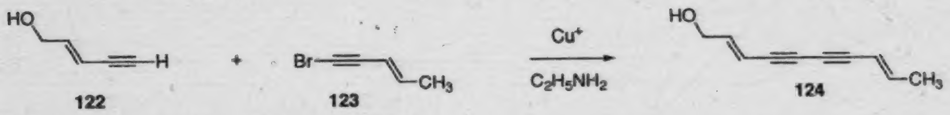

Scheme 1.7 Heterocoupling between a terminal alkyne **122** and a bromoalkyne **123**

The above discussion describes the homocoupling reaction between two terminal alkynes, but during the same period (1955), Cadiot and Chodkiewicz reported a heterocoupling protocol between a terminal alkyne **122** and a 1–bromoalkyne **123** in the presence of CuCl and EtNH$_2$ to produce the conjugated diyne **124** (Scheme 1.7).[13] This reaction, now called the Cadiot–Chodkiewicz reaction, is extensively used, even though the success of this reaction can vary widely and is often complicated by the formation of homocoupled byproducts. Bohlmann first proposed the reaction underwent a dinuclear Cu(II) acetylide complex, which collapsed to produce Cu(I) and a homocoupled diyne.[14,15] A Cu(III) acetylide intermediate has also been proposed for this reaction, followed by a reductive elimination to produce a diyne and Cu(I) halide, which can undergo another catalytic cycle.[16] This reaction can tolerate many functional groups such as alcohols, carboxylic acids, hydrocarbons, ethers, thioethers, quinols, amines, acetals and aldehydes. The yields of these reactions, however, can fluctuate widely between substrates.

Beginning in this time and extending through several decades, Bohlmann and others discovered hundreds of polyyne natural products, often using UV–vis spectroscopy to identify them. Many natural and unnatural polyyne products were subsequently synthesized. Bohlmann and coworkers tabulated a general table of λ_{max} absorbance bands for polyyne–enes and reported that two groups of absorptions were typically observed, a low energy and a high energy group.[2] During this period, Jones and coworkers also reported the isolation of scores of natural products (often from fungi) and used UV–vis spectroscopy to confirm structures.[17,18] For example, *Odyssic Acid* **125** and *Odyssin* **126** were isolated from fungal species.

The absorption wavelength and the relative intensity of the UV–vis spectra are useful diagnostic features to identify a polyyne framework. UV–vis spectroscopy is a very sensitive technique with a detection limit in the concentration range of 1–10 nM for some chromophores. This technique, however, does not always reveal the presence of impurities and the structure of non–absorbing groups.

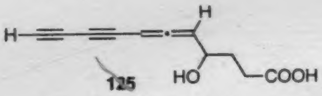

125

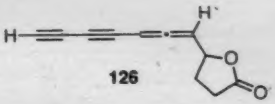

126

Finally, it was also during this timeframe that many of the new reactions developed for synthesis of natural products were applied to the formation of non–natural polyyne products. These efforts resulted in many extended polyynes, some reported as long as 32 sp–hybridized carbons. This work will be described in more detail in Chapter 4 of this thesis.

1.3 1970s to 1990s

This is an era dominated by the discovery and evolution of palladium–catalyzed coupling techniques and the many new reactions that were subsequently developed and are still used frequently today. Several of these well–known named reactions have been described below. In many cases, the original reaction involved only a monoyne, but has been later extended to polyynes over the years. Also presented during this timeframe was the prospect that polymeric polyynes could be synthesized from solid–state polymerization. Wegner and coworkers reported a solid–state polymerization of a 2,4,6–octatriyne derivatives in 1973 (Scheme 1.8).[19] In this solid–state transformation, the geometrical packing of the neighboring molecules is necessary for the reaction to take place. The products are directly controlled by the organization of the starting materials making this reaction regio– and stereoselective (See Chapter 6 for more details).[20] For example, triyne **127** could be polymerized under both thermo– and photochemical conditions (when heated to 100 °C or irradiated at 380 nm respectively) to form polymer **128** or **129**, depending on the geometry of the crystal lattice packing. In this particular case, either 1,6– or 1,4–topochemical polymerization takes place to form **128** and **129**, respectively.

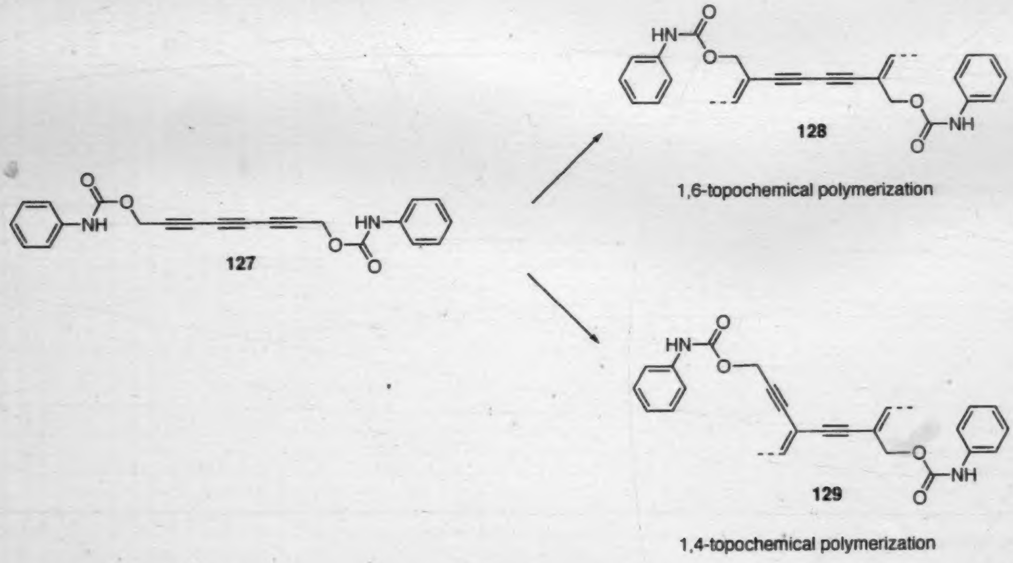
127
128
1,6-topochemical polymerization
129
1,4-topochemical polymerization

Scheme 1.8 1,4– and 1,6–topochemical polymerizations

1.4 1990s to Present

From 1990 to the present, traditional reactions have been continuously modified and new methods for the formation of polyynes via rearrangement processes have been developed. For example, the original Glaser reaction was problematic due to the unstable Cu(I) phenylacetylide precursor. Thus, this problem has been circumvented by combining the formation of Cu(I) phenylacetylide and oxidative step, resulting in the oxidative homocoupling of terminal acetylenes without the isolation of explosive intermediates. Although this reaction was discovered more than one hundred years ago, scientists routinely employ it in research with only small modifications from the traditional method, such as using CuOAc as a catalyst or using supercritical CO_2 as solvent.[21,22] The intramolecular coupling reaction of terminal alkynes with a mixture of $Cu(OAc)_2$ and CuCl in pyridine has also been used to form macrocycles.[23]

The Sonogashira reaction, initially reported in 1975,[24] outlined the coupling of a terminal monoyne with a halide derivative in the presence of Pd(II), CuI, and triethylamine to produce an alkynyl product. In this reaction, CuI acts to form a Cu(I)–acetylide which undergoes transmetallation with $PdCl_2$ to produce Pd(II)–diacetylide. The reductive elimination of a dimerized alkyne converts Pd(II) to Pd(0), which is accepted to be the active catalyst. Alternatively, $PdCl_2$ can coordinate to the lone pair of triethylamine and π–deinsertion forms an ammonium chloride species, which is followed by a reductive elimination to generate Pd(0) and HCl. The Pd(0) generated from either cycle can undergo oxidative addition with an aryl halide to form the Pd(II) complex and transmetallation between the Cu(I) acetylide and the Pd(II) halide produces a palladium acetylide complex. Reductive elimination of this complex affords the alkynyl coupling product and Pd(0) which can undergo another cycle.

The original Sonogashira reaction has also been used for the formation of natural occurring diynes (Scheme 1.9).[25] For example, López and coworkers reported the synthesis of marine polyyne Callyberyne A via intermediate **130**. Bromovinyl precursor **131** was reacted with the terminal diyne **132** in the presence of $PdCl_2(PPh_3)_2$ and CuI to produce the desired product **130** in good yield.

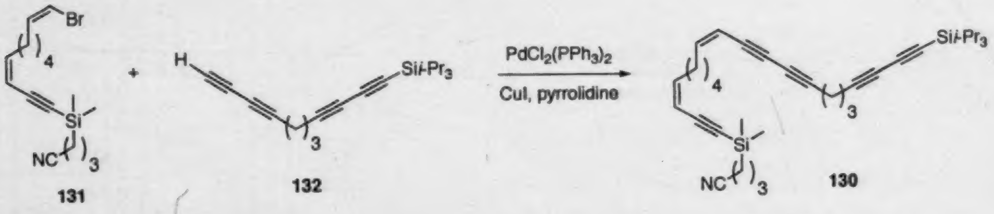

Scheme 1.9 A modified Sonogashira reaction for diyne **130**

The original Negishi reaction, reported in 1977, was not necessarily designed for the synthesis of polyynes, but is now used as a reliable method to synthesize unsymmetrical polyynes.[26] Once again, the Negishi reaction has been modified to suit the researchers' purposes. The Tykwinski group extended the Negishi reaction to the formation of triynes such as **133** in 2006 (Scheme 1.10).[27] In this reaction, the lithium acetylide **134** generated *in situ* underwent transmetalation to form zinc acetylide **135**. This zinc complex was coupled with an aryl iodide using a catalytic amount of $Pd(PPh_3)_4$ to produce the desired product **133** in good yield. This and related reactions will be discussed in Chapter 5 of this thesis.

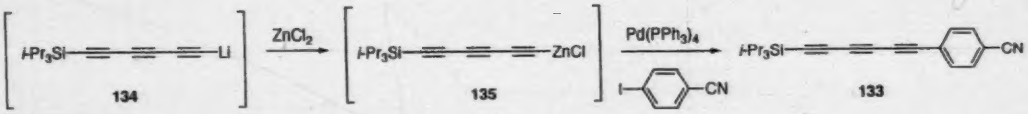

Scheme 1.10 A modified Negishi coupling for triyne **133**

Cross–coupling reactions were diversified to tin–species and acid chlorides. The original Stille coupling was reported in 1978 using a catalytic amount of palladium, and the catalytic cycle is similar to the Negishi coupling. Over the years, many compounds containing a polyyne core were synthesized using a modified Stille coupling reaction. For example, Tykwinski and coworkers have recently reported a one–pot reaction to synthesize diynone **136** using an *in situ* procedure to generate a tin–acetylide via lithium acetylide **137** (Scheme 1.11). This intermediate then underwent coupling with acid chloride **138**.[27] This reaction will also be discussed in Chapter 5 of this thesis.

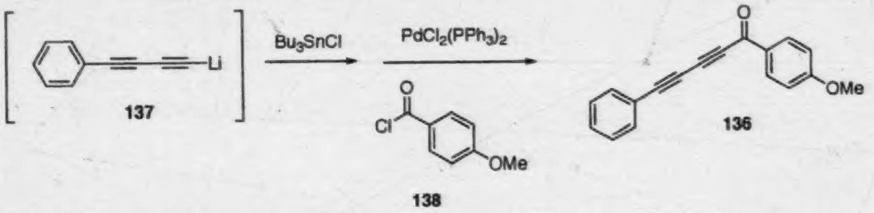

Scheme 1.11 A modified Stille reaction

Diederich and coworkers reported in 1991a new method to synthesize triyne **139**, as well as other polyynes, using Solution–Spray Flash Vacuum Pyrolysis (SSFVP) at 650 °C (Scheme 1.12).[28] Under these high temperature conditions, the diketone **140** underwent a two–fold CO elimination to produce polyyne **139**. This method converts the high molecular weight and nonvolatile cyclobutenediones to linear polyynes in a wide range of yields.

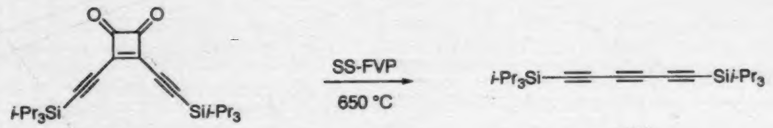

140 **139**

Scheme 1.12 Formation of triyne **139** by SS–FVP

Haley and coworkers in 1997 introduced a new method to synthesize diyne **141**. (Scheme 1.13).[29] The cobalt protecting group of the starting material **142** could be removed using iodine in THF to afford diyne **141**. The diyne, conversely, could also be protected using octacarbonyl dicobalt in ether, followed by the ligand exchange of CO with bis(diphenylphosphino)methane.

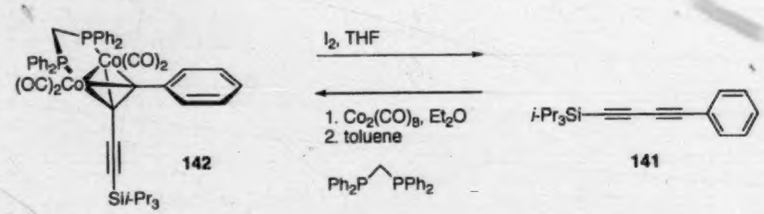

142 **141**

Scheme 1.13 Formation of diyne **141** from cobalt deprotection

The Tykwinski group reported a modified Fritsch–Buttenberg–Wiechell rearrangement to form triyne **139** (Scheme 1.14).[30] Dibromoolefin **143** undergoes a carbenoid rearrangement in the presence of BuLi in hexanes at low temperature. The mechanism of this reaction proceeds by lithium halogen exchange, followed by migration of an alkynyl group and lithium bromide elimination to form triyne **139**. This method can also be extended to longer polyynes, for example, via two-fold rearrangements.[31] The synthesis of several examples of larger polyynes will be outlined in Chapter 4 of this thesis.

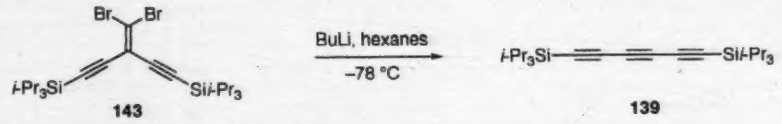

Scheme 1.14 Formation of triyne **139** from vinylidene rearrangement

In the same year, Tobe introduced a new method to obtain triyne **144** via a vinylidene precursor (Scheme 1.15).[32] Cheletropic extrusion of indane from starting material **145** by irradiating an ice–cooled solution of **145** with a low-pressure mercury lamp gave the triyne. This method was also expanded to multiple vinylidene precursors to form [*n*]cyclocarbons.[33]

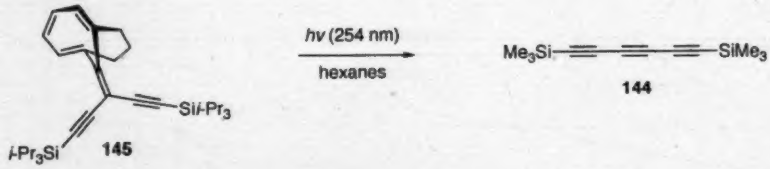

Scheme 1.15 Formation of triyne **144** from photolysis

During this period, applications of polyynes in materials chemistry became prominent. A variety of rod, ring, and spherical shapes were synthesized and characterized. Tykwinski and coworkers published the synthesis and application of rod–like compounds **146** and **147** (Figure 1.3). These two compounds show substantial nonlinear optical properties (NLO) when measured using the differential optical Kerr Effect (DOKE) technique. Compounds with phenyl end–caps, such as **146**, show molecular second hyperpolarizability values (γ) as a function of polyyne length that can be fit to the power–law relationship $\gamma \pm n^{3.79\pm0.25}$ (where *n* is the number of acetylene repeat units),[34] while those of the *i*–Pr$_3$Si end-capped series (e.g., **147**) show a slightly higher response ($\gamma \pm n^{4.28\pm0.13}$).[31,35]

Infinite expansion of the sp–hybridized framework of a polyyne affords carbyne, **148**. Carbyne constitutes a one-dimensional allotropic form of carbon that would ultimately be terminated with hydrogen or some other end-capping group. In its most basic form, carbyne would consist of a sufficient number of sp–hybridized carbon such that addition of an additional alkynyl unit does not change the polyyne properties, i.e., the property would be saturated. Research efforts toward determining the properties of carbyne have involved both theoretical and experimental studies, but up to now the synthesis of carbyne and its physical and chemical properties remain a mystery.[31,36–38]

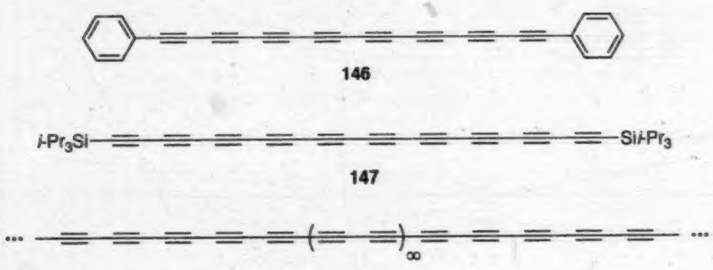

Figure 1.1 Polyynes **146**, **147**, and carbyne **148**

Vasella and coworkers synthesized acetylenosaccharide **149**, a novel cyclodextrin analogue (Figure 1.2).[39] Compound **149** binds poorly with *D*– and *L*–adenosine in aqueous solution, with association constants $K_a = 40$ and $32\ \mathrm{L\ mol^{-1}}$, respectively.

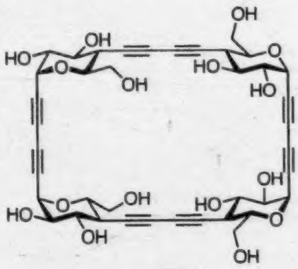

149

Figure 1.2 Acetylenosaccharide **149**

Graphite is a good conductor of heat and electricity. Haley and coworkers reported the synthesis of dehydrobenzoannulene **150** (Figure 1.3), a substructure of a larger form of graphite, called graphdiyne.[40,41] The authors also synthesized a variety of substructures of the cyclic diyne in an attempts toward the formation of the graphdiyne. The macrocycle **150** exhibits a characteristic pattern of four absorption bands. These bands come from the $\pi \rightarrow \pi^*$ transitions in the [18]annulene skeleton. Other groups have also targeted the synthesis of phenyldiacetylene macrocycles. For example, Fallis and coworkers constructed several macrocycles using a modified Cadiot–Chodkiewicz reaction.[42] As well, a simpler version of compound **150** was synthesized by Vollhardt and coworkers.[43]

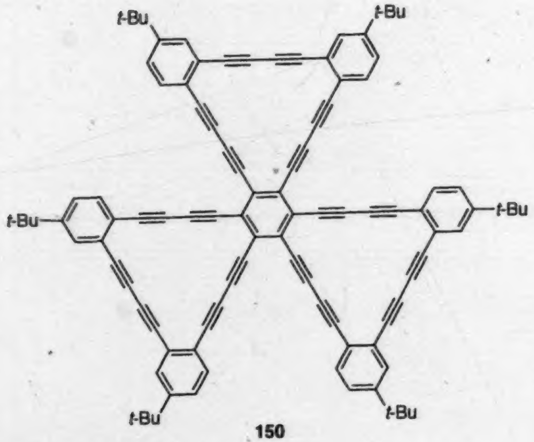

150

Figure 1.3 Dehydrobenzoannulene **150**

Diederich and coworkers synthesized bicyclic compound **151** via an oxidative homocoupling reaction (Figure 1.4).[44,45] Having compound **151** in hand, cyclic voltammetry was carried out and the voltammogram displayed a remarkably low first reduction potential at –0.81 V. The UV-vis spectrum of this compound shows a strong intramolecular charge transfer band, with a low energy absorption at 850 nm.

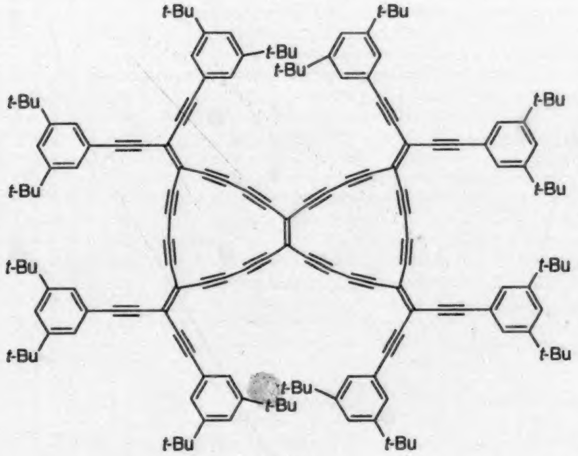
t-Bu
t-Bu
t-Bu
t-Bu
t-Bu
t-Bu
t-Bu
t-Bu
t-Bu
t-Bu
t-Bu
t-Bu
t-Bu
t-Bu
t-Bu
t-Bu

151

Figure 1.4 Bicyclic compound **151**

Self–assembled monolayers (SAMs) are a popular topic for shape–persistent macrocycles. Compound **152** was reported to bind to the surface of Au(III) (Figure 1.5).[46] This compound contains amide functional groups and additional thioethers for binding to the Au-surface. The adsorption properties of compound **152** were explored using scanning tunneling microscopy (STM), and the authors suggested that this macrocycle shows the potential to form new functional nanostructures.

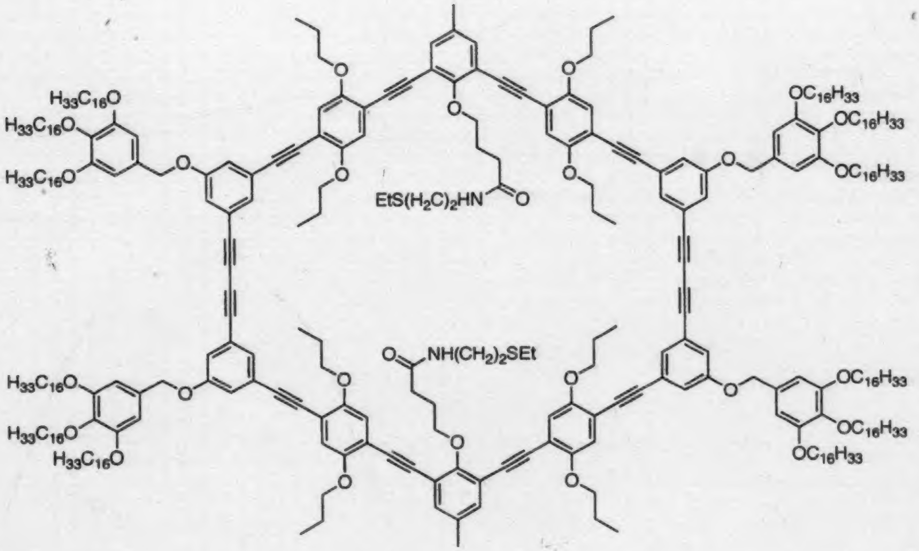
H33C16O
H33C16O
H33C16O
OC16H33
OC16H33
OC16H33
EtS(H2C)2HN
O
NH(CH2)2SEt
H33C16O
H33C16O
H33C16O
OC16H33
OC16H33
OC16H33

152

Figure 1.5 Macrocycle **152**

Tobe and coworkers reported the synthesis and association behavior of pyridine macrocycle **153** (Figure 1.6).[47] This compound was cyclized via an intramolecular homocoupling with $Cu(OAc)_2$ and pyridine. Compound **153** was tested for its binding selectivity for organic cations. Tropylium tetrafluoroborate was chosen as a guest and it has a slightly smaller size than the cavity of compound **153**. The host was titrated with the guest in $CDCl_3/CD_3CN$ (17:3) and the chemical shift of the aromatic protons of the complex was measured. The binding constant of this complex shows an association constant $K_a = 5 \times 10^2$ L mol^{-1}.

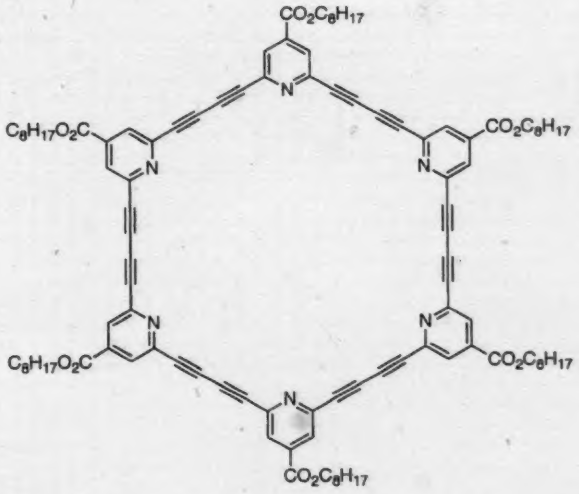

153

Figure 1.6 Pyridine macrocycle **153**

The discovery of polyynes and the synthetic efforts of numerous researchers have been briefly outlined here and used to introduce both the breadth of current polyyne chemistry and a number of aspects that will be addressed specifically in this thesis. The work of the pioneers of this area has been the stepping-stone for many modern chemists.

Clearly, however, there is ample room for growth in both synthetic chemistry and material applications.

1.5 References and Notes

(1) The term polyynes is used to denote compounds with two or more consecutive triple bonds. Such compounds can also be called conjugated alkynes. The term polyacetylenes has also been widely used, but this term can be ambiguous because the term polyacetylenes is referred to the material formed upon polymerization of acetylenes.

(2) Bohlmann, F.; Burkhardt, T.; Zdero, C. *Naturally Occurring Acetylenes*; Academic Press: New York, 1973.

(3) Glaser, C. *Ber. Dtsch. Chem. Ges.* **1869**, *154*, 137–171.

(4) Baeyer, A. *Chem. Ber.* **1882**, *15*, 55–60.

(5) Stobbe, H.; Ebert, E. *Chem. Ber.* **1911**, *44*, 1288–1298.

(6) Macbeth, A. K.; Stewart, A. W. *J. Chem. Soc.* **1917**, *111*, 829–841.

(7) Jones, E. R. H. *Acetylene Chemistry*; University of Notre Dane: Indiana, 1954.

(8) Sorensen, N. A.; Stavholt, K. *Acta Chem. Scand.* **1950**, *4*, 1080–1084.

(9) Sorensen, N. A.; Stene, J. *J. Liebigs Ann. Chem.* **1941**, *549*, 80–94.

(10) Eglinton, G.; Galbraith, A. R. *Chem. Ind.* **1956**, 737–738.

(11) Hay, A. S. *J. Org. Chem.* **1962**, *27*, 3320–3321.

(12) Hay, A. S. *J. Org. Chem.* **1960**, *25*, 1275–1276.

(13) Willemart, A.; Chodkiewicz, W.; Cadiot, P. *Bull. Soc. Chim. Fr.* **1957**, 455–456.

(14) Bohlmann, F.; Schonowsky, H.; Inhoffen, E.; Grau, G. *Chem. Ber.* **1964**, *97*.

(15) Siemsen, P.; Livingston, R. C.; Diederich, F. *Angew. Chem., Int. Ed.* **2000**, *39*, 2632–2657.

(16) Li, J. J. *Name Reactions*; Springer–Verlag: New York, 2003, pp 62.

(17) Bulock, J. D.; Jones, E. R. H.; Leeming, P. R. *J. Chem. Soc.* **1957**, 1097–1101.

(18) Bulock, J. D.; Jones, E. R. H.; Leeming, P. R. *J. Chem. Soc.* **1955**, 4270–4276.

(19) Kiji, J.; Kaiser, J.; Wegner, G.; Schulz, R. C. *Polymer* **1973**, *14*, 433–439.

(20) Fowler, F. W.; Lauher, J. W. *Carbon–Rich Compounds: From Molecules to Materials*; Haley, M. M.; Tykwinski, R. R., Eds; John & Sons: Weinheim, 2005.

(21) Fomina, L.; Vazquez, B.; Tkatchouk, E.; Fomine, S. *Tetrahedron* **2002**, *58*, 6741–6747.

(22) Li, J. H.; Jiang, H. F. *Chem. Commun.* **1999**, 2369–2370.

(23) Haley, M. M.; Bell, M. L.; Brand, S. C.; Kimball, D. B.; Pak, J. J.; Wan, W. B. *Tetrahedron Lett.* **1997**, *38*, 7483–7486.

(24) Sonogashira, K.; Tohda, Y.; Hagihara, N. *Tetrahedron Lett.* **1975**, 4467–4470.

(25) Lopez, S.; Fernandez–Trillo, F.; Midon, P.; Castedo, L.; Saa, C. *J. Org. Chem.* **2006**, *71*, 2802–2810.

(26) Negishi, E.; King, A. O.; Okukado, N. *J. Org. Chem.* **1977**, *42*, 1821–1823.

(27) Morisaki, Y.; Luu, T.; Tykwinski, R. R. *Org. Lett.* **2006**, *8*, 689–692.

(28) Rubin, Y.; Lin, S. S.; Knobler, C. B.; Anthony, J.; Boldi, A. M.; Diederich, F. *J. Am. Chem. Soc.* **1991**, *113*, 6943–6949.

(29) Haley, M. M.; Langsdorf, B. L. *Chem. Commun.* **1997**, 1121–1122.

(30) Eisler, S.; Tykwinski, R. R. *J. Am. Chem. Soc.* **2000**, *122*, 10736–10737.

(31) Eisler, S.; Slepkov, A. D.; Elliott, E.; Luu, T.; McDonald, R.; Hegmann, F. A.; Tykwinski, R. R. *J. Am. Chem. Soc.* **2005**, *127*, 2666–2676.

(32) Tobe, Y.; Iwasa, N.; Umeda, R.; Sonoda, M. *Tetrahedron Lett.* **2001**, *42*, 5485–5488.

(33) Hisaki, I.; Eda, T.; Sonoda, M.; Tobe, Y. *Chem. Lett.* **2004**, *33*, 620–621.

(34) Luu, T.; Elliott, E.; Slepkov, A. D.; Eisler, S.; McDonald, R.; Hegmann, F. A.; Tykwinski, R. R. *Org. Lett.* **2005**, *7*, 51–54.

(35) a) Slepkov, A. D.; Eisler, S.; Luu, T.; Elliott, E.; Tykwinski, R. R.; Hegmann, F. A. *Proc. SPIE Int. Soc. Opt. Eng.* **2005**, *4*, 5935; b) Slepkov, A. D.; Hegmann, F. A.; Eisler, S.; Elliott, E.; Tykwinski, R. R. *J. Chem. Phys.* **2004**, *120*, 5807–6810.

(36) Chalifoux, W. A.; Tykwinski, R. R. *Chemical Record* **2006**, *6*, 169–182.

(37) Tobe, Y.; Wakabayashi, T. *Acetylene Chemistry: Chemistry, Biology, and Material Science*; Diederich, F.; Stang, P. J.; Tykwinski, R. R., Eds.; John–VCH: Weiheim, 2005.

(38) Gibtner, T.; Hampel, F.; Gisselbrecht, J. P.; Hirsch, A. *Chem. Eur. J.* **2002**, *8*, 408–432.

(39) Burli, R.; Vasella, A. *Angew. Chem., Int. Ed. Engl.* **1997**, *36*, 1852–1853.

(40) Wan, W. B.; Haley, M. M. *J. Org. Chem.* **2001**, *66*, 3893–3901.

(41) Spitler, E. L.; Johnson, C. A.; Haley, M. M. *Chem. Rev.* **2006**, *106*, 5344–5386.

(42) Heuft, M. A.; Collins, S. K.; Fallis, A. G. *Org. Lett.* **2003**, *5*, 1911–1914.

(43) Boese, R.; Matzger, A. J.; Vollhardt, K. P. C. *J. Am. Chem. Soc.* **1997**, *119*, 2052–2053.

(44) Gholami, M.; Tykwinski, R. R. *Chem. Rev.* **2006**, *106*, 4997–5027.

(45) Mitzel, F.; Boudon, C.; Gisselbrecht, J. P.; Seiler, P.; Gross, M.; Diederich, F. *Helv. Chim. Acta* **2004**, *87*, 1130–1157.

(46) Borissov, D.; Ziegler, A.; Höger, S.; Freyland, W. *Langmuir* **2004**, *20*, 2781–2784.

(47) Tobe, Y.; Nagano, A.; Kawabata, K.; Sonoda, M.; Naemura, K. *Org. Lett.* **2000**, *2*, 3265–3268.

Chapter 2. Synthesis and Stability of a Homologous Series of Triynol Natural Products and Their Analogues

2.1 Introduction

Natural products bearing a conjugated polyyne framework have been isolated from plants, fungi, bacteria, sponges, and even an insect.[1–6] In fact, they are surprisingly common natural products, despite the fact that these compounds can demonstrate significant instability as a result of their often fragile, *sp*–hybridized carbon cores. When sufficient quantities of the natural product are available, studies of biological and physiological properties have been conducted and they have revealed a broad scope of activities such as larvicidal,[7] antimicrobial,[8,9] antiviral (HIV),[10] and cytotoxicity toward a range of cell lines.[11] Due to their inherently unstable nature, polyynes are often difficult to isolate from natural sources, particularly in the case of longer derivatives such as triynes, tetraynes, and pentaynes.[12] For example, polyynols **201a,b**, **202** and **203** were isolated from natural sources (Figure 2.1). Triynene derivatives **201a,b** were isolated and identified as allergens from *Chrysanthemum leucanthemum* L. by Ohta and coworkers.[13] It is known that *Chrysanthemum leucanthemum* has caused allergic contact dermatitis to children. These compounds were very unstable and turned into an insoluble grayish solid.[13] Diol **202** was extracted from *Bidens campylotheca*, which is traditional Hawaiian folk medicine for the treatment of throat and stomach disorders and asthma.[14] Terminal tetrayne **203** was extracted from the liquid culture of *Pseudomonas caryophylli*. This bacterium exhibited potent antibiotic activity against a pathogen of halo blight of the kidney bean, *Pseudomonas syringae*. Compound **203** was extremely unstable in a concentrated or coagulated state.[15]

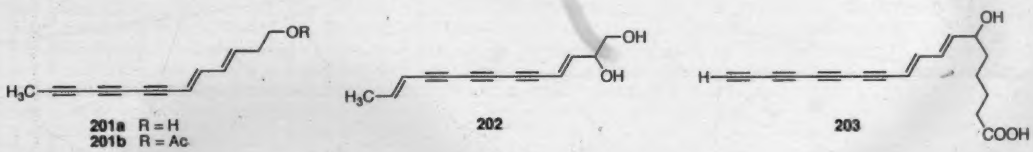

201a R = H
201b R = Ac

202

203

Figure 2.1 Naturally occurring polyynols **201a,b, 202** and **203**

Over the past 50 years, there have been a number of strategies used for the synthesis of polyyne–based natural products. The most common method by far is the copper–catalyzed oxidative coupling procedure developed by Cadiot and Chodkiewicz,[16] as well as the palladium–catalyzed variants of the original protocol that have been subsequently developed.[17–19] There are, however, a number of challenges associated with this strategy, including the significant instability of one or both of the precursors and the formation of troublesome byproducts. The byproduct within the reaction results from the competition of oxidative homocoupling reactions. For example, compound **204** was synthesized by Prévost and coworkers, using the cross–coupling of diyne **205** with bromoalkyne **206** (Scheme 2.1).[16] However, the requisite starting material **205**, and others like it, are often difficult to obtain in a pure form and in a substantial yield. Because of these challenges, a carbenoid Fritsch–Buttenberg–Wiechell (FBW) rearrangement has been developed as an alternative method for the formation of biologically interesting polyynes.[20–25]

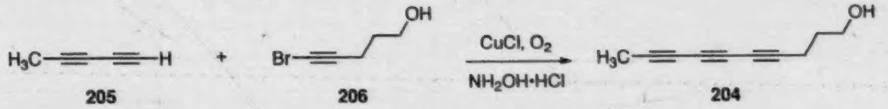

Scheme 2.1 Formation of compound **204** via Cadiot–Chodkiewicz coupling

In the development of new polyynes and their derivatives, we explored the synthesis and chemical stability of conjugated triynols as a function of structure. Using the FBW rearrangement as a key step, a homologous series of polyynes with a terminal proton, methyl, or phenyl moiety, **207a–c**, **208a,b**, **204**, and **209a–c**, respectively, have been synthesized (Figure 2.2). The stability of these compounds as a function of the terminal group and the length of the methylene tether to the alcohol moiety has been explored.

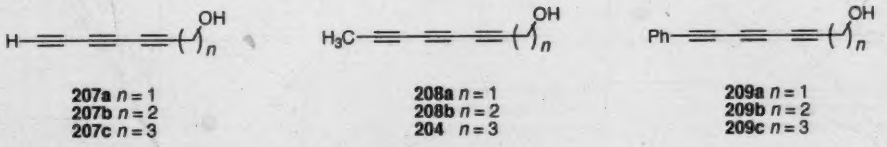

Figure 2.2 Targeted triynols **207a–c, 208a,b, 204**, and **209a–c**

The original FBW rearrangement for the formation of tolan was involved in the generation of the carbenoid species; however, the reaction conditions were strongly basic and the temperature was very high (180–200 °C).[26–28] Such harsh conditions are not compatible with many functional groups. Tykwinski and coworkers reported a modified FBW rearrangement suits many functional groups by using mild conditions (BuLi, –78 °C). Dibromoolefin **210** can undergo lithium–bromide exchange to form either a carbenoid **211** following Path A or the carbenoid intermediate can quickly proceed by α elimination to form a carbene **212** following Path B. Both species **211** and **212** are very reactive and can undergo the 1,2–migration to afford acetylene **213**.[19,21,29]

The original FBW rearrangement for the formation of tolans involved the generation of a carbenoid species. The reaction conditions were, however, strongly basic, and the temperature required was very high (180–200 °C).[26–28] Such harsh conditions were not compatible with many functional groups. Tykwinski and coworkers have reported a modified FBW rearrangement that tolerates many functional groups by using milder conditions (BuLi, –78 °C). Under this protocol, dibromoolefin **210** can undergo lithium–bromide exchange to form either a carbenoid intermediate **211** following Path A or a free carbene intermediate **212** following Path B. Both species **211** and **212** are very reactive and can undergo the 1,2–migration to afford acetylene **213**. To date, most experimental evidence supports formation of only the carbenoid intermediate **211**, although a free alkylidene carbene intermediate **212** can still not be ruled out completely.[19,21,29]

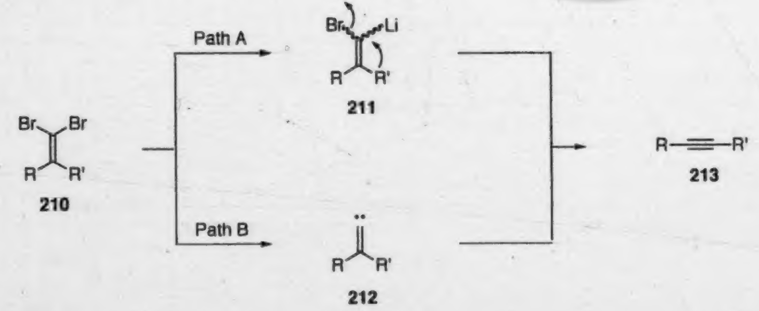

Figure 2.3 Possible reaction pathways of carbenoid **211** or alkylidene carbene **212** rearrangement

2.2 Results and Discussion

The initial route in exploring triyne formation employed the *t*–BuMe$_2$Si–protected alcohol **214** (Scheme 2.2), the synthesis of which has been reported by Diederich.[30]

Reaction of lithiated trimethylsilylacetylene with **214** in THF gave the alcohol **215** in 69% yield, which was then readily oxidized to the ketone with MnO_2. The next step in the synthesis, however, proved problematic. Attempts to convert the ketone to the dibromoolefin **216** were of limited success. Typical Corey–Fuchs dibromoolefination conditions[31] were met primarily with frustration when applied to the ketone. In addition, modifications of this standard protocol barely improved the outcome of these reactions. Yields were low, with a maximum of 17% for compound **216**. Numerous byproducts were observed in all cases. For example, propargyl bromide derivative **217** resulted from the desilylation and subsequent bromination of the alcohol, as previously reported by Mattes and Benezra.[32] Its kinetic instability[33] further complicated the formation and use of compound **216**. The pure compound decomposed over a period of days, even when stored at low temperature. Analysis of the decomposed material suggested that the Me_3Si group of compound **216** was slowly removed when stored either as a neat oil or in solution of, for example, hexanes.

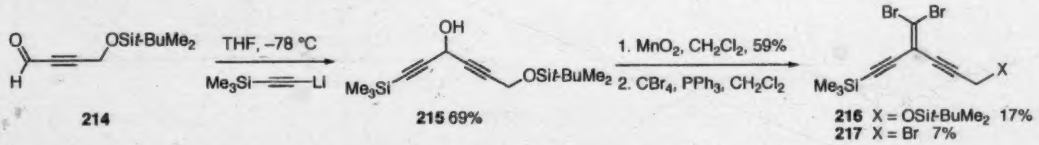

Scheme 2.2 Attempted synthesis of dibromoolefin **216**

Similar results were achieved when a *i*-Pr_3Si protecting group was used in place of the Me_3Si group to prevent the premature desilylation (Scheme 2.3). Addition of *i*-$Pr_3SiC{\equiv}CLi$ to aldehyde **214** gave **218** in good yield, following workup and column chromatography. Using $BaMnO_4$, alcohol **218** was cleanly oxidized to ketone **219** in 91% yield. Ultimately, it was demonstrated that the dibromoolefination reported by McIntosh *et al.* gave the best results in the formation of **220** using one equivalent of Et_3N.[34] Following this protocol, reducing the reaction time to 3 min, and workup with aqueous $NaHCO_3$ gave **220** in yields as high as 77%. This reaction was, however, remarkably irreproducible, and lower yields were more common than higher yields due to the loss of the *t*–$BuMe_2Si$ protecting group during the reaction. Nonetheless, pure **220** was considerably more stable under ambient conditions than its analogue **216**. With **220**, the conversion to triyne **221** was obtained via reaction with BuLi at –78 °C. It is worth noting that while the isolated yield of **221** was reasonable, in some cases up to 61%, its formation was always accompanied by compound **222**, a byproduct formed by reaction of the intermediate carbenoid of the FBW reaction with water in the medium.[21] Frustratingly all procedures that were previously effective in preventing this side reaction were found to be unsuccessful in this case. The similar retention factors of **221** and **222** on common chromatographic supports made separation difficult and time–consuming. Thus, a third protection scheme was explored.

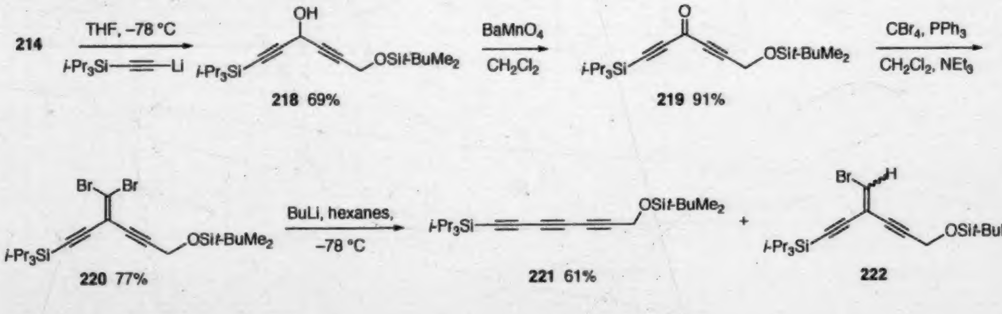
214
THF, –78 °C
i-Pr3Si—≡—Li
OH
i-Pr3Si
OSit-BuMe2
218 69%
BaMnO4
CH2Cl2
O
i-Pr3Si
OSit-BuMe2
219 91%
CBr4, PPh3
CH2Cl2, NEt3
Br
Br
i-Pr3Si
OSit-BuMe2
220 77%
BuLi, hexanes,
–78 °C
i-Pr3Si
OSit-BuMe2
221 61%
+
Br
H
i-Pr3Si
OSit-BuMe2
222

Scheme 2.3 Synthesis of triyne **221** and byproduct **222**

As a result of its robustness as a protecting group, the *t*-$BuPh_2Si$ group was subsequently used in an attempt to solve the problems encountered with the reactivity of the *t*-$BuMe_2Si$ ether. Aldehydes **223a**[35] and **223b**[36] were the target precursors of the desired triynols and could be achieved by two different methods (Scheme 2.4). Starting with the known precursor **224a** or **224b**, deprotonation with BuLi in THF generated the lithium acetylide, which was then reacted with DMF to produce either **223a** or **223b** in moderate yield. Unfortunately, this transformation was often accompanied by a side reaction that resulted from the addition of dimethyl amine to the *α,β*–unsaturated product. To avoid the formation of this byproduct, an alternative route was explored. Acetylene **224a** or **224b** was deprotonated with BuLi at –78 °C, followed by the addition of excess paraformaldehyde to produce alcohols **225a,b** in yields of 76% and 77%, respectively, as reported by Baltas and coworkers.[37] The alcohols were purified by column chromatography and oxidized with $BaMnO_4$ to give aldehydes **223a,b** in good yield. The advantage of the latter route was that the desired products were purified more easily than by the former route, and the overall yield was also slightly higher.

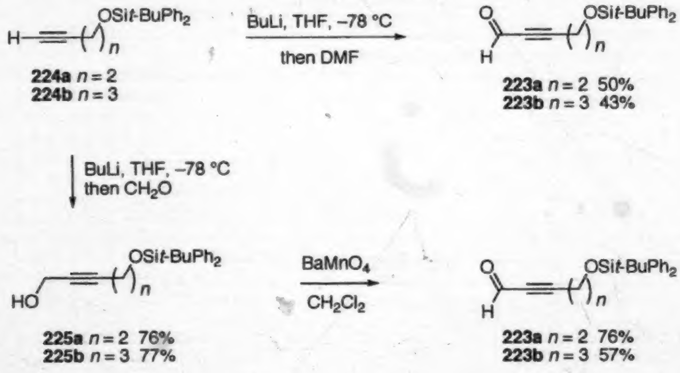
OSi*t*-BuPh$_2$
H
n
224a *n* = 2
224b *n* = 3
BuLi, THF, –78 °C
then DMF
O
H
OSi*t*-BuPh$_2$
n
223a *n* = 2 50%
223b *n* = 3 43%
BuLi, THF, –78 °C
then CH$_2$O
HO
OSi*t*-BuPh$_2$
n
225a *n* = 2 76%
225b *n* = 3 77%
BaMnO$_4$
CH$_2$Cl$_2$
O
H
OSi*t*-BuPh$_2$
n
223a *n* = 2 76%
223b *n* = 3 57%

Scheme 2.4 Formation of aldehydes **223a** and **223b** by two different methods

Starting from aldehydes **223**,[23] **223a**, and **223b**, terminal triynol natural products **207a–c** were synthesized (Scheme 2.5). The reaction of i-$Pr_3SiC{\equiv}CLi$ with the appropriate aldehyde at low temperature, followed by workup and column chromatography, afforded **226a–c** in excellent yield. Oxidation of the alcohols with

$BaMnO_4$ gave the corresponding ketones, which were converted to dibromoolefination adducts **227a–c** in reasonable yield under standard conditions. The reaction was devoid of the troublesome byproducts. The use of Et_3N, which had improved the yield of **220**, had no effect on the yield of **227a**. Other attempts to optimize the formation of **227a** included the use of zinc as the reductant in place of PPh_3.[38] Monitoring of the reaction using ^1H NMR spectroscopy, however, showed less than 10% conversion in this reaction, based on integration of the propargylic methylene protons. The conversion of the dibromoolefins to triynes **228a–c** was effected via the FBW reaction with BuLi in hexanes at –78 °C.

Exhaustive desilylation of triynes **228a–c** to give terminal triynes **207a–c** was more challenging than anticipated. The desilylation by TBAF gave the terminal triyne **207a**. While this product could be identified and characterized in solution via IR spectroscopy, it was insufficiently stable to be isolated.

Desilylation of the longer derivative, triyne **228c**, was slightly more successful. Using typical desilylation conditions, **228c** was dissolved in wet THF at 0 °C and TBAF was slowly added. The progress of desilylation was monitored by TLC. Addition of Et_2O and aqueous NH_4Cl, however, resulted in an intractable and insoluble black precipitate, suggesting that the deprotected polyynol **207c** decomposed during workup. All attempts to spectroscopically determine the structure of the decomposition product(s) have been unsuccessful. TLC analysis showed that the desilylation was quite efficient, and after quenching and workup, crude **207c** was purified on neutral alumina. Upon concentration, however, decomposition once again occurred and identification was limited to IR and crude ^1H NMR spectroscopic analysis; no yield could be determined. The IR data for crude **207c** were consistent with those reported by Bohlmann,[39] who synthesized **207c** via the Cadiot–Chodkiewicz coupling of butadiyne and 5–bromo–4–pentaynol (no yield was reported).

Chemoselective desilylation of **228b** and **228c** (t-BuPh$_2$Si versus i-Pr$_3$Si) was also attempted but was not successful. For example, the slow addition of TBAF (0.5 equiv) to a solution of **228b** in THF at either 0 or –10 °C revealed that indiscriminate desilylation took place at both silyl groups. The use of the desilylation reagent KF was also explored[40] and gave results similar to those obtained with TBAF. The formation of **207b** via desilylation of **228b** with either TBAF or KF was also attempted under a number of conditions, and the results were similar to those obtained with **207c**. Product **207b** was insufficiently stable to be concentrated to dryness, although ^{1}H NMR and IR spectroscopy could be used to confirm its formation. These results were similar to those of Tokimoto *et al.*,[41] who extracted **207b** from the neutral culture of *Lentinus edodes* after the attack of *Trichoderma polysporum*. They reported that the triynol could be purified via preparative TLC on silica.

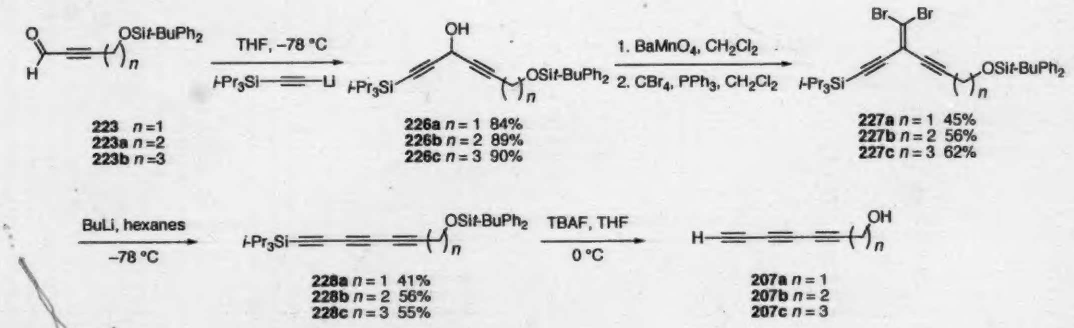
OSit-BuPh2
H
n
THF, –78 °C
i-Pr3Si—≡—Li
OH
i-Pr3Si
OSit-BuPh2
n
1. BaMnO4, CH2Cl2
2. CBr4, PPh3, CH2Cl2
Br
Br
i-Pr3Si
OSit-BuPh2
n
223 n=1
223a n=2
223b n=3
226a n = 1 84%
226b n = 2 89%
226c n = 3 90%
227a n = 1 45%
227b n = 2 56%
227c n = 3 62%
BuLi, hexanes
–78 °C
i-Pr3Si
OSit-BuPh2
n
TBAF, THF
0 °C
H
OH
n
228a n = 1 41%
228b n = 2 56%
228c n = 3 55%
207a n = 1
207b n = 2
207c n = 3

Scheme 2.5 Formation of terminal alcohols **207a–c**

The observed instability of **207b** and **207c** and the conditions of purification and isolation mirrors that of the shorter homologous natural product **207a**, which has been identified and isolated from *Ramaria flava* by Jones and coworkers.[42] Thus, with only a terminal proton, it is concluded that triynols are kinetically unstable species regardless of the number of methylene groups linking the alcohol moiety.

Numerous methyl terminated polyynes have been identified as naturally occurring species (Scheme 2.6).[1] Compound **208b** was isolated from the fungus *Collybia peronated*, first by Higham[43] and later from cultures of *Lentinus edodes* by Tokimoto.[41] Triynol **204** has been extracted from the culture fluids of *Psathyrella scobinacea* by Taha[44] and from *Tridax trilobata* by Bohlmann.[45] The shortest homologue **208a** has been obtained from neutral fractions of cultures of the sheathed wood tuft *Kuehneromyces mutabilis,* and also in *Psilocybe merdaria* and *Ramaria flava.*[42] Toward the formation of **208a,b,** and **204**, the reaction of aldehyde **223**, **223a**, or **223b** with MeC≡CLi in THF produced alcohols **229a–c** in good yields (Scheme 2.6). These intermediate products were oxidized with $BaMnO_4$ to produce the corresponding ketones. Dibromoolefination of the ketones provided the precursors **230a–c**. This two–step process provided rather modest yields, amounting to an average of ca. 60% yield per step. The formation of **230a** was resulted in a lower yield. FBW rearrangement yielded the triynol frameworks of **231a–c**. The reaction these triynes with TBAF in THF produced the free alcohols **208a,b, 204**. Triynols **208a** and **208b** were obtained as colorless crystalline solids that turned pink when exposed to light at room temperature. By contrast, compound **204** remained as a white, crystalline solid under ambient conditions, with a melting point of 68 °C, showing that the stability of the methyl terminated triynols improves to some extent as a function of the number of methylene units.

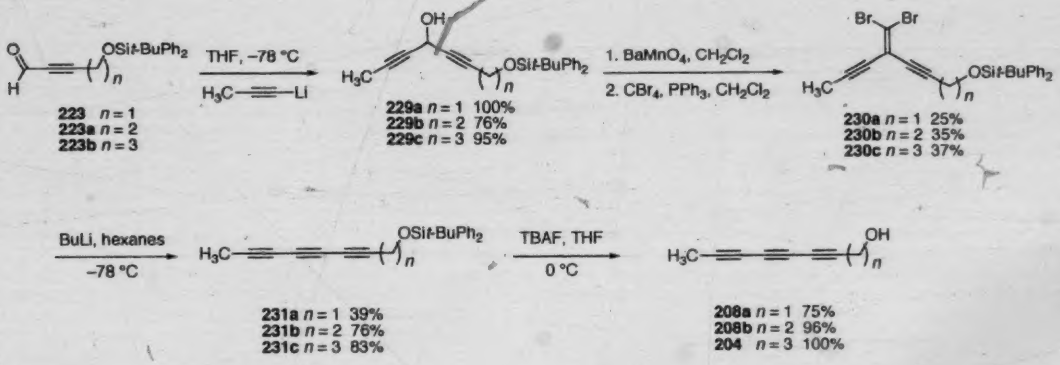
OSit-BuPh$_2$
H
n
223 $n = 1$
223a $n = 2$
223b $n = 3$
THF, –78 °C
H$_3$C—≡—Li
OH
H$_3$C
OSit-BuPh$_2$
229a $n = 1$ 100%
229b $n = 2$ 76%
229c $n = 3$ 95%
1. BaMnO$_4$, CH$_2$Cl$_2$
2. CBr$_4$, PPh$_3$, CH$_2$Cl$_2$
Br
Br
H$_3$C
OSit-BuPh$_2$
230a $n = 1$ 25%
230b $n = 2$ 35%
230c $n = 3$ 37%
BuLi, hexanes
–78 °C
H$_3$C
OSit-BuPh$_2$
231a $n = 1$ 39%
231b $n = 2$ 76%
231c $n = 3$ 83%
TBAF, THF
0 °C
H$_3$C
OH
208a $n = 1$ 75%
208b $n = 2$ 96%
204 $n = 3$ 100%

Scheme 2.6 Formation of methyl endcapped alcohols **208a,b, and 204**

The effect of replacing a terminal proton of the triyne with a phenyl group was then examined through the formation of triynols **209a–c** (Scheme 2.7), which form a homologous series of compounds based on natural product **209a**, which was isolated from a species of *Bidens*.[46,47] Thus, alcohols **232a–c** were formed in good yield from the reaction of lithium phenylacetylide with the appropriate aldehyde **223** or **223a,b**. The oxidation of the alcohols with BaMnO$_4$ to crude ketones, followed by the dibromoolefination resulted in **233a–c** in excellent yield. Although the ketones were reasonably stable intermediates that could be isolated without problem, higher yields were obtained when the crude products were subjected directly to the dibromoolefination step. FBW rearrangement of each dibromoolefin with BuLi provided triynes **234a–c** in excellent yield. The desired triynols **209a–c** were cleanly formed from **234a–c**, respectively, via desilylation with TBAF. In contrast to terminal triynes **207a–c**, the phenyl derivatives **209a–c** are kinetically stable to isolation under ambient conditions. Furthermore, the isolated oils can be stored indefinitely under refrigeration. It is quite clear that the phenyl end–capping groups have a stabilizing effect on the triynols, irrespective of the length of the methylene linker.

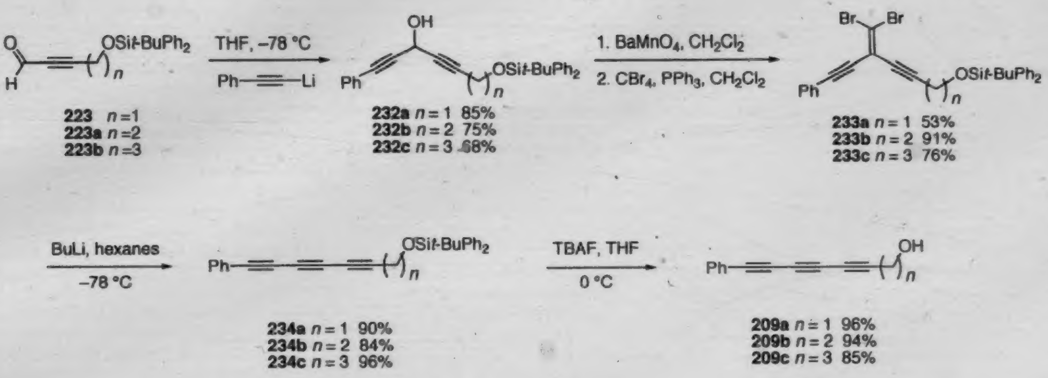

OSit-BuPh2
THF, –78 °C
Ph—≡—Li
OH
1. BaMnO4, CH2Cl2
2. CBr4, PPh3, CH2Cl2
Br
Br
223 n = 1
223a n = 2
223b n = 3
232a n = 1 85%
232b n = 2 75%
232c n = 3 68%
233a n = 1 53%
233b n = 2 91%
233c n = 3 76%
BuLi, hexanes
–78 °C
TBAF, THF
0 °C
234a n = 1 90%
234b n = 2 84%
234c n = 3 96%
209a n = 1 96%
209b n = 2 94%
209c n = 3 85%

Scheme 2.7 Formation of phenyl endcapped alcohols **209a–c**

2.3 Further Elaboration

Further elaboration of compound **209a** at oxygen through the formation of esters and glycosides was attempted (Figure 2.4). Triyne acetate **235a** was synthesized from triynol **209a** using Ac_2O, DMAP, and Et_3N. Compound **235a** was first isolated by Bohlmann and coworkers from several species of the genus *Bidens*, including *B. pilosus* and *B. leucanthus*,[46,47] and later in trace amount by Lam and coworkers from the flowering perennial *Dahlia pinnata*.[48] Furthermore, a talented graduate student under the tutelage of Professor Todd Lowary, Mr. Wei Shi, coupled triynol **209a** with different sugar moieties to afford a series of polyyne glycosides **235b–d**.[23]

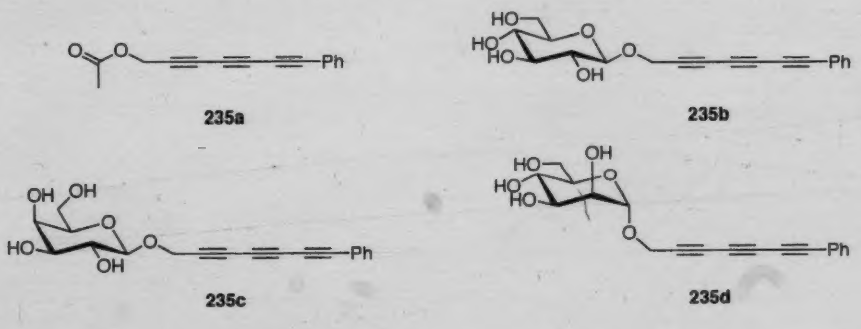

235a

235b

235c

235d

Figure 2.4 Acetylated and glycosylated triynols **235a–d**

2.4 Conclusions

In conclusion, the synthesis of a series of conjugated triynols (**207a–c, 208a,b, 204, 209a–c**) has been accomplished. It has been determined that the kinetic stability of these compounds can be generalized by three factors: (a) terminal triynols (**207a–c**) are unstable regardless of the number of methylene groups, (b) replacement of the terminal acetylenic proton with a methyl (**208a,b, 204**) or phenyl group (**209a–c**) affords increasingly more stable products, and (c) within the series of methyl–endcapped derivatives, more methylene groups is better.

2.5 References and Notes

(1) Shi Shun, A. L. K.; Tykwinski, R. R. *Angew. Chem., Int. Ed.* **2006**, *45*, 1034–1057.

(2) *Chemistry and Biology of Naturally Occurring Acetylenes and Related Compounds (NOARC)*; Elsevier: New York, 1988.

(3) Bohlmann, F.; Burkhardt, T.; Zdero, C. *Naturally Occurring Acetylenes*; Academic Press: New York, 1973.

(4) Jones, E. R.; Thaller, V. *The Chemistry of the Carbon–Carbon Triple Bond*; Patai, S., Ed.; John Wiley & Sons: New York, 1978; Vol. Part 2.

(5) Blunt, J. W.; Copp, B. R.; Munro, M. H. G.; Northcote, P. T.; Prinsep, M. R. *Nat. Prod. Rep.* **2003**, *20*, 1–48.

(6) Faulkner, D. J. *Nat. Prod. Rep.* **2001**, *18*, 1–49.

(7) Arnason, J. T.; Philogene, B. J. R.; Berg, C.; Maceachern, A.; Kaminski, J.; Leitch, L. C.; Morand, P.; Lam, J. *Phytochemistry* **1986**, *25*, 1609–1611.

(8) Kobaisy, M.; Abramowski, Z.; Lermer, L.; Saxena, G.; Hancock, R. E. W.; Towers, G. H. N.; Doxsee, D.; Stokes, R. W. *J. Nat. Prod.* **1997**, *60*, 1210–1213.

(9) Fusetani, N.; Toyoda, T.; Asai, N.; Matsunaga, S.; Maruyama, T. *J. Nat. Prod.* **1996**, *59*, 796–797.

(10) Rashid, M. A.; Gustafson, K. R.; Cardellina, J. H.; Boyd, M. R. *Nat. Prod. Lett.* **2001**, *15*, 21–26.

(11) Ito, A.; Cui, B. L.; Chavez, D.; Chai, H. B.; Shin, Y. G.; Kawanishi, K.; Kardono, L. B. S.; Riswan, S.; Farnsworth, N. R.; Cordell, G. A.; Pezzuto, J. M.; Kinghorn, A. D. *J. Nat. Prod.* **2001**, *64*, 246–248.

(12) Mukai, C.; Miyakoshi, N.; Hanaoka, M. *J. Org. Chem.* **2001**, *66*, 5875–5880.

(13) Shibata, H.; Deguchi, S.; Nijyo, S.; Ohta, K. *Agric. Biol. Chem.* **1989**, *53*, 2293–2295.

(14) Redl, K.; Breu, W.; Davis, B.; Bauer, R. *Planta Med.* **1994**, *60*, 58–62.

(15) Kusumi, T.; Ohtani, I.; Nishiyama, K.; Kakisawa, H. *Tetrahedron Lett.* **1987**, *28*, 3981–3984.

(16) Prévost, S.; Cadiot, P.; Willemart, A.; Chodkiewicz, W.; Meier, J. *Bull. Soc. Chim. Fr.* **1961**, 2171–2175.

(17) Siemsen, P.; Livingston, R. C.; Diederich, F. *Angew. Chem., Int. Ed.* **2000**, *39*, 2632–2657.

(18) Negishi, E. *Handbook of Organopalladium Chemistry for Organic Synthesis*; Negishi, E., Ed.; Wiley–VCH: New York, 2002.

(19) *Acetylene Chemistry – Chemistry, Biology, and Materials Science*; Diederich, F.; Stang, P. J.; Tykwinski, R. R., Eds.; Wiley–VCH: Weiheim, 2005.

(20) Shi Shun, A. L. K.; Tykwinski, R. R. *J. Org. Chem.* **2003**, *68*, 6810–6813.

(21) Eisler, S.; Chahal, N.; McDonald, R.; Tykwinski, R. R. *Chem. Eur. J.* **2003**, *9*, 2542–2550.

(22) Shi Shun, A. L. K.; Chernick, E. T.; Eisler, S.; Tykwinski, R. R. *J. Org. Chem.* **2003**, *68*, 1339–1347.

(23) Luu, T.; Shi, W.; Lowary, T. L.; Tykwinski, R. R. *Synthesis* **2005**, 3167–3178.

(24) Morisaki, Y.; Luu, T.; Tykwinski, R. R. *Org. Lett.* **2006**, *8*, 689–692.

(25) Luu, T.; Tykwinski, R. R. *J. Org. Chem.* **2006**, *71*, 8982–8985.

(26) Fritsch, P. *Liebigs Ann.* **1894**, *279*, 319–323.

(27) Buttenberg, W. P. *Liebigs Ann.* **1894**, *279*, 324–337.

(28) Wiechell, H. *Liebigs Ann.* **1894**, *279*, 337–344.

(29) Chalifoux, W. A.; Tykwinski, R. R. *Chemical Record* **2006**, *6*, 169–182.

(30) Livingston, R.; Cox, L. R.; Odermatt, S.; Diederich, F. O. *Helv. Chim. Acta* **2002**, *85*, 3052–3077.

(31) Corey, E. J.; Fuchs, P. L. *Tetrahedron Lett.* **1972**, 3769–3772.

(32) Mattes, H.; Benezra, C. *Tetrahedron Lett.* **1987**, *28*, 1697–1698.

(33) "Kinetic stability, in contrast to thermodynamic stability, is circumstantial as it is a property of the system and its immediate environment. Kinetic stability depends

not just on the system itself, but on factors extraneous to the system. For this reason kinetic stability cannot be classified as a state function (in contrast to thermodynamic stability)", see: Pross, A. *Pure Appl. Chem.* **2005**, *77*, 1905–1921.

(34) McIntosh, M. C.; Weinreb, S. M. *J. Org. Chem.* **1993**, *58*, 4823–4832.

(35) Dineen, T. A.; Roush, W. R. *Org. Lett.* **2003**, *5*, 4725–4728.

(36) Baldwin, J. E.; Romeril, S. P.; Lee, V.; Claridge, T. D. W. *Org. Lett.* **2001**, *3*, 1145–1148.

(37) Nacro, K.; Baltas, M.; Gorrichon, L. *Tetrahedron* **1999**, *55*, 14013–14030.

(38) Anthony, J.; Boldi, A. M.; Rubin, Y.; Hobi, M.; Gramlich, V.; Knobler, C. B.; Seiler, P.; Diederich, F. *Helv. Chim. Acta* **1995**, *78*, 13–45.

(39) Bohlmann, F.; Herbst, P.; Gleinig, H. *Chem. Ber.* **1961**, *94*, 948–957.

(40) Stang, P. J.; Ladika, M. *Synthesis* **1981**, 29–30.

(41) Tokimoto, K.; Fujita, T.; Takeda, Y.; Takaishi, Y. *Proc. Jpn. Acad.* **1987**, *63*, 277–280.

(42) Hearn, M. T. W.; Jones, E. R. H.; Pellatt, M. G.; Thaller, V.; Turner, J. L. *J. Chem. Soc., Perkin Trans. 1* **1973**, 2785–2788.

(43) Higham, C. A.; Jones, E. R. H.; Keeping, J. W.; Thaller, V. *J. Chem. Soc., Perkin Trans. 1* **1974**, 1991–1994.

(44) Taha, A. A. *Phytochemistry* **2000**, *55*, 921–926.

(45) Bohlmann, F.; Zdero, C.; Weickgen. G *J. Liebigs Ann. Chem.* **1970**, *739*, 135–143.

(46) Bohlmann, F.; Arndt, C.; Kleine, K.–M.; Wotschokowsky, M. *Chem. Ber.* **1965**, *98*, 1228–1232.

(47) Bohlmann, F.; Bornowski, H.; Kleine, K.–M. *Chem. Ber.* **1964**, *97*, 2135–2138.

(48) Bendixen, O.; Lam, J.; Kaufmann, F. *Phytochemistry* **1969**, *8*, 1021–1023.

Chapter 3. 1,2,3–Triazole Formation: Trapping Terminal Di–, Tri–, and Tetraynes with Benzyl Azide

3.1 Introduction

Natural products containing conjugated polyynes have been isolated from a variety of species such as fungi, bacteria, plants, sponges, and an insect.[1–7] Some of the naturally occurring polyynes have been reported as larvicidal,[8] antimicrobial,[9,10] and antiviral agents.[11] These conjugated polyynes are often too unstable to be isolated, particularly terminal polyynes. Terminal tri–, tetra–, and pentaynes, as shown in Figure 3.1, have been obtained from different species, some of which have exhibited potent biological activity. For example, triynol **301** has been isolated from the fungus *Ramaria flava* by Jones and coworkers.[12] Compound **302** is believed to be a product of hydrolysis of the fungal natural product marasin, isolated from *Aleurodiscus roseus* by Lowe and coworkers.[13] Tokimoto *et al.* also extracted this compound from the neutral culture of *Lentinus edodes* after the attack of *Trichoderma polysporum*.[14] Compound **303** also comes from the hydrolysis of the fungal natural product *Aleurodiscus roseus*.[13] Compounds **304a–c** were isolated from the culture medium of *Coprinus quadrifidus* by Jones and Stephenson.[15] Tetraynes **305a–c** have been obtained from a plant pathogen *Pseudomonas caryophylli*, which causes bacterial wilt of carnations and exhibits potent antibiotic activity against a pathogen of the halo blight of the kidney bean, *Pseudomonas* *syringae* and *P. phaseolicola.*[16] Pentayne **306** was isolated from several Peruvian plants of the *Leuceri* species and reported by Bohlmann and coworkers.[17] Many terminal polyynes, however, have likely not been obtained and fully characterized due to the kinetic instability[18] of such compounds, which may cause them to decompose during the isolation process or in neat form.[19]

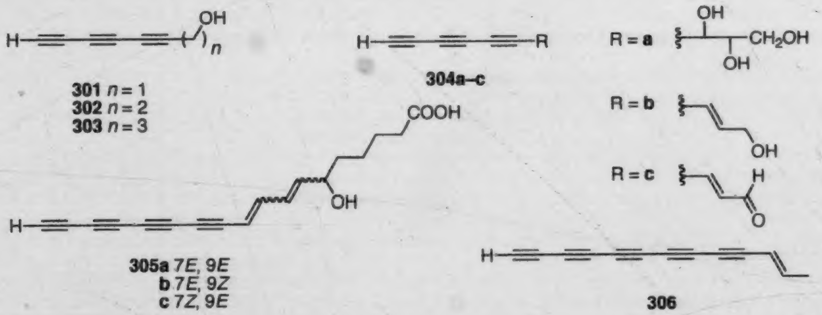

Figure 3.1 Naturally occurring tri–, tetra–, and pentaynes

A 1,3–dipolar cycloaddition can be used to convert a terminal alkyne into a five–member ring (e.g., 1,2,3–triazole).[20,21] 1,2,3–Triazoles exhibit potent biological activity, and are both anti–HIV[22] and antibacterial[23] agents. Over the years, many approaches have been reported for the formation of 1,2,3–triazoles via the reaction of a terminal alkyne with an azide, without a catalyst[24,25] and in the presence of a catalyst.[26–28] Unfortunately, the thermal and uncatalyzed so–called Huisgen reaction often produces mixtures of 1,4– and 1,5–substituted triazole isomers. The catalytic reaction using Cu(I/II) produces only the 1,4–substituted isomer, but can be complicated by the homocoupling that leads to byproduct formation.[26] Sharpless[29] and Meldal[30] reported independently the formation of only the 1,4–regioisomer using CuI or $CuSO_4 \cdot 5H_2O$ catalysis at room temperature.

We have modified the procedure developed by both Sharpless and Meldal to suit the reaction with unstable terminal polyynes.[31] The goal of this research has been to determine answers to the following questions:

a) What is the mechanism of the reaction?[26,32]

b) Would the regioselectivity of the reaction produce only 1,4–substituted adducts?[33]

c) Would the modified conditions be suitable for trapping di–, tri–, and tetraynes?[27,28,34,35]

d) Would multiple additions occur from the reaction of terminal polyynes with benzyl azide?[33]

e) Would the solvent system (DMF : H_2O) be important for the reaction?

3.2 Results and Discussion

3.2.1 Mechanistic Study

Sharpless named the reaction of trapping terminal alkynes with azides to form 1,4–trizoles as "Click" chemistry. The advantages of the reaction are that it can be conducted at room temperature, under an O_2 atmosphere, it is solvent independent, produces excellent yields, and purification can be achieved without column chromatography. It should be noted that the results from Sharpless' studies came from the reaction of azides with terminal monoynes.[29,32,34,36]

Sharpless and coworkers have proposed a catalytic cycle for the formation of 1,4–substituted adduct **307** as shown in Scheme 3.1.[29,37] The formation of 1,5–substituted adduct **308** was also included in the modified cycle based on Sharpless' original proposal.

Cu(I) is the main catalyst for a "Click" reaction; however, Cu(I) is not stable in aqueous media. It can disproportionate to Cu(0) and Cu(II). Thus, Cu(II) sulfate is used to generate Cu(I) *in situ* in the presence of the reductant ascorbic acid, and it is believed that this protocol is more effective. Cu(I) is inserted into terminal diyne **309** to generate Cu(I) acetylide **310**. Theoretical studies have shown that copper coordination with a terminal alkyne lowers the pK_a of the terminal alkyne by up to 9.8 pH units, allowing for acetylide formation.[37] The lone pair of the azide nitrogen atom coordinate to Cu(I) to form **311**. Compound **311** is likely at equilibrium with compound **312** where the lone pair of the terminal nitrogen coordinates to Cu(I). This intermediate **312** can potentially undergo a cyclization to form a 1,5–substituted adduct **308**. Formation of this 1,5–substituted adduct is not favorable due steric interactions of the benzyl substituent of the azide,[30] disfavoring the formation of **308**.

The intermediate **311** can undergo an interesting stepwise cycloaddition to form a six–membered copper–containing intermediate **313**. The nitrogen atom, initially coordinated to the copper, migrates to the allene carbon to form a five–membered copper–containing intermediate **314**. Protonation of this triazole–copper derivative followed by dissociation of the 1,4–substituted adduct **307** regenerates Cu(I) catalyst.

Conversely, it is possible that polyynes might also undergo a concerted [2+3] cycloaddition reaction with the BnN_3, as has been previously demonstrated in reaction conducted without Cu(I). It should be noted, however, that DFT calculations have shown that a concerted [2+3] mechanism is strongly disfavored by 12–15 kcal compared to this stepwise mechanism.[38]

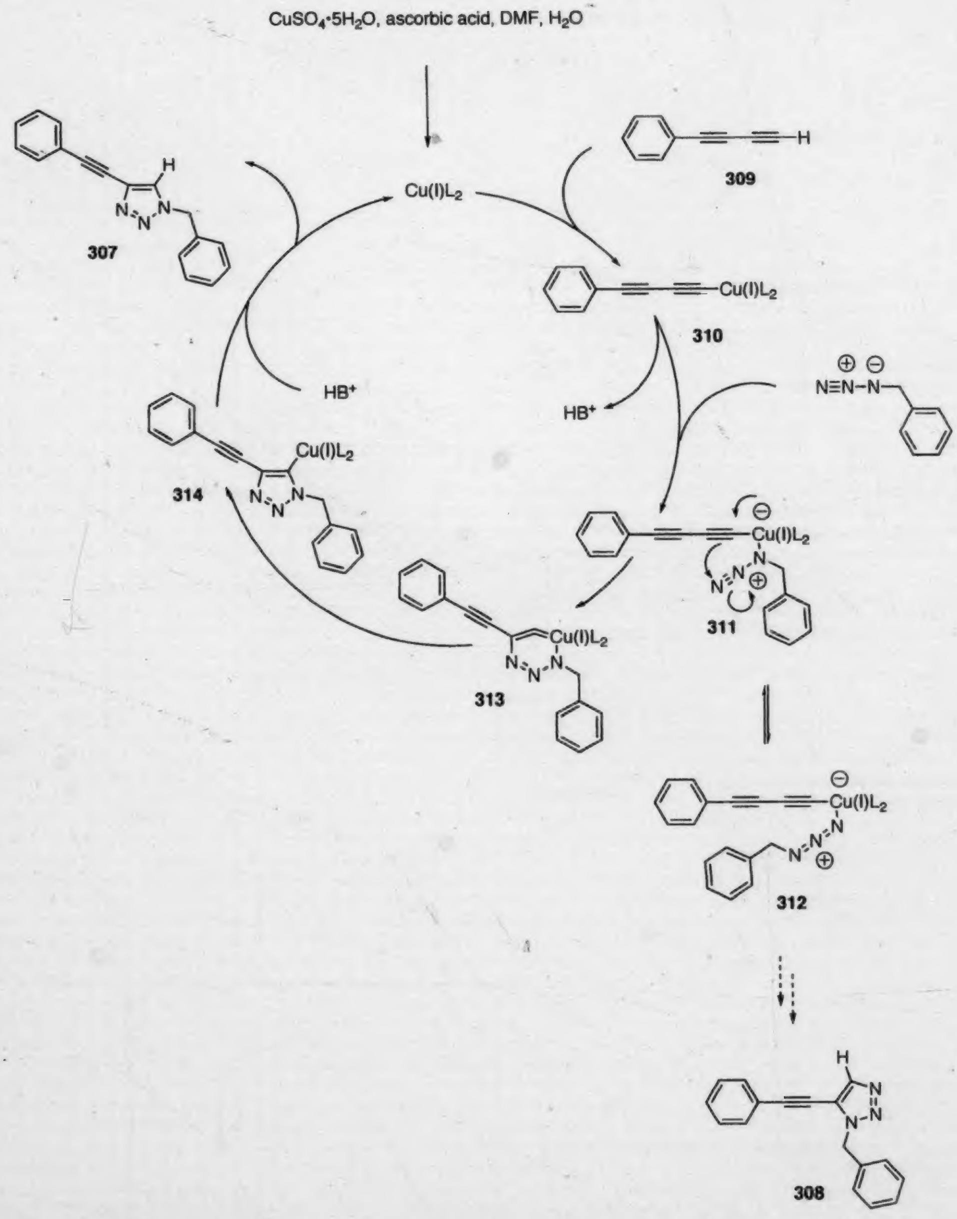
CuSO₄•5H₂O, ascorbic acid, DMF, H₂O
Cu(I)L₂
309
310
HB⁺
HB⁺
311
312
313
314
307
308
Cu(I)L₂

Scheme 3.1 Proposed mechanism for the formation of triazole **307**

The research reported herein worked with modified conditions ($CuSO_4$•$5H_2O$, ascorbic acid, DMF and H_2O), and questioned whether the triazole proton was provided by H_2O/D_2O present in the aqueous media, or from the terminal alkyne, as would be expected from a concerted cycloaddition reaction. Three simple tests were conducted to help establish the origin of the triazole proton (Table 3.1).

Table 3.1 Conditions and results for the formation of **307**

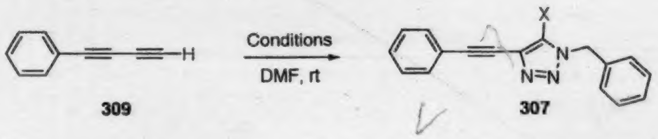

309 **307**

Entry	Conditions	X	Ratio H : CH_2 in ^1H NMR Spectrum
1	Sequence of BnN_3, ascorbic acid, $CuSO_4{\bullet}5H_2O$, and H_2O	H	1 : 2
2	Sequence of BnN_3, ascorbic acid, $CuSO_4{\bullet}5H_2O$, and then D_2O	H or D	0.8 : 2
3	Sequence of BnN_3, D_2O, ascorbic acid, and $CuSO_4{\bullet}5H_2O$	H or D	0.2 : 2

Entry 1 describes a reaction conducted under typical reaction conditions,[39] where H_2O is present as a cosolvent. In this case, the integration ratio of triazole proton/benzylic proton is 1:2, as would be expected from quenching of **314** in the last step of the catalytic cycle. In entry 2, D_2O was added last after all reagents other than H_2O were added. The integration ratio of the triazole proton/benzyl protons in the ^1H NMR spectrum of the resulting compound is 0.8:2, i.e., less than one. This experiment also suggests that the mechanism of the reaction likely involved protonation of the resulting triazole cuprate **314** with HD_2O^+ or H_3O^+.

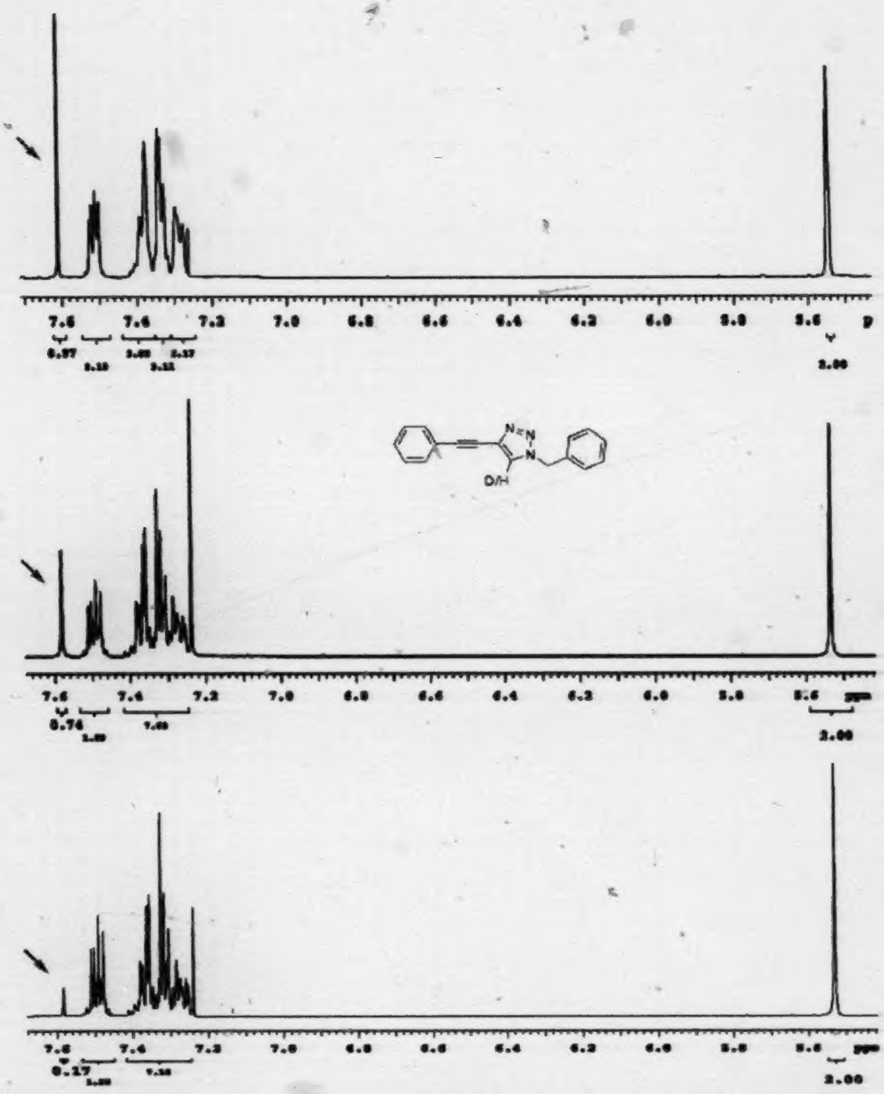

Figure 3.2 ^{1}H NMR spectra of compound **307** (arrow denotes the triazole proton)

In entry 3, D_2O was added first, before the oxidation reaction takes place. The integration ratio of the triazole proton/benzyl protons of the resulting compound is 0.2:2, much less than that in entry 2. Thus, the increased presence of D_2O in the reaction medium translates to increased deuterium in the product, likely due to quenching of the resultant triazole cuprate **314** by D^+ of D_2O.

In conclusion, the 1,2,3–triazole formation in this reaction likely involves initial deprotonation of the terminal alkyne and terminates by quenching of a triazole cuprate **314** with HD_2O^+ or H_3O^+ in the reaction medium. This is consistent with the mechanism suggested by Sharpless, although the above experiments were not conducted, to the best of my knowledge.

3.2.2 Synthesis

A series bis–triazoles **315a–d** with different methylene tethers was obtained (Scheme 3.2) starting with commercially available diynes **316a–d**. The procedure to this reaction is as follows: the diyne was added to a solution of DMF (10 mL). To this solution, benzyl azide (2 equiv), ascorbic acid (0.1 g), $CuSO_4•5H_2O$ (0.1 g), and H_2O (2 mL) were added in sequence. The reaction was monitored by TLC for 6–8 h until it was clear that the alkyne has been consumed. After the reaction was complete, saturated aqueous NH_4Cl (10 mL) and Et_2O (10 mL) were added, and the organic layer was separated. The resulting organic solution was washed with NaCl (10 mL), dried over $MgSO_4$, and the solution was concentrated to dryness. Purification of the triazoles **316a–d** could be accomplished by precipitating the crude products from hexanes or by column chromatography (silica gel, hexanes/EtOAc 1:1) to yield white crystalline solids.

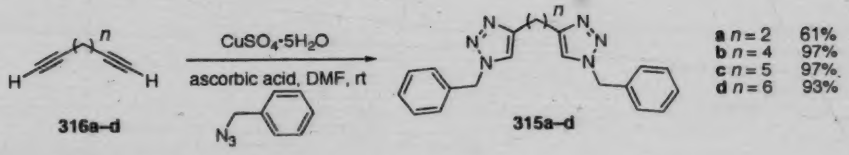

Scheme 3.2 Formation of bis–trizoles **315a–d**

Compound **315c** has been previously synthesized by Vereshchagin and coworkers by addition of benzyl azide (2 equiv) into a solution of **316c** in toluene at 110 °C.[40] The mixture was then stirred at this temperature for 2–6 h and gave both 1,4/1,4– and 1,5/1,5–disubstituted isomers in the ratio of 70:30, respectively. The same ratio was produced when acetone was used as solvent, whereas only 1,4/1,4–isomer **315c** was obtained when DMSO was used. In our case, the 1,4/1,4–isomer **315c** was the only product obtained.

Ethynyl triazoles **317a–r** were synthesized in a similar fashion as that of **315**.[23,41] Due to the kinetic instability of terminal diynes, silyl protected diynes **318a–r** were utilized as the immediate precursors (Table 3.2). The Me_3Si or i-Pr_3Si protecting group was first removed at room temperature by K_2CO_3 in THF/MeOH or TBAF in THF, respectively. The formation of the terminal alkyne was monitored by TLC (ca. 15–30 min). Once the desilylation was complete, the reaction mixture was subjected to an aqueous work–up. DMF (ca. 2 mL) was added to the resulting organic solution, which was then concentrated to approximately 1–2 mL. During the concentration, heat should not be applied and the solution should not be allowed to completely dry as this could result decomposition of the terminal alkyne. Additional DMF (10 mL) was added to the resulting solution, followed by the addition of the benzyl azide, $CuSO_4$•$5H_2O$, ascorbic acid, and water. The progress of the reaction was monitored by TLC. 1,2,3–Triazole adducts **317a–r** were produced in 46–83% yields. The triazoles could be purified by either column chromatography or recrystallization from hexanes (for the crystalline products).

The Me_3Si protecting groups of **318a,b** were selectively removed using K_2CO_3 in THF/MeOH, and the reaction of the resulting terminal diyne with benzyl azide afforded **317a,b** in good yield. Aryl derivatives **317c–m** were synthesized in the same fashion as those of **317a,b**. Precursor diynes with phenyl, pyrenyl, and thienyl substituents **317c–e** were first desilylated. The corresponding diynes were subjected to standard reaction conditions and yielded compounds **317c–e** with average yields of 67%. Compounds **317c–e** were purified simply by recrystallization from hexanes. *Trans*–enyne triazole **317f** was produced as a yellow powder in 69% yield. *Para*–substituted aryl derivatives **317g–k** were synthesized in yields ranging from 69–82%. No particular trend in yield was observed regarding the various electronic effects of substituents at the *para*–position. The presence of *t*-$BuPh_2Si$ protected hydroxyl groups was explored as found for **318l,m**. Desilylation of compound **318l** with potassium methoxide, followed by trapping the resulting terminal alkyne with benzyl azide produced **317l** in 68%. The *t*-$BuPh_2Si$ protective group remained intact. When TBAF (4 equiv) was used for desilylation of **318l**, complete desilylation occurred resulting in a diyne product terminated in a 4–benzyl alcohol group. Subjecting this compound to the general procedure generated triazole **317m**. Dibromoolefinic diyne **317n** was also subjected to the same protocol of desilylation and trapping the resulting terminal diyne with a benzyl azide, yielding **317n** in 65% yield with no product that results from the copper insertion into the bromide position observed. The formation of enone diyne **317o**, however, was not that successful.

A yield of only 5% was obtained which may have resulted from a kinetic decomposition of the terminal alkyne.

Table 3.2 Formation of ethynyl triazoles **317a–r**

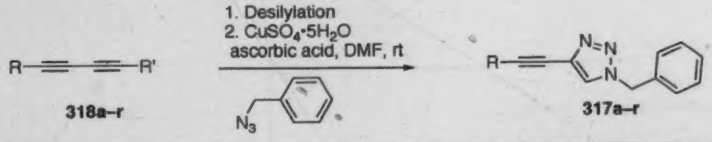
1. Desilylation
2. $CuSO_4 \cdot 5H_2O$
ascorbic acid, DMF, rt
R
R'
N_3
N
N
N
R

318a–r → **317a–r**

	R	R'	desilylation conditions	yield (%)
a	*t*-BuMe$_2$Si	Me$_3$Si	K_2CO_3/MeOH	75
b	*i*-Pr$_3$Si	Me$_3$Si	K_2CO_3/MeOH	67
c	Ph	Me$_3$Si	K_2CO_3/MeOH	73
d	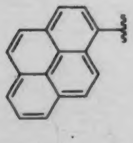	Me$_3$Si	K_2CO_3/MeOH	62
e	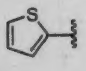	Me$_3$Si	K_2CO_3/MeOH	62
f	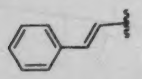	Me$_3$Si	K_2CO_3/MeOH	69
g	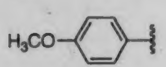	Me$_3$Si	K_2CO_3/MeOH	69
h	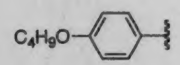	Me$_3$Si	K_2CO_3/MeOH	82
i	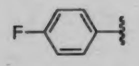	*i*-Pr$_3$Si	TBAF/THF	72
j	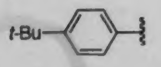	Me$_3$Si	K_2CO_3/MeOH	74
k	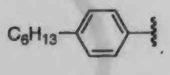	Me$_3$Si	K_2CO_3/MeOH	73
l	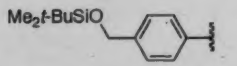	Me$_3$Si	K_2CO_3/MeOH	68[a]
m	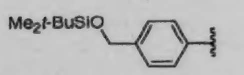	Me$_3$Si	TBAF/THF	86[b]

Table 3.2 (continued) Formation of ethynyl triazoles **317a–r**

	R	R'	desilylation conditions	yield (%)
n	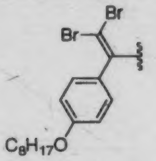	Me_3Si	K_2CO_3/MeOH	65
o	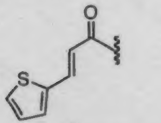	Me_3Si	K_2CO_3/MeOH	5
p	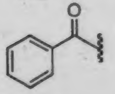	Me_3Si	K_2CO_3/MeOH	68
q	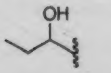	i-Pr_3Si	TBAF/THF	46
r	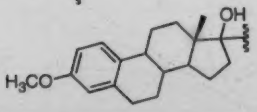	i-Pr_3Si	TBAF/THF	75

[a] Sit-BuMe_2 group is not removed during desilylation of the alkyne.
[b] Sit-BuMe_2 group is removed during desilylation of the alkyne.

This general method was also expanded to trap two naturally occurring diynes **318p’,q’**. A terminal ynone derived from **318p** has been isolated by Bohlmann from the crown daisy (*Chrysanthemum coronarium*).[42] After desilylation of **318p**, the terminal diyne was trapped with benzyl azide to produce **317p** in good yield. The desilylated alkyne, derived from **318q**, was obtained from *Gymnopilus spectabilis* by Jones[12] and also tested. The reaction with benzyl azide produced triazole **317q** in 46%. Finally, the steroid capped diyne **318r** was deprotected using TBAF and the resulting terminal diyne was subjected to the general conditions to give compound **317r** in good yield.

The isolation of terminal alkynes from natural sources such as plants or fungi often results in an aqueous solution of the polyyne. An undergraduate student, under my supervision, Danielle Vallee, explored the reaction of phenyl–1,3–butadiyne using the same conditions as described in Table 3.1, but varied the cosolvents (DMF: H_2O 1:1). This reaction produced the same yield as the condition that was used for synthesizing compound **317c**. Thus, varying of the solvent system does not seem to affect the outcome of the reaction.

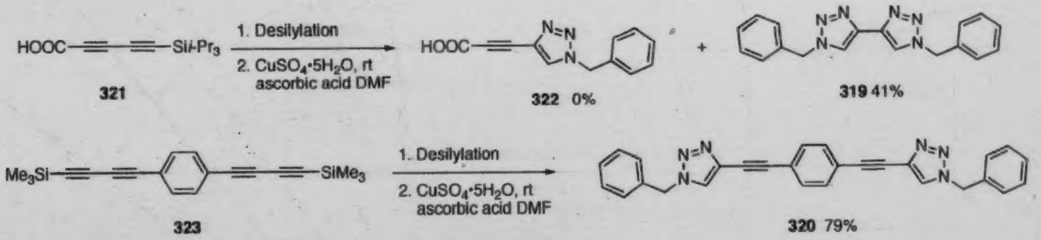
HOOC
Si*i*-Pr3
321
1. Desilylation
2. CuSO4•5H2O, rt
ascorbic acid DMF
HOOC
N=N
N
322 0%
+
N=N
N
N=N
N
319 41%
Me3Si
SiMe3
323
1. Desilylation
2. CuSO4•5H2O, rt
ascorbic acid DMF
N=N
N
N=N
N
320 79%

Scheme 3.3 Formation of bis–triazoles **319** and **320**

Interesting results were found the formation of **319** and **320** as shown in Scheme 3.3. *i*-Pr_3 protected diyne **321** was first desilylated with TBAF and the resulting terminal alkyne was subjected to typical reaction conditions with benzyl azide, toward the formation of compound **322**. Unexpectedly, disubstituted triazole **319** was produced in 41% yield as a result of the decarboxylation to form another terminal alkyne, which then underwent a second reaction with benzyl azide. The solubility of compound **319** was quite low and it simply precipitated out of solution as a white powder. The desired product **322** was not detected in the ^1H NMR spectrum of the crude product. Finally, this methodology was extended to the formation of bis–triazole **320** from precursor **323** in good yield. Purification of the yellow solid product was problematic due to the low solubility, and attempts to obtain a ^{13}C NMR spectrum of **320** were also unsuccessful.

Trapping a terminal triyne with benzyl azide was attempted and produced **324a–f** ranging from 47–82% yield (Table 3.3). Alkynyl derivative **325a** was subjected to the same conditions as those of the diynes to yield **324a** in 71% yield as a colorless oil. The reaction of *t*-$BuPh_2Si$ protected alcohol **325b** with TBAF (4 equiv) produced terminal the triyne which was then subjected to the general procedure to produce the desilylated alcoholic triazole **324b** in a reasonable yield of 47%. The terminal triynol[43] resulting from the exhaustive desilylation of **325b** has been predicted to be a product of hydrolysis of the fungal natural product marasin from *Aleurodiscus roseus.*[13] The terminal triyne resulting from the desilylation of **325c** was reacted with benzyl azide producing compound **324c** in good yield.

CAUTION: It should be noted that Armitage has reported that this intermediate terminal triyne "exploded at 0 °C in the absence of air,"[44] and therefore one should never attempt to isolate this, or any other, terminal triyne neat. Aryl derivatives **325d–e** also produced corresponding triazoles **324d–f** in good yield. In these reactions under the standard conditions, only 1,4–substituted triazole products were obtained and no 1,5–addition products were detected.

Table 3.3 Formation of butadiynyl triazoles **324a–f**

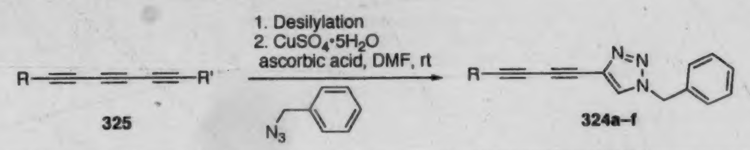

	R	R'	desilylation conditons	yield (%)
a	Bu	*i*-Pr$_3$Si	TBAF/THF	71
b	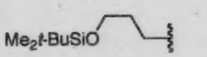	*i*-Pr$_3$Si	TBAF/THF	47[a]
c	Ph	Me$_3$Si	K$_2$CO$_3$/MeOH	68
d	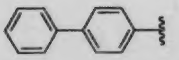	*i*-Pr$_3$Si	TBAF/THF	63
e	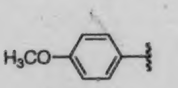	*i*-Pr$_3$Si	TBAF/THF	82
f	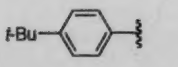	Me$_3$Si	K$_2$CO$_3$/MeOH	73

[a] Si*t*-BuMe$_2$ group also removed during desilylation of alkyne.

To extend the scope of the conjugated alkynes used to produce the hexa–1,3,5–triynyl triazoles **326a,b**, the reaction of two tetraynes **327a,b** was explored (Scheme 3.4). The desilylation of **327a,b** with K$_2$CO$_3$ in MeOH/THF produced terminal alkynes, and following workup, DMF (ca. 2 mL) was added to the resulting organic phase and this solution was then concentrated to ca. 1–2 mL. The resulting solution was subjected directly to the general reaction procedure with benzyl azide to produce **326a,b** in reasonable yields, considering the instability of the desilylated tetrayne precursors. Once again, only 1,4–substituted triazole products were produced with no trace of multiple addition of azide into the internal alkyne.

A one pot–reaction was attempted with **327a** toward the *in situ* formation and trapping of the terminal tetrayne. To the precursor **327a**, DMF, K_2CO_3, a few drops of methanol, $CuSO_4{\bullet}5H_2O$, ascorbic acid and benzyl azide were all added. The reaction was stirred at room temperature until all the benzyl azide had been consumed. This mixture was subjected to a standard aqueous work–up and column chromatography producing **326b** in very comparable yield (21%) versus the two–step route.

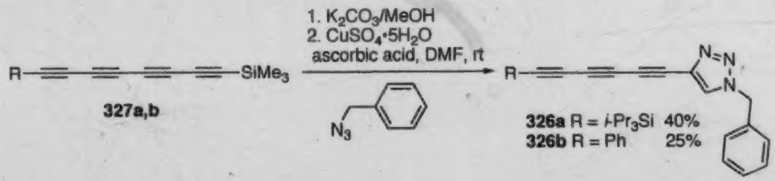

Scheme 3.4 Formation of triazoles **326a,b**

Generally, the products of these reactions were purified by simply quenching the reaction with water or NH_4Cl, then drying with saturated aqueous NaCl, $MgSO_4$, and concentrating down to give a solid (except for oily compound **324a**). A small amount of hexanes (ca. 10–20 mL) at 0 °C was added to the resulting solid and drained off to remove any remaining DMF and soluble byproducts. The compounds at this point were sufficiently pure for characterization. Once again, analysis of the products by ^1H NMR spectroscopy did not show any evidence of multiple additions to the alkyne.

3.2.3 Physical Properties

Chemical shifts of the triazole proton of the triazole ring and those of the methylene group of the benzyl moiety for compounds **315a–d, 317a–r, 319, 320, 324a–f,** and **326a,b** are summarized in Table 3.4. The chemical shifts of the triazole proton of the bis–triazole compounds **315a–d** are shifted upfield when compared to the corresponding ethynyl (**317a–r**), butadiynyl (**324a–f**), and hexatriynyl (**326a,b**) compounds. ^{1}H NMR spectroscopy could be used to distinguish isomers of 1,4– or 1,5–addition. Tikhonova *et al.* reported that the proton of the triazole ring resonates between 7.42–8.06 ppm for 1,4–isomers and 7.42–7.59 ppm for 1,5–isomers.[33] Unfortunately, there is no clear–cut point from this trend to rule out 1,5–addition. The triazole protons of ethynyl compounds **317a–r** have chemical shifts ranging from 7.81–7.47 ppm, and compounds **317d, 317o, 317p** show triazole proton resonances at above 7.70 ppm. The downfield chemical shift of the triazole proton of compound **317d** at 7.73 ppm might result from the deshielding from the large pyrene ring, while those of compounds **317o,p** at 7.77 and 7.81 ppm, respectively, might result from a strong carbonyl electronic withdrawing group. Symmetrical disubstituted triazole **319** shows the proton at 7.98 ppm. This may result from the effect of the adjacent triazole ring, which is also electron deficient. The benzylic protons of all compounds do not show any significant change except in compounds **315a,b** which are found at 5.39 and 5.33 ppm, respectively. The benzylic proton of other compounds range from 5.44–5.60 ppm.

Table 3.4 Chemical shift of compounds **315a–d, 317a–r, 324a–f, 326a,b**

Compound	Chemical Shift of Triazole proton (ppm)	Chemical Shift of Benzyl protons (ppm)
315a	7.11	5.39
315b	7.11	5.33
315c	7.16	5.46
315d	7.14	5.46
317a	7.51	5.49
317b	7.56	5.51
317c	7.61	5.55
317d	7.73	5.60
317e	7.60	5.54
317f	7.53	5.52
317g	7.47	5.44
317h	7.55	5.52
317i	7.60	5.52
317j	7.50	5.46
317k	7.56	5.53
317l	7.54	5.50
317m	7.58	5.53
317n	7.56	5.49
317o	7.77	5.56

317p	7.81	5.57
317q	7.50	5.49
317r	7.53	5.49
319	7.98	5.54
320	7.69	5.55
324a	7.53	5.49
324b	7.53	5.50
324c	7.30	5.52
324d	7.56	5.48
324e	7.58	5.52
324f	7.54	5.48
326a	7.65	5.53
326b	7.62	5.52

In the EIMS (70 eV) analysis of the triazole compounds, all of the spectra show a molecular parent peak, except compounds **317l** and **326a**. In these cases, the molecular parent peak is absent because the *t*-BuPh$_2$Si group of **317l** easily loses a *t*–Bu radical and compound **326a** readily loses N$_2$. This is a typical event for triazoles, and the fragmentation pattern of most of the triazole compounds in this study show the loss of N$_2$.

3.2.4 X–ray Crystallographic Analysis

X–ray crystallographic analysis can reveal a great deal of information about a molecule in the solid–state, such as bond lengths and angles. As well, details as to the manner in which the molecules pack in the solid–state can be determined by analysis of intermolecular close contacts such as H–bonding interactions and π–stacking. Utilizing the power of the X–ray crystallographic method, triazoles were analyzed and information about these compounds elucidated. Dihedral angles, selected bond lengths, and bond angles have been summarized in Tables 3.5 and 3.6.

The 1,4–addition of these reactions could be deduced from ^{1}H NMR spectroscopy and was confirmed by X–ray crystallographic analysis of compounds **315a, 317c,e,g,j,l,p, 324c,e,** and **326b** (Figures 3.3–3.12).

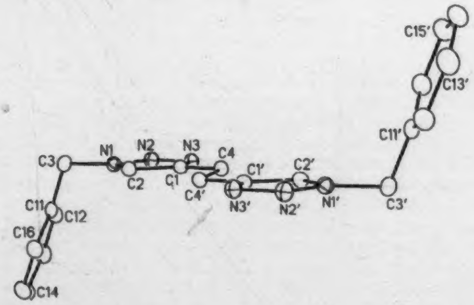
C15'
C13'
C11'
C3
N1
N2
N3
C4
C1'
C2'
C2
C1
C4'
N3'
N2'
N1'
C3'
C11
C12
C16
C14

Figure 3.3 ORTEP drawing (20% probability level, hydrogen atoms are omitted for clarity) of compound **315a**. Dihedral angle between plane 1 (N1, N2, N3, C1, C3, C4) and plane 2 (C11, C12, C13, C14, C15, C16) is 69.33(6)°.

A single crystal of compound **315a** was obtained by slow diffusion of hexanes into a solution of **315a** in CH_2Cl_2 at 4 °C (Figure 3.3). The geometry of **315a** in the solid state is centrosymmetric.

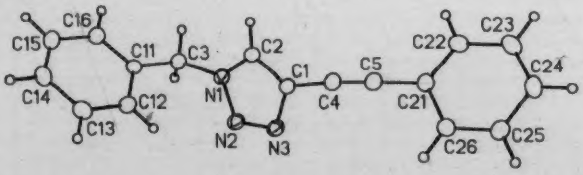
C16
C15
C11
C3
C2
C1
C5
C22
C23
C24
C14
C12
N1
C4
C21
C13
N2
N3
C26
C25

Figure 3.4 ORTEP drawing (20% probability level) of compound **317c**.

X–ray crystallographic analyses for monoyne products **317c,e,g,j,l,p** were obtained. Crystals of phenyl derivative **317c** were produced by vapor diffusion of hexanes into a CH_2Cl_2 solution at room temperature (Figure 3.4). X–ray crystallographic analysis of compound **317c** shows that the C≡C bond length is 1.1948(18) Å as expected for a triple bond. The structure of **317c** shows that the dihedral angle between phenyl ring (C21–C26) and the triazole ring is 39.3(4)°. This significant twist disrupts the electron communication between these two rings through the alkyne bond in its solid–state conformation.

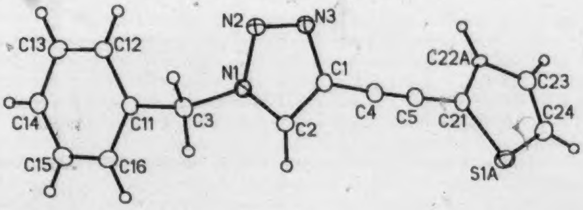
C13
C12
N2
N3
N1
C1
C22A
C23
C14
C11
C3
C2
C4
C5
C21
C24
C15
C16
S1A

Figure 3.5 ORTEP drawing (20% probability level) of compound **317e**.

Crystals of thiophenyl derivative **317e** were produced from slow evaporation of a solution of CH_2Cl_2 (Figure 3.5). The C≡C bond length is 1.193(3) Å. The dihedral angle of the triazole ring and the thiophene is 71.70(6)°. The sulfur atom in the thiophene ring does not appear to have any significant effects in the solid–state packing.

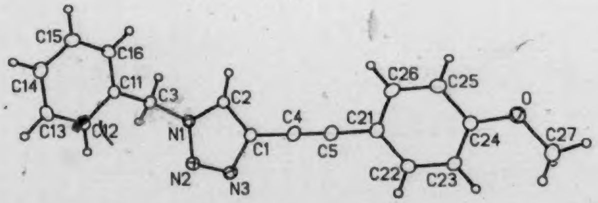
C15
C16
C26
C25
C14
C11
C3
C2
O
C4
C21
C13
C12
N1
C1
C5
C24
C27
N2
N3
C22
C23

Figure 3.6 ORTEP drawing (20% probability level) of compound **317g**.

Single crystals of 4–methoxyphenyl derivative **317g** were obtained from diffusion of hexanes into a solution of CH_2Cl_2 at room temperature (Figure 3.6). The alkyne bond length is unremarkable. The dihedral angle between the triazole ring and the phenyl ring in the anisole group is 20.43(8)°. This twist angle is smaller than that of phenyl derivative **317c** [39.30(4)°] by 20°. However, these two planes are not sufficiently coplanar to permit to extend the conjugated electronic communication through the alkyne bond.

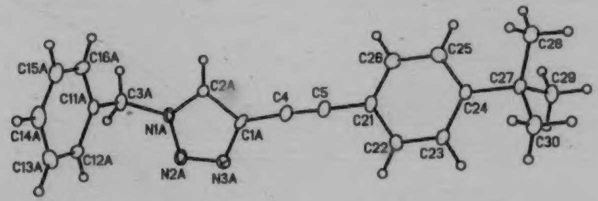
C15A
C16A
C11A
C3A
C14A
C13A
C12A
N1A
N2A
N3A
C2A
C1A
C4
C5
C26
C25
C21
C22
C23
C24
C27
C28
C29
C30

Figure 3.7 ORTEP drawing (20% probability level) of compound **317j**.

Single crystals were obtained from slow evaporation of a solution of $CHCl_3$ containing compound **317j** at 4 °C (Figure 3.7). The C≡C bond length is unremarkable. The dihedral angle between the triazole ring and the *t*–butylphenyl ring is 27.1(2)°. This observation is similar to the result found for the phenyl derivative **317c** and anisole derivative **317e** in terms of disrupting the electron communication between the aryl ring and triazole via the alkyne.

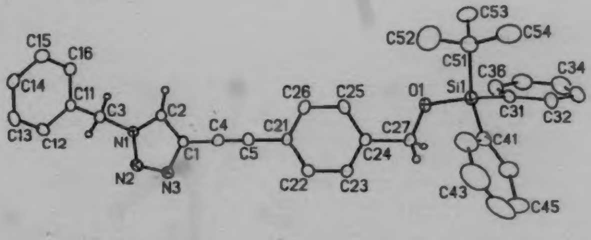
C15
C16
C14
C11
C3
C13
C12
N1
N2
N3
C2
C1
C4
C5
C26
C25
C21
C22
C23
C24
C27
O1
Si1
C51
C52
C53
C54
C36
C34
C31
C32
C41
C43
C45

Figure 3.8 ORTEP drawing (20% probability level, selected hydrogen atoms are omitted for clarity) of compound **317l**

By slow evaporation of the CHCl$_3$ solution of compound **317l** at 4 °C, single crystals were obtained (Figure 3.8). The C≡C bond is a typical length for a triple bond, at ca. 1.2 Å. The dihedral angle between the aryl ether and the triazole groups is 14.1(2)° (Figure 3.8). This is the smallest dihedral angle observed among compounds **317c,g,j,l**.

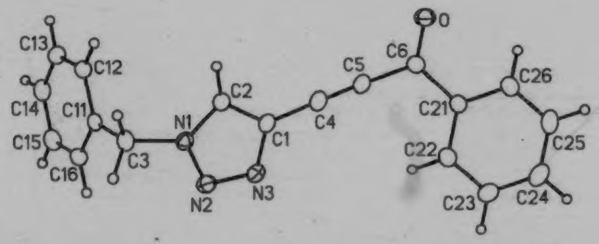
O
C13
C12
C14
C11
C15
C16
C3
N1
C2
N2
N3
C1
C4
C5
C6
C21
C22
C23
C24
C25
C26

Figure 3.9 ORTEP drawing (20% probability level) of compound **317p**

Single crystals of ketone **317p** suitable for X–ray crystallography were obtained from slow diffusion of hexanes into a solution of hexanes/CH$_2$Cl$_2$ at room temperature (Figure 3.9). The alkyne C≡C bond length is ca. 1.2 Å. The bond angle of the ketone (C5–C6–C21) is 117.18(16)° as is expected for an sp^2–hybrized carbon. The dihedral angle between the triazole ring and the phenyl ring adjacent to the ketone is 25.07(7)°.

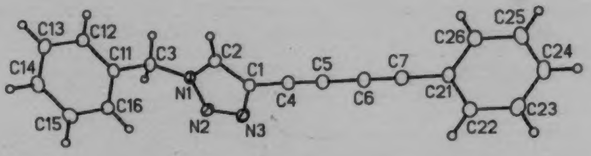
C13
C12
C11
C3
C2
C14
C1
C16
N1
C15
N2
N3
C4
C5
C6
C7
C21
C26
C25
C24
C23
C22

Figure 3.10 ORTEP drawing (20% probability level) of compound **324c**

X–ray crystallographic structures were obtained of two diyne triazoles, **324c** and **324e**. Single crystals of compound **324c** were produced by slow evaporation of hexanes into a solution of hexanes/CH$_2$Cl$_2$ at 4 °C (Figure 3.10). The alkyne bond length for all

C≡C bonds is approximately 1.2 Å. The dihedral angle between the phenylacetylene and the triazole 62.92(5)°; it is also twisted like the series of alkynyl derivatives **317c,g,j,l**.

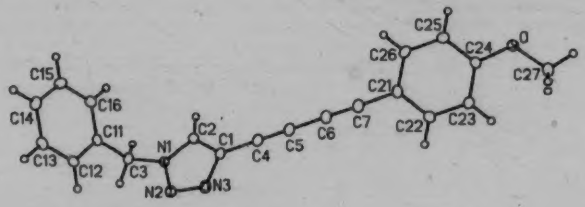
C25
C26
C24
O
C27
C15
C21
C16
C14
C11
N1
C2
C1
C7
C22
C23
C6
C5
C4
C13
C12
C3
N2
N3

Figure 3.11 ORTEP drawing (20% probability level) of compound **324e**

Crystals of diyne derivative **324e** were produced by slow evaporation of a solution of $CDCl_3$ at 4 °C (Figure 3.11). The alkynyl C≡C bond lengths are approximately 1.2 Å. Dihedral angle between the aryl end group and the triazole is 27.70(7)° which is larger than **317g** by 7°.

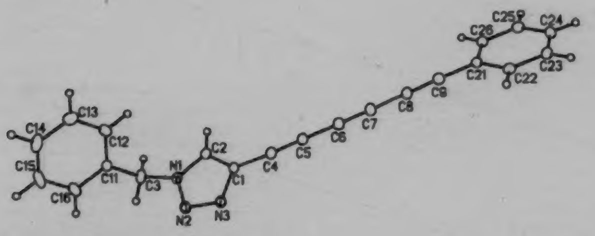
C25
C24
C26
C23
C21
C22
C9
C8
C7
C6
C13
C14
C12
C5
C2
C4
N1
C15
C11
C1
C3
C16
N2
N3

Figure 3.12 ORTEP drawing (20% probability level) of compound **326b**

Crystals of triyne product **326b** were produced by slow evaporation of a solution of compound **326b** in CH_2Cl_2 at 0 °C (Figure 3.12). The three C≡C bond lengths are also ca. 1.20 Å. The alkyne bridge is nearly linear with bond angles that range from 176.2 to 178.9°. The dihedral angle between the terminal phenyl group and the triazole ring is

22.84(11)°, which is the smallest result observed in comparison to those of the shorter analogues **317c** and **324c** with only an alkyne and diynyl linker, respectively.

Given the diverse range of structures analyzed by X–crystallography (**317c,e,g,j,l,p, 324c,e**, and **326b**), it is hard to draw any significant trends common to all or even a majority of the compounds. What can be said, however, is that all alkyne C≡C bond lengths are near the expected value of ca. 1.2 Å and there seems to be no driving force for the aryl end group and the triazole to achieve coplanarity in the solid–state.

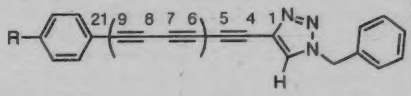

Table 3.5 Dihedral angles and selected bond lengths of compounds **317c,e,g,j,l, 324c,e,** and **326b**

Compound	Dihedral Angle (deg)	Selected Bond Lengths (Å)						
Monoynes		C1–C4	C4–C5	C5–C21				
317c	39.30(4)	1.4301(18)	1.1948(18)	1.4378(18)				
317e	24.87(10)	1.432(3)	1.193(3)	1.419(3)				
317g	20.43(8)	1.4284(19)	1.200(2)	1.4395(19)				
317j	27.1(2)	1.409(17)	1.192(2)	1.435(2)				
317l	14.1(2)	1.421(6)	1.202(6)	1.453(6)				
Diynes		C1–C4	C4–C5	C5–C6	C6–C7	C7–C21		
324c	62.92(5)	1.426(2)	1.196(2)	1.372(2)	1.200(2)	1.435(2)		
324e	27.70(7)	1.4262(18)	1.199(2)	1.376(2)	1.201(2)	1.4347(19)		
Triyne		C1–C4	C4–C5	C5–C6	C6–C7	C7–C8	C8–C9	C9–C21
326b	22.84(11)	1.425(3)	1.203(3)	1.368(3)	1.205(3)	1.334(3)	1.199(3)	1.430(3)

Table 3.6 Alkynyl bond angles of compounds **317c,e,g,j,l,p, 324c,e,** and **326b**

Compound	Bond Angle (deg)					
Monoynes	C1–C4–C5	C4–C5–C21				
317c	174.45(14)	176.95(14)				
317e	176.3(2)	178.8(2)				
317g	179.25(17)	177.01(16)				
317j	173.9(8)	178.9(3)				
317l	179.5(6)	175.3(5)				
	C1–C4–C5	C4–C5–C6				
317p	177.7(2)	173.9(2)				
Diyne	C1–C4–C5	C4–C5–C6	C5–C6–C7	C6–C7–C21		
324c	176.85(18)	178.12(18)	177.64(19)	178.33(18)		
324e	177.69(16)	179.06(16)	178.27(17)	177.14(17)		
Triyne	C1–C4–C5	C4–C5–C6	C5–C6–C7	C6–C7–C8	C7–C8–C9	C8–C9–C21
326b	178.4(2)	179.5(3)	178.9(3)	177.8(3)	177.5(3)	176.2(3)

3.2.5 Trapping Diynone 318p' from Chrysanthemum coronarium

Preliminary attempts to extend the scope of this methodology by trapping terminal polyynes from natural sources with BnN_3 were conducted. Plants of *Chrysanthemum coronarium* were chosen because they grow widely in Asia or North America, and in fact Asians have used this type of plant as food. Bohlmann isolated diynone **318p'** only from the roots of the *C. coronarium*; no yield was reported. In this study, fresh roots and aerial–flower parts were ground and extracted with a mixture of Et_2O, hexanes, benzene, and H_2O by stirring at rt for 10 h, followed by an aqueous workup. DMF (10 mL) was added to the resulting organic solution and the mixture was

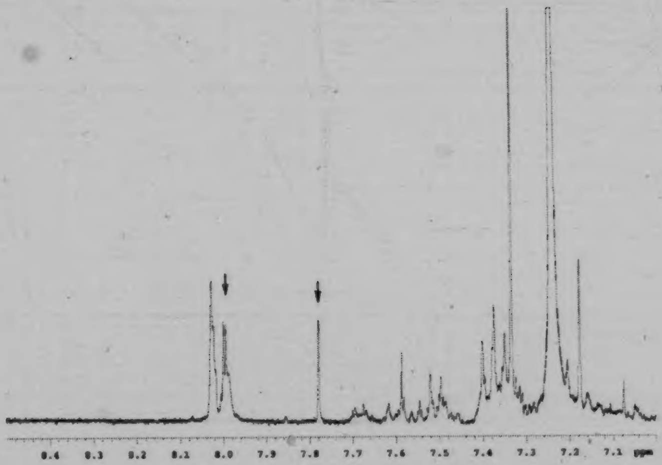

Figure 3.13 ^{1}H NMR spectrum of a solution containing fractions from a trapping experiment involving the extract of *Chrysanthemum coronarium* and benzyl azide.

3.3 Conclusions

We have successfully demonstrated that terminal di–, tri–, and tetraynes can be trapped with benzyl azide using DMF as a solvent, Cu(II) and ascorbic acid as catalysts, to yield ethynyl, butadiynyl, and hexatriynyl triazoles in reasonable to good yields. This method has also been used to trap two synthetic natural products. Using this procedure, our initial exploration has answered those questions stated in the introduction. Under the conditions described above, only 1,4–adducts were produced and no 1,5–addition was observed. No multiple addition on the polyyne skeleton was detected. X–ray crystallographic analyses of compounds **315a, 317c,e,g,j,l,p, 324c,e,** and **326b** have been concentrated via aspirator to ca. 8–10 mL. To this solution was added additional DMF (5 mL), ascorbic acid (0.1 g), $CuSO_4 \cdot 5H_2O$ (0.1 g), BnN_3 (1.6 m L) and H_2O (5 mL) in sequence. This mixture was allowed to stir at rt for 12 h, followed by an aqueous workup, solvent removal, and purification via column chromatography. Fractions were spotted against a known product **317p**, and fractions containing compounds with an R_f similar to that of compound **317p** were collected. ^1H NMR spectroscopic analysis of these fractions showed two signals (7.8 and 8.0 ppm) similar to that of pure synthetic **317p**, among many impurity signals (Figure 3.13). This preliminary result suggests that the diynone could have been converted to the trizole. This experiment shows that the methodology could be used to trap terminal polyynes from natural sources. However, more trials of the trapping experiment as well as quantity of the precursor **318p'** isolated from *Chrysanthemum coronarium* need to be carried out.

conducted and have confirmed the formation of the 1,4–adducts. No particular trend is observed when comparing a series such as the Ph terminal **317c, 324c,** and **326b**.

Given the success of this work, in the future this protocol should be extended toward trapping naturally occurring terminal alkynes from the natural sources, such as mushrooms or plants. There are several readily available natural sources of terminal polyynes, such as chrysanthemums and coneflowers. Different solvents and catalysts could be tested.

3.4 References and Notes

(1) Shi Shun, A. L. K.; Tykwinski, R. R. *Angew. Chem., Int. Ed.* **2006**, *45*, 1034–1057.

(2) *Chemistry and Biology of Naturally Occurring Acetylenes and Related Compounds (NOARC)*; Elsevier: New York, 1988.

(3) Bohlmann, F.; Burkhardt, T.; Zdero, C. *Naturally Occurring Acetylenes*; Academic Press: New York, 1973.

(4) Blunt, J. W.; Copp, B. R.; Munro, M. H. G.; Northcote, P. T.; Prinsep, M. R. *Nat. Prod. Rep.* **2003**, *20*, 1–48.

(5) Faulkner, D. J. *Nat. Prod. Rep.* **2001**, *18*, 1–49.

(6) *Acetylene Chemistry – Chemistry, Biology, and Materials Science*; Diederich, F.; Stang, P. J.; Tykwinski, R. R., Eds.; Wiley–VCH: Weiheim, 2005.

(7) Meinwald, J.; Meinwald, Y. C.; Chalmers, A. M.; Eisner, T. *Science* **1968**, *160*, 890–892.

(8) Arnason, J. T.; Philogene, B. J. R.; Berg, C.; Maceachern, A.; Kaminski, J.; Leitch, L. C.; Morand, P.; Lam, J. *Phytochemistry* **1986**, *25*, 1609–1611.

(9) Kobaisy, M.; Abramowski, Z.; Lermer, L.; Saxena, G.; Hancock, R. E. W.; Towers, G. H. N.; Doxsee, D.; Stokes, R. W. *J. Nat. Prod.* **1997**, *60*, 1210–1213.

(10) Fusetani, N.; Toyoda, T.; Asai, N.; Matsunaga, S.; Maruyama, T. *J. Nat. Prod.* **1996**, *59*, 796–797.

(11) Rashid, M. A.; Gustafson, K. R.; Cardellina, J. H.; Boyd, M. R. *Nat. Prod. Lett.* **2001**, *15*, 21–26.

(12) Hearn, M. T. W.; Jones, E. R. H.; Pellatt, M. G.; Thaller, V.; Turner, J. L. *J. Chem. Soc., Perkin Trans. 1* **1973**, 2785–2788.

(13) Cambie, R. C.; Hirschbe.A; Jones, E. R. H.; Lowe, G. *J. Chem. Soc.* **1963**, 4120–4130.

(14) Tokimoto, K.; Fujita, T.; Takeda, Y.; Takaishi, Y. *Proc. Jpn. Acad.* **1987**, *63*, 277–280.

(15) Jones, E. R. H.; Stephenson, J. S. *J. Chem. Soc.* **1959**, 2197–2203.

(16) Kusumi, T.; Ohtani, I.; Nishiyama, K.; Kakisawa, H. *Tetrahedron Lett.* **1987**, *28*, 3981–3984.

(17) Bittner, M.; Jakupovic, J.; Bohlmann, F.; Silva, M. *Phytochemistry* **1989**, *28*, 271–273.

(18) "Kinetic stability, in contrast to thermodynamic stability, is circumstantial as it is a property of the system and its immediate environment. Kinetic stability depends not just on the system itself, but on factors extraneous to the system. For this reason kinetic stability cannot be classified as a state function (in contrast to thermodynamic stability)," see: Pross, A. *Pure Appl. Chem.* **2005**, *77*, 1905–1921.

(19) Luu, T.; Tykwinski, R. R. *J. Org. Chem.* **2006**, *71*, 8982–8985.

(20) Gothelf, K. V.; Jorgensen, K. A. *Chem. Rev.* **1998**, *98*, 863–909.

(21) *1,3–Dipolar Cycloaddition Chemistry*; Padwa, A., Ed.; Wiley: New York, 1984.

(22) Alvarez, R.; Velazquez, S.; Sanfelix, A.; Aquaro, S.; Declercq, E.; Perno, C. F.; Karlsson, A.; Balzarini, J.; Camarasa, M. J. *J. Med. Chem.* **1994**, *37*, 4185–4194.

(23) Reck, F.; Zhou, F.; Girardot, M.; Kern, G.; Eyermann, C. J.; Hales, N. J.; Ramsay, R. R.; Gravestock, M. B. *J. Med. Chem.* **2005**, *48*, 499–506.

(24) Harju, K.; Vahermo, M.; Mutikainen, I.; Yli–Kauhaluoma, J. *J. Comb. Chem.* **2003**, *5*, 826–833.

(25) Katritzky, A. R.; Singh, S. K. *J. Org. Chem.* **2002**, *67*, 9077–9079.

(26) Bock, V. D.; Hiemstra, H.; van Maarseveen, J. H. *Eur. J. Org. Chem.* **2005**, 51–68.

(27) Lee, J. W.; Kim, B. K. *Bull. Korean Chem. Soc.* **2005**, *26*, 658–660.

(28) Pirali, T.; Tron, G. C.; Zhu, J. P. *Org. Lett.* **2006**, *8*, 4145–4148.

(29) Rostovtsev, V. V.; Green, L. G.; Fokin, V. V.; Sharpless, K. B. *Angew. Chem., Int. Ed.* **2002**, *41*, 2596–2599.

(30) Tornoe, C. W.; Christensen, C.; Meldal, M. *J. Org. Chem.* **2002**, *67*, 3057–3064.

(31) Luu, T.; McDonald, R.; Tykwinski, R. R. *Org. Lett.* **2006**, *8*, 6035–6038.

(32) Yoo, E. J.; Ahlquist, M.; Kim, S. H.; Bae, I.; Fokin, V. V.; Sharpless, K. B.; Chang, S. *Angew. Chem., Int. Ed.* **2007**, *46*, 1730–1733.

(33) Tikhonova, L. G.; Serebryakova, E. S.; Proidakov, A. G.; Sokolov, I. E.; Vereshchagin, L. I. *J. Org. Chem. USSR* **1981**, *17*, 645–648.

(34) Lee, L. V.; Mitchell, M. L.; Huang, S. J.; Fokin, V. V.; Sharpless, K. B.; Wong, C. H. *J. Am. Chem. Soc.* **2003**, *125*, 9588–9589.

(35) Aucagne, V.; Leigh, D. A. *Org. Lett.* **2006**, *8*, 4505–4507.

(36) Kolb, H. C.; Finn, M. G.; Sharpless, K. B. *Angew. Chem., Int. Ed.* **2001**, *40*, 2004–2021.

(37) Bock, V. D.; Hiemstra, H.; van Maarseveen, J. H. *Eur. J. Org. Chem.* **2006**, 51–68.

(38) Himo, F.; Lovell, T.; Hilgraf, R.; Rostovtsev, V. V.; Noodleman, L.; Sharpless, K. B.; Fokin, V. V. *J. Am. Chem. Soc.* **2005**, *127*, 210–216.

(39) For a general procedure, see the Experimental Section.

(40) Vereshchagin, L. I.; Bolshedvorskaya, R. L.; Maksikova, A. V.; Serebryakova, E. S.; Kozyrev, S. V.; Bratilov, B. I.; Proidakov, A. G. *J. Org. Chem. USSR* **1987**, *23*, 2303–2307.

(41) Gerard, B.; Ryan, J.; Beeler, A. B.; Porco, J. A. *Tetrahedron* **2006**, *62*, 6405–6411.

(42) Bohlmann, F.; Bornowski, H.; Kleine, K.–M. *Chem. Ber.* **1964**, *97*, 2135–2138.

(43) Compound **303** has been renamed as **325** for convenience.

(44) Armitage, J. B.; Entwistle, N.; Jones, E. R. H.; Whiting, M. C. *J. Chem. Soc.* **1954**, 147–154.

Chapter 4. Synthesis and Physical Properties of α,ω–diarylpolyynes

4.1 Introduction

The synthesis of carbyne[1–6] has been an interesting subject in organic synthesis because it is a linear form of entirely sp–hybridized carbon, and traditionally it has been difficult to obtain systems in which there are greater than 10 triple bonds.[1] Thus, its physical properties, e.g., electronic, magnetic, optical, mechanical, thermal, etc.,[7–9] are not fully understood. Over the years, polyynes of different length and with a variety of different end capping groups have been reported, and a few selected examples are shown in Figure 4.1.[10,11] Hirsch and coworkers have synthesized and studied dicyano end capped polyynes **401**.[12] The series of compounds **401** was synthesized by vaporization of graphite under Krätschmer–Huffman conditions in the presence of dicyan $(CN)_2$.[13] Whiting synthesized and studied the optical properties of dimethyl end capped **402** to predict the behavior of carbyne.[10] Compounds **402** were produced by a homocoupling reaction of two terminal alkynes. Due to the instability of polyynes with methyl end caps, the *i*–Pr_3Si protecting group was introduced in recent years. Tykwinski and coworkers utilized a modified Fritsch–Buttenberg–Wiechell (FBW) rearrangement to synthesize the series **403** with 10 units of C≡C.[1,14] More importantly, they showed nonresonant molecular second hyperpolarizabilities (γ) were greater than theoretically predicted, which suggested a possible materials application for polyynes.[1,15–17] Hirsch and coworkers reported polyynes with aryl end caps **404**. The large aryl groups were used to provide better solubility and stability for the polyynes.[6] In addition to the terminal silyl and carbon protecting groups described above, transition metals (e.g., Re and Pt) have been used. Rhenium end capped polyynes **405** were synthesized by the combination of Cu–catalyzed oxidative homocoupling and cross–coupling reactions. These polyynes are reasonably stable and highly crystalline. They have a reversible oxidation state of +2 based on electrochemical measurements showing communication between the metal centers. Gladysz and coworkers have successfully constructed platinum end capped polyynes **406** by oxidative coupling of two terminal alkynes in the presence of CuCl. The PtC_nPt complexes were air–stable and no significant decomposition was observed after several days.[18]

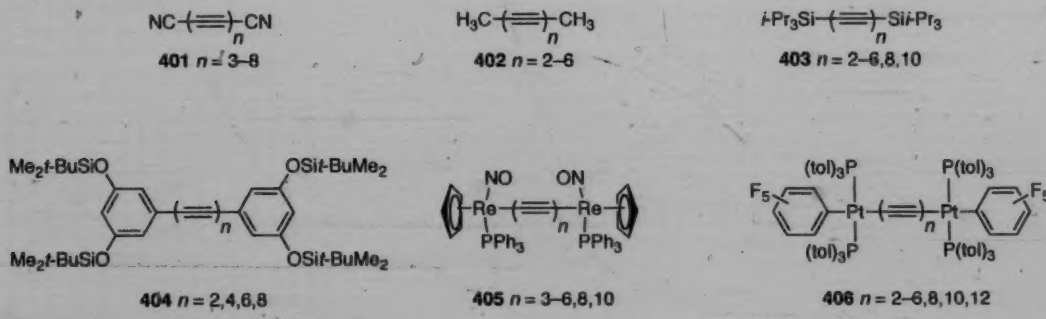
NC–(≡)n–CN
401 n = 3–8
H3C–(≡)n–CH3
402 n = 2–6
i-Pr3Si–(≡)n–Sii-Pr3
403 n = 2–6,8,10
Me2t-BuSiO
OSit-BuMe2
Me2t-BuSiO
OSit-BuMe2
404 n = 2,4,6,8
NO
ON
Re
Re
PPh3
PPh3
405 n = 3–6,8,10
(tol)3P
P(tol)3
F5
F5
Pt
Pt
(tol)3P
P(tol)3
406 n = 2–6,8,10,12

Figure 4.1 Polyynes **401–406**

Traditionally, conjugated polyynes have been synthesized by the homocoupling reaction between two terminal alkynes catalyzed by Cu(I/II). For example, the classic Glaser reaction used CuCl in NH_4OH, EtOH and O_2,[19] the Eglinton coupling reaction employed a Cu(I) halide, pyridine and O_2,[20] and the common Hay coupling reaction used a Cu(I) halide, TMEDA, and O_2.[21] Alternatively, polyynes can be synthesized by the cross–coupling reaction between a terminal alkyne and an alkynyl or aryl/vinyl halide derivative via the Cadiot–Chokiewicz reaction utilizing a Cu(I) halide in NEt_3,[22] the Castro–Stephens reaction using a Cu(I) halide in pyridine,[23] and the Sonogashira reaction using Pd(0), CuI, and NEt_3.[24] Polyynes can often be obtained under the conditions above, but utilizing terminal polyynes as a precursor is quite difficult, particularly in the case of longer terminal polyynes.[10,25] Thus, a variety of methods have been developed over the years to avoid the use of potentially hazardous precursors. For example, Tobe and coworkers have designed a method to form polyynes using indane as an alkyne protecting group. In the final step, the authors generate polyynes via a photochemical [2+2] cycloreversion process to generate the desired product.[26] An alternative approach to synthesizing conjugated alkynes using an octacarbonyl cobalt complex as an alkyne protecting group was explored by Diederich and coworkers. In this case the desired product could be formed by reductive elimination of the octacobalt precursor.[27]

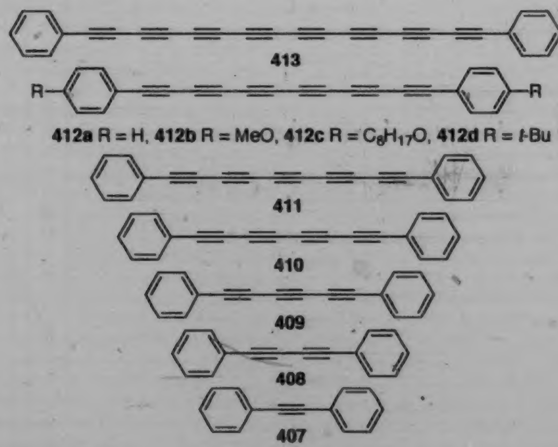

Figure 4.2 A series of conjugated polyynes **407–413**

We are interested in the formation of polyynes and their physical properties (Figure 4.2). In this chapter, we have overcome some of the synthetic challenges to obtain the polyynes **407–413** in good to excellent yield using a modified Fritsch–Buttenberg–Wiechell rearrangement.[1,14,28,29] Having polyynes **407–413** in hand, we explored their physical properties (UV–vis, ^{13}C NMR, nonlinear optical spectroscopic and X–ray crystallographic), and these results were compared with analogues such as compounds **403** and **404**. As well, some properties of carbyne can be predicted through extrapolation for our data.

4.2 Results and Discussion

4.2.1 Synthesis

A series of conjugated diarylpolyynes **407–413** were targeted. Monoyne **407** and diyne **408** have been reported previously.[10] The monoyne **407** can be synthesized by a number of means, including the rearrangement of a dichloroolefin[30–32] whereas the diyne **408** can be obtained from the Hay coupling reaction of phenylacetylene.[33] In this study, we report the syntheses of odd numbered polyynes **409** and **411**, the even numbered polyynes **410**, **412a**, **413**, unsymmetrical triynes **424a–c**, as well as several other ^{13}C–enriched polyyne derivatives via the FBW rearrangement.[15]

4.2.1.1 Synthesis of Odd Numbered Polyynes 409 and 411

The syntheses of triyne **409** and pentayne **411** were derived from the known aldehyde **414** (Scheme 4.1). The reaction of compound **414** with lithium acetylide **415a** or **415b**, generated from an appropriate alkyne, produced alcohol **416a**[34] in 80% yield and **416b** in lower yield (36%). These alcohols were oxidized with PCC and the resulting ketones were obtained by passing the reaction mixture through a short plug of silica gel and celite. A Corey–Fuchs reaction of the crude ketones gave dibromoolefin **417a** as a light yellow solid and tetrabromoolefin **417b**[34] as a yellow crystalline solid in good yield. A one– or two–fold FBW rearrangement effected on precursors **417a** or **417b** proceeded smoothly via slow addition of 1.2 or 2.4 equiv of BuLi to a solution of the respective precursor in toluene at –78 °C to give diphenyltriyne **409** in 79% yield and diphenylpentayne **411** in 50% yield, respectively.

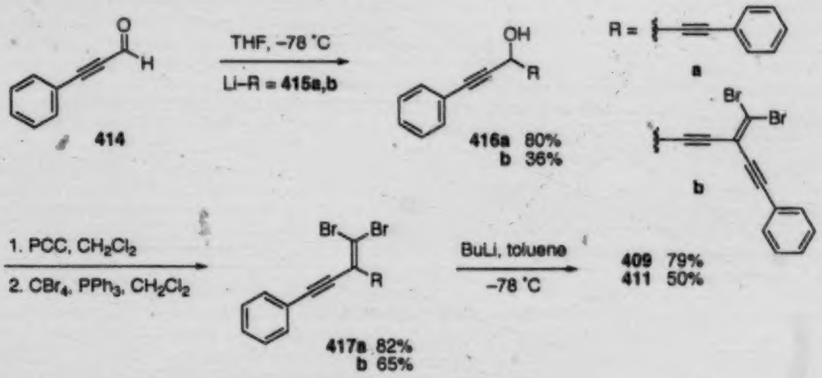

Scheme 4.1 Synthesis of unsymmetrical polyynes **409** and **411**

Diederich and coworkers have previously synthesized both triyne **409** and pentayne **411** using the solution–spray flash vacuum pyrolysis (SS–FVP) method. The authors converted 3,4–bis(1–phenylethynyl)–3–cyclobutene–1,2–dione and 3,4–bis(1,3–phenylbutadiynyl)–3–cyclobutene–1,2–dione into triyne **409** and pentayne **411**, respectively.[35] Triyne **409** has also been previously obtained by the Negishi coupling of a terminal alkyne with iodobenzene.[36]

4.2.1.2 Synthesis of Even Numbered Polyynes 410, 412, and 413 via a Double Rearrangement

Even numbered diaryl tetrayne **410**, hexayne **412a**, and octayne **413** were synthesized by a two–fold rearrangement (Scheme 4.2).[14] The desilylation of monoyne **418a** or diyne **418b** in a mixture of K_2CO_3, MeOH and THF (1:1 v:v), produced a terminal alkyne.[36] The solution of a crude terminal alkyne was quenched with sat. aq. NH_4Cl, washed with sat. aq. NaCl, and the resulting solution was concentrated to ca. 2 mL. This solution of the terminal alkyne was added to a Hay catalyst (prepared mixture of CuCl, TMEDA and CH_2Cl_2) to produce tetrabromoolefins **419a,b** in good to excellent yield. The FBW rearrangement of the bromide **419b** in toluene at –20 °C produced tetrayne **410** in 53%, but formation of hexayne **412a** was unsuccessful due to the low solubility of precursor **419b** in hexanes or toluene. Attempts to rearrange compound **419b** in toluene at 0 °C gave intractable material and recovered trace amounts of starting material.

Hexayne **412a** and octayne **413** could be obtained by an alternative method, as previously shown by a talented undergraduate, Erin Elliott (Scheme 4.2). Dibromoolefins **420a,b** were first desilylated, followed by oxidative homocoupling to generate tetrabromoolefins **421a,b** in good yield. Precursors **421a,b** were nearly insoluble in hexanes. Toluene was thus chosen as a solvent for the rearrangement step, which then afforded the hexayne **412a** and octayne **413** in low yield.

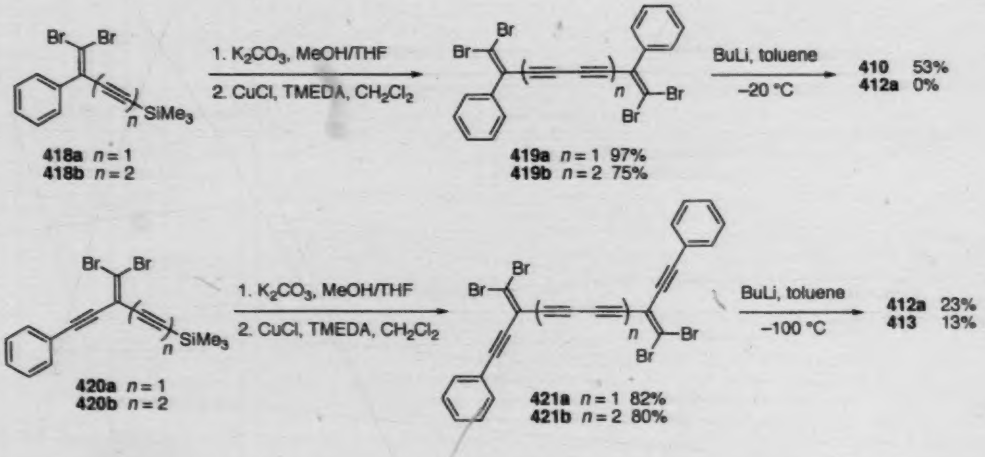
Br
Br
SiMe$_3$
n
418a n = 1
418b n = 2
1. K$_2$CO$_3$, MeOH/THF
2. CuCl, TMEDA, CH$_2$Cl$_2$
419a n = 1 97%
419b n = 2 75%
BuLi, toluene
–20 °C
410 53%
412a 0%
420a n = 1
420b n = 2
421a n = 1 82%
421b n = 2 80%
–100 °C
412a 23%
413 13%

Scheme 4.2 Syntheses of symmetrical polyynes **410, 412a** and **413**

It can be noted that polyynes **410**, **412a**, and **413** were previously synthesized by Walton and coworkers using an oxidative homocoupling reaction of two corresponding terminal alkynes in the presence of CuCl and TMEDA.[10,37]

4.2.1.3 Synthesis of Aryl Hexaynes 412a–e

Aryl hexaynes **412a–e** were targeted (Scheme 4.3). Dibromoolefins **422a–e** were synthesized from the corresponding acid chlorides and 1,4–bis(trimethylsilyl)butadiyne, followed by dibromoolefination. Rearrangement of the dibromoolefins was induced with BuLi in hexanes to produce triynes **423a–d** in good to excellent yield. Unfortunately, the reaction of nitro derivative **422e** does not lead to a FBW rearrangement, and no starting material was recovered. The desilylation of triynes **423a–d** with K_2CO_3 in MeOH/THF afforded kinetically unstable terminal triynes. These crude triynes were subjected to Hay conditions to produce the desired hexaynes **412a–d** in good yield. Contrary to their terminal alkyne precursors, compounds **412a–d** were isolated as kinetically stable orange solids.

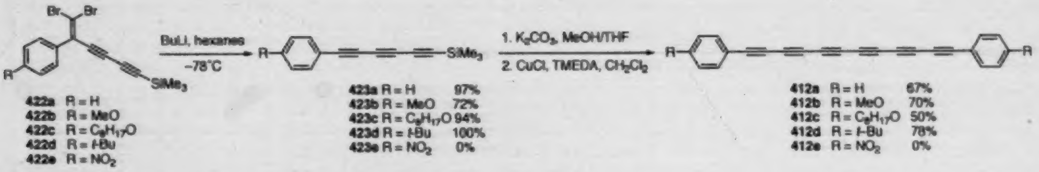
BuLi, hexanes
−78°C
1. K₂CO₃, MeOH/THF
2. CuCl, TMEDA, CH₂Cl₂
422a R = H
422b R = MeO
422c R = C₈H₁₇O
422d R = t-Bu
422e R = NO₂
423a R = H 97%
423b R = MeO 72%
423c R = C₈H₁₇O 94%
423d R = t-Bu 100%
423e R = NO₂ 0%
412a R = H 67%
412b R = MeO 70%
412c R = C₈H₁₇O 50%
412d R = t-Bu 78%
412e R = NO₂ 0%

Scheme 4.3 Syntheses of symmetrical hexaynes **412a–d**

4.2.1.4 Synthesis of Aryl Triynes 424a–c

Monoaryl triynes **424a–c** bearing either electron–donating or eletron–withdrawing groups were synthesized as shown in Scheme 4.4. The reaction of dibromoolefin **425** with LDA in Et_2O afforded lithium acetylide **426**. This intermediate reacted with aldehydes **427a,b** to form alcohols **428a,b** in low yield. It also underwent transmetallation with $ZnCl_2$ to form the zinc acetylide, which was then coupled to iodoalkyne **429** in the presence of a catalytic amount of $Pd(PPh_3)_4$ to produced triyne **424c** in good yield. Oxidation of alcohols **428a** and **428b** with PCC formed the corresponding ketones, which were isolated simply by passing the crude mixture through a plug of silica gel and Celite. Corey–Fuchs reaction of the ketones resulted in dibromoolefins **430a** or **430b**[38] in low yield over the two steps. FBW arrangement of the dibromoolefins with BuLi under standard conditions produced triynes **424a,b** in excellent yield.

The formation of **412e** from **424c** was also attempted. Desilylation of **424c** gave the terminal triyne, as monitored by TLC. When this crude triyne was subjected to Hay conditions at room temperature or 0 °C, the starting materials disappeared and a new spot appeared that was monitored by TLC. This new product was stable to column chromatography and isolation. Unfortunately, this product was not the desired hexayne **412e**, and the product remained unidentified.

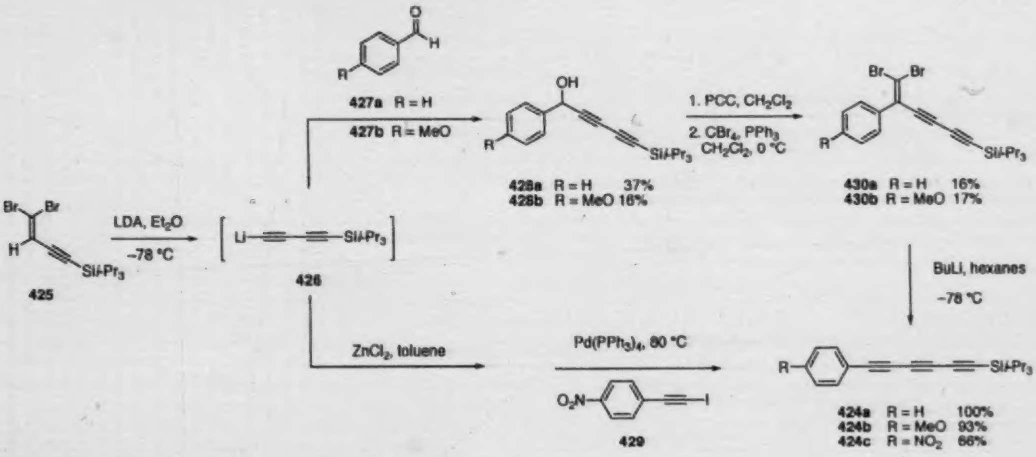

427a R = H
427b R = MeO
OH
428a R = H 37%
428b R = MeO 16%
1. PCC, CH_2Cl_2
2. CBr_4, PPh_3, CH_2Cl_2, 0 °C
430a R = H 16%
430b R = MeO 17%
425
LDA, Et_2O, −78 °C
426
BuLi, hexanes, −78 °C
$ZnCl_2$, toluene
$Pd(PPh_3)_4$, 80 °C
429
424a R = H 100%
424b R = MeO 93%
424c R = NO_2 66%
Si*i*-Pr$_3$

Scheme 4.4 Synthesis of triynes **424a–c**

4.2.1.5 Synthesis of ^{13}C Labeled Polyynes 431–433

Well resolved alkyne signals were found in the ^{13}C NMR spectra for unlabeled polyynes **407–413**. Attempting to identify the resonance of each individual alkynyl carbon, however, was more of a challenge than anticipated. Thus, three labeled compounds **431–433** were prepared to determine chemical shifts of individual sp–hybridized carbon as a function of alkyne unit (Scheme 4.5) Triyne **431** was formed in two steps starting from ketone **434**. A mixture of CBr_4 (containing 20% of $^{13}CBr_4$) and PPh_3 added to a solution of the ketone afforded labeled dibromoolefin **435** in 79% yield. The enriched carbon introduced at the alkylidene position was verified by ^{13}C NMR spectroscopy. Standard rearrangement of the dibromoolefin with BuLi produced triyne

431 in 62% yield. During the rearrangement, either of the phenylacetylene groups could migrate to form compound **431** with only one carbon enrichment at position C3.

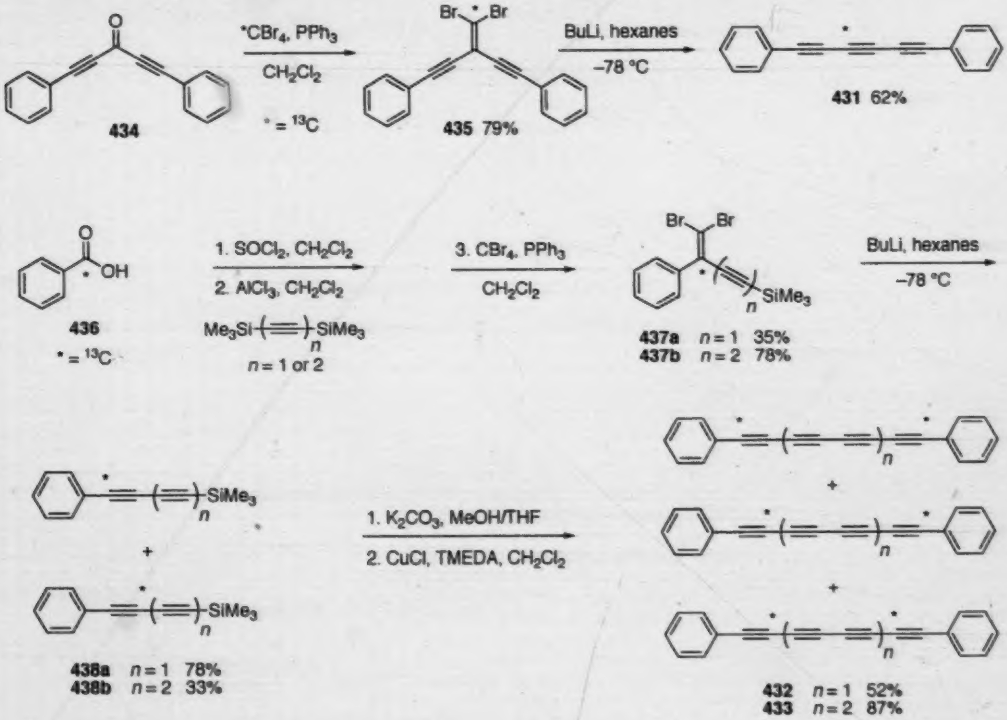

434
*CBr4, PPh3
CH2Cl2
* = 13C
Br
Br
435 79%
BuLi, hexanes
−78 °C
431 62%
436
* = 13C
OH
1. SOCl2, CH2Cl2
2. AlCl3, CH2Cl2
Me3Si(≡)nSiMe3
n = 1 or 2
3. CBr4, PPh3
CH2Cl2
SiMe3
437a n = 1 35%
437b n = 2 78%
BuLi, hexanes
−78 °C
SiMe3
438a n = 1 78%
438b n = 2 33%
1. K2CO3, MeOH/THF
2. CuCl, TMEDA, CH2Cl2
n
432 n = 1 52%
433 n = 2 87%

Scheme 4.5 Synthesis of labeled polyynes **431–433**

The formation of tetrayne **432** and hexayne **433** was also achieved. The reaction of benzoic acid **436** (100% ^{13}C enrichment) in CH_2Cl_2 with thionyl chloride produced the crude acid chloride. This acid chloride reacted with 1,2–bis(trimethylsilyl)acetylene or 1,4–bis(trimethylsilyl)butadiyne in the presence of the Lewis acid $AlCl_3$ to produce ketone, which was subsequently subjected to Corey–Fuchs conditions to produce the dibromoolefins **437a,b**. Rearrangement of the dibromoolefins with BuLi yielded alkynes **438a,b**. In these reactions, either the alkyne or the phenyl group can migrate to form di– or triyne **438a** or **438b** with a single enriched carbon at either the α– or β–position, denoted with an asterisk (*). A sequence of desilylation to form a terminal alkyne and homocoupling of the resulting alkyne produced targeted compounds **432** and **433** as a mixture of α,α–, α,β–, and β,β–isotopomers. Unfortunately, the yields for the reactions in Scheme 2.5 are lower than those of the unlabeled polyynes because the products generally required an extensive purification by column chromatography to remove the byproducts containing ^{13}C enrichment. Contamination of the byproducts would hinder the ^{13}C NMR spectroscopic analysis.

4.2.2 Physical Properties

The thermal stability of compounds **407–413** and **424a–c** was investigated via conventional melting point and differential scanning calorimetry (DSC) analyses and the results are shown in Table 4.1. Monoyne **407** has a reported melting point of 56–61 °C (Aldrich) and diyne **408** has an observed melting point of 81–83 °C. Diphenyltriyne **409** has an observed melting point of 87–89 °C. The melting point of the first three polyynes **407–409** in the series thus increases as a function of number of triple bonds.

Table 4.1 Melting points and DSC data of polyynes **403–412d,** and **413**

Compound	Observed Melting Point or DSC Analysis (°C)[a]
407	56–61[b,c]
408	81–83[c]
409	87–89[c]
410	$T_o = 115$, $T_{max} = 120$ (sharp, endotherm)[d]
	$T_o = 120$, $T_{max} = 162$ (medium, exotherm)[d]
411	$T_o = 170$, $T_{max} = 173$[d]
412a	$T_o = 133$, $T_{max} = 148$[d]
412b	$T_o = 138$, $T_{max} = 166$[d]
412c	$T_o = 132$, $T_{max} = 134$ (sharp, endotherm)[d]
	$T_o = 157$, $T_{max} = 196$ (broad, exotherm)[d]
412d	$T_o = 144$, $T_{max} = 157$[d]
413	$T_{o1} = 84$, $T_{max1} = 94$[d]
	$T_{o2} = 98$, $T_{max2} = 111$[d]

[a] T_o defines the onset temperature and T_{max} the maximum of the endotherm or exotherm. Sharp, medium, and broad are an empirical description of the event. [b] Purchased from Aldrich. [c] Melting Point analysis. [d] DSC analysis.

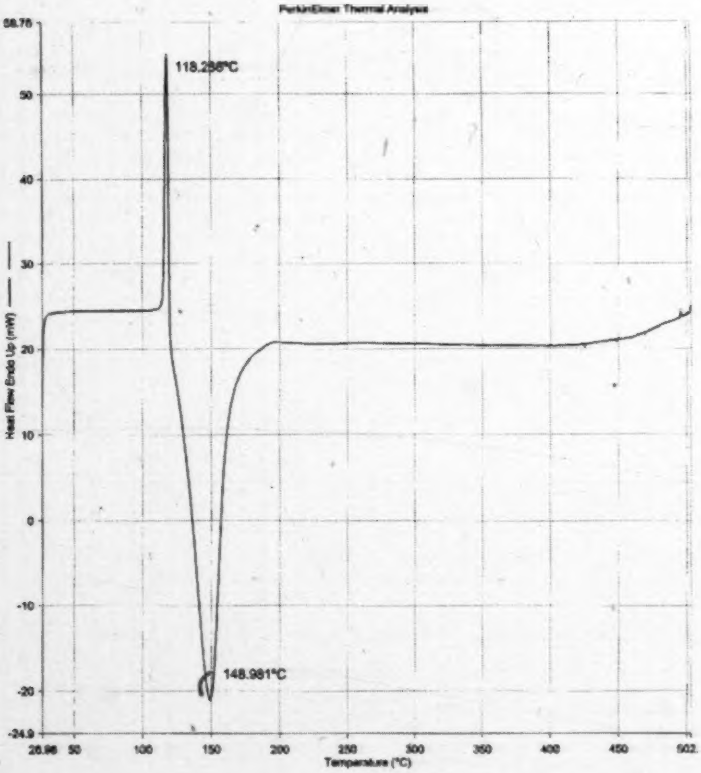

Figure 4.3 DSC trace of tetrayne **410**

The thermal behavior of the remaining seven polyynes **410–413** was assessed using DSC. Tetrayne **410** has a sharp endotherm (T_o = 115, T_{max} = 120 °C) that was quickly followed by an exotherm (T_o = 120, T_{max} = 162 °C) as shown in Figure 4.3. The sharp endotherm is an indication that the molecules may undergo a phase transition, which is followed by exothermic decomposition (reaction or polymerization).

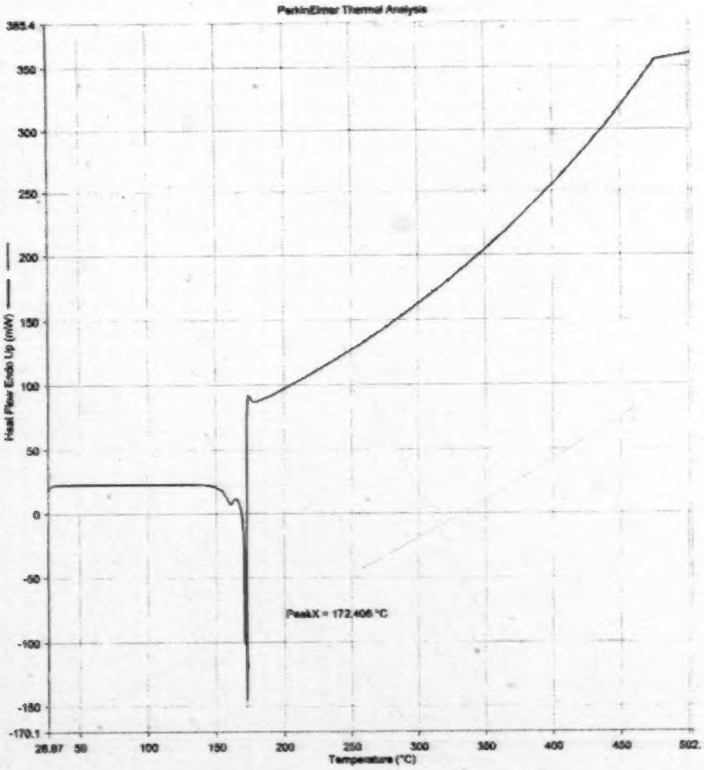

Figure 4.4 DSC trace of pentayne **411**

DSC analysis of pentayne **411** shows a sharp exotherm at 173 °C, T_o = 170 and T_{max} = 173 °C, an indication of polymerization (Figure 4.4). In fact, Diederich and coworkers have previously suggested that this pentayne could undergo a 1,4–topochemical polymerization.[35]

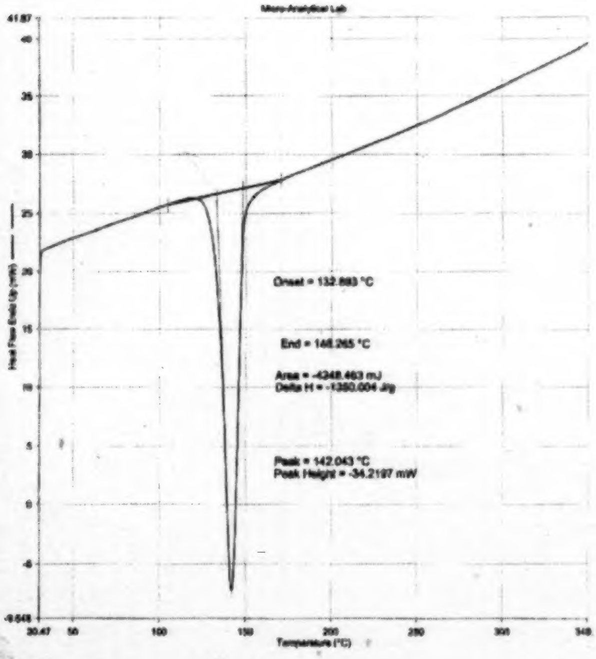

Figure **4.5** DSC trace of hexayne **412a**

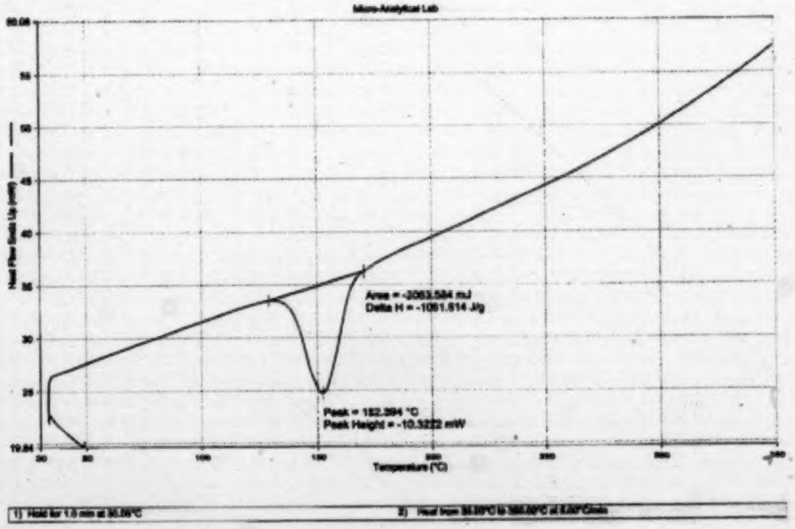

Figure **4.6** DSC trace of hexayne **412b**

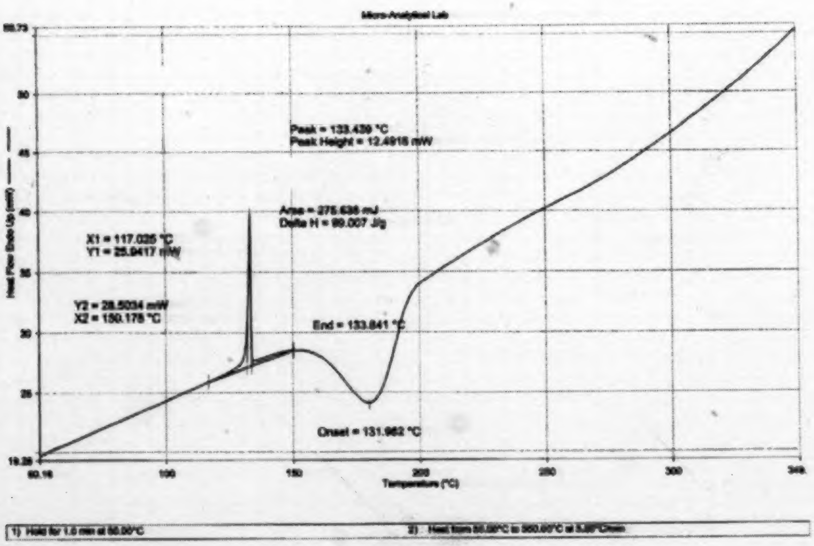

Figure 4.7 DSC trace of hexayne **412c**

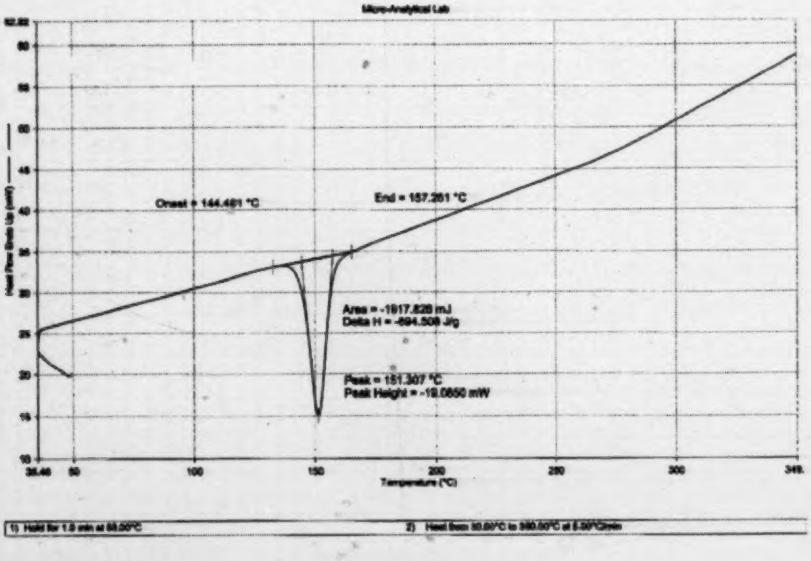

Figure 4.8 DSC trace of hexayne **412d**

In the DSC analysis of the diphenylhexayne series **412a–d**, hexayne **412a** shows no melting point, but a rather sharp exothermic peak with T_o = 133 and T_{max} = 148 °C, and anisyl derivative **412b** displays a similar, but broader, exotherm (T_o = 138, T_{max} = 166 °C). An interesting result is observed for the octyl derivative **412c**, which shows a sharp endotherm (T_o = 132, T_{max} = 134 °C), quickly followed by a rather broad exothermic peak with an onset temperature of 157 °C and a maximum temperature of 196 °C. This implies that compound **412c** undergoes a phase transition that leads to polymerization. Butyl derivative **412d** shows a narrow exotherm with an onset temperature of 144 °C and a maximum temperature of 157 °C.

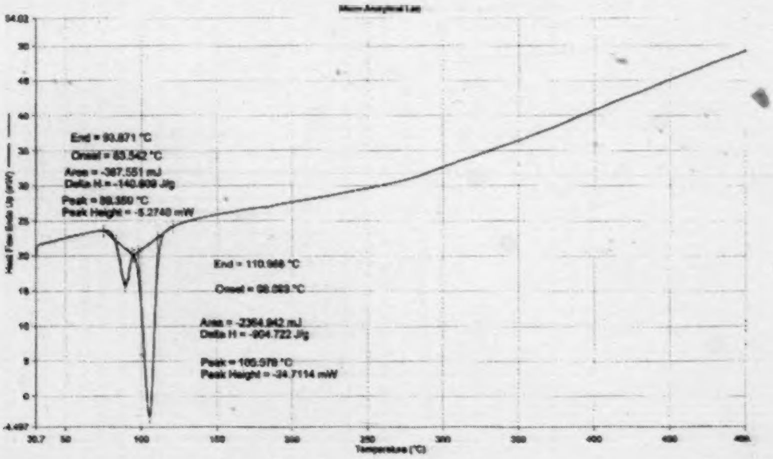

Figure 4.9 DSC trace of octayne **413**

The DSC analysis of diphenyloctayne **413** shows two rather distinctive exothermic peaks. The first peak has an onset temperature of 84 °C and ends at 94 °C. This second peak has a larger exotherm, T_{o2} = 98 °C and T_{max2} = 111 °C. At present, the reason for this behavior is unknown. In summary, DSC data of compounds **410–413** do not show any remarkable observation, other than exotherms and endotherms

In summary, there does not seem to be a distinct trend between the length of the polyyne and the observed thermal behavior as measured by DSC. Nonetheless, a wealth of information for each individual molecule can be extracted, including clues as to whether a particular system is prone to topochemical polymerization.

The observed melting points of the unsymmetrical triynes **424a–c** were also measured. Phenyltriyne **424a** is a yellow oil at room temperature and crystallizes at –4 °C; the other two aryl triynes have melting points of 67–70 °C and 112–115 °C for compounds **424b** and **424c**, respectively.

Table 4.2 Melting points of triynes **424a–c**

Triyne	Observed Melting Point (°C)
424a	Yellow oil
424b	67–70
424c	112–115

4.2.3 ^{13}C NMR Spectroscopy

Chemical shifts of individual alkynyl carbons in diaryl phenyl polyynes **407–412a**, and **413** have been investigated. The spectra of these polyynes have been obtained in $CDCl_3$ at 125 MHz and are summarized in Table 4.3. The ^{13}C chemical shifts of the phenyl end groups are omitted for clarity. Two distinct areas of interest are assigned as Regions 1 and 2 (Figure 4.10). Region 1 contains lower field resonances (90–73 ppm). Region 2 contains the remaining sp–carbon resonances at higher field (68–62 ppm). The sp–carbon connecting to one phenyl ring is assigned as C1 and the adjacent sp–carbon to C1 is consequently numbered as C2, and so on up to C8 in the octayne **413**.

Carbon C1 can be easily identified using the long–range (two and three bond, but not one bond) proton–carbon couplings between carbon C1 and the *ortho*–proton of the phenyl ring in the HMBC (Heteronuclear Multiple Bond Coherence) experiment. The chemical shift of the sp–hybridized carbon in diphenylacetylene **407** is 89.4 ppm. Diyne **408** shows two signals in Region 1. C1 can be assigned as described above and the other signal is thus carbon C2 at 73.9 ppm.

Identifying the sp–hydridized carbons in triyne **409** can be complicated. Carbon C1 appears at 78.6 ppm. The other two higher field carbons resonate at 74.4 ppm and 66.5 ppm. ^{13}C enrichment is a powerful tool to solve this challenge. The enhanced signal at 66.5 ppm in the ^{13}C NMR spectrum of the carbon enrichment **431** shows this arises from the middle triple bond carbon C3 and the remaining sp–hybridized carbon is thus assigned as C2 at 74.4 ppm.

Four alkynyl signals are observed in the ^{13}C NMR spectrum for tetrayne **410**, one of which is assigned as C1 (77.7 ppm) from the HMBC experiment. The remaining three signals (C2, C3, C4) could not be identified, and the ^{13}C NMR spectrum of carbon–enriched tetrayne **432** was used to distinguish the three unassigned signals. Two intense signals of the ^{13}C labeled carbons were assigned as carbons C1 at 77.7 ppm and C2 at 74.4 ppm. Alkynyl carbons C3 and C4 are resolved based on the carbon–carbon coupling constant. Carbon C3 (63.7 ppm) has a larger coupling constant of 158 Hz ($^{1}J_{C3\text{–}C2}$), and a smaller value of 20 Hz ($^{2}J_{C4\text{–}C2}$) is observed for C4.

The chemical shifts of the sp–carbons of hexayne **412a** can be assigned via the ^{13}C NMR spectrum of the labeled compound **433**. Six sp–hybridized carbon signals are observed as expected. C1 has a chemical shift of 77.5 ppm, one of the two enhanced signals from the labeled compound. The remaining intense signal is C2 at 74.3 ppm. A signal C3 at 62.6 ppm has the largest coupling constant to C3 ($^1J_{C3–C2}$ = 159 Hz) and the signal of C4 at 67.3 ppm has a smaller constant to C4 ($^2J_{C4–C2}$ = 19 Hz). Fortunately, internal sp–carbon C5 (63.6 ppm) can also be determined with the smallest coupling constant of 5 Hz ($^3J_{C5–C2}$) and the remaining signal is assigned as C6 at 64.6 ppm.

The chemical shifts of the sp–hybridized carbons of pentayne **411** have not been assigned, except C1 at 77.5 ppm from HMBC experiment. Likewise, only the chemical shift of carbon C1 at 77.6 ppm of octayne **413** is identified.

Table 4.3 Summary of alkyne chemical shifts for polyynes **407–412a,** and **413**

Compound	Chemical Shifts (ppm, in CDCl$_3$)
413	77.6, 74.3, 67.2, 64.5, 63.6, 63.4, 63.3, 62.6
412a	77.5, 74.3, 67.3, 64.6, 63.6, 62.6
411	77.5, 74.4, 67.3, 64.5, 62.8
410	77.7, 74.4, 67.2, 63.7
409	78.6, 74.4, 66.5
408	81.6, 73.9
407	89.4

As a result of this study, one might tentatively assign the alkynyl carbons in the diphenyl polyynes based on following guidelines: (a) signals for the C1 atoms starting from the most downfield in Region 1 shift upfield toward the $CDCl_3$ signals centered at 77.0 ppm; (b) signals for C2 atoms stay at ca. 74.4 ppm, except for C2 in the diyne at 73.9 ppm; (c) signals for C3 atoms in Region 2 shift upfield with the most variation, from 66.5 ppm → 63.7 ppm → 62.8 ppm → 62.6 ppm → 62.6 ppm for the triyne to hexayne (octayne), respectively; and (d) signals for C4 atoms are unchanged ca. 67.2 ppm.

Assuming the trends outlined above for shorter polyynes hold true for longer derivatives, one can predict the 13C NMR chemical shift of the carbons of carbyne (i.e., Ph–$(C\equiv C)_n$–Ph with *n* approaching infinity). We expect the first four alkynyl carbons C1–C4 of carbyne to vary as they do in the diphenyl end capped polyynes with C1 near 77.5 ppm, C2 at 74.3 ppm, C3 at 62.6 ppm and C4 at 67.2 ppm. The remaining carbon resonances should be found as a single signal, or range of very closely spaced signals, between 63.6–63.4 ppm, as observed for the octayne **413**.

The results for the alkynyl carbon assignment in the diphenyl polyynes **407–412a** and **413** were compared to the known polyynes **403** and **404** (Figure 4.1). The results of the chemical shift of the sp–hybridized carbons in diarylpolyynes **404** is similar to our polyynes than the silyl protective group **403.** Hirsch and coworkers reported the ^{13}C chemical shifts for the alkynyl signals (tetrayne, hexayne, and octayne of compounds **404**) measured in the same solvent as our experiment ($CDCl_3$). Signals for C1 atoms were assigned at 73.9 ppm, 73.8 ppm, and 73.7 ppm for the tetrayne, hexayne, and octayne, respectively. The upfield shift of the C1 signals in Hirsch's study is the same as our results of C2. The chemical shifts of the C2 atoms were reported at ca. 77 ppm (77.6 ppm, 77.4 ppm, and 77.5 ppm). The conclusion from Hirsch's observation is, however, slightly different from that of our studies. We show that the signals of the C1 atoms shift upfield and approach the deuterated chloroform signals; the C2 signals stay at ca. 74 ppm. In Hirsch's studies of **404**, signals for C3 atoms were assigned at 67 ppm (67.10 ppm, 67.13 ppm, and 67.04 ppm).[6] In our case, the most upfield signals C3 continue to shift upfield as each triple bond added. Finally, in Hirsch's study the chemical shifts of C4 at ca. 63.6 ppm but ours have a chemical shift at 67.4 ppm. Thus, the assignment of the signals for C3 and C4 in Hirsch's study are reversed from ours.

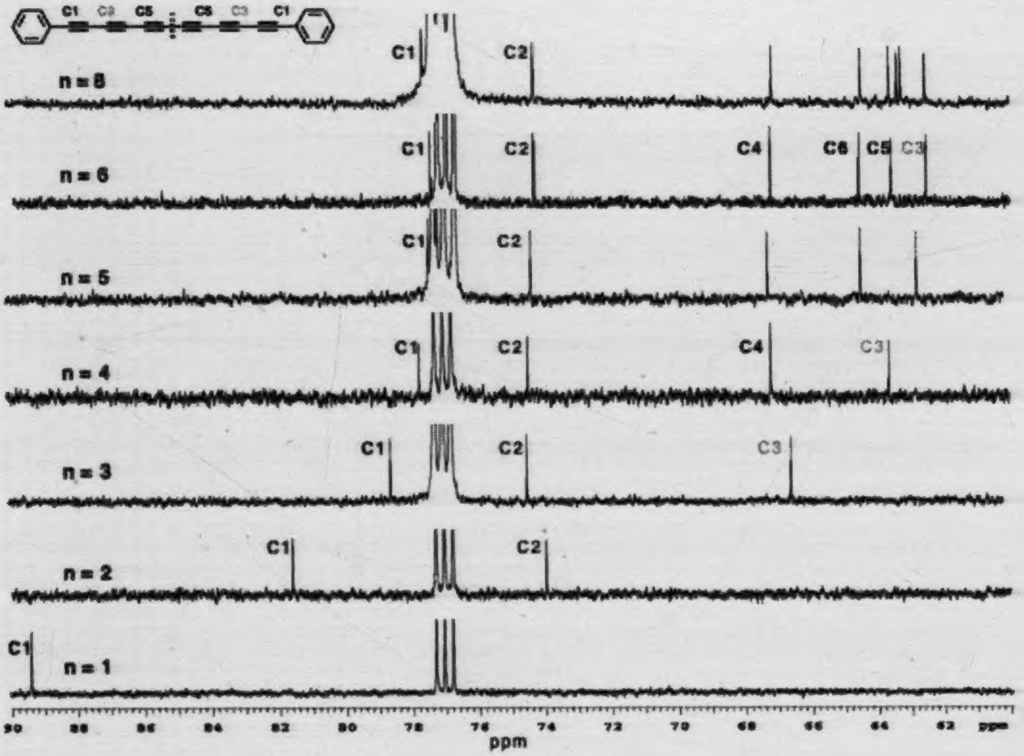

Figure 4.10 ^{13}C NMR spectra of diphenyl polyynes **407–412a** and **413**

The chemical shifts of the triple bond carbons in the diphenyl polyynes **407–412a** and **413** are also compared to the series of polyynes **403** (See Figure 4.1). The measurements of **403** were, however, done in a different solvent (CD_2Cl_2). A former graduate student from the Tykwinski group, Dr. Sara Eisler, showed that the chemical shifts of C1 of the series **403** moves downfield dramatically from 82.2 ppm for diyne to 88.8 ppm for decayne.[1] This study also showed that the chemical shift of the C1 carbon is significantly affected by each additional triple bond, but that of the C2 carbon is essentially unaffected (ca. 90 ppm). Those of the C3 atoms move downfield from 61.5 ppm for triyne to 63.0 ppm for hexayne. These results for C3 are different from the diphenyl polyyne series, where the signals shift in an opposite direction. The signals for C4 in the case of **403** stay unchanged, as for the Ph–polyynes.

Overall, the trend for the diphenyl polyynes (**407–412a** and **413**) is more similar to that of the Hirsch's studies than to the series **403**.[6] The aryl end caps and the diphenyl polyyne presumably have a similar effect on the chemical shifts of the alkynyl carbons whereas the *i*–Pr_3Si end caps do not. It is currently unknown whether this difference arises from the different end groups or the solvent ($CDCl_3$ vs CD_2Cl_2).

Overall, the observed trend in chemical shifts for the diphenyl polyynes $CDCl_3$ (**407–412a** and **413**) is more similar to that determined by Hirsch in his studies of the series **404** (in $CDCl_3$) than to found by Eisler for the series **403** (in CD_2Cl_2).[6] The aryl end caps and the diphenyl polyyne presumably have a similar effect on the chemical shifts of the alkynyl carbons. This stands to reason, since the aryl groups of **404** conjugate to the polyyne chain in the same was as the phenyl groups of phenyl end–capped series, whereas the silyl groups of series **403** are electronically inert. It is also possible, although less likely, that the difference in solvent between the two studies ($CDCl_3$ vs CD_2Cl_2), also plays a role.

The chemical signals of the six sp–hybridized carbons for the homologues **412a–d** do not show any significant distinctive trends. However, the signals do not overlap within a series. Thus, *para*–substituents such as methoxyl, octoxyl, and tert–butyl, have little effect on the resonances of the alkynyl carbons.

Unsymmetrical triynes **424a–c** with different *para*–substituents, ranging from electron–donating to electron–withdrawing groups, have also been examined. The alkynyl carbons C1 (directly bonded to the aryl group) appear at ca. 77 ppm for all three cases, as determined by HMBC experiments.

4.2.4 Electronic Properties

Data from infrared, mass, and UV–vis spectroscopic analyses for the diphenyl polyynes **407–413** and unsymmetrical triynes **424a–c** are summarized in Table 4.4 and Table 4.5.[15] Infrared spectroscopy is a very useful technique to identify functional groups, but it is not particularly suitable for symmetrical molecules, such as diphenyl polyynes, since the intensity of an IR spectrum depends on the dipole moment of the compounds. The IR spectra of the diphenyl polyynes were measured as films cast from a solution of CH_2Cl_2. A very weak alkynyl signal is observed for diyne **408** whereas two signals are observed for triyne **409**, a weak intensity signal at 2245 cm^{-1} and a medium intensity signal at 2192 cm^{-1}. Infrared spectra of tetrayne **410** and pentayne **411** contain a medium intensity signal at 2200 cm^{-1} and 2185 cm^{-1}, respectively. The intensity of the alkynyl stretching signal increases in hexaynes **412a–c**. The band becomes a doublet for **412a** and **412c**, but not in methoxy derivative **412b**. This splitting band is useful for alkyne identification.[39] Octayne **413** shows a medium intensity band at 2184 cm^{-1} and a strong signal at 2105 cm^{-1}. Other than the additional signals and stronger stretches for the longer polyynes, no particular trends have been observed.

Table 4.4 Summary data for IR and EIMS for **408–413**

Compound	IR (cm^{-1}, in DCM, cast)	EIMS (70 eV, m/z)
408	2150 (w)	M$^+$ (100%)
409	2245 (w), 2192 (m)	M$^+$ (100%)
410	2200 (m)	M$^+$ (100%)
411	2185 (m)	M$^+$ (100%)
412a	2159 (s), 2174 (s)	M$^+$ (100%)
412b	2171 (s)	M$^+$ (100%)
412c	2168 (s), 2152 (s)	NA[a]
412d	2173 (s), 2158 (s)	M$^+$ (84%)
413	2184 (m), 2105 (s)[b]	NA[c]

[a] Obtained by MALDI MS. [b] Cast from THF. [c] Not obtained.

Electron impact mass spectroscopy (EIMS) was used to analyze diaryl polyynes **408–413**. In most cases, the molecular ion peak was the base peak. For octoxyl derivative **412c**, MALDI MS was used, but a molecular ion peak was not observed.

The IR and EIMS spectroscopic analyses of unsymmetrical triynes **426a–c** do not show any significant trends. The triynes show a base peak (100%) for molecular ion (M – iPr)$^+$. Their data are reported in the Appendix.

UV–vis spectroscopy is a useful technique to characterize conjugated polyynes. The absorption spectra for diphenyl polyynes **407–412a** and **413** are shown in Figure

4.11 and these results are summarized in Table 4.5. Two significant regions are observed, a higher energy Region 1 containing signals with greater absorbance coefficients, and a lower energy Region 2 containing signals with smaller absorbance coefficients. Monoyne **407** and diyne **408** show only one significant absorption in Region 1, but the other polyynes show absorptions in both regions. As the number of triple bonds is increased, the absorptions show a bathochromic shift for both regions. For example, tetrayne **410** has a higher energy absorption (288 nm) than octayne **413** (344 nm). Likewise the tetrayne and octayne have maximal absorption peaks at 399 nm and 512 nm, respectively, in Region 2. Furthermore, the molar absorptivities also increase as a function of the number of triple bonds for Region 1. However, in Region 2 the molar absorptivities decrease with an increase in the conjugated system. For example, triyne **409** has a molar absorptivity of 21600 L mol^{-1} cm^{-1} (at 361 nm) whereas octayne **413** has a molar absorptivity of 3600 L mol^{-1} cm^{-1} (at 512 nm).

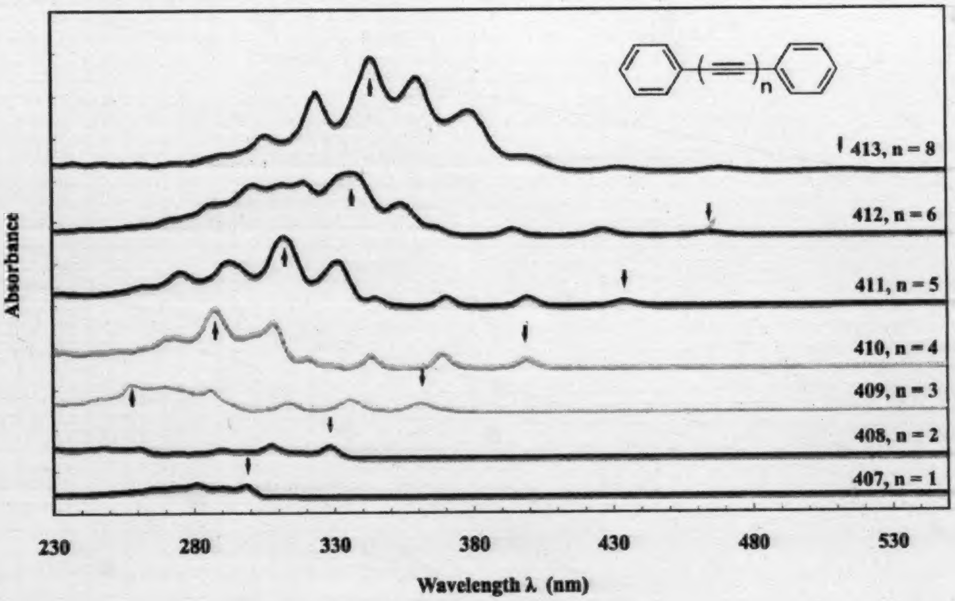

Figure 4.11 UV–vis spectra of polyynes **407–412a** and **413**. Up arrows denote λ_{max} for Region 1 and down arrows λ_{max} for Region 2.

Table 4.5 UV–vis data for the λ_{max} in both regions in THF for **407–412a** and **413**

Compound	λ_{max} (nm) Region 1 ε (L mol^{-1} cm^{-1})	λ_{max} (nm) Region 2 ε (L mol^{-1} cm^{-1}),
413	344 (272 000)	512 (3 600)
412a	337 (155 000)	476 (13 300)
411	312 (167 000)	434 (12 500)
410	288 (143 000)	399 (22 000)
409	258 (70 900)	361 (21 600)
408	328 (30 000)	NA
407	299 (22 400)	NA

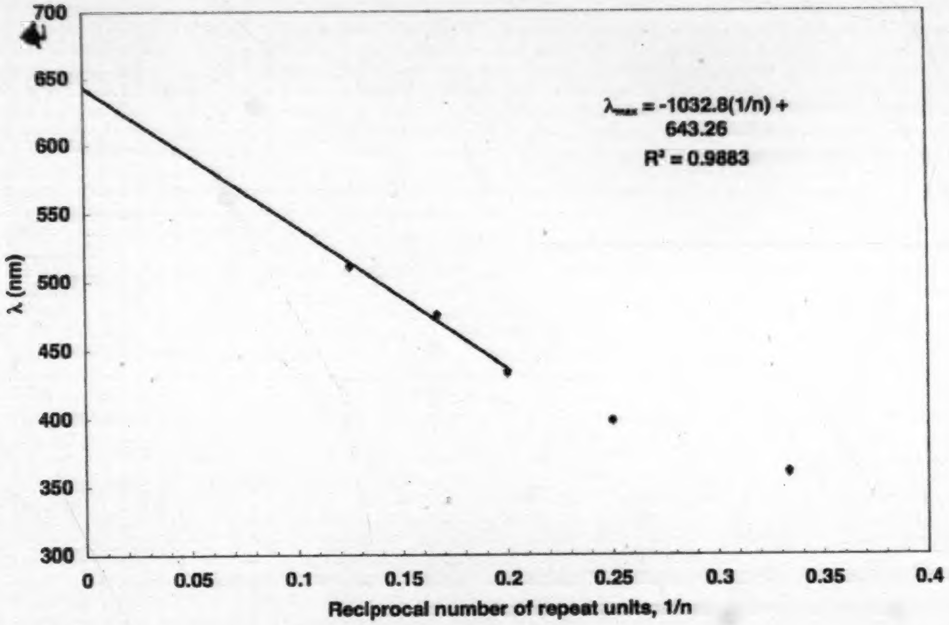

Figure 4.12 Plot of λ_{max} of lowest energy absorption versus the reciprocal of the number of triple bonds for compounds **407–409**

A red shift in λ_{max} indicates a decrease in the HOMO–LUMO energy gap. This trend can be used to estimate the HOMO–LUMO band–gap of carbyne. By plotting the lowest energy wavelength against the reciprocal number of repeat units (1/n), a plot is obtained that allows one to estimate a λ_{max} of a saturated polyyne system, i.e., one in which extension of the polyyne length by another alkyne unit has no effect (Figure 4.12). The extrapolation of the last three points (pentayne **411**, hexayne **412a** and octayne **413**) with the reciprocal number of triple bonds (1/5, 1/6, 1/8) generates a linear equation λ_{max} (nm) = –1032.8(1/*n*) + 643.26. When $n \rightarrow \infty$, the term (1/*n*) becomes zero and the term –1032.8(1/*n*) is thus zero. The constant term is 643.26 nm, and this is then the estimated

λ_{max} for an infinite polyyne, i.e., carbyne. The result obtained from α,ω–diphenylpolyyne **407–412a**, **413** (i.e., λ_{max} ca. 643 nm) is different from that predicted for the *i*–Pr_3Si polyyne series **403** (λ_{max} ca. 570 nm) by 73 nm.[16] Given that this estimation of λ_{max} using diphenyl polyynes as a model relies on shorted molecules than that of the series **403**, the estimate of this series can be considered tentative. Further investigation, such as synthesizing longer diphenyl polyynes, is required.

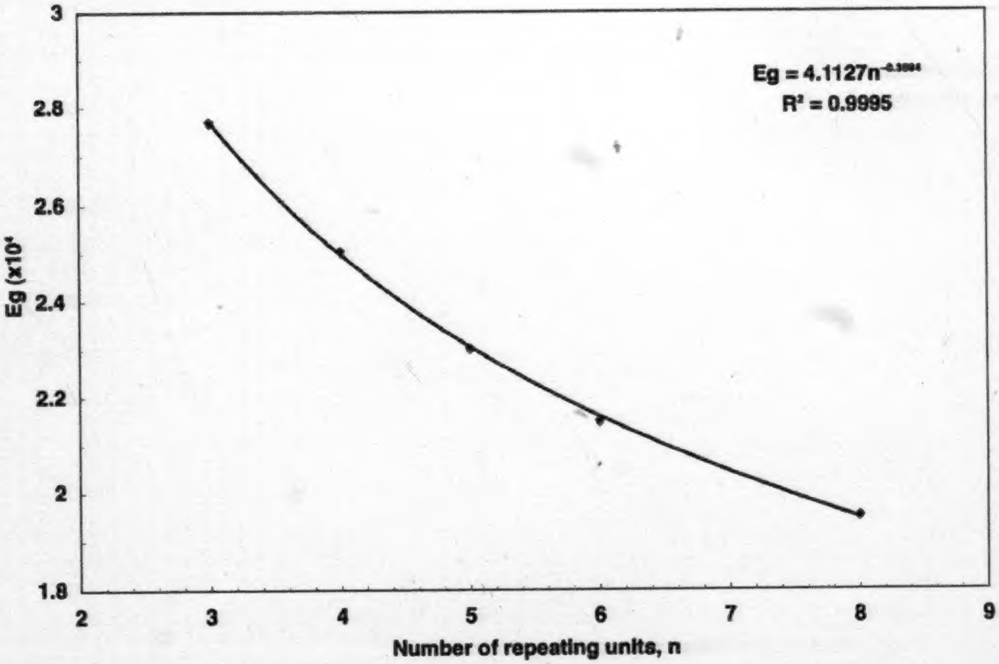

Figure 4.13 Plot of the energy gap vs the number of repeat alkyne units in the diphenyl polyyne series.

The graph for estimating the energy gap of the diphenyl polyynes is generated by plotting the energy gap (E_g, where $E_g = 1/\lambda_{max}$) versus the number of repeat alkyne units. The exponential equation [E_g ($\times 10^4$ cm^{-1}) $= 4.1127n^{-0.3594}$] shows that by increasing the conjugated alkyne units, the LUMO–HOMO gap decreases. Once again, the result obtained for the α,ω–diphenylpolyyne is different from that found the α,ω–diisopropylsilylpolyyne series [E_g (x10^4 cm^{-1}) = $64.9n^{-0.379}$]. The exponent of the series of polyynes with *i*–Pr_3Si end capping groups is lower than that of the phenyl endcapped series. These differences show that each additional triple bond to the polyyne framework lowers the energy gap more for the *i*–Pr_3Si series than for the diphenyl series. This is likely due to the fact that the diphenyl end groups have an effect on λ_{max} where as the *i*–Pr_3Si end groups do not.

The UV–vis spectra of diaryl hexaynes **412a–d** also show two distinctive absorption regions, one at high energy and one at low energy (Table 4.6). In both regions, there is a small difference in the λ_{max} values. Derivatives **412b,c** have a slightly lower energy λ_{max} values than does the phenyl derivative **412a**. This is likely due to the lone pair of the oxygen atom extending slightly the conjugated framework. It is not clear why absorptivity of the methoxy derivative is larger than that of the octoxyl derivative.[15]

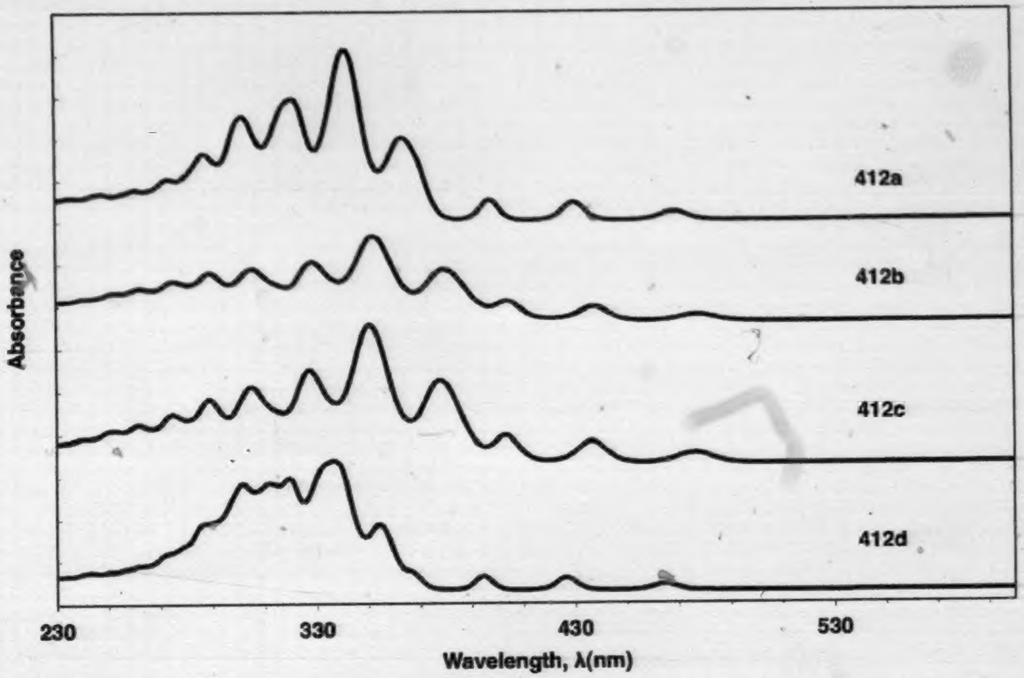

Figure 4.14 UV–vis spectra of polyynes **412a–d**.

Table 4.6 UV–vis data for symmetrical hexaynes **412a–d** in THF.

Compound	λ_{max} (nm) Region 1 ε (L mol^{-1} cm^{-1})	λ_{max} (nm) Region 2 ε (L mol^{-1} cm^{-1})
412a	337 (155 000)	465 (8 000)
412b	351 (164 000)	476 (13 300)
412c	352 (103 000)	477 (8 500)
412d	342 (206 000)	469 (10 900)

The UV–vis spectra for triynes **424a–c** were analyzed and the spectral data are shown in Table 4.7 and the spectra are shown in Figure 4.15. Nitroaryl derivative **424c** shows the lowest energy λ_{max} (361 nm) among compounds **424a–c** and phenyl derivative **424a** has the highest energy absorption (345 nm).

Table 4.7 UV–vis spectra data for unsymmetrical triynes **424a–c** in THF.

Compound	λ_{max} (nm), ε (L mol^{-1} cm^{-1})
424a	284 (13 900), 302 (24 100), 322 (32 0000), 345 (22 800)
424b	309 (26 700), 329 (37 000), 353 (27 300)
424c	315 (16 500), 337 (25 0000), 361 (21 600)

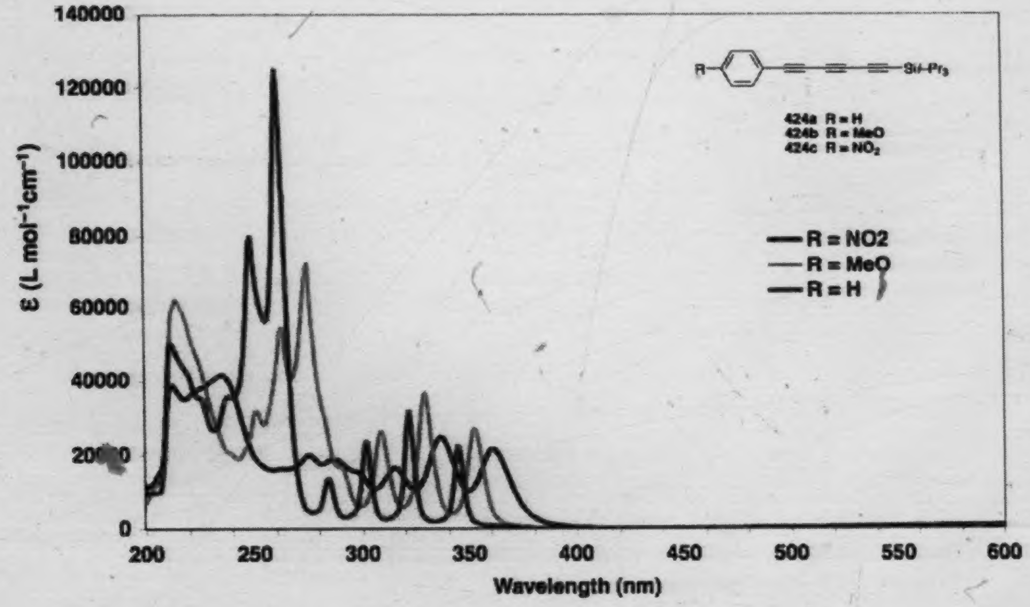

Figure 4.15 UV–vis absorption spectra for triynes **424a–c**

4.2.5 X–ray Crystallography

Crystals suitable for X–ray crystallographic analysis were obtained for compound **410** grown from a solution of $CHCl_3$ at 4 °C. Crystals suitable for X–ray crystallographic analysis were obtained for compound **412a** and **412d** grown from a solution of $CDCl_3$ at 4 °C. Crystals suitable for X–ray crystallographic analysis for compound **410** were grown from a solution of hexanes/CH_2Cl_2 at 4 °C. Crystals for diphenyl pentayne **411** were obtained from a solution of $CDCl_3$ and the structure obtained by X–ray crystallography is consistent with the data reported by Diederich.[35] In the solid–state, tetrayne **410** and pentayne **411** are centrosymmetric whereas hexaynes **412a,d** are not. Of the four structures, the *t*–butyl hexayne derivative has the most unusual shape. The two aryl end groups bend outward, and this will be discussed in more detail in the following section.

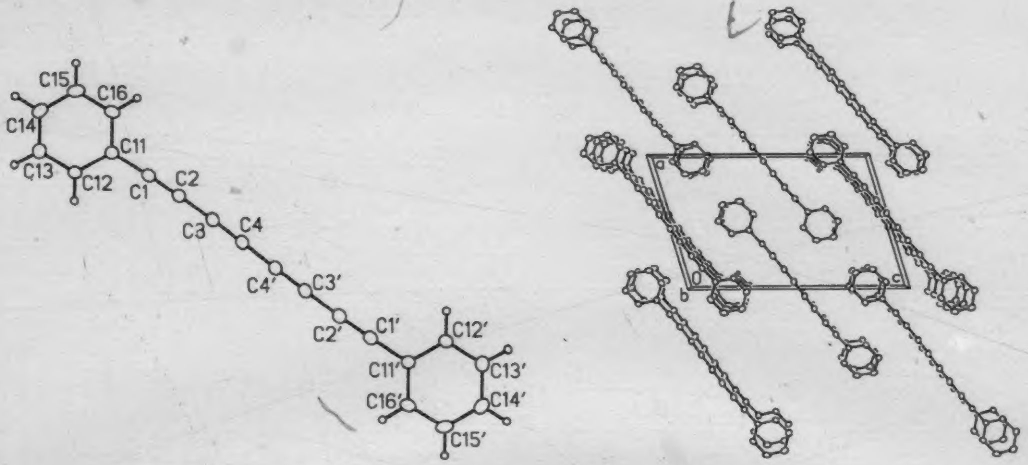

Figure 4.16 ORTEP drawing of compound **410** showing several parallel–oriented molecules. Selected interatomic distances (Å): C1≡C2 1.2067(14), C3≡C4 1.2109(14). Selected bond angles (deg): C11–C1≡C2 177.00(10), C1≡C2–C3 178.53(11), C2–C3≡C4 178.21(11), C3≡C4–C4' 179.38(15).

The alkynyl bond lengths of tetrayne **410** are unremarkable (Figure 4.16). The alkyne bond angles range from 177.0–179.4°, and thus the alkyne framework is essentially linear.

The X–ray crystal structure of pentayne **411** has been reported by Diederich and coworkers, and shows that the compound is also nearly linear.[35] The largest deviation from linearity being 1.92(06)° for the C2≡C1–C11 angle. The compound has an interesting arrangement of molecules in the solid–state in which packing along the *a*–axis in a parallel fashion with a very short distance between neighboring molecules of 3.645

Å. Diederich suggested that this compound can potentially undergo topochemical polymerization, which is consistent with the DSC results reported in section 4.2.2.

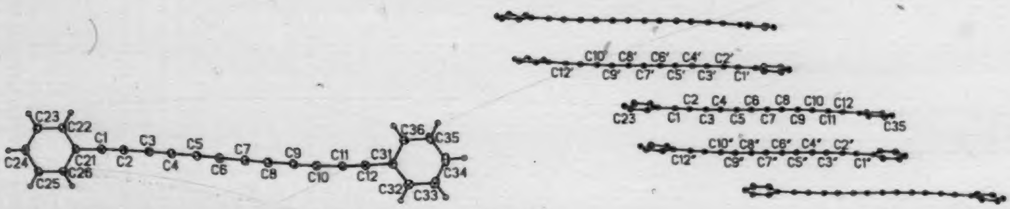
C23
C22
C24
C21
C26
C25
C1
C2
C3
C4
C5
C6
C7
C8
C9
C10
C11
C12
C31
C32
C33
C34
C35
C36
C10'
C8'
C6'
C4'
C2'
C12'
C9'
C7'
C5'
C3'
C1'
C2
C4
C6
C8
C10
C12
C23
C1
C3
C5
C7
C9
C11
C35
C10''
C8''
C6''
C4''
C2''
C12''
C9''
C7''
C5''
C3''
C1''

Figure 4.17 ORTEP drawing of diphenyl hexayne **412a**. Selected interatomic distances: C1≡C2 1.199(3), C3≡C4 1.206(3), C5≡C6 1.209(3), C7≡C8 1.211(3), C9≡C10 1.211(3), C11≡C12 1.201(3); Selected bond angles: C21–C1≡C2 178.2(3), C1≡C2–C3 178.4(3), C2–C3≡C4 178.5(3), C3≡C4–C5 179.4(3), C4–C5≡C6 179.1(3), C5≡C6–C7 179.5(3), C6–C7≡C8 179.0(3), C7≡C8–C9 178.9(3), C8–C9≡C10 178.5(3), C9≡C10–C11 178.0(3), C10–C11≡C12 177.1(3), C11≡C12–C31 178.0(3). Dihedral angle between plane 1 (C21, C22, C23, C24, C25, C26) and plane 2 (C31, C32, C33, C34, C35, C36) is 5.13(13)°.

In contrast to the geometry of compounds **410** and **411** in the solid state, hexayne **412a** is not centrosymmetric (Figure 4.17). The structure is nearly linear, with all sp–sp carbon bond angles between 177° and 180°. The intermolecular distances between sp–hybridized carbons are within 3.5–3.7 Å. This small intermolecular distance suggests that the compound can potentially undergo topochemical polymerization. The DSC analysis of hexayne **412a** shows no endotherm, but rather a sharp exotherm with an onset temperature of 133 °C and a maximum temperature of 142 °C. The DSC and X–ray crystallographic results also imply that the compound might undergo a topochemical reaction.

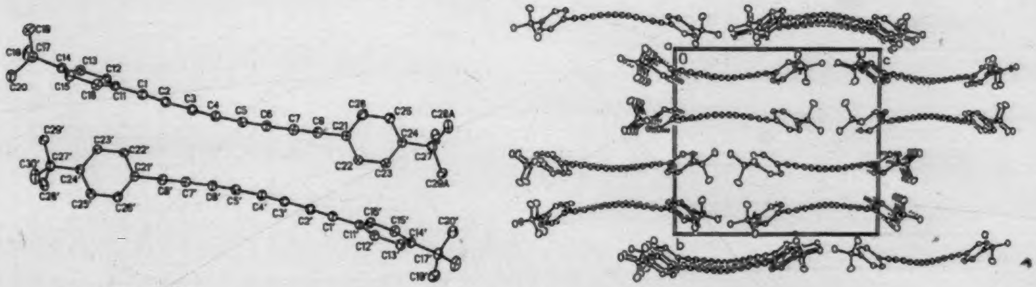
C18
C17
C19
C14
C13
C12
C20
C15
C16
C11
C1
C2
C3
C4
C5
C6
C7
C8
C26
C25
C28A
C21
C24
C27
C22
C23
C29A
C29'
C23'
C22'
C27'
C21'
C30'
C24'
C28'
C25'
C26'
C8'
C7'
C6'
C5'
C4'
C3'
C2'
C1'
C16'
C15'
C20'
C11'
C14'
C12'
C13'
C17'
C19'
0
c
b

Figure 4.18 ORTEP drawing of *t*-butyl derivative **412d**. Selected interatomic distances: C1≡C2 1.204(3), C3≡C4 1.210(3), C5≡C6 1.207(3), C7≡C8 1.215(3), C9≡C10 1.212(3), C11≡C12 1.201(3); Selected bond angles: C21–C1≡C2 178.2(3), C1≡C2–C3 176.6(3), C2–C3≡C4 178.0(3), C3≡C4–C5 178.0(3), C4–C5≡C6 178.6(3), C5≡C6–C7 178.35(3), C6–C7≡C8 178.0(3), C7≡C8–C9 178.5(3), C8–C9≡C10 177.9(3), C9≡C10–C11 178.4(3), C10–C11≡C12 176.5(3), C11≡C12–C31 177.5(3). Dihedral angle between plane 1 (C21, C22, C23, C24, C25, C26) and plane 2 (C31, C32, C33, C34, C35, C36) is 84.85(7)°.

The geometry of compound **412d** in the solid state is not centrosymmetric, but there is a pseudo center of inversion between two neighboring and crystallographically independent molecules (Figure 4.18). The C–C≡C bond angles range from 176.5(3)° to 178.6(3)°. The terminal aryl groups of each molecule are nearly orthogonal. DSC analysis of compound **412d** shows a narrow exotherm (T_o = 144 °C, T_{max} = 151 °C). The DSC and X–ray crystallographic results suggest that this compound can also potentially undergo a topochemical polymerization process. From the X–crystallographic analysis of polyynes **410–412** and **412d**, a significant trend was observed which suggests the these compounds could undergo topochemical polymerization.

4.3 Conclusions

In this chapter, the synthesis of a series of diaryl polyynes ranging from a diyne to an octayne **408–413**, three diaryl hexaynes **412b–d**, and three unsymmetrical triynes **424a–c** with electron–donating and eletron–withdrawing groups has been discussed. Unfortunately, the attempted synthesis of *para*–substituted nitro aryl hexayne derivative was not successful. Some difficulties encountered include: (a) the nitro group is not compatible with BuLi during the FBW rearrangement, and (b) the terminal alkyne did not undergo the homocoupling reaction to form hexayne **412e**. In addition to the synthesis of unlabeled diaryl polyynes, the ^{13}C enrichment at specific positions of triyne **431**, tetrayne **432**, and hexayne **433** was achieved. The enhanced signals from the ^{13}C NMR spectra facilitated identification of each alkyne resonance in the ^{13}C NMR spectra. These results show that, in an infinite diphenyl polyyne system, C1 and C3 will approach 77.5 ppm and 62.5 ppm, respectively, whereas C2 and C4 stay at 74.3 ppm and 67.2 ppm, respectively. DSC analyses of compounds **410–413** were undertaken. As well, as single X–ray crystallography of compounds **409–412** and **412d** was accomplished. The sharp exotherm from the DSC analysis and the correct geometric crystal packing in the solid–states imply that the tetrayne, pentayne, hexayne, *t*–butyl hexayne could undergo topochemical polymerization. UV–vis spectroscopic analyses of the diphenyl polyynes demonstrated that the molar absorptivity and maximum absorption wavelength increase with the number of triple bonds. A plot of E_g vs $1/n$ demonstrates that the HOMO–LUMO band gap decreases as the conjugated polyyne system is extended. The UV–vis spectra of triynes **424a–c** show a red shift for nitro– and methoxy–derivatives.

4.4 References and Notes

(1) Eisler, S.; Slepkov, A. D.; Elliott, E.; Luu, T.; McDonald, R.; Hegmann, F. A.; Tykwinski, R. R. *J. Am. Chem. Soc.* **2005**, *127*, 2666–2676.

(2) Vonhelden, G.; Gotts, N. G.; Bowers, M. T. *Nature* **1993**, *363*, 60–63.

(3) Clemmer, D. E.; Jarrold, M. F. *J. Am. Chem. Soc.* **1995**, *117*, 8841–8850.

(4) Goroff, N. S. *Acc. Chem. Res.* **1996**, *29*, 77–83.

(5) Faust, R. *Angew. Chem., Int. Ed.* **1998**, *37*, 2825–2828.

(6) Gibtner, T.; Hampel, F.; Gisselbrecht, J. P.; Hirsch, A. *Chem. Eur. J.* **2002**, *8*, 408–432.

(7) Nagano, Y.; Ikoma, T.; Akiyama, K.; Tero–Kubota, S. *J. Chem. Phys.* **2001**, *114*, 1775–1784.

(8) Nagano, Y.; Ikoma, T.; Akiyama, K.; Tero–Kubota, S. *J. Am. Chem. Soc.* **2003**, *125*, 14103–14112.

(9) Slepkov, A. D.; Hegmann, F. A.; Zhao, Y.; Tykwinski, R. R.; Kamada, K. *J. Chem. Phys.* **2002**, *116*, 3834–3840.

(10) Armitage, J. B.; Entwistle, N.; Jones, E. R. H.; Whiting, M. C. *J. Chem. Soc.* **1954**, 147–154.

(11) Akiyama, S.; Nakasuji, K.; Akashi, K.; Nakagawa, M. *Tetrahedron Lett.* **1968**, 1121–1126.

(12) Schermann, G.; Grosser, T.; Hampel, F.; Hirsch, A. *Chem. Eur. J.* **1997**, *3*, 1105–1112.

(13) Hare, J. P.; Kroto, H. W. *Acc. Chem. Res.* **1992**, *25*, 106–112.

(14) Eisler, S.; Chahal, N.; McDonald, R.; Tykwinski, R. R. *Chem. Eur. J.* **2003**, *9*, 2542–2550.

(15) Luu, T.; Elliott, E.; Slepkov, A. D.; Eisler, S.; McDonald, R.; Hegmann, F. A.; Tykwinski, R. R. *Org. Lett.* **2005**, *7*, 51–54.

(16) Slepkov, A. D.; Eisler, S.; Luu, T.; Elliott, E.; Tykwinski, R. R.; Hegmann, F. A. *Proc. SPIE Int. Soc. Opt. Eng.* **2005**, *4*, 5935.

(17) Slepkov, A. D., Ph.D. Thesis, University of Alberta, Canada, 2006.

(18) Szafert, S.; Gladysz, J. A. *Chem. Rev.* **2003**, *103*, 4175–4205.

(19) Glaser, C. *Ber. Dtsch. Chem. Ges.* **1869**, *154*, 137–171.

(20) Eglinton, G.; Galbraith, A. R. *Chem. Ind.* 1956, 737–738.

(21) Hay, A. S. *J. Org. Chem.* **1962**, *27*, 3320–3321.

(22) Willemart, A.; Chodkiewicz, W.; Cadiot, P. *Bull. Soc. Chim. Fr.* **1957**, 455–456.

(23) Stephens, R. D.; Castro, C. E. *J. Org. Chem.* **1963**, *28*, 3313–3315.

(24) Sonogashira, K.; Tohda, Y.; Hagihara, N. *Tetrahedron Lett.* **1975**, 4467–4470.

(25) Métay, E.; Hu, Q.; Negishi, E. *Org. Lett.* **2006**, *8*, 5773–5776.

(26) Tobe, Y.; Ohki, I.; Sonoda, M.; Niino, H.; Sato, T.; Wakabayashi, T. *J. Am. Chem. Soc.* **2003**, *125*, 5614–5615.

(27) Diederich, F.; Rubin, Y.; Knobler, C. B.; Whetten, R. L.; Schriver, K. E.; Houk, K. N.; Li, Y. *Science* **1989**, *245*, 1088–1090.

(28) Shi Shun, A. L. K.; Chernick, E. T.; Eisler, S.; Tykwinski, R. R. *J. Org. Chem.* **2003**, *68*, 1339–1347.

(29) Eisler, S.; Tykwinski, R. R. *J. Am. Chem. Soc.* **2000**, *122*, 10736–10737.

(30) Wiechell, H. *Liebigs Ann.* **1894**, *279*, 337–344.

(31) Buttenberg, W. P. *Liebigs Ann.* **1894**, *279*, 324–337.

(32) Fritsch, P. *Liebigs Ann.* **1894**, *279*, 319–323.

(33) Heuft, M. A.; Collins, S. K.; Yap, G. P. A.; Fallis, A. G. *Org. Lett.* **2001**, *3*, 2883–2886.

(34) Diederich, F.; Philp, D.; Seiler, P. *J. Chem. Soc., Chem. Commun.* **1994**, 205–208.

(35) Rubin, Y.; Lin, S. S.; Knobler, C. B.; Anthony, J.; Boldi, A. M.; Diederich, F. *J. Am. Chem. Soc.* **1991**, *113*, 6943–6949.

(36) Morisaki, Y.; Luu, T.; Tykwinski, R. R. *Org. Lett.* **2006**, *8*, 689–692.

(37) Johnson, T. R.; Walton, D. R. M. *Tetrahedron* **1972**, *28*, 5221–5236.

(38) Corey, E. J.; Fuchs, P. L. *Tetrahedron Lett.* **1972**, 3769–3772.

(39) *The Chemistry of Carbon–Carbon Triple Bond*; Patai, S., Ed.; Wiley and Sons: New York, 1978.

Chapter 5. A One–Pot Synthesis and Functionalization of Di– and Triynes Based on the Fritsch–Buttenberg–Wiechell Rearrangement[†]

5.1 Introduction

Conjugated carbon–carbon triple bonds are important building blocks for organic chemistry because they are found in a wide variety of natural products,[1–3] and they can function as carbon–rich scaffolds and organic materials.[4] As well, they can be utilized as high–energy precursors for forming many cyclic and acyclic derivatives.[5] The synthesis of organic compounds containing multiple carbon–carbon triple bonds can be a challenge. Over the years, a number of metal–catalyzed hetero– and homocoupling reactions have been developed for the formation of sp–sp^2 and sp–sp bonds, many of which have been refined and applied to the synthesis of structurally diverse derivatives.[6] The use of terminal polyynes in these coupling reactions can, however, be problematic due to the fact that they often show limited stability.[7] Metal acetylides **501** (Scheme 5.1), on the other hand, are often stable intermediates when kept in solution. Although the most obvious route to an intermediate Li–acetylide might be through a two–step approach consisting of desilylation and lithiation (i.e., Scheme 5.1A), instability of the terminal polyyne renders such an approach problematic. Thus, a number of methods have been developed for the *in situ* generation of the metal acetylide **501**, typically based on one of two strategies. One approach relies on the derivatization of an existing polyyne core through, for example, desilylation/metalation of a 1–trimethylsilyl–1,3–butadiyne or 1,3,5–hexatriyne (**502** or **503**) with MeLi–LiBr[8–10] or Si–Sn[11,12] exchange mediated by TBAF (Scheme 1B and 1C, respectively). The second approach utilizes an initial elimination reaction using, for example, 1–halo–1–buten–3–ynes **504**[13–17] or (*Z*)–1–methoxy–1–buten–3–ynes **505**[18,19] to construct a conjugated diyne, followed by metal acetylide formation (Scheme 1D and 1E, respectively). In either case, the result is a nucleophilic acetylide that can be subsequently derivatized, and both approaches have been quite successful for the formation of diynes. Much less has been done to generalize these protocols to triynes, although a recent report by Negishi and coworkers provides a viable route to not only triynes, but tetra– and pentaynes as well.[20]

[†] Some of the work in this chapter has been done in collaboration with a PDF, Dr. Yasuhiro Morisaki, and the text has been adapted almost entirely from: Luu, L.; Morisaki, Y.; Cunningham, N.; Tykwinski, Rik R. *J. Org. Chem.*, accepted.

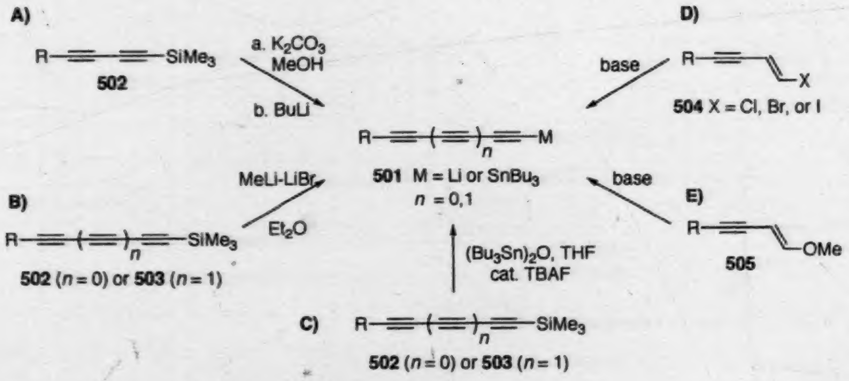

Scheme 5.1 Formation of metal acetylides **501**

We envisioned a one–pot, divergent route for the formation and substitution of di– and triynes based on the α–elimination of a 1,1–dibromoolefin **506** (Scheme 5.2) to initiate a sequence consisting of a Fritsch–Buttenberg–Wiechell (FBW) rearrangement[21–24] and deprotonation. The result would be a Li–acetylide intermediate **507** that could then be trapped directly with electrophiles to give diynes **508** or triynes **509**. Alternatively, the Li–acetylide could be subjected to transmetalation to give a) Zn–acetylides **510** for Negishi coupling to provide α,ω–tolans **511**, b) Cu–acetylides **512** for Glaser–Hay homocoupling to polyynes **513**, c) alkynylstannanes **514** for Stille coupling to ynones **515**, and d) the stable platinum σ–acetylide complexes **516**. The successful development of this divergent process for the one–pot formation of polyynes and its scope for the construction of substituted derivatives are described in this Chapter.[25]

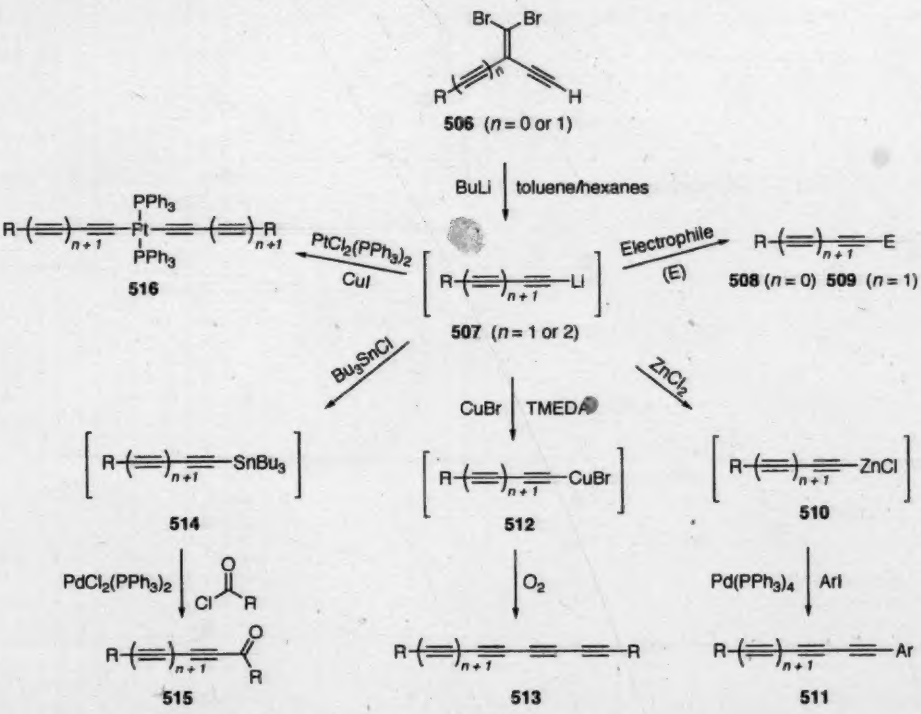
Br
Br
R
n
H
506 (n = 0 or 1)
BuLi
toluene/hexanes
PPh3
R
Pt
R
n + 1
n + 1
PPh3
516
PtCl2(PPh3)2
CuI
R
Li
n + 1
507 (n = 1 or 2)
Electrophile
(E)
R
E
n + 1
508 (n = 0) 509 (n = 1)
Bu3SnCl
CuBr
TMEDA
ZnCl2
R
SnBu3
n + 1
514
R
CuBr
n + 1
512
R
ZnCl
n + 1
510
PdCl2(PPh3)2
O
Cl
R
O2
Pd(PPh3)4
ArI
R
O
R
n + 1
515
R
R
n + 1
513
R
Ar
n + 1
511

Scheme 5.2 General Scheme for the divergent route for the formation and substitution.

5.2 Result and Discussions

The requisite precursors, terminal alkynes **506a–g**, were synthesized in good yield from the corresponding Me_3Si protected enynes **517a–g**[11,22] (Scheme 5.3) via desilylation with K_2CO_3 in methanol/THF. The most important aspect in the preparation of compounds **506a–g** is the purification process, which must ensure that the terminal alkyne products are absolutely anhydrous before being carried on to the deprotonation–rearrangement step to follow (vide infra). Typically, this can be accomplished by passing the terminal alkyne product through a short column of unactivated alumina before proceeding to the FBW reaction.

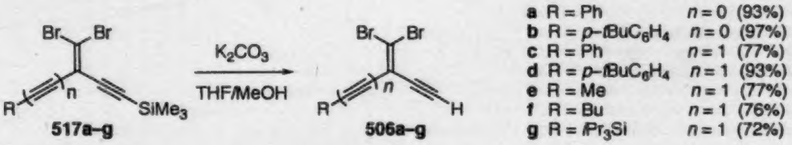

Scheme 5.3 Desilylation of compounds **517a–g**

Initial studies were aimed at optimizing the FBW/deprotonation and trapping sequence. It was known that the formation of polyynes using a FBW requires that the reaction be run in an apolar solvent such as hexanes.[22] In the present case, however, the dibromoolefins **506a–g** showed only minimal solubility in hexanes, especially upon cooling to the desired reaction temperature. Optimization studies determined that this problem could be circumvented if the dibromoolefin **506** (ca. 0.5–1 mmol) was initially dissolved in ca. 2 mL of toluene and this solution then diluted with ca. 10 mL of hexanes.[26] In the second step of the reaction, it was quickly discovered that addition of electrophiles directly to the solution of intermediate **507** in hexanes/toluene typically gave a low yield of the desired products **508** or **509**. It was surmised that the nonpolar reaction medium that favored the FBW rearrangement concurrently disfavored the subsequent reaction with an electrophile. This problem was easily solved by adding the electrophile as an ethereal solution to the intermediate **507**.

During the initial optimization of this procedure, the deleterious effect of water on the reaction was also probed (Table 5.1). Using dry hexanes and toluene,[27] the reaction of dibromoolefin **506a** with BuLi at –20 °C followed by quenching with methyl iodide (dissolved in 2 mL of ether) gave **508a** in 67% yield (Conditions A).[28] Conversely, when the reaction was repeated using either "wet" toluene (Conditions B) or "wet" hexanes (Conditions C) only a trace amount of the desired diyne **508a** was observed.[29] The major product formed in both cases was the terminal diyne **518**,[7] along with a trace of the protonated species **519** that resulted from quenching of the carbenoid intermediate of the reaction.[22] Thus, the success of the reactions described in this Chapter is linked vitally to the use of strictly anhydrous solvents and reagents.

Table 5.1 Effect of solvent and conditions on the FBW–deprotonation reaction.

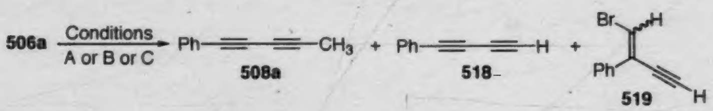

Conditions[a]	yield **508a**	yield **518**	yield **519**
A	67%	not observed	not observed
B	trace[b]	major product[b]	trace[b]
C	trace[b]	major product[b]	trace[b]

[a] Conditions: A) BuLi, dry toluene/hexanes (1:5) at –20 °C, then CH_3I in Et_2O; B) BuLi, wet toluene/hexanes (1:5) at –20 °C, then CH_3I in Et_2O; C) BuLi, toluene/wet hexanes (1:5) at –20 °C, then CH_3I in Et_2O. [b] As determined by ^1H NMR spectroscopy.

5.2.1 Formation of Diynes and Triynes by Trapping Li–Acetylides with Electrophiles

Using the general procedure as described above, the scope of this one–pot reaction was then explored, using precursor **506a** as a model system. The first targets were unsymmetrical substituted diynols. Both di– and triynols have been isolated from a range of natural sources and show a vast array of biological activity,[1,3,30–33] and they can be challenging synthetic targets.[34] Thus, dibromoolefin **506a** was subjected to BuLi to generate the lithium acetylide intermediate **507a**, which was subsequently trapped with a variety of carbonyl electrophiles, including formaldehyde, aryl and alkyl aldehydes, ketones, and CO_2. The products **508b–i** were isolated typically in good yields (57–95%) following aqueous work–up and chromatographic purification (Table 5.2). The latter three examples (**508g–i**) are perhaps the most noteworthy. Compound **508g** represents a substrate that could easily be carried on to the formation of an unsymmetrical tetrayne via a sequence of oxidation, dibromoolefination, and a FBW rearrangement,[35] while **508h** provides an interesting building block for three dimensional carbon–rich architectures.[36] The formation of **508i** demonstrated the potential of this protocol for reactions with alkyl aldehydes with acidic α–protons.

The successful formation of unsymmetrical diynes then directed efforts to the formation of triynes using an analogous route. Gratifyingly, the reaction of dibromoolefin **506c** with BuLi at –20 °C followed by trapping with a variety of electrophiles gave triyne derivatives **509a–e**.[37] While the overall yields of 54–72% for these reactions might only be labeled as moderate, it is worth emphasizing in a single step, the triyne core is both constructed and functionalized. This is a significant advantage over existing routes to triyne products that either require two steps to accomplish the same process (i.e., triyne formation and functionalization) or necessitate the prior formation of a functionalized di– or triyne as one of the partners for a metal mediated coupling reaction (e.g., Cadiot–Chodkiewicz conditions[38]).

Table 5.2 One pot formation of di– and triynes through trapping with carbon based electrophiles.

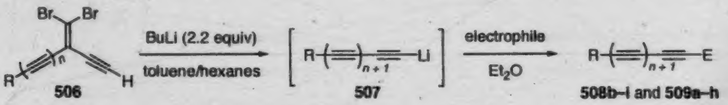

BuLi (2.2 equiv)
toluene/hexanes
electrophile
Et$_2$O

506 **507** **508b–i and 509a–h**

dibromoolefin	electrophile	product	yield (%)
506a	CO$_2$	$\mathrm{Ph{-}C{\equiv}C{-}C{\equiv}C{-}CO_2H}$ **508b**	64
	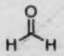	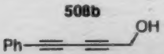 **508c**	58
	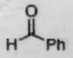	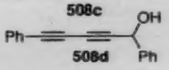 **508d**	70
	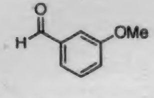	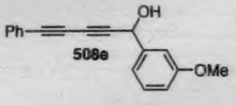 **508e**	72
	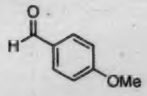	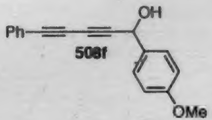 **508f**	72
	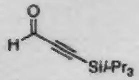	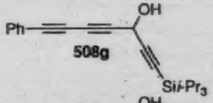 **508g**	75
	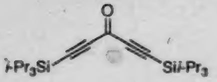	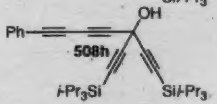 **508h**	95
	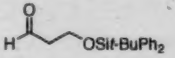	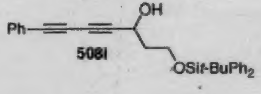 **508i**	57
506c	CH$_3$I	$\mathrm{Ph{-}C{\equiv}C{-}C{\equiv}C{-}C{\equiv}C{-}CH_3}$ **509a**	65
	CO$_2$	$\mathrm{Ph{-}C{\equiv}C{-}C{\equiv}C{-}C{\equiv}C{-}COOH}$ **509b**	65
	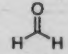	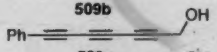 **509c**	72
	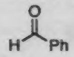	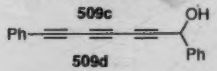 **509d**	54
	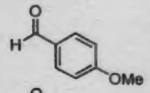	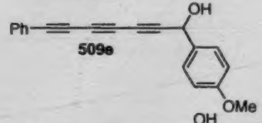 **509e**	54
506e	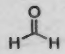	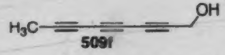 **509f**	59
506f	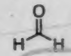	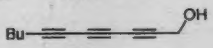 **509g**	55
	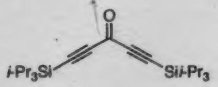	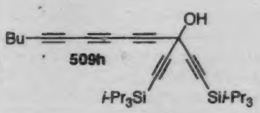 **509h**	82

An analogous reaction of alkyl terminated dibromoolefins **506e** and **506f** with paraformaldehyde produced the triynols **509f** and **509g** in reasonable yields.[39] Compound **509f** was obtained as a white crystalline solid, but slowly turned magenta in color when exposed to light. Triyne **509g**, on the other hand, was isolated as a pale yellow oil that remained unchanged when exposed to light. Finally, the Li–acetylide **507f** generated from **506f** reacted with a highly conjugated diyne ketone to produce tertiary alcohol **509h** as a stable brown oil in an excellent 86% yield.

5.2.1.1 X–ray Crystallographic Structure 509a

The product **509a** (1–phenylhepta–1,3,5–triyne) is a particularly interesting molecule that has been isolated as a natural product from many plant species such as *Bidens pilosa* (Asteraceae)[40] and several members of the *Coreopsis* family.[3] This triyne has significant insecticidal activity against larvae of the army worm *Spodoptera frugiperda*, and it has also exhibited antimicrobial and nematicidal activity, as well as phototoxicity toward *Aedes aegypti* larvae.[41] Since single crystals of **509a** were easily grown from a concentrated solution in $CHCl_3$ at 4 °C, the X–ray crystallographic analysis of the molecule was explored. The molecular structure shows a slight bending of the C–C≡C bonds, with angles in the range of 177.6–179.0° (Figure 1).[42] The solid–state packing of **509a** shows no intermolecular close contacts of <4 Å between neighboring triyne segments, which precludes solid–state polymerization and likely contributes to the observed stability of this molecule in the solid state.

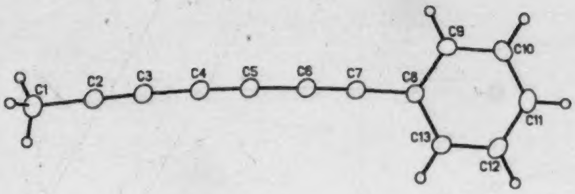

Figure 5.1 ORTEP drawing of **509a** (20% probability level). Selected interatomic distances (Å): C1–C2, 1.4522(17); C2≡C3, 1.1949(17); C3–C4, 1.3685(17); C4≡C5, 1.2067(16); C5–C6, 1.3665(17); C6≡C7, 1.2024(17); C7–C8, 1.4308(17). Selected bond angles (Å): C1–C2≡C3, 178.95(13); C2≡C3–C4, 177.58(13); C3–C4≡C5, 178.24(13); C4≡C5–C6, 177.48(13); C5–C6≡C7, 177.57(14); C6≡C7–C8, 178.12(13)

Complementary to targeting di– or triynes with an alcohol in the propargylic position through the reaction of an acetylide with a carbonyl compound would be synthesis of the homopropargylic alcohols through addition of an acetylide to an epoxide (Table 5.3). Thus, the reaction of **506a** with BuLi in pure toluene at –20 °C gave Li–acetylide intermediate **507a**, which was then trapped with (*S*)–propylene oxide to produce (*S*)–**508j** as a light yellow oil in 30% yield ($[\alpha]^{20}_{D}$ = –9.3, *c* 1.3, MeOH); a reaction conducted by an undergraduate student under my supervision, Ms. Nina Cunningham. The use of the Lewis acid catalyst BF_3•Et_2O did little to improve the yield,[43] and provided 16% yield of (*S*)–**508j** in a ca. 5:1 ratio with (*S*)–**508k**, the product resulting from addition at the more hindered site of the epoxide. Similarly, the addition of (*R*)–propylene oxide dissolved in a combination of DMSO and Et_2O to a solution of **507a** did not improve the yield, giving (*R*)–**508j** in only 20%. The product (*R*)–**508j** ($[\alpha]^{20}_{D}$ +6.4, *c* 0.55, MeOH) shows analogous spectral data and optical rotation as pilosol A, a diyne isolated from *Bidens pilosa*, thus, confirming both the structure and (*R*)–stereochemistry for this natural product.[44] The reaction of acetylide **507a** with the (*R*)–(+)–glycidyl ether was attempted using HMPA as an additive,[45] but gave (*R*)–**508l** in only 22% yield. Given the limited success of these addition reactions, only a single attempt was made to form a triyne. Dibromoolefin **506e** was used to provide **507e** in toluene, and to this solution was added a mixture of excess oxirane, ammonia, and THF at –20 °C. This procedure ultimately gave 58% of the triyne product **509i** as a colorless oil.[46] Thus, the last set of conditions may ultimately provide a general path to triyne homopropargylic alcohols, and an investigation of this possibility is ongoing.

Table 5.3 Acetylide addition to epoxides.

dibromoolefin	epoxide	product	yield (%)
506a	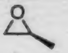	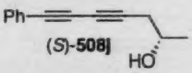 (*S*)-**508j**	30
	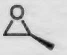	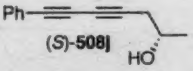 (*S*)-**508j** 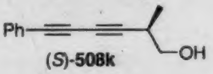 (*S*)-**508k**	16^a
	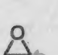	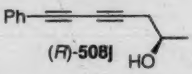 (*R*)-**508j**	20^b
	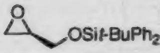	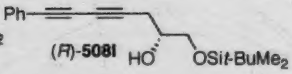 (*R*)-**508l**	22^c
506e		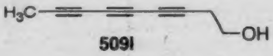 **509l**	58^d

^{a}BF$_3$•OEt$_2$ added, ~5:1 ratio of **508j**:**508k** formed, not separated; ^{b}DMSO added; ^{c}HMPA added; ^{d}NH$_3$ added.

5.2.2 Formation of Di–, Tri–, and Tetraynes from the Negishi Coupling

Polyynes terminated with aryl groups are attractive synthetic targets due to their potential as electronic and optical materials.[35] The ease with which the polyyne framework of intermediate acetylides **507** could be formed *in situ* suggested their use as nucleophilic coupling partners in the formation of aryl polyynes via the Negishi coupling reaction (Table 5.4).[47] Thus, the reaction of the appropriate dibromoolefinic precursors **506** with BuLi (2.2 equiv) at –40 °C in pure toluene generated the Li–acetylide **507**. To ensure the rearrangement was complete, the reaction mixture was warmed slowly to ca. –20 °C and then recooled to –40 °C. To this mixture was added $ZnCl_2$ (1.2 equiv, 0.5 M in THF) to effect transmetalation to the Zn–acetylide **510**. The appropriate aryl iodide and $Pd(PPh_3)_4$ (5 mol%) were added, and the mixture was heated at 70 °C for 20 h. Work–up and column chromatography provided diyne **511a** and triynes **511b–i.** With the exception of **511g**, the desired diaryl polyynes were formed in generally good yields. In the reaction of the intermediate **510f** with 4–iodo–*N,N*–dimethylaniline, the unfortunate low yield of triyne **511g** was not unexpected given the known issues of Pd(0)–insertion into electron–rich C–I bonds.[48] This method could also be extended to multiple couplings, as demonstrated by Negishi reaction of **510a** with 1,3–diiodobenzene to yield **511j** in 64%.

Table 5.4 One–pot formation and Negishi coupling of di– and triynes.

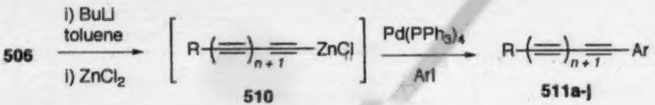
506
i) BuLi
toluene
i) ZnCl2
R
ZnCl
n + 1
510
Pd(PPh3)4
ArI
R
Ar
n + 1
511a-j

dibromoolefin	ArI	product	yield (%)
506a	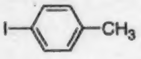	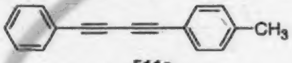 **511a**	90
506c	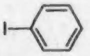	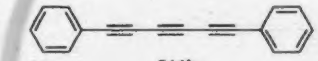 **511b**	70
	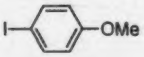	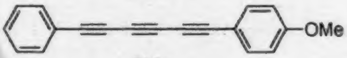 **511c**	80
	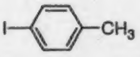	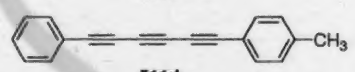 **511d**	81
	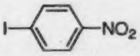	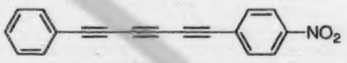 **511e**	84
506d	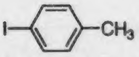	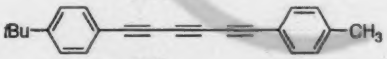 **511f**	60
506f	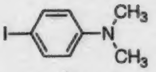	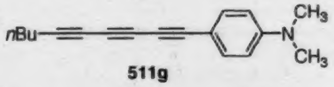 **511g**	24
506g	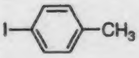	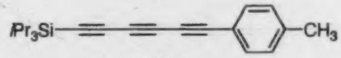 **511h**	69
	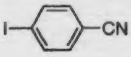	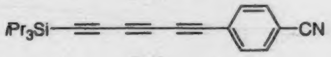 **511i**	78
506a	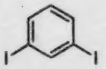	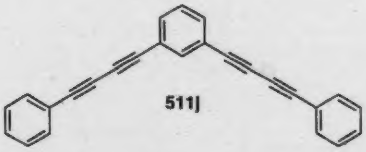 **511j**	64

An attempt was made to parlay this methodology toward the cross–coupling of alkynyl iodides using a hybrid of the Negishi and Cadiot–Chodkiewicz protocols (Scheme 5.4). Zinc–acetylide **510c** was formed from **506c** and reacted with iodoalkyne

520[49] to afford tetrayne **521** in 34% yield, as well as diyne **522** (24% yield), the result of homocoupling of precursor **520**. Competition between the desired heterocoupling and the undesirable homocoupling is a well–known problem in Cadiot–Chodkiewicz type reactions[6] and attempts to eliminate or reduce the formation of this byproduct were not successful. Given the difficulty in separating the two products chromatographically due to their similar polarities on common supports, efforts toward optimizing this potentially useful reaction were abandoned.

Scheme 5.4 Formation of tetrayne **521**

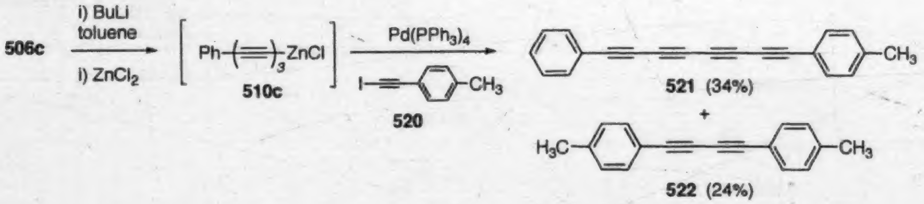

Attempts to extend this Negishi coupling reaction to synthesize **523** were not successful (Scheme 5.5). Both Negishi[20] and Kim[50] reported that di– or triynyl Zn–acetylides could be coupled in situ to a dibromoolefin and subsequent elimination of HBr should give the desired polyyne. Precursor **506a** first went through deprotonation–rearrangement and the resulting Li–acetylide was transmetalated to the Zn–acetylide according to the general procedure. To this mixture, dibromoolefin **524**, $Pd(PPh_3)_4$, and NEt_3 were added and the reaction was heated to 70 °C overnight to give a colorless oil **525** in 55% yield; none of the target tetrayne **523** was detected. The failure to observe the tetrayne may due to a different solvent system used in the present case, because it is known that at times solvent can play a significant role in the coupling reaction. Negishi and coworkers used THF and NEt_3 whereas we needed to use toluene for the initial rearrangement, which was then diluted by the addition of THF and NEt_3.

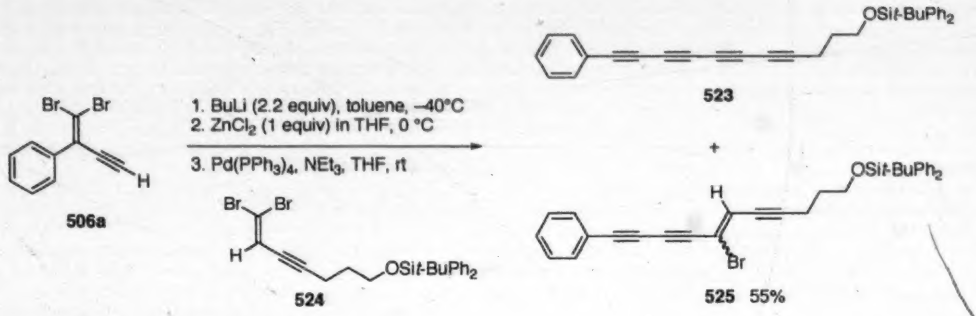
506a
1. BuLi (2.2 equiv), toluene, –40°C
2. ZnCl2 (1 equiv) in THF, 0 °C
3. Pd(PPh3)4, NEt3, THF, rt
524
OSit-BuPh2
523
+
525 55%
Br
H

Scheme 5.5 Synthesis of **525**

5.2.3 Formation of Tetra– and Hexaynes

Transmetalation to Cu(I) was next explored toward effecting oxidative homocoupling under Glaser–Hay conditions (Table 5.5). Intermediates **507a,b,g** were generated from **506a,b,g** under standard conditions in toluene. To the intermediate Li–acetylide was added CuBr (1 equiv) and TMEDA (17 equiv) to give Cu–acetylides **512**,[51] and oxygen gas was then bubbled into the mixture for 15 min. After TLC analysis revealed the reaction was completed, the mixture was passed through a plug of alumina to remove the copper salts and the crude products were purified by column chromatography to produce tetraynes **513a**[35] and **513b**,[52] as well as hexayne **513c**[24] (Table 5). By way of comparison, the previous synthesis of **513c**, also from **506g**, required two–additional steps and provided an overall yield of only 35%, whereas the current procedure provides **513c** in 68% yield and only one step.[24]

Table 5.5 One–pot formation and oxidative homocoupling of di– and triynes

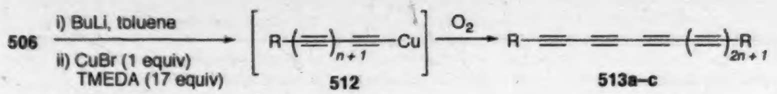

dibromoolefin	product	yield (%)
506a	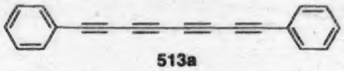 **513a**	69
506b	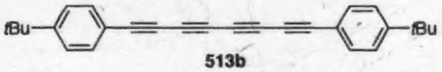 **513b**	93
506g	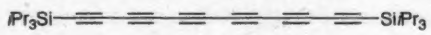 **513c**	68

5.2.4 Formation of Di– and Triynones

Conjugated ynones are desirable synthetic targets[53] because they are versatile precursors and are also known to possess interesting biological activity.[54] Thus, a one–pot protocol using the Stille cross–coupling reaction based on transmetalation to tin was also explored (Table 5.6). In collaboration with a postdoctoral fellow in our group, Dr. Yasuhiro Morisaki, ynones **515** as well as some of di– and triynes **511** were synthesized. The dibromoolefin (**506a** or **506c**) was rearranged at –40 °C in toluene to form the corresponding Li–acetylide, which was then converted to the Sn–acetylide **514** via reaction with Bu_3SnCl. The reaction mixture was warmed to room temperature to ensure complete transmetalation, then the acyl chloride (dissolved in a minimal amount of CH_2Cl_2) was added, followed by a catalytic amount of $PdCl_2(PPh_3)_2$. After heating at reflux overnight, work–up gave the crude ynones **515a–d**, which could be isolated pure by column chromatography. Stille coupling of the stannylacetylenes **514** was successful with a variety of aryl acyl chlorides, ranging from electron donating to electron withdrawing groups, although the yield for neutral and electron donating aryl acyl products **515a–c** was slightly higher than that with an electron deficient aryl group, **515d**.[55,56] Compound **515e** was derived from the combination of tin species **514a** and acetyl chloride and resulted in an unstable orange oil in low yield. Attempts to extend this method to triynones such as **515f** were unsuccessful, and it was not possible to isolate this product pure due to its instability, although TLC analysis of the reaction mixture did suggest that **515f** had been formed.

Table 5.6 One–pot formation, stannylation, and Stille coupling of diynes.

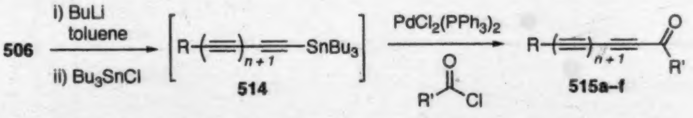

dibromoolefin	acyl chloride	product	yield (%)
506a	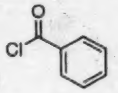	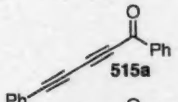 **515a**	75
	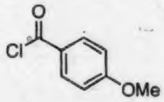	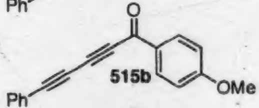 **515b**	71
	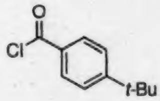	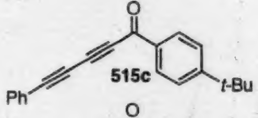 **515c**	71
	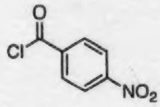	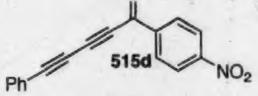 **515d**	56
	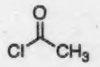	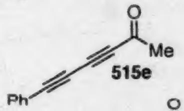 **515e**	33
506c	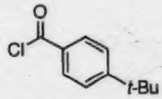	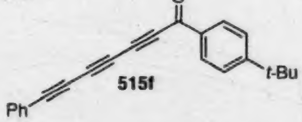 **515f**	–[a]

[a] Not isolated due to decomposition.

5.2.5 Formation of Pt–Complexes

Pt–acetylide complexes have recently been explored for the formation of a wide range of carbon–rich oligomers,[57] macrocycles,[58] as well as supramolecular complexes.[59] Thus, the final transformation explored was the one–pot assembly of Pt–acetylides starting from precursors **506a,f,g** (Table 5.7). The general procedure was used to provide the Li–acetylide **507** in toluene, and to this intermediate was added CuI, followed by $PtCl_2(PPh_3)_2$. The reaction mixture was stirred at room temperature for 12 h and then at 50 °C for 4 h. Using this procedure, tetrayne **516a** was generated as a marginally soluble, off–white solid in excellent yield. Compound **516b** was synthesized from precursor **506f** as a soluble colorless solid in 82% yield. Formation of the *i*–Pr_3Si–derivative **506g** was also successful, providing a marginally soluble product in 74% yield, although all attempts to achieve purity >90% for this derivative have been unsuccessful. The *trans*–stereochemistry of **516a–516c** was easily established based on the $^1J_{Pt-P}$ coupling constants observed in the ^{31}P NMR spectra (CD_2Cl_2). Values of $^1J_{Pt-P}$ 2570, 2525, and 2540 Hz, respectively, indicated formation of the *trans*–isomer, whereas the *cis*–isomer would show smaller $^1J_{Pt-P} \approx 2300$ Hz.[60]

Table 5.7 Pt–acetylide formation from di– and triynes.

$$\mathbf{506} \xrightarrow[\text{ii) CuI, PtCl}_2(\text{PPh}_3)_2]{\text{i) BuLi, toluene}} \mathbf{516a\text{–}c}$$

dibromoolefin	product	yield (%)
506a	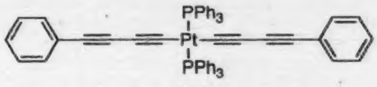 **516a**	91
506f	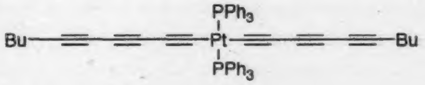 $\mathrm{Bu{-}C{\equiv}C{-}C{\equiv}C{-}C{\equiv}C{-}Pt(PPh_3)_2{-}C{\equiv}C{-}C{\equiv}C{-}C{\equiv}C{-}Bu}$ **516b**	82
506g	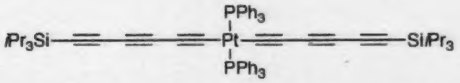 $\mathrm{\mathit{i}Pr_3Si{-}C{\equiv}C{-}C{\equiv}C{-}C{\equiv}C{-}Pt(PPh_3)_2{-}C{\equiv}C{-}C{\equiv}C{-}C{\equiv}C{-}Si\mathit{i}Pr_3}$ **516c**	74

5.2.6 Synthesis of cis Pt–complexes

Unfortunately, *trans*–isomers of Pt–acetylides **516a–c** have very low solubility. They are quite difficult to purify and characterize, whereas it is known that the corresponding *cis*–isomers have higher solubility. Thus, this study was extended and the *trans*–isomers were converted to *cis*–isomers (Scheme 5.10). The respective *trans*–acetylide **516a–c** was reacted with *cis*–1,2–bis(diphenylphosphino)ethylene in CH_2Cl_2 at room temperature overnight to produce the corresponding *cis*–isomers **526a–c** in good yields. In all cases, TLC analysis (sorbent, solvent) showed that the *trans*–isomers are less polar than the *cis*–isomers, as expected. The *cis*–isomers are easier to purify by column chromatography. *Cis*–isomers have a lower melting point compared to their *trans*–counterparts. The *cis*–isomers all have a smaller ^{31}P–Pt coupling constant value than the analogous *trans*–isomers, and the ${}^1J_{P-Pt}$ values for compounds **516a–c** are 2294, 2294, and 2298 Hz, respectively.

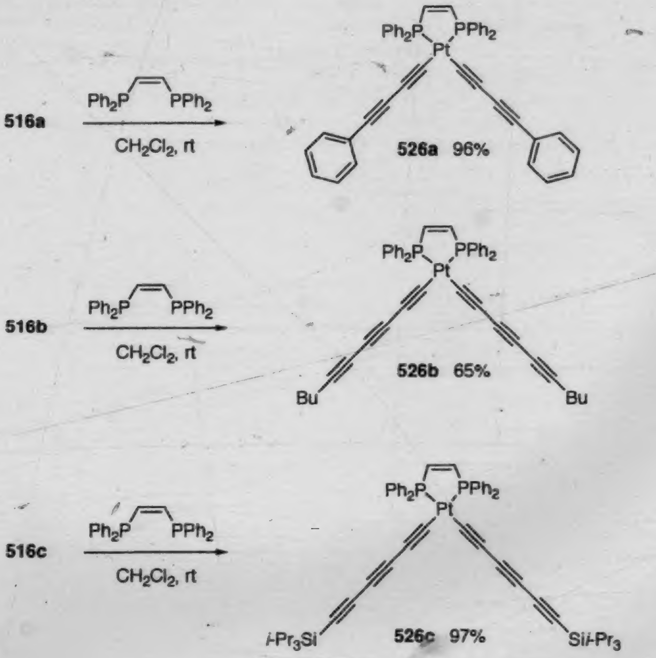

Scheme 5.6 Transformation of *trans*–acetylides **516a–c** to *cis*–acetylides **526a–c**

Further elaboration on *trans*–platinum complexes **516a–b** to form chiral *cis*–platinum complexes has been done by a coworker, Ms. Amber Sadowy. These results include the synthesis of the *cis*–Pt–acetylide derivatives and analysis of their physical properties by as UV–vis and circular dichroism spectroscopies. This work has been described in her masters thesis.[61]

5.3 Toward Optically Active Polyynols

Chiral polyynols have been attractive targets in natural product synthesis because some of them have been used as an intermediate building blocks for complex organic molecules; many of which have been isolated from nature and proved to have medicinal properties. Traditionally, enantioselective syntheses of propargylic alcohols are often obtained from the reaction of a terminal alkyne with an aldehyde in a presence of a catalytic amount of a chiral ligand, such as (+)–*N*–methylephendrine, (*S*)–BINOL, (1*S*,2*S*)–2–dimethylamino–1–(*p*–nitrophenyl)–3–(*tert*–butyldimethylsilyloxy)propan–1–ol, or salen, and a Lewis acid, such as $ZnMe_2$, $Zn(OTf)_2$, or CuOTf.[62,63] These methods require a terminal alkyne as a precursor. However, obtaining terminal polyynes in pure form is problematic. The one–pot methodology described earlier is being extended toward the synthesis of optical active polyynols utilizing in situ transmetalation of the intermediate Li–acetylide. This work is still in progress, but a brief introduction is provided here.

Determining the enantiomeric excess of secondary polyynols is quite a challenge because they are relatively unstable in neat form and at high temperature. This is particularly true for the longer polyynes. Several techniques to determine enantiomeric excess have been used, such as a chiral HPLC, chiral shift reagents in NMR spectroscopy, Mosher ester derivatives, etc. The Mosher ester method was chosen to determine the enantiomeric excess in the present work because this method does not require a large quantity of sample (ca. 1–2 mg) and the Mosher ester derivatives are typically stable in solution. Three different propargylic alcohols were used as a model to test this method, and the results are shown in Scheme 5.7.[64] A series of racemic proparylic alcohols **528**,[65] **508d** and **509e** was synthesized via the normal one–pot FBW reaction described above. Each of the alcohols (1 equiv), (*R*)–Mosher acid chloride (1.5 equiv), pyridine (20 μL), and $CDCl_3$ (0.70 mL) were placed in a NMR test tube to produce ester derivatives **527a–c**. ^{1}H and ^{19}F NMR spectra of each sample were measured.

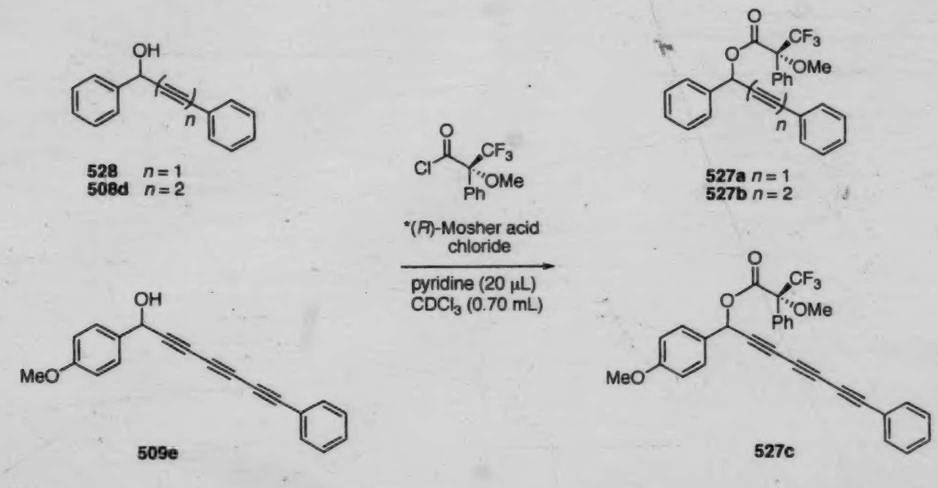

OH
n
528 n = 1
508d n = 2
O
Cl
CF3
OMe
Ph
*(R)-Mosher acid chloride
pyridine (20 μL)
CDCl3 (0.70 mL)
OH
MeO
509e
527a n = 1
527b n = 2
MeO
527c

Scheme 5.7 Conversion of the propargylic alcohols to Mosher ester using *R*–Mosher acid chloride

The ^{1}H NMR spectrum of monoyne **527a** shows two signals with similar integration at 3.5 and 3.4 ppm (multiplets) due to the diastereotopic methyl groups of the products (the signal of the Me of the starting material, the Mosher acid chloride, is also observed at 3.6 ppm). The ^{1}H NMR spectrum of diyne **527b** displays also two signals for the methyl groups at 3.6 and 3.4 ppm, again with identical integrations. Triyne **527c**, however, shows an unresolved series of four signals at 3.77 ppm that appears to be a quartet.

Similar observations are seen in the ^{19}F NMR spectra. Two signals are observed for monoyne **527a** at –72.0 and –72.2 ppm, whereas that of the Mosher acid chloride starting material appears at –71.7 ppm. Similarly, diyne **527b** displays two signals, at –72.1 and –72.2 ppm. Unfortunately, the reaction to form triyne **527c** shows only a single signal at –73.6 ppm in the ^{19}F NMR spectrum after 48 h at room temperature.

The similar integration values of methyl protons in the ^{1}H NMR spectra for **527a** and **527b** suggest that starting materials **528** and **508d** are racemic mixtures as would be expected. This is confirmed by the analysis of the ^{19}F NMR spectra of these two product mixtures as well. The results for triyne **527c** are, however, ambiguous. Thus, the Mosher ester method might be a reasonable method for determining enantiomeric excess for diynols by ^{1}H and ^{19}F NMR spectroscopy, but its usefulness for triynes such as **527c** remains unproven.

5.4 Conclusions

A one–pot protocol for the synthesis and derivatization of di– and triynes has been developed based on a FBW rearrangement–deprotonation sequence. The main advantage of this method is that from a common dibromoolefinic precursor, a substantial range of polyyne products can be achieved simply through the choice of the electrophile introduced in the second step of the reaction. The efforts to date have shown that carbon based electrophiles such as aldehydes, ketones, MeI, and CO_2 work quite well, whereas the use of epoxide based electrophiles results in only low yields of the desired products. Use of an electrophilic transition metal allows for transmetalation from the initial Li–acetylide and the formation of Zn–, Cu–, Sn–, Pt–acetylides, which greatly increases the range of products that may be achieved. Given the ease with which this one–pot reaction sequence can be effected, the possibility for structure function analysis of di– and triynes for both materials and medicine has been greatly expanded.

5.5 References and Notes

(1) Shi Shun, A. L. K.; Tykwinski, R. R. *Angew. Chem., Int. Ed.* **2006**, *45*, 1034–1057.

(2) *Chemistry and Biology of Naturally Occurring Acetylenes and Related Compounds*; Lam, J.; Breteler, H.; Arnason, T.; Hansen, L., Eds.; Elsevier: Amsterdam, 1988.

(3) Bohlmann, F.; Burkhardt, T.; Zdero, C. *Naturally Occurring Acetylenes*; Academic Press: New York, 1973.

(4) *Acetylene Chemistry: Chemistry, Biology, and Material Science*; Diederich, F.; Stang, P. J.; Tykwinski, R. R., Eds.; Wiley–VCH: Weinheim, Germany, 2005.

(5) Larock, R. C. In *Acetylene Chemistry: Chemistry, Biology, and Material Science*; Diederich, F., Stang, P. J., Tykwinski, R. R., Eds.; Wiley–VCH: Weinheim, Germany, 2005, p Chapter 2.

(6) Siemsen, P.; Livingston, R. C.; Diederich, F. *Angew. Chem., Int. Ed.* **2000**, *39*, 2632–2657.

(7) West, K.; Wang, C.; Batsanov, A. S.; Bryce, M. R. *J. Org. Chem.* **2006**, *71*, 8541–8544.

(8) Holmes, A. B.; Jennings–white, C. L. D.; Schulthess, A. H.; Akinde, B.;

Walton, D. R. M. *J. Chem. Soc., Chem. Commun.* **1979**, 840–842.

(9) Fiandanese, V.; Bottalico, D.; Marchese, G.; Punzi, A. *J. Organomet. Chem.* **2005**, *690*, 3004–3008.

(10) Fiandanese, V.; Bottalico, D.; Marchese, G.; Punzi, A. *Tetrahedron* **2006**, *62*, 5126–5132.

(11) Mukai, C.; Miyakoshi, N.; Hanaoka, M. *J. Org. Chem.* **2001**, *66*, 5875–5880.

(12) Warner, B. P.; Buchwald, S. L. *J. Org. Chem.* **1994**, *59*, 5822–5823.

(13) Himbert, G.; Umbach, H.; Barz, M. *Z. Naturforsch. B* **1984**, *39*, 661–667.

(14) Negishi, E. I.; Okukado, N.; Lovich, S. F.; Luo, F. T. *J. Org. Chem.* **1984**, *49*, 2629–2632.

(15) Kende, A. S.; Smith, C. A. *J. Org. Chem.* **1988**, *53*, 2655–2657.

(16) Alami, M.; Crousse, B.; Linstrumelle, G. *Tetrahedron Lett.* **1995**, *36*, 3687–3690.

(17) See also: a) Bartlome, A.; Stämfli, U.; Neuenschwander, M. *Helv. Chim. Acta* **1991**, *74*, 1264–1272; b) Faul, D.; Himbert, G. *Liebigs Ann. Chem.* **1986**, 1466–1473; c) Okuhara, K. *J. Org. Chem.* **1976**, *41*, 1487–1494.

(18) Stracker, E. C.; Zweifel, G. *Tetrahedron Lett.* **1990**, *31*, 6815–6818.

(19) Kwon, J. H.; Lee, S. T.; Shim, S. C.; Hoshino, M. *J. Org. Chem.* **1994**, *59*, 1108–1114.

(20) Métay, E.; Hu, Q.; Negishi, E. *Org. Lett.* **2006**, *8*, 5773–5776.

(21) Chalifoux, W. A.; Tykwinski, R. R. *Chem. Rec.* **2006**, *6*, 169–182.

(22) Eisler, S.; Chahal, N.; McDonald, R.; Tykwinski, R. R. *Chem. Eur. J.*

2003, *9*, 2542–2550.

(23) Eisler, S.; Tykwinski, R. R. *J. Am. Chem. Soc.* **2000**, *122*, 10736–10737.

(24) Eisler, S.; Slepkov, A. D.; Elliott, E.; Luu, T.; McDonald, R.; Hegmann, F. A.; Tykwinski, R. R. *J. Am. Chem. Soc.* **2005**, *127*, 2666–2676.

(25) Morisaki, Y.; Luu, T.; Tykwinski, R. R. *Org. Lett.* **2006**, *8*, 689–692.

(26) Pure toluene can also be used for the FBW/deprotonation. Due to the higher boiling point of toluene, however, it is more difficult remove during product isolation, which can cause problems in cases where the di– or triyne product show limited thermal stability.

(27) Hexanes were dried by distillation from CaH_2, toluene was dried by distallation from Na/benzophenone ketyl.

(28) Compound **508a** a well–known Chinese folk medicine isolated from the shrub Yin Chen Hao, see: Tang W.; Eisenbrand, G. Chinese Drugs of Plant Origin, Springe, Berlin, 1992.

(29) "Wet" toluene and hexanes were arrived at by storing reagent grade solvent over molecular sieves (4Å) for 24 h.

(30) In *Biologically Active Natural Products – Potential Use in Agriculture*; Cutler, H., Ed.; ACS: Washington, DC, 1988; Vol. 380.

(31) Blunt, J. W.; Copp, B. R.; Munro, M. H. G.; Northcote, P. T.; Prinsep, M. R. *Nat. Prod. Rep.* **2003**, *20*, 1–48.

(32) Faulkner, D. J. *Nat. Prod. Rep.* **2001**, *18*, 1–49.

(33) Meinwald, J.; Meinwald, Y. C.; Chalmers, A. M.; Eisner, T. *Science* **1968**, *160*, 890–892.

(34) Luu, T.; Tykwinski, R. R. *J. Org. Chem.* **2006**, *71*, 8982–8985.

(35) Luu, T.; Elliott, E.; Slepkov, A. D.; Eisler, S.; McDonald, R.; Hegmann, F. A.; Tykwinski, R. R. *Org. Lett.* **2005**, *7*, 51–54.

(36) Manini, P.; Amrein, W.; Gramlich, V.; Diederich, F. *Angew. Chem., Int. Ed.* **2002**, *41*, 4339–4343.

(37) Triyne **509c** is a natural product isolated from several species, such as Bidens pilosus, Bidens leucanthus, and Dahlia pinnata, see: a) Bohlmann, F.; Bornowski, H.; Kleine, K.–M. *Chem. Ber.* **1964**, *97*, 2135–2138; b) Bohlmann, F.; Arndt, C.; Kleine, K.–M.; Wotschokowsky, M. *Chem. Ber.* **1965**, *98*, 1228–1232; c) Bendixen, O.; Lam, J.; Kaufmann, F. *Phytochemistry* **1969**, *8*, 1021–1024.

(38) Cadiot, P.; Chodkiewicz, W. In *Chemistry of Acetylenes*; Viehe, H. G., Ed.; Marcel Dekker: New York, 1969, p pp 597–647.

(39) The product **509f** (octa–2,4,6–triynol) has been isolated by Jones and coworkers from the fungus Kuehneromyces mutabilis, see: a) Hearn, M. T. W.; Jones, E. R. H.; Pellatt, M. G.; Thaller, V.; Turner, J. L. *J. Chem. Soc., Perkin, Trans. 1* **1973**, 2785–2788; b) for a previous synthesis, see Luu, T.; Shi, W.; Lowary, T. L.; Tykwinski, R. R. *Synthesis* **2005**, 3167–3178.

(40) Wat, C. K.; Biswas, R. K.; Graham, E. A.; Bohm, L.; Towers, G. H. N.; Waygood, E. R. *J. Nat. Prod.* **1979**, *42*, 103–111.

(41) Arnason, T.; Swain, T.; Wat, C.–K.; Graham, E. A.; Parington, S.; Towers, G. H. N. *Biochem. Syst. Ecol.* **1981**, *9*, 63–68.

(42) Crystal data for **509a**: $C_{13}H_8$, M = 164.19, monoclinic space group $P2_1/n$ (an alternate setting of $P2_1/c$ [No. 2]), $D_c = 1.158$ g cm^{-3}, a = 6.1920(8), b = 7.7938(11), c

= 19.640(3) Å, b = 96.640(2), V = 941.5(2) Å^3, Z = 4, m = 0.066 mm^{-1}. Final $R(F)$ =0.0400, $wR_2(F^2)$ = 0.1163 for 119 variables and 1925 data with $F_o^2 \geq -3\sigma(F_o^2)$ (1415 observations $[F_o^2 \geq 2\sigma(F_o^2)]$).

(43) Yamaguchi, M.; Hirao, I. *Tetrahedron Lett.* **1983**, *24*, 391–394.

(44) Chang, M.–H.; Wang, G.–J.; Kuo, Y.–H.; Lee, C.–K. *J. Chin. Chem. Soc.* **2000**, *47*, 1131–1136.

(45) Xie, X.; Yue, G.; Tang, S.; Huo, X.; Liang, Q.; She, X.; Pan, X. *Org. Lett.* **2005**, 7, 4057–4059.

(46) Triyne **509i** is a natural product first isolated from the fungus *Collybia peronata* and later from cultures of *Lentinus edodes*, see: Higham, C. A.; Jones, E. R. H.; Keeping, J. W.; Thaller, V. *J. Chem. Soc., Perkin Trans. 1* **1974**, 1991–1994; b) Tokimoto, K.; Fujita, T.; Takeda, Y.; Takaishi, Y. *Proc. Japan Acad.* **1987**, *63*, 277–280.

(47) Negishi, E.; Zeng, X.; Tan, Z.; Qian, M.; Hu, Q.; Huang, Z. In *Metal–Catalyzed Cross–Coupling Reactions, 2nd Edition*; de Meijere, A., Diederich, F., Eds.; Wiley–VCH: Weinheim, 2004, Chapter 15.

(48) Bréfort, J. L.; Corriu, R. J. P.; Gerbier, P.; Guérin, C.; Henner, B. J. L.; Jean, A.; Kuhlmann, T.; Garnier, F.; Yassar, A. *Organometallics* **1992**, *11*, 2500–2506.

(49) Xu, W.; Chen, Q. Y. *J. Org. Chem.* **2002**, *67*, 9421–9427.

(50) Lee, H. B.; Huh, D. H.; Oh, J. S.; Min, G. H.; Kim, B. H.; Lee, D. H.; Hwang, J. K.; Kim, Y. G. *Tetrahedron* **2001**, *57*, 8283–8290.

(51) Ruitenberg, K.; Kleijn, H.; Westmijze, H.; Meijer, J.; Vermeer, P. *J. R. Neth. Chem. Soc.* **1982**, *101*, 405–409.

(52) Haley, M. M.; Bell, M. L.; Brand, S. C.; Kimball, D. B.; Pak, J. J.; Wan,

W. B. *Tetrahedron Lett.* **1997**, *38*, 7483–7486.

(53) Walton, D. R. M.; Waugh, F. *J. Organomet. Chem.* **1972**, *37*, 45–56.

(54) Chretien, R.; Wetroff, P.; Wetroff, G.; Thillay, L. U.S. Patent 3483257, 1969.

(55) Nash, B. W.; Thomas, D. A.; Warburton, W. K.; William, T. D. *J. Chem. Soc.* **1965**, 2983–2988.

(56) Fukumaru, T.; Awata, H.; Hamma, N.; Komatsu, T. *Agr. Biol. Chem.* **1975**, *39*, 519–527.

(57) Liu, Y.; Jiang, S.; Glusac, K.; Powell, D. H.; Anderson, D. F.; Schanze, K. S. *J. Am. Chem. Soc.* **2002**, *124*, 12412–12413.

(58) Campbell, K.; Kuehl, C. J.; Ferguson, M. J.; Stang, P. J.; Tykwinski, R. R. *J. Am. Chem. Soc.* **2002**, *124*, 7266–7267.

(59) Kaiser, A.; Bäeuerle, P. *Top. Curr. Chem.* **2005**, *249*, 127–201.

(60) Campbell, K.; McDonald, R.; Ferguson, M. J.; Tykwinski, R. R. *J. Organomet. Chem.* **2003**, *683*, 379–387.

(61) Sadowy, A., M.Sc. Thesis, University of Alberta, Fall, 2007.

(62) Cozzi, P. G.; Hilgraf, R.; Zimmermann, N. *European J. Org. Chem.* **2004**, 4095–4105.

(63) *Acetylene Chemistry – Chemistry, Biology, and Materials Science*; Wiley–VCH: Weiheim, 2005.

(64) Rieser, M. J.; Hui, Y. H.; Rupprecht, J. K.; Kozlowski, J. F.; Wood, K. V.; McLaughlin, J. L.; Hanson, P. R.; Zhuang, Z. P.; Hoye, T. R. *J. Am. Chem. Soc.* **1992**, *114*, 10203–10213.

(65) Takita, R.; Yakura, K.; Ohshima, T.; Shibasaki, M. *J. Am. Chem. Soc.* **2005**, *127*, 13760–13761.

Chapter 6. Synthesis and Structural Analysis of Tetraynes

6.1 Introduction

Synthesis of conjugated polyenynes is an attractive goal because they can be used as semiconductors, as components of solar cells, and they show substantial optical nonlinearities.[1–5] One of the premier methods for forming polyenynes is via topochemical polymerization. Topochemical reactions are solid–state reactions in which a product is formed by controlling the regio– and stereochemistry of the starting materials. Over the years, scientists have investigated optimal parameters for polymerizing one-dimensional molecular polyynes to form two-dimensional polydi– and polytriacetylenes.[6–11] In their review of solid–state polyyne chemistry, Gladysz and Szafert most recently summarized the optimal packing parameters for 1,4–, 1,6–, 1,8–polymerization for conjugated polyynes (Figure 6.1).[12] The parameters can be divided into three categories:

(a) The distance separating two reacting atoms (C1–C4, denoted as $R_{1,4}$; C1–C6, denoted as $R_{1,6}$; or C1–C8 denoted as $R_{1,8}$) of the neighboring molecules should be approximately 3.4–3.5 Å and certainly less than 4Å.

(b) The translation spacing (d) should be 5.1, 7.4, or 9.6 Å for 1,4–, 1,6–, and 1,8–polymerization, respectively.

(c) The angle (θ) with respect to the stacking axis should be 45, 28, or 21° for 1,4–, 1,6–, and 1,8–polymerization, respectively.

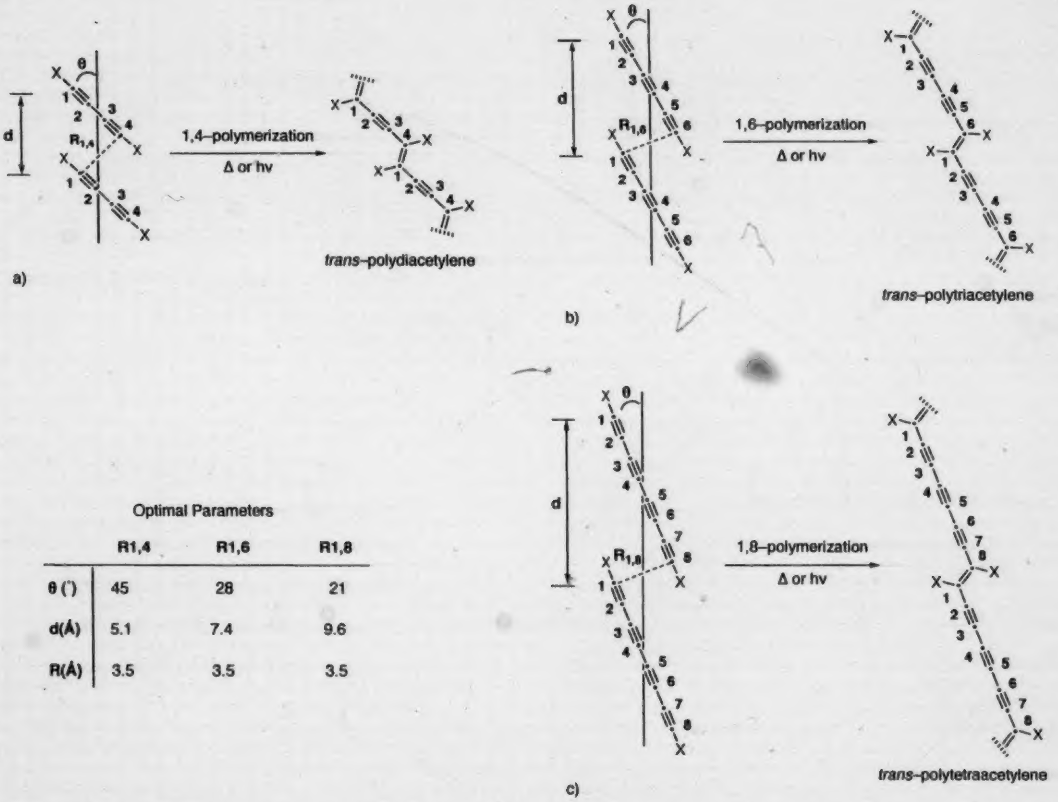

a)
d
θ
X
$R_{1,4}$
1,4–polymerization
Δ or hv
trans–polydiacetylene
b)
$R_{1,6}$
1,6–polymerization
Δ or hv
trans–polytriacetylene
c)
$R_{1,8}$
1,8–polymerization
Δ or hv
trans–polytetraacetylene

Optimal Parameters

	R1,4	R1,6	R1,8
θ (°)	45	28	21
d(Å)	5.1	7.4	9.6
R(Å)	3.5	3.5	3.5

Figure 6.1 Optimal geometry and parameters for topochemical polymerization. a) 1,4–polymerization. b) 1,6–polymerization. c) 1,8–polymerization.

Several strategies have been developed to orient polyynes such that these optimal parameters are achieved, including carefully growing single crystals and introducing a guest molecule to direct a host polyyne during the crystal growing process.[2,7] Wegner and coworkers reported the first 1,4–polymerization of a diacetylene, and produced a completely conjugated single crystalline polymer.[13] Fowler and Lauher introduced the guest–host strategy. They slowly evaporated a solution of methanol containing a 1:1 ratio of a guest oxalamide and a diacetylene. On standing at room temperature or by heating the crystals at 110 °C, the single crystalline monomers were converted to polydiacetylenes.

In addition to the synthesis of a polydiacetylene, Fowler and Lauher have also synthesized polytriacetylenes by irradiating single crystalline triynes. Obtaining the correct geometrical parameters for the polymerization of the single crystalline triynes can be difficult. However, the authors obtained an X–ray crystallographic structure of single crystals grown from slow evaporation of a 2:1 solution of a pyridine host and a triacetylene in methanol. By γ–irradiation these single crystals, the triacetylenes were transformed into polytriacetylenes, as determined by Raman spectroscopy and X–ray diffraction.[14]

In the work described in this Chapter, a 1,6–polymerization process has been investigated toward transforming disubstituted tetraynes into polytriacetylenes. The primary results from IR, UV–vis, and NMR spectroscopies, differential scanning calorimetry (DSC), and X–ray crystallography suggest that the formation of polytriacetylenes is successful under thermal conditions.[2,15–17]

6.2 Results and Discussion

6.2.1 Synthesis

Disubstituted tetraynes **601a–d** were targeted (Scheme 6.1) and they were synthesized from commercially available acid chlorides **602a–d**. Under Friedel–Crafts acylation conditions, the acid chlorides were reacted with 1,4–bis(trimethylsilyl)butadiyne to afford an intermediate ketone after quenching with aqueous HCl (10%). The crude ketones were then converted to dibromoolefins **603a–d**, in good to excellent yield, via a Corey–Fuchs reaction. Me_3Si protected diynes **603a–d** were obtained as crystalline solids with melting points of 86, 73, 98, and 82 °C, respectively.[18,19] With diyne precursors **603a–d** in hand, desilylation proceeded under mild conditions, K_2CO_3 in MeOH and THF, to give terminal alkynes.[20] After desilylation was complete, the reaction mixture was washed with an excess aqueous NH_4Cl, NaCl, and dried over $MgSO_4$. This solution was concentrated to ca. 1–2 mL and then used without further purification. A solution of Hay catalyst (premixed CuCl, TMEDA in CH_2Cl_2) was added, and O_2 gas was bubbled through the resulting solution. The tetraynes could be purified either by column chromatography or recrystallization from hexanes. The desired products **601a–d** were obtained in good yield (51–80%).

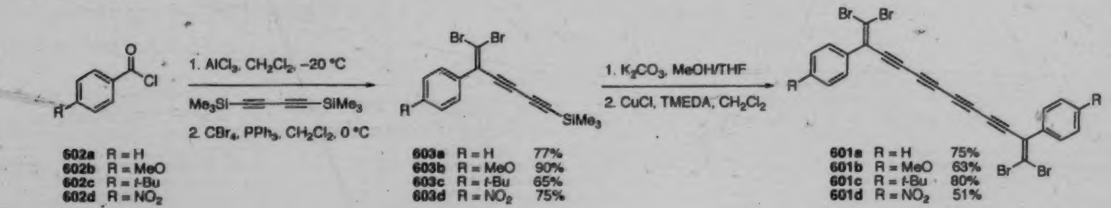
O
Cl
R
1. $AlCl_3$, CH_2Cl_2, –20 °C
Me_3Si—≡—≡—$SiMe_3$
2. CBr_4, PPh_3, CH_2Cl_2, 0 °C
Br
Br
$SiMe_3$
1. K_2CO_3, MeOH/THF
2. CuCl, TMEDA, CH_2Cl_2
602a R = H
602b R = MeO
602c R = t-Bu
602d R = NO_2
603a R = H 77%
603b R = MeO 90%
603c R = t-Bu 65%
603d R = NO_2 75%
601a R = H 75%
601b R = MeO 63%
601c R = t-Bu 80%
601d R = NO_2 51%

Scheme 6.1 Synthesis of tetraynes **601a–d**

6.2.2 Physical Properties

Results from IR, mass, and ^{13}C NMR spectroscopic analyses of tetraynes **601a–d** are shown in Table 6.1. Infrared absorption spectroscopy is a reliable technique for the identification of functional groups. To simplify the discussion, only alkyne stretches are considered for **601a–d**. Internal alkynyl stretches of the tetraynes vary little, with the highest energy signal found for phenyl derivative **601a** at 2192 cm^{-1} and the lowest energy nitro aryl derivative **601d** at 2188 cm^{-1}. The results from the mass spectroscopic analysis for tetraynes **601a–d** show a molecular ion peak in all cases and a fragment ion that corresponds to $[M - 4Br]^+$ in compounds **601a**, **601b**, and **601d**. This fragment is interesting in that it may represent a gas phase FBW rearrangement product that results from losing four bromides. ^{13}C NMR spectroscopic data do not show any trends in the chemical shifts of the four internal alkynes with only small differences, within ca. 1 ppm, for these carbons. This observation implies that the electronic structure in tetrayne framework is not affected by the substituents.

Table 6.1 IR, mass, and ^{13}C NMR spectroscopic data for compounds **601a–d**

Compound	IR (cm^{-1}, $CHCl_3$)	M^+ (intensity) (70 eV, *m/z*)	$[M - 4Br]^+$ (intensity) (70 eV, *m/z*)	^{13}C NMR (ppm, in $CDCl_3$)
601a	2192	617.7488 (80%)	298.0785 (100%)	82.0, 76.5, 71.6, 65.0
601b	2190	677.7697 (100%)	358.0911 (69%)	81.5, –[a], 70.7, 64.8
601c	2182	729.8750 (30%)	–	81.8, –[a], 70.9, 65.0
601d	2188(w)	707.7217 (23%)	388.0490 (6%)	82.6, 75.4, 71.2, 64.8

[a] Peaks overlap with $CDCl_3$ solvent peaks.

The thermal stability of tetraynes **601a–d** has been investigated via conventional melting point and differential scanning calorimetry (DSC) analyses, and the results are shown in Table 6.2.[21] It is interesting to note that the melting or decomposition point observed by traditional melting point analysis is not identical to the result obtained from the DSC measurement. This may be due to uncorrected melting point apparatus. Crystalline phenyl derivative **601a** has an observed decomposition point greater than 185 °C in an open glass plate. In DSC measurements, this compound shows a similar result, with a sharp exotherm with an onset temperature, T_o = 191 °C and a maximum temperature, T_{max} = 192 °C. The DSC spectrum of tetrayne **601b** shows a sharp onset endotherm at ~176 °C, quickly followed by a broad exotherm with T_{max} = 179 °C. Because no melting point has been observed in the melting point experiment, it is likely that the initial endotherm observed by DSC is a phase transition that leads to decomposition. Compound **601c** has an observed melting point of 168–170 °C and it turns dark slowly as the temperature is increased. The DSC analysis shows an initial onset exothermic temperature of 229 °C and it sharpens quickly with a maximum exothermic temperature of 233 °C. DSC analysis of nitro derivative **601d** shows a decomposition point of 190 °C (T_o = 189 °C, and T_{max} = 191 °C), which corresponds well to the observed decomposition point of 190 °C. The sharp, symmetrical, exotherms observed by DSC for compounds **601a**, **601c** and **601d** are characteristic of a topochemical polymerization reaction. Furthermore, tetraynes **601a**, **601c**, and **601d** (Figure 6.2) do not show any significant phase transition after this exotherm, which suggests the products of polymerization are thermally stable. In summary, DSC data of tetraynes **601a–d** do not show any particularly remarkable trends, other than the exotherm observed for each material in a range of ca. 180–230 °C.

Table 6.2 Observed melting points and DSC data of tetraynes **601a–d**

Compound	Observed Melting or Decomposition Point (°C)	DSC Analysis
601a	~185 (dec)	$T_o = 191$, $T_{max} = 192$
601b	~230 (dec)	$T_o = 176^a$, $T_{max} = 179$ (br)

601c	168–170	$T_o = 229$, $T_{max} = 233$
601d	~190 (dec)	$T_o = 189$, $T_{max} = 191$

[a] Sharp onset melting point.

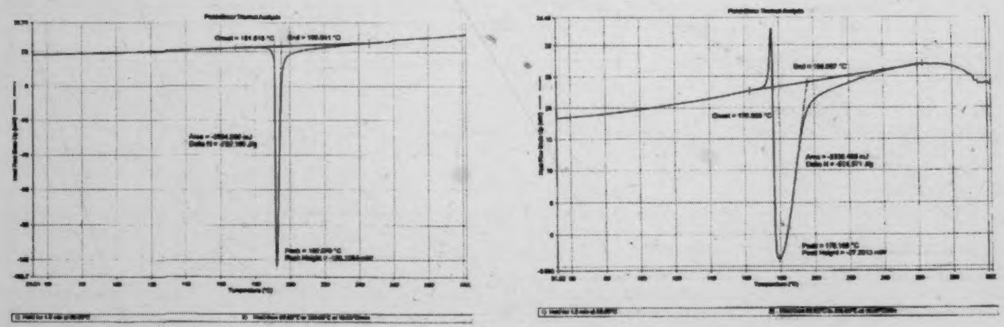

Compound **601a** Compound **601b**

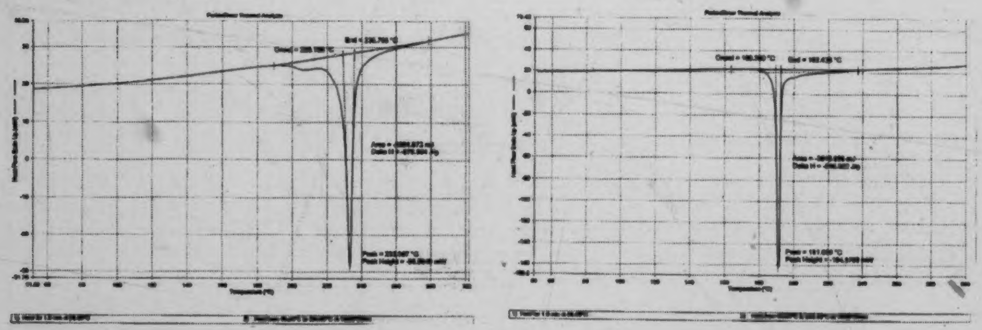

Compound **601c** Compound **601d**

Figure 6.2 DSC plots of the tetraynes **601a–d**

WARNING: An explosion occurred at approximately 190 °C when heating a small quantity of compound **601d** (60 mg) in a capped tightly packed solid–state NMR rotor. When handling any polyyne, one should always take the appropriate safety precautions when the sample is heated above room temperature. If the sample is a terminal polyyne, precautions should be taken at all temperatures.

Thermogravimetric analysis (TGA) has been used to investigate compound **601d** (Figure 6.3). At ca. 191 °C, a sudden change in mass occurs with a small loss of mass (ca. 1%), in agreement with the proposed topochemical polymerization temperature. Significant mass loss (55%) is observed in the temperature range of 200–600 °C, which is probably due to decomposition.

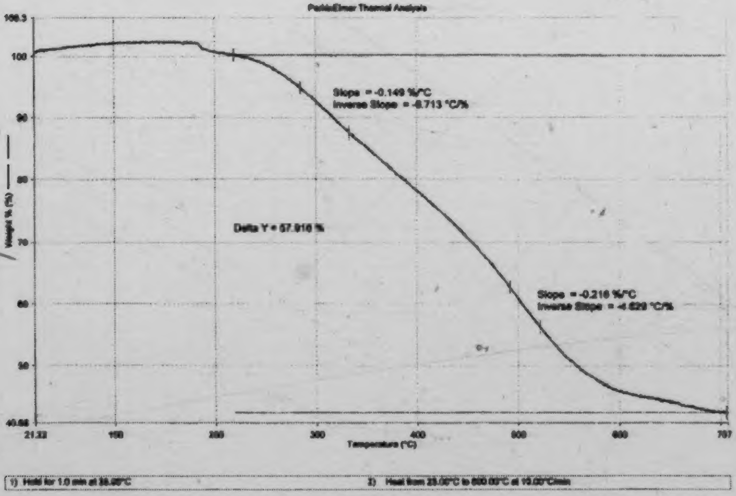

Figure 6.3 TGA plot for compound **601d** scanned from 20 to 700 °C at a rate of 10 °C/min.

6.2.3 X–ray Crystallographic Analysis

Single crystals suitable for X–ray crystallographic analysis were obtained for compounds **601a** and **601c** by the slow diffusion of hexanes into hexanes/CH_2Cl_2 at 4 °C and for compound **601d** by slow evaporation of $CDCl_3$. The solid-state structure of compound **601a** (Figure 6.4) is not centrosymmetric whereas those of compounds **601c**

(Figure 6.5) and **601d** (Figure 6.5) are centrosymmetric. The C≡C lengths are all unremarkable, and the alkynyl framework of each tetrayne is almost linear.

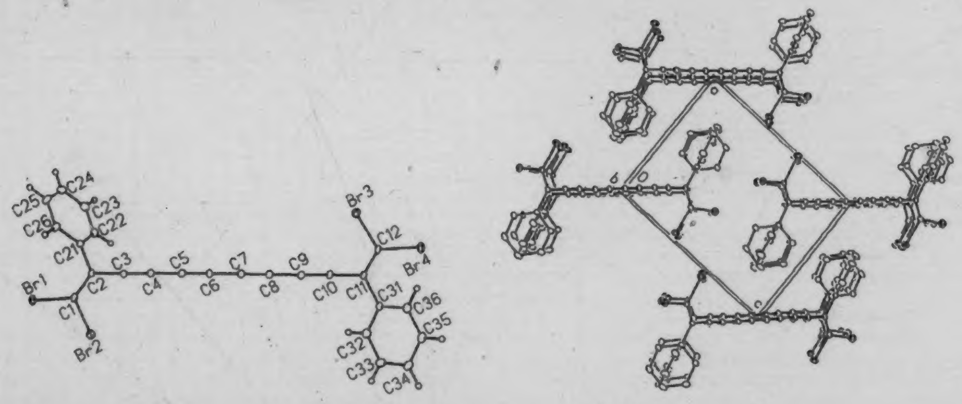

Figure 6.4 ORTEP drawing of compound **601a** (20% probability level) and packing diagram as viewed along the crystallographic *b*-axis. Selected interatomic distances (Å): C3–C4, 1.207(4); C5–C6, 1.199(4); C7–C8, 1.211(4); C9–C10, 1.207(4). Selected bond angles (deg): C2–C3≡C4, 177.4(4); C3≡C4–C5, 179.0(4); C4–C5≡C6, 179.4(4); C5≡C6–C7, 179.3(4); C6–C7≡C8, 179.8(4); C7≡C8–C9, 179.7(4); C8–C9≡C10, 177.8(4); C9≡C10–C11, 176.8(4).

Although very close to the expected value of 180°, the terminal C–C≡C angles of **601a** (177.4°) are slightly more bent than the internal angles (Figure 6.4). The planes generated from two dibromoolefins (C1, C2, Br1, Br2 and C11, C12, Br3, Br4) are not coincident, but are twisted with an angle of 8.7°. The two phenyl rings are approximately perpendicular with an angle of 81.4°. Analysis of the solid–state packing shows that the tetrayne groups of neighboring molecules are aligned. The distance separating the two atoms with $R_{1,6}$ is 3.4 Å. The θ angle is 29° and the longest side d is 7.1 Å. These results are close to the optimal theoretical values of 3.5 Å, 7.4 Å, and 29°. Combined with the intense and sharp exotherm in the DSC measurement, evidence suggests that compound **601a** can undergo a 1,6–topochemical polymerization.

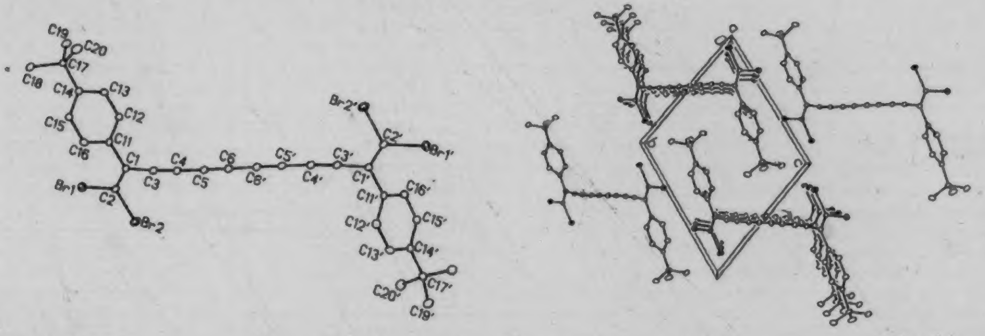
C19
C20
C17
C18
C14
C13
C12
C15
C11
C16
C1
C4
C6
C5'
C3'
C3
C5
C6'
C4'
C1'
Br2'
C2'
Br1'
C16'
C11'
Br1
C2
Br2
C12'
C15'
C13'
C14'
C17'
C20'
C19'

Figure 6.5 ORTEP drawing of compound **601c** (20% probability level) and packing diagram as viewed along the crystallographic *a*-axis. Selected interatomic distances (Å): C3–C4, 1.207(4); C5–C6, 1.203(4). Selected bond angles (deg): C1–C3≡C4, 175.9(3); C3≡C4–C5, 178.3(3); C4–C5≡C6, 178.5(3); C5≡C6–C6', 179.6(4).

Analysis of the solid-state structure of compound **601c** (Figure 6.5) shows that the terminal C–C≡C angle (175.9°) is bent slightly more than the internal C–C≡C angles. Analysis of the crystal packing shows that molecules of compound **601c**, as viewed along either the *a*– or *b*–axis, are parallel to one another. The distance between carbons C3 and C5' of the adjacent molecule ($R_{1,6}$) is 3.7 Å; the transitional spacing between the two adjacent molecules $d = 8.1$ Å and $\theta = 27°$. These deviate slightly from the optimal values for a topochemical 1,6–polymerization as described in the introduction section of $R_{1,6} = 3.5$ Å, $d = 7.4$ Å, and $\theta = 29°$.

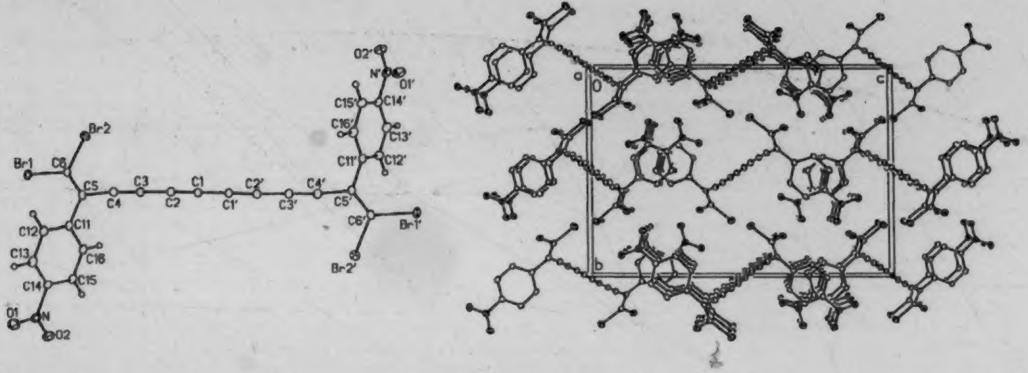

Figure 6.6 ORTEP drawing of compound **601d** (20% probability level) and packing diagram as viewed along the crystallographic *a*-axis. Selected interatomic distances (Å): C1–C2, 1.204(5); C3–C4, 1.204(4). Selected bond angles (deg): C3≡C4–C5, 174.3(4); C2–C3≡C4, 179.1(4); C1≡C2–C3, 177.1(4); C1'–C1≡C2, 179.8(6).

As with **601a** and **601c**, the terminal C–C≡C angles (174.3°) of compound **601d**, (Figure 6.8) are bent more than the internal C–C≡C angles. Molecules of compound **601d** as viewed along either *a*– or *b*–axis are packed parallel to each other. The distance separating the two reacting atoms C4 and C2' of the adjacent molecule ($R_{1,6}$) is 3.5 Å; the transitional distance between carbons (C4 to C4') of the two adjacent molecules d = 7.5 Å; θ = 28°. These values are very close to the optimal values for a 1,6–topochemical polymerization (3.5 Å, 7.4 Å, and 29°) as discussed in Section 6.1. Moreover, DSC analysis shows no melting point (endotherm) but a rather sharp exotherm at 190 °C. The distance between two neighboring molecules along with the sharp exotherm relationship implies that compound **601d** is suitable for a 1,6–topochemical polymerization. The study of this prospect is discussed in more detail below. Analysis of the solid-state packing for the three molecules was, however, quite surprising. Remarkably, these packing parameters show that the all three systems are suitable for solid–state polymerization via a 1,6–topochemical reaction. To our knowledge, this is the first series of structurally similar tetraynes that shows a consistent packing motif conducive to topochemical polymerization.

6.2.4 Electronic Properties

6.2.4.1 Solution State

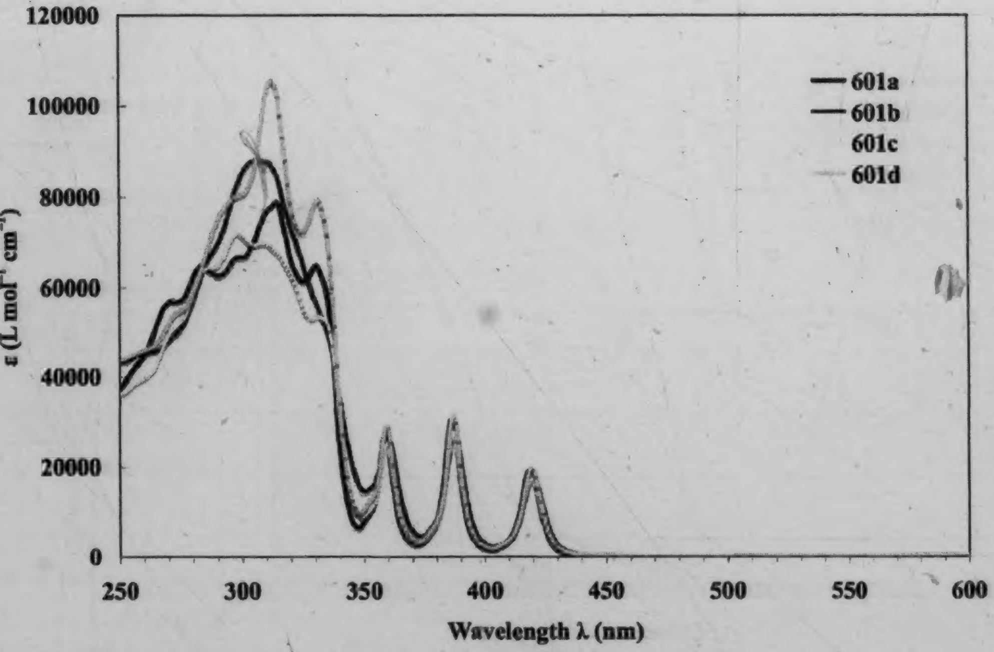

Figure 6.7 UV–vis absorption spectra of tetraynes **601a–d**

As a result of interest in the electronic properties of polyynes, the ultraviolet spectra of many such compounds are known and have been used for structure elucidation.[2,11,22] Thus, UV–vis spectroscopy was used to measure the electronic absorption characteristics of tetraynes **601a–d** in THF at room temperature (Figure 6.7). Within 1 nm, each tetrayne displays three identical peaks at 359, 387, and 419 nm in the low energy region 350–450 nm (Table 6.3). Thus, varying the aryl substituents does not change λ_{max}. In addition, the four compounds have almost identical molar absorbility values (ε). The chromophore of these compounds is likely limited to the 1,1,12,12–tetrabromododeca–1,11–dien–3,5,7,9–tetrayne as λ_{max} is independent of the aryl substituent.

Table 6.3 Maximum absorbance of tetraynes **601a–d**, measured in THF

Compound	Maximum Absorbance, λ_{max} (nm), in THF (ε)
601a	359 (27600), 386 (30600), 419 (19500)
601b	360 (26900), 388 (27800), 420 (18300)
601c	359 (25200), 387 (27600), 419 (17500)
601d	359 (29200), 387 (31700), 419 (19900)

6.2.4.2 Solid State

Crystallographic analysis of nitroaryl derivative **601d** (previous section) shows that the solid–state packing for this molecule is nearly optimal for a 1,6–topochemical reaction. Thus, **601d** was chosen to study this transformation. The UV–vis absorption spectrum of compound **601d** was measured in the solid–state (Figure 6.8),[22,23] on thin films produced by applying a solution of compound **601d** in CH_2Cl_2 onto a quartz slide and allowing the solvent to evaporate. The UV–vis spectrum of a thin film shows absorbance values of 368, 400, and 434 nm. These systematically differ from those obtained from the sample in solution (359, 384, and 419 in THF). Furthermore, the peaks are broader in the solid state than in solution. These differences are due to the solvent effect of THF and the free rotation of the compound in solution.

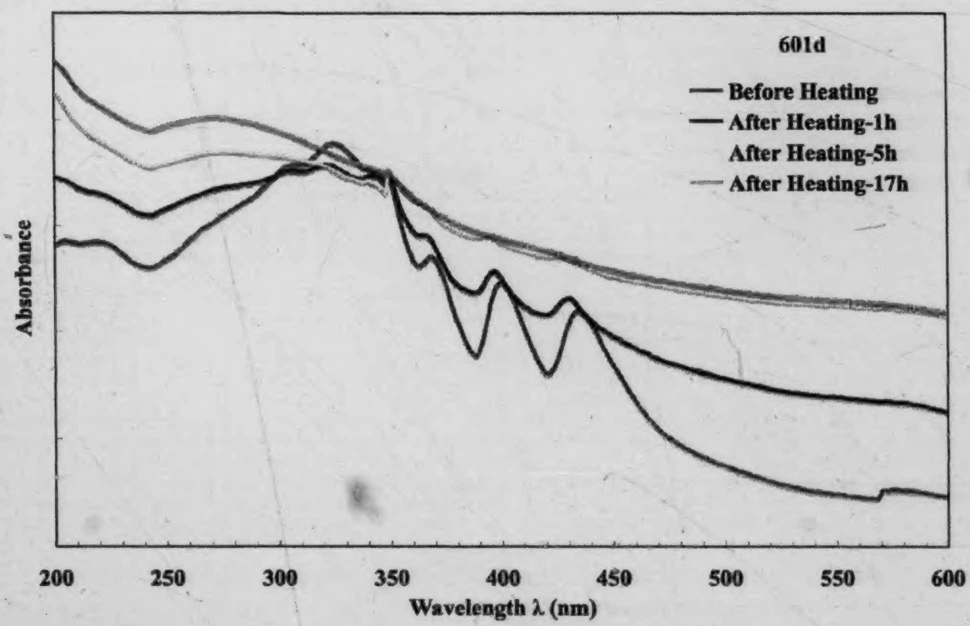

Figure 6.8 Solid–state UV–vis spectra for compound **601d**

The thin film was then heated at 170 °C under an Ar atmosphere for 1, 5, or 17 hours and UV–vis spectra were acquired (Table 6.4). After heating for 1 hour, the intensity of the absorbance signals decreased and λ_{max} values were blue shifted by ca. 3 nm. After heating the same film for an additional 4 hours, two distinct signals remained in the low energy region. These two signals merged into one signal after heating for a total of 17 hours (12 hours after the second experiment). The low energy signal intensity decreased and broadened substantially, and the λ_{max} values were blue shifted as a function of the heating time. This implies that the 1,1,12,12–tetrabromododeca–1,11–

dien–3,5,7,9–tetrayne framework has been transformed into a less conjugated system, rather than a more conjugated system that would be expected upon formation of a polytriacetylene product. This result may still be due to a topochemical polymerization, but the ultimate product would not seem to be the desired one based on UV-vis analysis.

Table 6.4 UV–vis absorption of compound **601d** in the solid state on a quartz

	Maximum Absorbance, λ_{max} (nm), in Argon
Before Heating	368, 400, 434
After Heating 1 h	365, 397, 430
After Heating 5 h	393, 424
After Heating 17 h	422

IR spectroscopy was used to explore the structure of **601d** after heating (Figure 6.9). Similar to the thin films cast for the solid–state UV–vis spectroscopic analysis, a solution of compound **601d** in CH_2Cl_2 was slowly applied to a gold plate and the solvent was slowly removed by evaporation at room temperature to produce a thin film suitable for an IR spectroscopic measurement. The reflection IR technique was used for monitoring changes of the alkenyl and alkynyl regions of the spectrum. Unfortunately, the alkynyl signals at ca. 2200 cm^{-1} are weak because the compound is symmetrical and there is no significant dipole moment to generate a strong alkynyl stretch. However, the alkenyl and aromatic signals are enhanced after heating the thin films in an Ar atmosphere for 6 hours. Furthermore, the positions of these signals after heating do not change appreciably. This signal enhancement suggests that additional alkenyl groups may be present as chromophores in the heated sample. This may be an indication that topochemical polymerization results in the conversion of some triple bonds to double bonds, as would be expected.

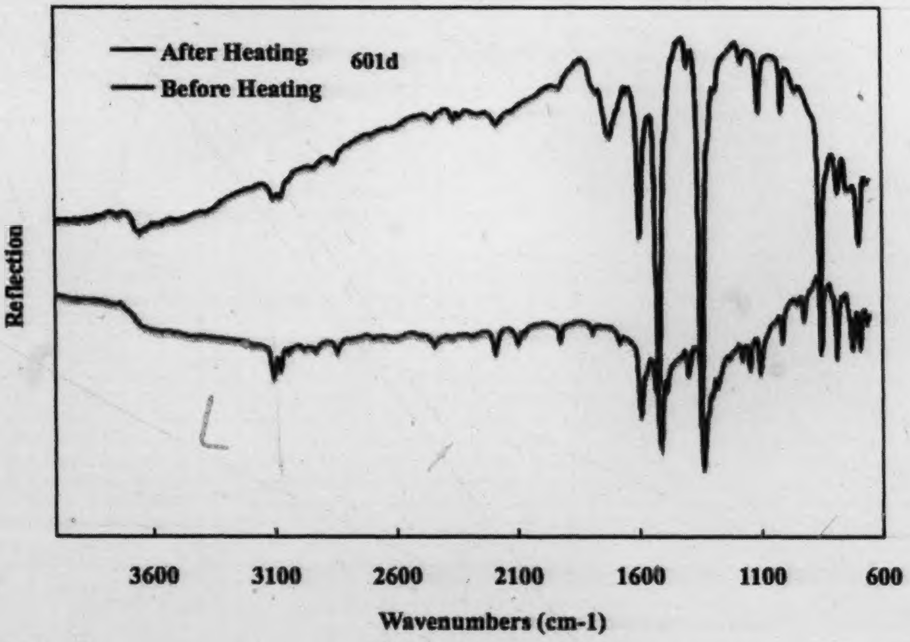

Figure 6.9 Reflection IR spectra of solid–state compound **601d** on gold.

6.2.4.3 Solvent Optimization for Growing Single Crystals

In collaboration with an undergraduate student, Mr. Tyler Taerum, a variety of solvent ratios for growing good single crystals for compound **601d** have been conducted. Obtaining good polyyne single crystals in a large quantity is necessary for topochemical polymerization studies. The solvent is often a critical factor for crystal growth. Thus, a series of solvents have been explored to optimize the crystallizations of **601d** (Table 6.5).

Two different approaches were explored, diffusion (Figure 6.10a) and layering (Figure 6.10b).

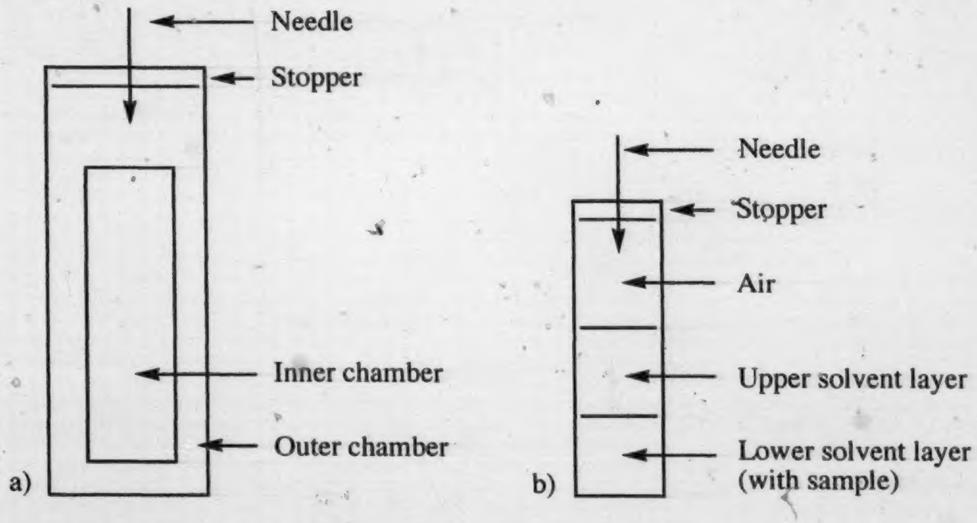
Needle
Stopper
Inner chamber
Outer chamber
a)
Needle
Stopper
Air
Upper solvent layer
Lower solvent layer
(with sample)
b)

Figure 6.10 a) Inner–outer chambers. b) Upper–lower layers.

Figure 6.10 diagram shows the two different processes explored for growing crystals. Compound **601d** was first dissolved in CH_2Cl_2 in entries 4, 6, and 7 or in $CHCl_3$ in entries 1–3, and 5 (Table 6.5). This solution was placed in an inner vial (a) or vial (b). The solvent was placed gently on top of the lower layer solution. The solvent for the outer chamber was placed where a stopper was placed on the outer vial, not the inner vial. A small needle penetrated the top of the vial for ventilation. The vial was left undisturbed at –4 °C. Under these conditions, single crystals, a stringy–like fine powder, or both were produced. The single crystals were suitable for X–ray crystallography, whereas the stringy fine powders were not. The solvent ratio in entries 1–5 and 7 (Table 6.5) gave good crystals. The solvent system in entry 7 was chosen to produce single crystals for solid–state polymerization and analysis.

Table 6.5 Solvent systems and results obtained for crystallization of compound **601d**

Entry	Solvent System	Single Crystals	Stringy Fine Powder
1	Inner chamber: Hexanes/$CHCl_3$ (1:1) Outer chamber: Hexanes/$CHCl_3$ (2:1)	Many small	No
2	Inner chamber: Hexanes/$CHCl_3$ (1:1) Outer chamber: Hexanes/$CHCl_3$ (3:1)	Many small	No
3	Inner chamber: Hexanes/$CHCl_3$ (1:1) Outer chamber: Hexanes/$CHCl_3$ (4:1)	Many small	No
4	Inner chamber: Hexanes/ CH_2Cl_2 (1:1) Outer chamber: Hexanes/CH_2Cl_2 (2:1)	Many small	No
5	Upper layer: Ether Lower layer: $CHCl_3$	Many small	Yes
6	Upper layer: Ether Lower layer: CH_2Cl_2	Few small and big	Yes
7	Upper layer: Hexanes Lower layer: CH_2Cl_2	Many small	No

6.2.4.4 Solid–state NMR Spectroscopic Analysis

$^1H/^{13}C$ NMR spectroscopy is also a good method to help deduce the structure of a compound. Unfortunately, after heating single crystals of compound **601d**, the resulting polymer was not soluble, precluding the acquisition of solution–state $^1H/^{13}C$ NMR spectra.[15,23] Therefore, solid–state ^{13}C NMR spectroscopy was chosen to monitor the transformation of compound **601d**. Single crystals of **601d** were formed from hexanes/CH_2Cl_2 as described in entry 7 (in Table 6.5). In collaboration with Dr. Guy Bernard in the Wasylishen group, ^{13}C NMR spectra of compound **601d** have been obtained before and after heating (Figure 6.11). Aromatic and alkenyl peaks are labeled as Region 1 (150–120 ppm) and alkynyl peaks are labeled as Region 2 (90–60 ppm). Region 1 shows the alkenyl and aromatic signals. Four distinct signals (83.6, 78.9, 73.1, and 66.9 ppm) in Region 2 of the spectrum obtained before heating come from four alkynyl peaks and correlate well with the four signals observed in the solution–state spectrum at 82.6, 75.9, 71.2 and 64.8 ppm. After the compound was heated at 170 °C under an Ar atmosphere for 6 hours, one signal in Region 1 is split into two signals; one signal (83.6 ppm) in region 2 is split into two signals (84.7 and 83.4 ppm) and the intensity of this alkynyl peak decreases. The spectral changes in Regions 1 and 2 for the spectrum acquired after heating suggest that there is a loss of molecular symmetry through the presence additional sp^2 and sp carbon resonances. This is strong evidence for polymerization. Unfortunately, it is not clear whether the process of the topochemical polymerization proceeds via a 1,6– or via other manners.

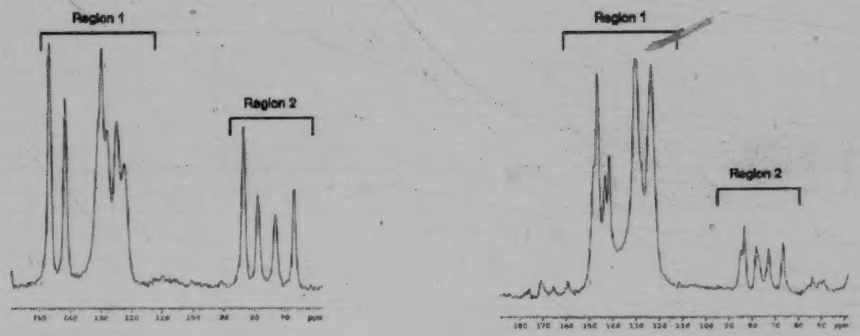

a) Before Heating. b) After Heating at 170 °C for 6 hours in Ar.

Figure 6.11 Solid–state ^{13}C NMR spectra of compound **601d** at 75 MHz

6.2.5 Synthesis of Compound 604 ^{13}C–enriched at a Specific Position

To decipher the polymerization process described for **601d**, a ^{13}C atom was introduced into the tetrayne framework at a specific position to facilitate ^{13}C NMR analysis. Labeled nitro derivative **604** was synthesized with ca. 34% ^{13}C enrichment introduced at the C1 alkyne carbon (Scheme 6.2). Starting with the known aldehyde **605**, dibromoolefin **606** was produced in good yield with a labeled carbon at the C1 position, denoted with an asterisk (*). The reaction of the dibromoolefin with LDA induced elimination and the intermediate lithium diyne was trapped with Me_3SiCl to give diyne **607**. The reaction of diyne **607** and acid chloride **602d** under normal Friedel–Crafts acylation conditions and subsequent Corey–Fuchs dibromoolefination afforded **608** in reasonable yield over the two steps. Target compound **604** was achieved via desilylation of compound **608** to form a terminal diyne that was quickly subjected to homocoupling using of CuCl and TMEDA in CH_2Cl_2. The ^{1}H/^{13}C NMR spectra of this compound are identical to those of the unlabelled compound **601d** except for an enhanced signal of the C1 carbon at 75.6 ppm.

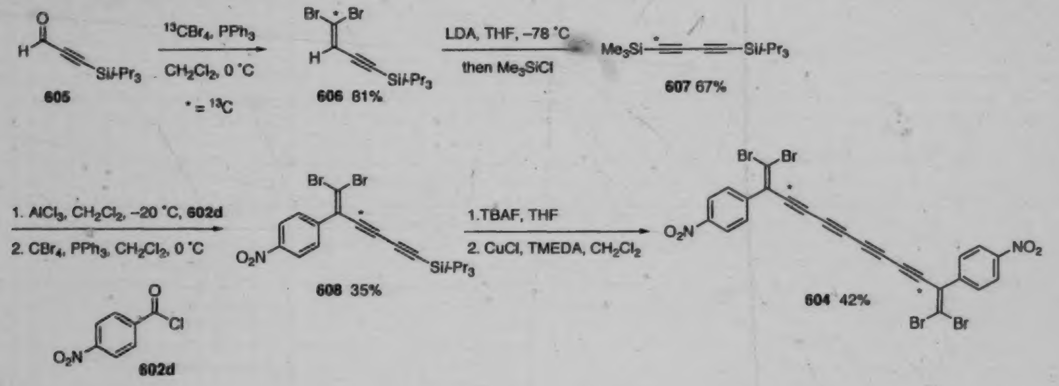

605
^{13}CBr$_4$, PPh$_3$
CH$_2$Cl$_2$, 0 °C
• = ^{13}C
606 81%
LDA, THF, –78 °C
then Me$_3$SiCl
607 67%
1. AlCl$_3$, CH$_2$Cl$_2$, –20 °C, 602d
2. CBr$_4$, PPh$_3$, CH$_2$Cl$_2$, 0 °C
602d
608 35%
1.TBAF, THF
2. CuCl, TMEDA, CH$_2$Cl$_2$
604 42%

Scheme 6.2 Synthesis of labeled tetrayne **604**

6.2.6 *Solid–State ^{13}C NMR Spectroscopy of 604*

The purpose of synthesizing compound **604** is to facilitate monitoring of this alkyne carbon during the polymerization process. Scheme 6.3 demonstrates a 1,6–topochemical polymerization for compound **604** with the enriched carbon denoted with an asterisk. If the transformation of monomers proceeds as shown in Scheme 6.3, then in the solid–state ^{13}C NMR spectra, half of the enriched carbon signals should shift from the alkynyl region to the alkenyl region and the other half should remain virtually unchanged.

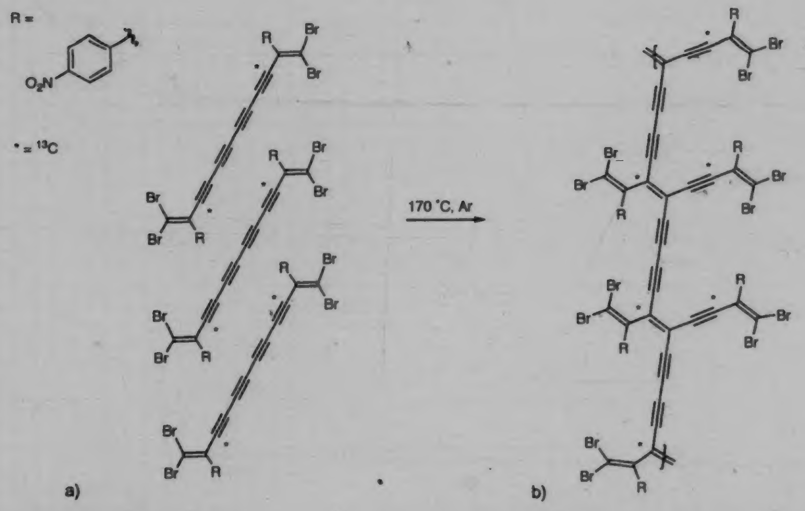

Scheme 6.3 Predicted 1,6–topochemical polymerization of labeled **604**. a) Before heating. b) After heating.

With the labeled compound **604** in hand, single crystals were grown with the same solvent system as that for unlabeled **601d** (entry 7 in Table 6.5). Good crystals (ca. 1 mg) have been produced and X–ray crystallography established that the solid–state geometric packing is identical to those for **601d**. Due to ^{13}C enrichment, two strong signals for the labeled alkynyl carbon were observed at 81.5 and 75.4 ppm in the solid–state ^{13}C NMR spectra as shown in Figure 6.12a, whereas a single enhanced signal at 75.6 ppm is found in the solution state ^{13}C NMR spectrum. Because the solid-state structure of **604** should be centrosymmetric (based on the crystallographic analysis), it should result in only a single resonance (at 75.6 ppm) for the labeled carbon; the origin of the second signal, is at present unexplained. Unfortunately, spinning side bands are also quite intense. After obtaining a ^{13}C NMR spectrum before heating, the sample holder containing compound **604** was heated at 170 °C under Ar for 3 days. A ^{13}C NMR spectrum of the resulting sample was obtained (Figure 6.12b). The spectrum shows signals at 81.5 and 75.4 ppm from the enriched ^{13}C. This observation contradicts the previous spectrum of unlabeled **601d**, to which some of the alkyne signals still remained after heating. Furthermore, according to the reasoning above, one would observe at least one or more signals in the alkyne region (80–70 ppm), albeit at low intensity, since these ^{13}C are at natural abundance. The fact that no signals were detected may indicate that this process did not proceed ideally or that the alkyne signals are too weak to be identified above the noise. Thus, compound **604** may undergo a 1,6-topochemical polymerization, but more trials are required as discussed in the Future Study section.

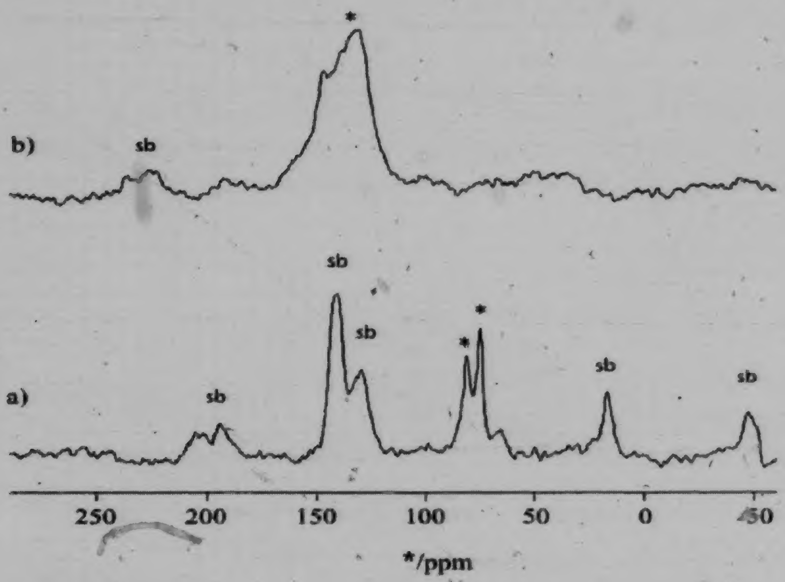

sb = spinning side band. * = Labeled ^{13}C signal

Figure 6.12 Solid–state ^{13}C NMR spectra for compound **604**. a) Before Heating. b) After Heating. Spectra were acquired at 11.75 T (125 MHz for ^{13}C) using *CP/MAS* and a

spinning frequency of 8 kHz. A spectrum acquired at 12 kHz (not shown) confirmed that the peak in the 100–150 ppm region in a) are only from a spinning sideband.

6.3 Conclusions

In this chapter, the syntheses of four functionalized arylene end capped tetraynes **601a–d** and a ^{13}C labeled analogue of **601d** have been described. DSC analyses of the four unlabeled compounds show that the phenyl and nitro aryl derivatives **601a** and **601d**, respectively, show a sharp exothermic signal. This result implies that these two derivatives are suitable candidates for topochemical polymerization. X–ray crystallographic analyses of compounds **601a**, **601c**, and **601d** also confirm that they are suitable for solid–state polymerization. The interatomic distances between each molecule in the solid–state correspond well to the optimal parameters for topochemical polymerization in a 1,6–polymerization manner. The solution-state UV–vis spectroscopic analyses of tetraynes **601a–d** with varying electronic groups at *para*-position (EDG or EWG) show no effect on λ_{max} absorptions and absorbance coefficients. Three λ_{max} UV–vis absorptions in the low energy region are probably due to the 1,1,12,12–tetrabromododeca–1,11–dien–3,5,7,9–tetrayne framework. UV–vis spectroscopic analyses of a thin film of compound **601d** show three λ_{max} bands in the low energy region with a small shift. The intensity of the alkenyl stretches, measured by reflection IR spectroscopy, increased after heating, possibly due to the transformation of the alkyne bonds into alkene bonds in the polymerization process. Solid–state ^{13}C NMR spectroscopic analysis for **601d** shows each aryl and alkynyl peaks are split into two signals after heating. Furthermore, the alkenyl region in the solid–state ^{13}C NMR spectrum suggests the transformation of alkyne to akene. The overall preliminary results support the contention that a topochemical polymerization takes place upon heating the nitro aryl derivatives **601a** and **604**.

6.4 References and Notes

(1) Keibooms, R.; Menon, R.; Lee, K. In *The Handbook of Advanced Electronic and Photonic Materials and Devices*; Halwa, H. S., Ed.; Academic Press: San Diego, 2001; Vol. 8, Chapter 1.

(2) Zhao, Y., Ph.D. Thesis, University of Alberta, Canada, 2002.

(3) Slepkov, A. D.; Hegmann, F. A.; Zhao, Y.; Tykwinski, R. R.; Kamada, K. *J. Chem. Phys.* **2002**, *116*, 3834–3840.

(4) Tykwinski, R. R.; Zhao, Y. *Synlett* **2002**, 1939–1953.

(5) Zhao, Y.; McDonald, R.; Tykwinski, R. R. *Chem. Commun.* **2000**, 77–78.

(6) Fowler, F. W.; Lauher, J. W. *Carbon–Rich Compounds: From Molecules to Materials*; Haley, M. M.; Tykwinski, R. R., Eds. John–VCH: Weinheim, 2005.

(7) Fowler, F. W.; Lauher, J. W. *J. Phys. Org. Chem.* **2000**, *13*, 850–857.

(8) Kiji, J.; Kaiser, J.; Wegner, G.; Schulz, R. C. *Polymer* **1973**, *14*, 433–439.

(9) Enkelmann, V. *Chem. Mater.* **1994**, *6*, 1337–1340.

(10) Baughman, R. H.; Yee, K. C. *Macromol. Rev.* **1978**, *13*, 219–239.

(11) Vellutini, L.; Errien, N.; Froyer, G.; Lacoudre, N.; Boileau, S.; Tran–Van, F.; Chevrot, C. *Chem. Mater.* **2007**, *19*, 497–502.

(12) Szafert, S.; Gladysz, J. A. *Chem. Rev.* **2003**, *103*, 4175–4205.

(13) Wegner, G. *Z. Naturforsch. B: Chem. Sci.* **1969**, *B 24*, 824–832.

(14) Xiao, J.; Yang, M.; Lauher, J. W.; Fowler, F. W. *Angew. Chem. Int., Ed.* **2000**, *39*, 2132–2135.

(15) Okada, S.; Hayamizu, K.; Matsuda, H.; Masaki, A.; Nakanishi, H. *Bull. Chem. Soc. Jpn* **1991**, *64*, 857–863.

(16) Okada, S.; Matsuda, H.; Masaki, A.; Nakanishi, H.; Hayamizu, K. *SPIE–Nonlinear Optical Properties of Organic Materials IV* **1991**, *1560*, 25–34.

(17) Hayamizu, K.; Okada, S.; Tsuzuki, S.; Matsuda, H.; Masaki, A.; Nakanishi, H. *Bull. Chem. Soc. Jpn* **1994**, *67*, 342–345.

(18) Luu, T.; Elliott, E.; Slepkov, A. D.; Eisler, S.; McDonald, R.; Hegmann, F. A.; Tykwinski, R. R. *Org. Lett.* **2005**, *7*, 51–54.

(19) Shi Shun, A. L. K.; Chernick, E. T.; Eisler, S.; Tykwinski, R. R. *J. Org. Chem.* **2003**, *68*, 1339–1347.

(20) Morisaki, Y.; Luu, T.; Tykwinski, R. R. *Org. Lett.* **2006**, *8*, 689–692.

(21) Cammenga, H. K.; Epple, M. *Angew. Chem. Int., Ed. Engl.* **1995**, *34*, 1171–1187.

(22) Kijima, M.; Kinoshita, I.; Shirakawa, H. *Chem. Lett.* **1999**, 531–532.

(23) Okada, S.; Matsuda, H.; Masaki, A.; Nakanishi, H.; Hayamizu, K. *Chem. Lett.* **1990**, 2213–2216.

Chapter 7. Conclusions and Future Plans

This thesis covers five projects undertaken as part of my doctoral studies ranging from the synthesis of natural products to the development of methodology and solid–state polymerization.

At the beginning of my graduate studies, I had an interest in the synthesis of triynol natural products and their analogues. A conjugated triynol framework was constructed from the alkyne migration in a carbenoid FBW rearrangement. We demonstrated that the kinetic stability of these compounds depended on both the terminus substituents and methylene linker between the alkynyl and hydroxyl groups. We showed that the terminal triynol is the most unstable.

This discovery directed our efforts to develop a method to convert the unstable terminal polyynes to a relatively stable 1,2,3–triazole derivative. We trapped terminal polyynes with benzyl azides based on Sharpless' and Meldal's original ideas. We demonstrated that trapping of terminal di–, tri–, and tetraynes with benzyl azide under Cu catalysis produces 4–ethyl, 4–butadiynyl, and 4–hexatriynyl triazoles. The reaction occurs exclusively at the terminal alkyne units and with no trace of multiple additions to the polyyne framework.

I am also interested in the synthesis, physical and nonlinear optical properties of both α,ω–diarylpolyynes and diaryltetraynes. For diarylpolyynes, we constructed a series of symmetrical and unsymmetrical polyynes via a carbenoid rearrangement. The UV–vis spectroscopic analysis of the polyynes demonstrated that molar absorptivity and maximum absorption increase with the number of triple bonds. The X–ray crystallographic analysis of the packing of the diarylenetetraynes reveals that their geometry is suitable for 1,6–polymerization. Solid–state ^{13}C NMR spectroscopic analysis of the thermal polymerization of the 4–nitroaryl derivative demonstrates that this compound can undergo 1,6–polyymeriztion.

A recent project has focused on the development of a method that can be used to synthesize triynols and polyynes in a one–pot reaction via a tandem Fritsch–Buttenberg–Wiechell (FBW) rearrangement and deprotonation step. This method allows one to start with relatively stable and easily accessed precursors and assemble the desired products in a single step.

There are numerous avenues possible for future study. I would like to emphasize two follow–up projects that I believe need to be completed: (a) Trapping the terminal diynone **312q** (and potentially other terminal polyynes) from *Chrysanthemum coronarium* with benzyl azide as identified in Chapter 3, and (b) the solid–state polymerization of the tetraynes, discussed in Chapter 6.

(a) Bohlmann detected the presence of diynone **312q** in the roots of the *C. coronarium*, but no yield was reported. From our study, the ^{1}H NMR spectroscopic analysis of the preliminary efforts to trap compound **312q** from *C. coronarium* with benzyl azide show that two signals from the crude product have similar chemical shifts to those of the synthetic compound corresponding to 1,2,3–triazole. It would be desirable to be able to determine the quantity of this compound (and other polyynes, as the case may be) present in the extract before reacting the solution with benzylazide, based on the characterization of product **311q** after this reaction.

(b) The preliminary results from solid–state ^{13}C NMR, UV–vis, and IR spectroscopic analyses as well as the X–ray crystallographic analysis of compound **604** suggest that this compound can undergo 1,6–polymerization to form polytriacetylenes. Future plans for this project include the need to synthesize a greater quantity of the labeled tetrayne **604** and resolve the signals from the solid–state ^{13}C NMR spectrum. If possible, obtaining a single crystal of the polytriacetylene product suitable for X–ray crystallographic analysis would be desirable.

Chapter 8. Experimental Section

8.1 General Details

Reagents: Reagents were purchased in reagent grade from commercial suppliers and used without further purification. Et_2O, THF, and toluene were distilled from sodium/benzophenone ketyl; hexanes and CH_2Cl_2 were distilled from CaH_2; *N,N*–dimethylformamide (DMF), hexamethylphosphoramide (HMPA), and tetramethylethylenediamine (TMEDA) were dried over molecular sieves immediately prior to use. Anh. $MgSO_4$ or Na_2SO_4 was used as the drying agent after aqueous work–up. Evaporation and concentration *in vacuo* was done at water–aspirator pressure. All reactions were performed in standard, dry glassware under an inert atmosphere of Ar.

Column chromatography: *silica gel–60* (230–400 mesh) from silicycle. Thin Layer Chromatography (TLC): aluminum sheets covered with *silica gel–60* F_{254} from *Macherey–Nagel*; visualization by UV light or $KMnO_4$ stain. Aluminum oxide, neutral, Brockman 1, 150 mesh from *Aldrich Chemical Company, Inc.* (5% water)

Mp: *Gallenkamp* or *Fisher–Johns* apparatus; uncorrected.

IR spectra (cm^{-1}): *Nicolet Magna–IR 750* (neat) or *Nic–Plan IR Microscope* (solids).

^{1}H– and ^{13}C–NMR: *Varian Inova–300, 400* or *500* instruments, at rt in $CDCl_3$ or CD_2Cl_2; solvent peaks (7.24 and 5.32 for ^{1}H and 77.0 and 53.8 for ^{13}C, respectively) as reference. For ^{1}H NMR data, coupling constants are expressed in Hertz (Hz) and are considered precise to within ±0.5 Hz. For simplicity, the coupling constants for the aryl protons of *para*–substituted phenyl groups have been reported as pseudo first–order even though they are second order spin systems. Precursors not a part of a Scheme or Figure in the main text of each Chapter have been assigned a sequential compound number in this Chapter that is preceded by the letter S.

UV–visible spectra: *Pharmacia Biotech Ultrospecc 300* or *Varian Cary 400* at ambient temperature and THF as solvent; λ_{max} in nm (ε in cm^{-1} M^{-1}).

Differential Scanning Calorimetry (DSC); *Perkin Elmer Pyris 1 Differential Scanning Calorimeter*. Thermal analysis performed under a N_2 atmosphere.

EI MS (*m/z*): *Kratos MS 50* instrument. ESI MS (*m/z*): *Micromass Zabspec oaTOF* or *PE Biosystems Mariner TOF* instruments; solvents as noted. MALDI MS (*m/z*): *PE Voyager Elite* instrument in reflectron mode with delayed extraction; matrices as noted; solvents as noted. For mass spectral analyses, low–resolution data are provided in cases when M^+ is not the base peak; otherwise, only high–resolution data are provided. Elemental analyses, DSC, and TGA were conducted by Spectral Services at the University of Alberta.

For IR data, useful functional groups and 3–4 of the strongest absorptions are reported, including but not limited to C–H, C=C and C≡C bond stretches.

Crystallographic data for unpublished compounds are available from the X–ray Crystallography Laboratory, Department of Chemistry, University of Alberta.

All solvent ratios reported are volume:volume, unless otherwise noted.

Measurements of the third order nonlinear optical second hyperpolarizabilities (γ) were acquired using differential optical Kerr effect (DOKE) detection and the data were measured by the collaborator Dr. Aaron Slepkov under the supervision of Dr. Frank A. Hegmann, Department of Physics, University of Alberta.

In cases where crude reaction mixtures were passed through a plug of silica gel and celite, the following procedure was employed: To a fritted funnel (35 mL), a mixture of silica gel and hexanes was added, which was then covered by celite. A sample solution was introduced and flushed with the solvent (as indicated below). Progress of separation was monitored by means of TLC.

8.2 General Experimental Procedures

General Procedure A – Desilylation. The appropriate trimethyl–, triisopropyl–, *t*–butyldimenthyl–, or *t*–butyldiphenylsilyl–protected polyyne was dissolved in wet THF/MeOH [1:1, 10 mL, for deprotection using K_2CO_3 (ca. 0.1 equiv)] or wet THF [10 mL, for deprotection using TBAF (ca. 2.2 equiv)] was added, and the resulting solution was stirred, in the presence of air at rt, until TLC analysis indicated complete conversion to the desilylated intermediate. Et_2O (10 mL) was added, and the resulting solution was washed with satd. NH_4Cl (2 x 10 mL), washed with satd. NaCl (2 x 10 mL), and dried over $MgSO_4$. Solvent was reduced to ca. 1 mL and the deprotected polyyne was carried on or the deprotected polyyne can be purified using column chromatography (silica gel), if necessary.

General Procedure B – Palladium Catalyzed Cross–Coupling. The respective terminal acetylene (ca. 0.4 mmol) was combined with the appropriate aryl halide (one equiv per terminal acetylene) and dissolved in dry THF or DMF (40 mL). Et_3N (3 mL) was added and the resulting solution was degassed for at least 45 min. $Pd(PPh_3)_4$ or

$PdCl_2(PPh_3)_2$ (ca. 0.05 equiv per coupling event) was added and the reaction mixture was stirred at rt for 5 min. CuI (ca. 0.15 equiv per coupling event) was added and the reaction mixture was stirred at the temperature indicated in the individual procedure. Reactions performed at elevated termperatures were sealed under Ar for heating. When TLC analysis indicated full consumption of the starting polyyne, the reaction mixture was cooled to rt, Et_2O (20 mL) was added, and the resulting solution was washed with satd. NH_4Cl (2 x 25 mL) and dried. Solvent removal followed by purification via column chromatography and/or recrystallization yielded the desired product.

General Procedure C – Formation of Alcohols. To the terminal alkyne (1.1 equiv) in THF (ca. 20 mL) at –78 °C was added BuLi (ca. 1.1 equiv). After stirring for 1 h at –78 °C, the corresponding aldehyde (1 equiv) was added in one portion and the reaction was warmed to rt. Et_2O (20 mL) and satd. aq. NH_4Cl (2 x 20 mL) were added, the organic phase was separated, washed satd. aq. NaCl (2 x 20 mL), and dried over $MgSO_4$. Solvent removal and purification by column chromatography (silica gel) afforded the desired alcohol.

General Procedure D – Formation of Ketones. To the alcohol (1 equiv) in anhyd CH_2Cl_2 (10 mL) at rt was added MnO_2 (2–8 equiv), $BaMnO_4$ (2 equiv), or PCC (2 equiv) in one portion. After stirring for overnight at rt, the mixture was filtered through a plug of celite and silica gel (CH_2Cl_2) affording a crude ketone. This ketone can be carried on to the next step or purified by using column chromatography (silica gel) if necessary.

General Procedure E – Formation of Dibromoolefins. To CBr_4 (2 equiv) in CH_2Cl_2 (10 mL) at 0 °C was added PPh_3 (4 equiv) and the mixture was stirred for 30 min. This mixture was added to the ketone in CH_2Cl_2 (3 mL) at 0 °C and stirred for 3 h. The mixture was filtered through celite and purified by column chromatography (silica gel) to afford the desired dibromoolefin.

General Procedure F – Fritsch–Buttenberg–Wiechell Rearrangement (FBW) for the Formation of Polyynes. To the dibromoolefin (1 equiv) in anhyd hexanes (10 mL) at –78 °C was added dropwise BuLi (1.1 equiv). The reaction was stirred at –78 °C for 30 min, and then warmed to rt for 30 min. Et_2O (10 mL) and satd. aq. NH_4Cl (10 mL) were added. The organic phase was separated, washed with satd. aq. NaCl (2 x 10 mL), and dried over $MgSO_4$. Solvent removal and purification by column chromatography afforded the desired triynol.

General Procedure G – Friedel–Crafts Acylation. Unless otherwise noted in the individual procedures, $SOCl_2$ (42 mmol) was added to the carboxylic acid (7.0 mmol) in a dry flask protected from moisture with a drying tube containing $CaCl_2$, and the mixture allowed to stir overnight at rt. The excess thionyl chloride was then removed *in vacuo* to provide the acid chloride. CH_2Cl_2 (50 mL) was added and the temperature of the solution lowered to 0 °C. Bis(trimethylsilyl)acetylene (7.0 mmol) or bis(trimethylsilyl)butadiyne (7.0 mmol) and $AlCl_3$ (8.0 mmol) was added and the reaction mixture warmed to rt over 3 h. The reaction was carefully quenched by the addition of the reaction to 10% HCl (50 mL) in ice (50 mL). Et_2O (70 mL) was added, the organic layer separated, washed with satd. aq. $NaHCO_3$ (2 x 20 mL), satd. aq. NaCl (2 x 20 mL), dried over $MgSO_4$, and the solvent removed *in vacuo*. Column chromatography (silica gel), if necessary, provided the pure ketone.

General Procedure H – Oxidative Coupling. The terminal alkyne was added to a solution of the Hay catalyst [CuCl (0.30 mmol) and TMEDA (0.60 mmol) in CH_2Cl_2

(60 mL), previously stirred until homogeneous] and a stream of oxygen was bubbled into the reaction until the solution turned blue. This mixture was stirred at rt under oxygen until TLC analysis no longer showed the starting material (ca. 3 h). Et_2O (30 mL) and satd. aq. NH_4Cl (2 x 20 mL), dried over $MgSO_4$, and the solvent removed *in vacuo*. Column chromatography (silica gel) and/or recrystallization gave the desired product.

General Procedure I – Lithium Diisopropyl Amide Deprotonation. To a mixture of diisopropylamine (3.0 mmol) in Et_2O (10 mL) or THF (10 mL) at –78 °C was added BuLi (3.0 mmol). The mixture was stirred for 1 h, then transferred via cannula into a round bottom flask containing a solution of the terminal acetylene (3.0 mmol) in Et_2O (100 mL) at –78 °C.

General Procedure J – The Reaction of Di–, Tri–, and Tetraynes with Benzyl Azide. A mixture of the appropriate trimethylsilyl– or triisopropylsilyl–protected polyyne and K_2CO_3 (ca. 0.5 g) or TBAF (2.0 equiv) in wet THF/MeOH (1:1 v/v, 5 mL) or THF (10 mL), respectively, was combined and stirred at rt until TLC analysis showed the formation of the terminal alkyne. Et_2O and satd. aq. NH_4Cl were added, the organic phase was separated, washed with satd. aq. NH_4Cl (2 x 10 mL), satd. aq. NaCl (10 mL), and then dried over $MgSO_4$. DMF (1 mL) was then added and the solution concentrated to 1–2 mL via rotary evaporation to remove Et_2O, THF, or MeOH. To the mixture above, DMF (10 mL) was added, followed by benzyl azide (0.85 equiv based on the starting silylated polyyne), $CuSO_4{\bullet}5H_2O$ (0.1 g), ascorbic acid (0.1 g), and H_2O (2 mL). This mixture was then stirred at rt until TLC analysis no longer showed the presence of benzyl azide. Satd. aq. NH_4Cl (10 mL) and Et_2O (10 mL) were added, the organic phase was separated, washed with satd. aq. NaCl (2 x 10 mL), and dried over $MgSO_4$, solvent removal and purification via column chromatography (silica gel) or recrystallization from hexanes gave the desired triazole.

General procedure K – Synthesis of Functionalized Polyynes by Trapping with Electrophiles. The appropriate dibromoolefin (0.5–1.0 mmol) was dissolved in toluene (2 mL) and this mixture was then diluted with hexanes (10 mL) and cooled to –20 °C under an Ar atmosphere. To this solution with stirring, BuLi (2.2 equiv, 1.6 or 2.5 M in hexanes) was added via syringe over a period of ca. 1 min. The reaction mixture was allowed to slowly warm to 0 °C. The reaction was then cooled to –20 °C again, and Et_2O (10 mL) was added, followed by the addition of the electrophile (dissolved in 2 mL of Et_2O) via a canula. The reaction mixture was allowed to slowly warm to rt overnight. Satd. aq. NH_4Cl (10 mL) and Et_2O (10 mL) were added, the organic phase was separated, washed with satd. aq. NaCl (2 x 10 mL), and dried over $MgSO_4$. Solvent removal and purification by column chromatography (silica gel) gave the desired product. Additional steps, as required, are also indicated below.

General procedure L – The FBW–Negishi Method. The appropriate dibromoolefin (1.0 mmol) in toluene (10 mL) was cooled to –40 °C under N_2 atmosphere. To this solution with stirring, BuLi (2.5 M in hexanes, 0.90 mL, 2.2 mmol) was added by a syringe over a period of ca. 5 min. The reaction mixture was allowed to slowly warm to –20 °C. The reaction mixture was cooled to –40 °C again. To this mixture with stirring, $ZnCl_2$ (0.50 M in THF, 2.4 mL, 1.2 mmol) was added by a syringe over a period of ca. 5 min. The reaction mixture was allowed to slowly warm to 0 °C. Aryl halide (1.1 mmol) and $Pd(PPh_3)_4$ (58 mg, 0.050 mmol) were added directly under a flow of N_2, and this mixture was heated up to 70 °C. After 20 h, the reaction mixture was filtered through a Celite plug. After the solvent was removed under reduced pressure, the residue was purified by column chromatography (silica gel) to give the targeted compound.

General procedure M – FBW–Hay Method. The appropriate dibromoolefin (0.70 mmol) in toluene (10 mL) was cooled to –40 °C under N_2 atmosphere. To this solution with stirring, BuLi (1.40 mmol) was added by a syringe over a period of ca. 5 min. The reaction mixture was allowed to slowly warm to –20 °C. To this mixture with stirring, CuBr (14 mmol) and TMEDA (13 mmol) were added, followed by bubbling oxygen in the solution for 15 min. The reaction mixture was allowed to slowly warm to rt overnight. The reaction mixture was filtered through a plug of alumina oxide and purified by column chromatography to give the targeted compound.

General procedure N – FBW–Stille Method. A solution of the dibromoolefin (0.70 mmol) in toluene (3.0 mL) was cooled to –40 °C under N_2 atmosphere. To this solution with stirring, BuLi (2.5 M in hexanes, 0.65 mL, 1.6 mmol) was added by a syringe over a period of ca. 5 min. The reaction mixture was allowed to slowly warm to –20 °C. The reaction mixture was cooled to –40 °C again. To this mixture with stirring, Bu_3SnCl (0.45 mL, d = 1.2 g/mL, 0.54 g, ca 1.2 mmol) was added by a syringe over a period of 5 min. The reaction mixture was allowed to slowly warm to rt and stirred for 2 h. Acid chloride (0.70 mmol) and $PdCl_2(PPh_3)_2$ (25 mg, 0.035 mmol) in CH_2Cl_2 (15 mL) were added, and this mixture was refluxed overnight. The reaction mixture was cooled to rt. Aqueous KF solution (30 mL) and ether (30 mL) were added and stirred vigorously for 15 min. This solution was filtered by using a Celite column. The organic phase was separated, washed with water, and dried over $MgSO_4$. After the solvent was removed under reduced pressure, the residue was purified by column chromatography (silica gel) to give the target compound.

General procedure O – FBW–Pt Acetylide Formation. A solution of dibromoolefin (0.50 mmol) in toluene (5.0 mL) was cooled to –40 °C under nitrogen atmosphere. To this solution with stirring, BuLi (1.12 mmol) was added dropwise by a syringe. The reaction mixture was allowed to slowly warm to –20 °C. The reaction was then cooled to –40 °C again. To this mixture with stirring, CuI (0.656 mmol) was added directly under a flow of nitrogen, followed by the addition of *cis*–$PtCl_2(PPh_3)_2$ (0.252 mmol). The reaction mixture was stirred at rt overnight and 50 °C for 4 h. After the mixture was cooled, H_2O (5.0 mL) and CH_2Cl_2 (5.0 mL) were added. The organic phase was separated, washed with H_2O, and dried over $MgSO_4$. After removal of $MgSO_4$, the solvent was removed under reduced pressure. The brown solid residue was dissolved in a small amount of CH_2Cl_2 and recrystalized with MeOH or purified by column chromatography (silica gel) to give the desired product.

General procedure P – *Trans* Pt–Complexes to *Cis* Pt–Complexes Method. A solution of the *trans*-platinum complex (0.099 mmol) and dppe (0.030 mmol) in CH_2Cl_2 (5 mL) was stirred under an Ar atmosphere overnight. CH_2Cl_2 and satd. aq. NH_4Cl were added, the organic phase was separated, washed with satd. aq. NH_4Cl (2 x 10 mL), satd. aq. NaCl (10 mL), and then dried over $MgSO_4$. After removal of $MgSO_4$, the solvent was removed under reduced pressure. *Cis*-Pt–complexes were purified by column chromatography (silica gel) to give desired product.

8.3 Experimental Procedures

8.3.1 Chapter 2

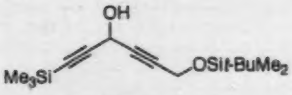

215

6–(*tert*–Butyldimethylsilanyloxy)–1–trimethylsilanylhexa–1,4–diyn–3–ol (215)

To $Me_3SiC{\equiv}CH$ (341 mg, 3.47 mmol) in THF (14 mL) at –78 °C was added BuLi (2.4 M in hexanes; 1.4 mL, 3.5 mmol) and aldehyde **210**[1] (561 mg, 2.81 mmol) were used according to general procedure C yielding **215** (572 mg, 69%) as a light yellow oil. R_f = 0.4 (CH_2Cl_2).

IR (cast, $CDCl_3$) 3395, 2958, 2179, 1363 cm^{-1}; ^1H NMR (400 MHz, $CDCl_3$) δ 5.12 (d, J = 7.0 Hz, 1H), 4.37 (s, 1H), 4.36 (s, 1H), 2.16 (d, J = 7.0 Hz, 1H), 0.95 (s, 9H), 0.18 (s, 9H), 0.13 (s, 6H); ^{13}C NMR (100 MHz, $CDCl_3$) δ 101.7, 89.5, 83.2, 81.9, 52.6, 51.7, 25.8, 18.3, –0.3, –5.0. EIMS m/z 239.1 ($[M - t\text{–}Bu]^+$, 8); HRMS calcd. for $C_{11}H_{19}O_2Si_2$ ($[M - t\text{–}Bu]^+$) 239.0924, found 239.0923. Anal. calcd. for $C_{15}H_{28}O_2Si_2$: C, 60.75; H, 9.52. Found: C, 60.60; H, 9.46.

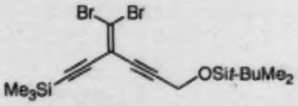

216

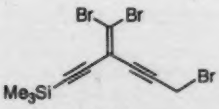

217

6–(*tert*–Butyldimethylsilanyloxy)–3–(dibromomethylidene)–1–trimethylsilanylhexa–1,4–diyne (216) and 6–Bromo–3–(dibromo-methylidene)–1–trimethylsilanylhexa–1,4–diyne (217)

Compound **215** (442 mg, 1.49 mmol) in anhyd CH_2Cl_2 (7 mL) and MnO_2 (1.55 g, 17.8

mmol) in one portion according to general procedure D affording a ketone (257 mg, 59%) as a yellow oil. *R*$_f$ = 0.6 (hexanes–CH_2Cl_2, 1:2).

IR (cast, $CHCl_3$) 2958, 2930, 2858, 2229, 2147, 1634 cm^{-1}; ^{1}H NMR (300 MHz, $CDCl_3$) δ 4.47 (s, 2H), 0.89 (s, 9H), 0.23 (s, 9H), 0.13 (s, 6H); ^{13}C NMR (100 MHz, $CDCl_3$) δ 160.0, 102.2, 99.5, 91.5, 84.8, 51.6, 25.7, 18.2, –0.99, –5.22. EIMS *m/z* 294.1 (M$^+$, 1), 237.1 ([M – *t*–Bu]$^+$, 95), 209.1 ([M – *t*–Bu – Me$_2$]$^+$, 100); HRMS calcd. for $C_{11}H_{17}O_2Si_2$ (M – *t*–Bu)$^+$ 237.0767, found 237.0767. Anal. calcd. for $C_{15}H_{26}O_2Si_2$: C, 61.17; H, 8.90. Found: C, 61.03; H, 8.84.

CBr_4 (512 mg, 1.54 mmol) in CH_2Cl_2 (3 mL), PPh_3 (809 mg, 3.08 mmol) and the ketone (227 mg, 0.772 mmol) in CH_2Cl_2 (3 mL) were used according to general procedure E affording **216** and **217**.

Compound 216

Yield: 57.5 mg (17%); light yellow oil; *R*$_f$ = 0.2 (hexanes).

IR (cast, $CHCl_3$) 2957, 2929, 2857, 2159 cm^{-1}; ^{1}H NMR (400 MHz, $CDCl_3$) δ 4.43 (s, 2H), 0.89 (s, 9H), 0.20 (s, 9H), 0.13 (s, 6H); ^{13}C NMR (100 MHz, $CDCl_3$) δ 113.9, 108.9, 102.5, 100.1, 94.7, 81.1, 52.2, 25.8, 18.2, –0.52, –5.08. EIMS *m/z* 450.0 (M$^+$, 2), 145.0 ([M – Br$_2$ – *t*–BuMe$_2$SiCH$_2$O]$^+$, 100); HRMS calcd. for $C_{16}H_{26}OSi_2{}^{81}Br^{79}Br$ (M$^+$) 449.9869, found 449.9854.

Compound 217

Yield: 20 mg (7%); light yellow oil; *R*$_f$ = 0.4 (hexanes).

IR (cast, $CHCl_3$) 2959, 2150, 1250 cm^{-1}; ^{1}H NMR (300 MHz, $CDCl_3$) δ 4.05 (s, 2H), 0.23 (s, 9H); ^{13}C NMR (100 MHz, $CDCl_3$) δ 113.4, 111.0, 103.1, 99.7, 90.6, 82.5, 14.1, –0.53. EIMS *m/z* 399.8 (M$^+$, 46); HRMS calcd. for $C_{10}H_{11}Si^{79}Br^{81}Br_2$ (M$^+$) 399.8139, found 399.8138.; HRMS calcd. for $C_{10}H_{11}Si^{79}Br_2{}^{81}Br$: 397.8160, found 397.8159.

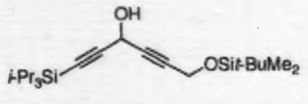

218

6–(*tert*–Butyldimethylsilanyloxy)–1–triisopropylsilanylhexa–1,4–diyn–3–ol (218)

To *i*–$Pr_3SiC{\equiv}CH$ (565 mg, 3.10 mmol) in THF (10 mL) at –78 °C was added BuLi (2.5 M in hexanes; 1.25 mL, 3.1 mmol) and aldehyde **214**[1] (511 mg, 2.58 mmol) according to general procedure C affording **218** (805 mg, 82%). Spectral data were consistent with that reported in the literature.[2]

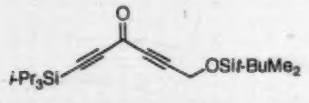

219

6–(*tert*–Butyldimethylsilanyloxy)–1–triisopropylsilanylhexa–1,4–diyn–3–one (219)

Compound **218** (576 mg, 1.52 mmol) in anhyd CH_2Cl_2 (30 mL) and $BaMnO_4$ (1.31 g, 5.12 mmol) in one portion were used according to general procedure D affording **219** (523 mg, 91%). Spectral data were consistent with that reported in the literature.[3]

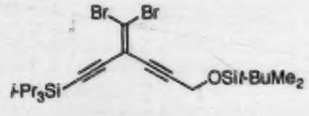

220

6–(*tert*–Butyldimethylsilanyloxy)–3–(dibromomethylidene)–1–triisopropylsilanylhexa–1,4–diyne (220)

CBr_4 (648 mg, 1.95 mmol) in CH_2Cl_2 (8 mL) at 0 °C was added PPh_3 (1.02 g, 3.90 mmol). The mixture was stirred for 30 min and Et_3N (0.1 mL) was added. The mixture was transferred to a solution of **219** (369 mg, 0.974 mmol) in CH_2Cl_2 (1 mL) at 0 °C according to general procedure E affording **220** (402 mg, 77%), as a colorless oil. R_f =

0.7 (hexanes/CH_2Cl_2, 2:1).

IR (cast, $CHCl_3$) 2944, 2892, 2865, 2223, 2156, 1463 cm^{-1}. ^1H NMR (400 MHz, $CDCl_3$) δ 4.44 (s, 2H), 1.08 (s, 21H), 0.89 (s, 9H), 0.12 (s, 6H); ^{13}C NMR (100 MHz, $CDCl_3$) δ 114.2, 108.7, 101.9, 99.5, 94.5, 81.3, 52.2, 25.7, 18.6, 18.2, 11.1, –5.1. EIMS *m/z* 534.1 (M^+, 11); HRMS calcd. for $C_{22}H_{38}O^{79}Br^{81}BrSi_2$ (M^+) 534.0808, found 534.0815. Anal. calcd. for $C_{22}H_{38}OBr_2Si_2$: C, 49.43; H, 7.17. Found: C, 49.43; H, 7.49.

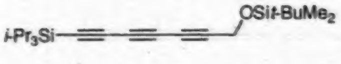

221

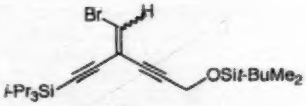

222

7–(*tert*–Butyldimethylsilanyloxy)–1–triisopropylsilanyl–1,3,5–heptatriyne (221) and 5–(*tert*–Butyldimethylsilanyloxy)–1–bromo–2–triisopropylsilanyl–3–yn–1–pentene (222)

Compound **220** (402 mg, 0.751 mmol) in anhyd hexanes (6 mL) and BuLi (2.5 M in hexanes; 0.6 mL, 1.5 mmol) according to general procedure F yielding **221** and **222**.

Compound 221

R_f = 0.4 (hexanes/CH_2Cl_2, 6:1).

IR (cast, $CHCl_3$) 2942, 2891, 2865, 2154 cm^{-1}. ^1H NMR (400 MHz, $CDCl_3$) δ 6.88 (s, 1H), 4.391 (s, 1H), 4.390 (s, 1H), 1.10 (s, 21H), 0.90 (s, 9H), 0.11 (s, 6H); ^{13}C NMR (100 MHz, $CDCl_3$, APT) δ 123.1, 112.1, 100.9, 99.0, 88.4, 80.8, 52.0, 25.8, 18.5, 18.2, 11.1, –5.1. EIMS *m/z* 485.2483.2 (M^+, 1).

Compound 222

Yield: 172 mg (61%) as a colorless oil. R_f = 0.5 (hexanes/CH_2Cl_2, 6:1).

IR (cast, $CHCl_3$) 2945, 2865, 2194, 2164, 2078, 1463 cm^{-1}; ^1H NMR (400 MHz, $CDCl_3$) δ 4.37 (s, 2H), 1.06 (s, 21H), 0.88 (s, 9H), 0.10 (s, 6H); ^{13}C NMR (100 MHz, $CDCl_3$, APT) δ 89.6, 84.9, 69.8, 63.5, 60.3, 52.1, 25.8, 18.5, 11.3, –5.2, two coincident signals not observed. EIMS *m/z* 374.2 (M^+, 7), 287.2 ($[M - t\text{–Bu} - Me_2]^+$, 100); HRMS calcd. for $C_{22}H_{38}OSi_2$ (M^+) 374.2461, found 374.2465.

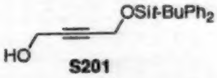

S201

4–(*tert*–Butyldiphenylsilanyloxy)–2–butyn–1–ol (S201)

To 1,4–butynediol (15 g, 174 mmol) in THF (100 mL) at rt were added t–$BuPh_2SiCl$ (8.46 g, 30.8 mmol), Et_3N (5 mL), and DMAP (0.100 g, 0.819 mmol). After stirring overnight, the mixture was washed with H_2O (100 mL). The organic phase was separated, washed with sat. aq NH_4Cl (2 × 100 mL), sat. aq NaCl (2 × 100 mL), and dried over $MgSO_4$. Solvent removal and purification by column chromatography (CH_2Cl_2) afforded **S201** [starting material 1,4–butynediol was also recovered, (8.38 g, 84%)] as a colorless oil; $R_f = 0.3$ (CH_2Cl_2).

IR (cast, $CHCl_3$) 3214, 3070, 2957, 2857, 1589 cm^{-1}; ^1H NMR (500 MHz, $CDCl_3$) δ =7.71–7.68 (m, 4H), 7.44–7.36 (m, 6H), 4.35 (t, $J = 2.0$ Hz, 2H), 4.18 (t, $J = 2.0$ Hz, 2H), 1.33 (br s, 1H), 1.04 (s, 9H); ^{13}C NMR (500 MHz, $CDCl_3$) δ 135.7, 133.1, 129.8, 127.7, 84.3, 83.4, 52.6, 51.2, 26.7, 19.1. EIMS *m/z* 267.1 ($[M - t\text{–Bu}]^+$, 41); HRMS calcd. for $C_{16}H_{15}O_2Si$ ($[M - t\text{–Bu}]^+$) 267.0841, found 267.0835.

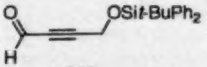

214

4–(*tert*–Butyldiphenylsilanyloxy)–2–butyn–1–al (214)

Compound **S201** (866 mg, 2.67 mmol) in CH_2Cl_2 (100 mL) and $BaMnO_4$ (2.05 g, 8.01 mmol) according to general procedure D yielding **214** (498 mg, 58%, 84% based on recovered starting material), as a colorless oil. $R_f = 0.7$ (CH_2Cl_2).

IR (cast, $CHCl_3$) 3071, 2958, 2858, 2262, 2188, 1674 cm^{-1}; ^{1}H NMR (500 MHz, $CDCl_3$) δ 9.14 (s, 1H), 7.69–7.66 (m, 4H), 7.46–7.37 (m, 6H), 4.47 (s, 2H), 1.06 (s, 9H); ^{13}C NMR (100 MHz, $CDCl_3$) δ 176.4, 135.6, 132.3, 130.1, 127.9, 94.4, 84.5, 52.4, 26.6, 19.1. EIMS *m/z* 309.1 (M^+, 1), 265.1 ($[M - t\text{–}Bu]^+$, 100); HRMS calcd. for $C_{20}H_{22}O_2Si$ (M^+) 309.1389, found 309.1384.

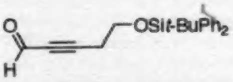

223a

5–(*tert*–Butyldiphenylsilanyloxy)–2–pentyn–1–al (219a) – Method 1

Compound **224a**[4] (2.29 g, 7.42 mmol) in THF (30 mL) at –78 °C was added BuLi (1.6 M in hexanes; 4.2 mL, 6.7 mmol). After stirring for 2 h at –78 °C, *N,N*–dimethylformamide (1.2 g, 16 mmol) was added dropwise by syringe and the reaction was warmed to rt overnight. Et_2O (50 mL) and 10% aq HCl (2 x 100 mL) were added. The organic phase was separated, neutralized with sat. aq $NaHCO_3$, washed with sat. aq NaCl (2 × 100 mL), and dried over $MgSO_4$. Solvent removal and purification by column chromatography (hexanes/CH_2Cl_2, 3:1) afforded **223a** (1.13 g, 50%) as a colorless oil. R_f = 0.3 (hexanes/CH_2Cl_2, 3:1).

IR (microscope): 3071, 2932, 2858, 2281, 2206, 1670 cm^{-1}; ^{1}H NMR (400 MHz, $CDCl_3$) δ 9.13 (s, 1H), 7.66–7.64 (m, 4H), 7.43–7.38 (m, 6H), 3.82 (t, *J* = 6.6 Hz, 2H), 2.63 (t, *J* = 6.6 Hz, 2H), 1.05 (s, 9H); ^{13}C NMR (100 MHz, $CDCl_3$) δ 176.8, 135.4, 133.0, 129.7, 127.6, 96.0, 82.2, 61.1, 26.6, 23.2, 19.1; EIMS *m/z* 336.2 (M^+, 1), 279.1 ($[M - t\text{–}Bu]^+$, 90); HRMS calcd. for $C_{21}H_{24}O_2Si$ (M^+) 336.1546, found 336.1543.

5–(*tert*–Butyldiphenylsilanyloxy)–2–pentyn–1–al (223a) – Method B

To **224a**[4] (1.03 g, 3.04 mmol) in CH_2Cl_2 (50 mL) at rt was added $BaMnO_4$ (1.61 g, 6.28 mmol). After stirring overnight, the mixture was filtered through a plug (celite, CH_2Cl_2).

Solvent removal and purification by column chromatography (CH_2Cl_2) afforded **223a** (0.780 g, 76%) as a colorless oil. Spectral data were consistent with those of **223a** described above.

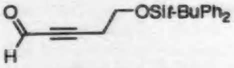

223a

6–(*tert*–Butyldiphenylsilanyloxy)–2–hexyn–1–al (223b) – Method A

To **224b**[4] (5.00 g, 15.5 mmol) in THF (150 mL) at –78 °C was added BuLi (2.5 M in hexanes; 6.2 mL, 15 mmol). After stirring for 2 h at –78 °C, *N,N*–dimethylformamide (1.2 g, 16 mmol) was added dropwise by syringe and the reaction was warmed to rt overnight. Et_2O (50 mL) and 10% aq HCl (2 x 100 mL) were added. The organic phase was separated, neutralized with sat. aq $NaHCO_3$ (50 mL), washed with sat. aq NaCl (2 × 100 mL), and dried over $MgSO_4$. Solvent removal and purification by column chromatography (hexanes/CH_2Cl_2, 3:1) afforded **223b** (2.3 g, 43%) as a colorless oil. R_f = 0.2 (hexanes/CH_2Cl_2, 3:1).

IR (microscope) 3071, 2957, 2932, 2868, 2279, 2204, 1671 cm^{-1}; ^{1}H NMR (400 MHz, $CDCl_3$) δ 9.11 (s, 1H), 7.66–7.63 (m, 4H), 7.44–7.35 (m, 6H), 3.73 (t, J = 6.0 Hz, 2H), 2.56 (t, J = 7.2, 2H), 1.81 (tt, J = 7.2 Hz, 6.0 Hz, 2H), 1.04 (s, 9H); ^{13}C NMR (100 MHz, $CDCl_3$) δ 176.9, 135.4, 133.4, 129.6, 127.6, 98.7, 81.6, 61.8, 30.3, 26.7, 19.1, 15.6; EIMS *m/z* 393.1 ([M – *t*–Bu]$^+$, 100); HRMS calcd. for $C_{18}H_{17}O_2Si$ ([M – *t*–Bu]$^+$) 293.0998, found 293.1001.

6–(*tert*–Butyldiphenylsilanyloxy)–2–hexyn–1–al (223b) – Method B

Compound **224b**[4] (1.52 g, 4.31 mmol) in CH_2Cl_2 (50 mL) and $BaMnO_4$ (1.72 g, 6.71 mmol) according to general procedure D yielding **223b** (0.862 g, 57%) as a colorless oil. Spectral data were consistent with those of **223b** described above.

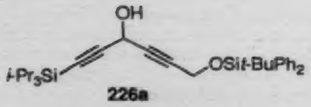

226a

6–(*tert*–Butyldiphenylsilanyloxy)–1–triisopropylsilanylhexa–1,4–diyn–3–ol (226a)

To *i*–Pr$_3$SiC≡CH (621 mg, 3.41 mmol) in THF (65 mL) at –78 °C was added BuLi (1.6 M, hexanes; 2.3 mL, 3.7 mmol) and aldehyde **223** (1.00 g, 3.10 mmol) according to general procedure C yielding **226a** (1.31 g, 84%), as a colorless oil. R_f = 0.2 (hexanes/CH$_2$Cl$_2$, 2:1).

IR (cast, CHCl$_3$) 3405, 3071, 2942, 2180, 1589 cm^{-1}; ^{1}H NMR (500 MHz, CDCl$_3$) δ 7.70–7.68 (m, 4H), 7.44–7.3 (m, 6H), 5.05 (br d, *J* = 4.0 Hz, 1H), 4.35(3) (d, *J* = 1.0 Hz, 1H), 4.35(0) (d, *J* = 1.0 Hz, 1H), 1.95 (br s, 1H), 1.07 (s, 21H), 1.05 (s, 9H); ^{13}C NMR (100 MHz, CDCl$_3$) δ 135.6(5), 135.6(7), 133.0, 133.0, 129.8, 127.7, 103.8, 85.9, 82.7, 82.3, 52.6(4), 52.5(8), 26.7, 19.1, 18.4, 11.1; two coincident signals not observed. HRMS (ES, MeOH/toluene, 3:1) *m/z* calcd. for C$_{31}$H$_{44}$O$_2$Si$_2$Na ([M + Na]$^+$) 527.2772, found 527.2770. Anal. calcd. for C$_{31}$H$_{44}$O$_2$Si$_2$: C, 73.75; H, 8.78. Found: C, 73.48; H, 8.95.

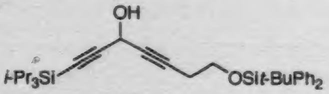

226b

7–(*tert*–Butyldiphenylsilanyloxy)–1–triisopropylsilanylhepta–1,4–diyn–3–ol (226b)

To *i*–Pr$_3$SiC≡CH (599 mg, 3.28 mmol) in THF (30 mL) at –78 °C was added BuLi (1.6 M in hexanes; 2.0 mL, 3.2 mmol) and aldehyde **223a** (1.01 g, 3.00 mmol) according to general procedure C yielding **226b** (1.38 g, 89%) as a colorless oil. R_f = 0.5 (hexanes/CH$_2$Cl$_2$, 1:2).

IR (CHCl$_3$, cast) 3421, 3071, 2942, 2864, 2232(w), 2171(w), 1112 cm^{-1}; ^{1}H NMR (500 MHz, CDCl$_3$) δ 7.67–7.65 (m, 4H), 7.43–7.35 (m, 6H), 5.05 (dt, *J* = 2.0 Hz, 7.5 Hz, 1H), 3.76 (t, J = 7.5 Hz, 2H), 2.48 (td, J = 7.5 Hz, 2.0 Hz, 2H), 1.99–1.96 (m, 1H), 1.04 (s, 21H), 1.03(7) (s, 9H); ^{13}C NMR (100 MHz, $CDCl_3$) δ 135.4, 133.4, 129.5, 127.5, 104.4, 85.4, 82.1, 78.6, 62.1, 52.6, 26.7, 22.7, 19.1, 18.4, 11.0; EIMS *m/z* 461.2 ([M – *t*–Bu]$^+$, 41); HRMS calcd. for $C_{28}H_{37}O_2Si_2$ ([M – *t*–Bu]$^+$) 461.2347, found 461.2312. Anal. calcd. for $C_{32}H_{46}O_2Si_2$: C, 74.07; H, 8.94. Found: C, 73.90; H, 9.56.

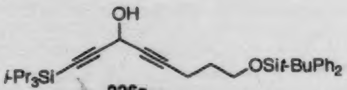

226c

8–(*tert*–Butyldiphenylsilanyloxy)–1–triisopropylsilanylocta–1,4–diyn–3–ol (226c)

To *i*–$Pr_3SiC{\equiv}CH$ (575 mg, 3.15 mmol) in THF (30 mL) at –78 °C was added BuLi (2.5 M in hexanes; 1.3 mL, 3.2 mmol) and aldehyde **223b** (1.01 g, 2.88 mmol) according to general procedure C yielding **226c** (1.38 g, 90%) as a colorless oil. R_f = 0.4 (hexanes/CH_2Cl_2, 1:1).

IR (microscope) 3420, 3072, 2943, 2865, 2290(w), 2233(w), 2174(w), 1111 cm^{-1}; ^{1}H NMR (400 Hz, $CDCl_3$) δ 7.66–7.63 (m, 4H), 7.43–7.34 (m, 6H), 5.01–5.02 (m, 1H), 3.72 (t, J = 6.0 Hz, 2H), 2.37 (td, J = 6.8 Hz, 2.4 Hz, 2H), 1.97 (br d, J = 7.6 Hz, 1H), 1.74 (tt, J = 6.8 Hz, 6.0 Hz, 2H), 1.05 (s, 21H), 1.03 (s, 9H); ^{13}C NMR (100 MHz, $CDCl_3$) δ 135.5, 133.7, 129.4, 127.5, 104.6, 85.2, 84.8, 77.7, 62.1, 52.7, 31.2, 26.7, 19.1, 18.4, 15.1, 11.0; EIMS *m/z* 475.2 ([M – *t*–Bu]$^+$, 67); HRMS calcd. for $C_{29}H_{39}O_2Si_2$ ([M – *t*–Bu]$^+$) 475.2489, found 275.2478. Anal. calcd. for $C_{32}H_{46}O_2Si_2$: C, 74.38; H, 9.08. Found: C, 74.41; H, 9.13.

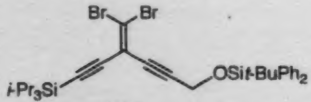

227a

6–(*tert*–Butyldiphenylsilanyloxy)–3–(dibromomethylidene)–1–

triisopropylsilanylhexa–1,4–diyne (227a)

Compound **226a** (576 mg, 1.14 mmol) in CH_2Cl_2 (30 mL) and $BaMnO_4$ (1.31 g, 5.11 mmol) in one portion according to general procedure D affording a crude ketone (523 mg, 91%) as a yellow oil, which was used in the next step without further purification. $R_f = 0.5$ (hexanes/CH_2Cl_2, 1:1).

CBr_4 (660 mg, 1.99 mmol) in CH_2Cl_2 (10 mL) at 0 °C was added PPh_3 (1.05 g, 4.00 mmol). The mixture was stirred for 30 min and Et_3N (0.1 mL) was added. The mixture then was added to the ketone (501 mg, 0.998 mmol) in CH_2Cl_2 (1 mL) at –20 °C according to general procedure E affording **227a** (293 mg, 45%), as a colorless oil. $R_f =$ 0.7 (hexanes/CH_2Cl_2, 2:1).

IR (cast, CH_2Cl_2) 3071, 2942, 2864, 2224, 2156, 1589, 1471 cm^{-1}; ^1H NMR (300 MHz, $CDCl_3$) δ 7.72–7.67 (m, 4H), 7.44–7.34 (m, 6H), 4.43 (s, 2H), 1.09 (s, 21H), 1.04 (s, 9H); ^{13}C NMR (125 MHz, $CDCl_3$) δ = 135.6, 132.9, 129.8, 127.8, 114.2, 108.8, 102.0, 99.5, 94.2, 81.5, 53.2, 26.7, 19.2, 18.6, 11.2. EIMS *m/z* 601.0 ([M – *t*–Bu]$^+$, 100); HRMS calcd. for $C_{28}H_{33}OSi_2{}^{79}Br^{81}Br$ ([M – *t*–Bu]$^+$) 601.0416, found 601.0417. Anal. calcd. for $C_{32}H_{42}OBr_2Si_2$: C, 58.35; H, 6.43. Found: C, 58.12; H, 6.24.

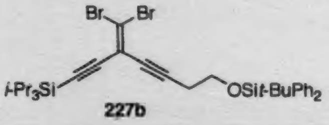

227b

7–(*tert*–Butyldiphenylsilanyloxy)–3–(dibromomethylidene)–1–triisopropylsilanylhepta–1,4–diyne (227b)

Compound **226b** (1.37 g, 2.64 mmol) in CH_2Cl_2 (30 mL) and $BaMnO_4$ (1.32 g, 5.15 mmol) in one portion according to general procedure D affording the ketone as a yellow oil, which was used in the next step without further purification. R_f = 0.7

(hexanes/CH_2Cl_2, 1:1).

CBr_4 (1.31 g, 3.95 mmol) in CH_2Cl_2 (30 mL), PPh_3 (2.12 g, 8.08 mmol) and ketone in CH_2Cl_2 (1 mL) according to general procedure E affording **227b** (874 mg, 50%) as a colorless oil. $R_f = 0.6$ (hexanes/CH_2Cl_2, 3:1).

IR (CH_2Cl_2, cast) 3071, 2942, 2864, 2230(w), 2151(w), 1112 cm^{-1}; ^1H NMR (500 MHz, $CDCl_3$) δ 7.67–7.65 (m, 4H), 7.43–7.35 (m, 6H), 3.80 (t, J = 7.0 Hz, 2H), 2.58 (t, J = 7.0 Hz, 2H), 1.07 (s, 21H), 1.04 (s, 9H); ^{13}C NMR (100 MHz, $CDCl_3$) δ 135.4, 133.4, 129.6, 127.6, 114.5, 107.7, 102.3, 98.8, 94.6, 78.4, 61.8, 26.7, 23.8, 19.1, 18.5, 11.0; HRMS calcd. for $C_{29}H_{35}OSi_2{}^{79}Br^{81}Br$ ($[M - t\text{-}Bu]^+$) 615.0544, found 615.0544. Anal. calcd. for $C_{33}H_{44}OBr_2Si_2$: C, 58.92; H, 6.59. Found: C, 58.71; H, 6.57.

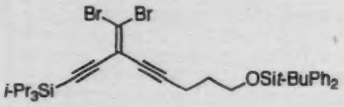

227c

8–(*tert*–Butyldiphenylsilanyloxy)–3–(dibromomethylidene)–1–triisopropylsilanylocta–1,4–diyne (227c)

Compound **226b** (1.32 g, 2.48 mmol) in CH_2Cl_2 (25 mL) and $BaMnO_4$ (1.27 g, 4.96 mmol) in one portion according to general procedure D affording the ketone as a yellow oil, which was used in the next step without further purification. $R_f = 0.5$ (hexanes/CH_2Cl_2, 3:1).

CBr_4 (1.64 g, 4.94 mmol) in CH_2Cl_2 (10 mL), PPh_3 (2.60 g, 9.91 mmol) and the ketone in CH_2Cl_2 (1 mL) at 0 °C according to general procedure E affording **227c** (1.06 g, 62%) as a colorless oil. $R_f = 0.5$ (hexanes/CH_2Cl_2, 3:1).

IR (CH_2Cl_2, cast) 3071, 2943, 2865, 2223, 2156(w), 1111 cm^{-1}; ^1H NMR (500 MHz, $CDCl_3$) δ 7.66–7.64 (m, 4H), 7.43–7.35 (m, 6H), 3.77 (t, J = 6.5 Hz, 2H), 2.49 (t, J = 6.5

Hz, 2H), 1.81 (quint, J = 6.5 Hz, 2H), 1.09 (m, 21H), 1.04 (s, 9H); ^{13}C NMR (125 MHz, $CDCl_3$) δ 135.6, 133.8, 129.6, 127.7, 114.7, 107.4, 102.6, 98.8, 97.4, 78.0, 62.3, 31.1, 26.9, 19.2, 18.6, 16.3, 11.2; HRMS calcd. for $C_{30}H_{37}OSi_2{}^{79}Br^{81}Br$ ([M – t–Bu]$^+$) 629.0729, found 629.0730.

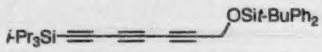

228a

7–(*tert*–Butyldiphenylsilanyloxy)–1–triisopropylsilanyl–1,3,5–heptatriyne (228a)

Compound **227a** (228 mg, 0.345 mmol) in anhyd hexanes (15 mL) and dropwise BuLi (2.5 M in hexanes; 0.17 mL, 0.42 mmol) according to general procedure F afforded **228a** (71.0 mg, 41%) as a colorless oil. R_f = 0.6 (hexanes/CH_2Cl_2, 4:1).

IR (cast, $CHCl_3$) 3071, 2943, 2864, 2164, 2078, 1463, 1369 cm^{-1}; ^{1}H NMR (400 MHz, $CDCl_3$) δ 7.69–7.64 (m, 4H), 7.45–7.36 (m, 6H), 4.35 (s, 2H), 1.07 (s, 21H), 1.04 (s, 9H); ^{13}C NMR (100 MHz, $CDCl_3$) δ 135.6, 132.6, 130.0, 127.8, 89.6, 85.0, 76.3, 70.0, 63.6, 60.4, 53.1, 26.7, 19.2, 18.6, 11.3. EIMS m/z 498.3 (M$^+$, 4), 441.2 ([M – t–Bu]$^+$, 24); HRMS calcd. for $C_{32}H_{42}OSi_2$ (M$^+$) 498.2774; found: 498.2776.

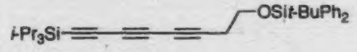

228b

8–(*tert*–Butyldiphenylsilanyloxy)–1–triisopropylsilanyl–1,3,5–octatriyne (228b)

Compound **227b** (349 mg, 0.519 mmol) in dry hexanes (10 mL) and dropwise BuLi (2.5 M in hexanes; 0.23 mL, 0.58 mmol) according to general procedure F afforded **228b** (149 mg, 56%) as a colorless oil. R_f = 0.6 (hexanes/CH_2Cl_2, 3:1).

IR (microscope) 3071, 2944, 2865, 2214, 2078, 1112 cm^{-1}; ^{1}H NMR (400 MHz, $CDCl_3$) δ 7.66–7.64 (m, 4H), 7.44–7.35 (m, 6H), 3.75 (t, J = 6.6 Hz, 2H), 2.52 (t, J = 6.6 Hz, 2H), 1.07 (s, 21H), 1.04 (s, 9H); ^{13}C NMR (100 MHz, $CDCl_3$) δ 135.4, 133.2, 129.6, 127.6, 89.9, 83.1, 77.5, 66.5, 61.6, 61.2, 60.5, 26.6, 23. 5, 19.1, 18.4, 11.2; EIMS *m/z* 512.3 (M^+, 7), 455.2 ($[M - t\text{–Bu}]^+$, 100). HRMS calcd. for $C_{33}H_{44}OSi_2$ (M^+) 512.2931, found 512.2944. Anal. calcd. for $C_{33}H_{44}OSi_2$: C, 77.28; H, 8.65. Found: C, 77.01; H, 8.59.

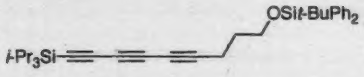

228c

9–(*tert*–Butyldiphenylsilanyloxy)–1–triisopropylsilanyl–1,3,5–nonatriyne (228c)

Compound **227c** (933 mg, 1.36 mmol) in dry hexanes (10 mL) and BuLi (2.5 M in hexanes; 0.65 mL, 1.62 mmol) according to general procedure F yielding **228c** (393 mg, 55%) as a colorless oil. $R_f = 0.7$ (hexanes/CH_2Cl_2, 3:1).

IR ($CHCl_3$, cast) 2944, 2866, 2212, 2166, 2078, 1111 cm^{-1}; ^1H NMR (400 MHz, $CDCl_3$) δ 7.66–7.63 (m, 4H), 7.44–7.35 (m, 6H), 3.71 (t, *J* = 6.5 Hz, 2H), 2.45 (t, *J* = 6.5 Hz, 2H), 1.75 (quint, *J* = 6.5 Hz, 2H), 1.08 (s, 21H), 1.04 (s, 9H); ^{13}C NMR (100 MHz, $CDCl_3$) δ 135.4, 133.5, 129.5, 127.6, 89.9, 82.9, 80.1, 78.4, 65.7, 61.8, 61.4, 60.3, 30.8, 26.7, 19.4, 15.9, 11.2; EIMS *m/z* 526.3 (M^+, 2), 469.2 ($[M - t\text{–Bu}]^+$, 100); HRMS calcd. for $C_{34}H_{46}OSi_2$ ($[M - t\text{–Bu}]^+$) 469.2383, found 469.2389.

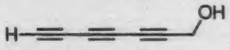

207a

2,4,6–Heptatriyn–1–ol (207a)

Compound **228a** (60.3 mg, 0.121 mmol) in wet THF (2 mL) at 0 °C and TBAF (1.0 M, THF; 0.2 mL, 0.2 mmol) according to general procedure A. The product was insufficiently stable to isolate and attempted purification by column chromatography (hexanes/EtOAc, 4:1) led to decomposition. $R_f = 0.5$ (hexanes/EtOAc, 4:1).

IR (cast, $CHCl_3$) 3350, 3156, 2960, 2179 cm^{-1}.

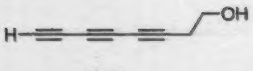

207b

3,5,7–octatriyn–1–ol (207b)

Compound **228b** (123 mg, 0.240 mmol) in wet THF (10 mL) at 0 °C and TBAF (1.0 M in THF; 0.5 mL, 0.5 mmol according to general procedure A. The product was insufficiently stable to isolate and attempted purification by column chromatography (hexanes/EtOAc, 4:1) led to decomposition. $R_f = 0.1$ (CH_2Cl_2).

IR ($CHCl_3$, cast) 3096, 2960, 2873, 2051 cm^{-1}; ^1H NMR (500 MHz, $CDCl_3$) δ 2.03 (s, 1H), 2.54 (t, $J = 6.0$ Hz, 2H), 3.73 (br s, 2H), (OH signal was not observed); ^1H NMR spectrum was consistent with that reported in the literature.[5]

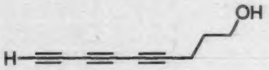

207c

4,6,8–nonatriyn–1–ol (207c)

Compound **228c** (0.067 g, 0.127 mmol) in wet THF (5 mL) at 0 °C and TBAF (1.0 M in THF; 0.25 mL, 0.25 mmol) according to general procedure A. The product was insufficiently stable to isolate and attempted purification by column chromatography (CH_2Cl_2) led to decomposition. $R_f = 0.1$ (CH_2Cl_2).

IR ($CHCl_3$, cast) 3400, 3181, 2957, 2863, 2218 cm^{-1}. (lit. IR ($CHCl_3$) 3600, 3450, 3170, 2200 cm^{-1}).[6]

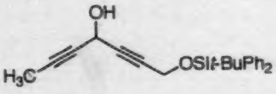

229a

1–(*tert*–Butyldiphenylsilanyloxy)hepta–2,5–diyn–4–ol (229a)

To excess propyne, condensed in THF (300 mL) at –78 °C, was added BuLi (1.6 M, hexanes; 5.3 mL, 8.5 mmol) and LiBr (0.5 g, 6 mmol), stirring for 2 h at –20 °C and aldehyde **223** (1.82 g, 5.65 mmol) according to general procedure C yielding **229a** (2.04 g, 100%) as a light yellow oil. $R_f = 0.4$ (hexanes/CH_2Cl_2, 1:4).

IR (cast, $CHCl_3$) 3396, 3071, 2958, 2893, 2258, 2226, 1472 cm^{-1}; ^1H NMR (400 MHz, $CDCl_3$) δ 7.72–7.68 (m, 4H), 7.45–7.35 (m, 6H), 4.99 (br s, 1H), 4.35(3) (s, 1H), 4.35(1) (s, 1H), 1.91 (br s, 1H), 1.84 (s, 3H) 1.04 (s, 9H); ^{13}C NMR (100 MHz, $CDCl_3$) δ =135.7(0), 135.6(9), 133.0(5), 133.0(4), 129.8, 127.7, 82.7, 82.6, 81.2, 76.4, 52.6, 52.3, 26.7, 19.1, 3.6; two coincident signals not observed. HRMS (ES, MeOH/toluene, 3:1) calcd. for $C_{23}H_{26}O_2SiNa$ ($[M + Na]^+$) 385.1594, found 385.1595.

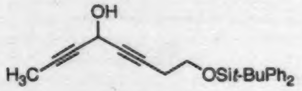

229b

1–(*tert*–Butyldiphenylsilanyloxy)octa–3,6–diyn–5–ol (229b)

To propyne (ca. 1 mL, 18 mmol), condensed in THF (20 mL) at –78 °C, was added BuLi (2.5 M in hexanes; 2.0 mL, 5.0 mmol), stirring for 2 h at –20 °C, and aldehyde **223a** (1.30 g, 3.86 mmol) according to general procedure C yielding **229b** (1.11 g, 76%) as a light yellow oil. $R_f = 0.5$ (CH_2Cl_2).

IR (microscope) 3405, 3071, 2931, 2858, 2292, 2260, 2228, 1112 cm^{-1}; ^1H NMR (300 MHz, $CDCl_3$) δ 7.77–7.66 (m, 4H), 7.44–7.34 (m, 6H), 5.02 (app. dsext, J = 7.0 Hz, 2.0 Hz, 1H), 3.77 (t, J = 7.0 Hz, 2H), 2.49 (td, J = 7.0 Hz, 2.0 Hz, 2H), 2.00 (d, J = 6.9 Hz, 1H), 1.83 (d, J = 3.0 Hz, 3H), 1.05 (s, 9H); ^{13}C NMR (100 MHz, $CDCl_3$) δ 135.5, 133.4, 129.6, 127.6, 82.0, 80.7, 78.9, 76.9, 62.0, 52.3, 26.7, 22.7, 19.1, 3.5; EIMS *m/z* 319.1 ([M

– *t*–Bu]$^+$, 4). Anal. calcd. for $C_{24}H_{28}O_2Si$: C, 76.55; H, 7.49. Found: C, 76.25; H, 7.33.

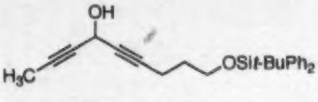

229c

1–(*tert*–Butyldiphenylsilanyloxy)nona–4,7–diyn–6–ol (229c)

To propyne (ca. 1 mL, 18 mmol), condensed in THF (35 mL) at –78 °C, was added BuLi (2.5 M in hexanes; 1.8 mL, 4.5 mmol), stirring for 2 h at –20 °C, and aldehyde **223b** (1.24 g, 3.54 mmol) according to general procedure C yielding **229c** (1.31 g, 95%) as a colorless oil. $R_f = 0.4$ (CH_2Cl_2).

IR (microscope) 3398, 3071, 2931, 2857, 2290, 2259, 2228, 1111 cm^{-1}; ^{1}H NMR (300 MHz, $CDCl_3$) δ 7.67–7.63 (m, 4H), 7.44–7.36 (m, 6H), 5.01 (br s, 1H), 3.72 (t, *J* = 6.0 Hz, 2H), 2.37 (td, *J* = 7.2 Hz, 2.1 Hz, 2H), 1.95 (brd, *J* = 5.7 Hz, 1H), 1.84 (d, *J* = 2.1 Hz, 3H), 1.76 (tt, *J* = 6.0 Hz, 5.7 Hz, 2H), 1.03 (s, 9H); ^{13}C NMR (100 MHz, $CDCl_3$) δ 135.6, 133.8, 129.6, 127.6, 84.7, 80.7, 78.1, 62.3, 52.5, 31.2, 26.8, 19.2, 15.3, 3.6, (one coincident signal not observed); EIMS *m/z* 320.1 ([M – *t*–Bu]$^+$, 11); HRMS calcd. for $C_{21}H_{21}O_2Si$ ([M – *t*–Bu]$^+$) 320.1311, found 320.1304. Anal. calcd. for $C_{25}H_{30}O_2Si$: C, 76.88; H, 7.74. Found: C, 76.87; H, 8.40.

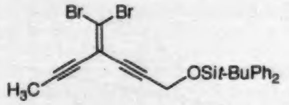

230a

1–(*tert*–Butyldiphenylsilanyloxy)–4–(dibromomethylidene)hepta–2,5–diyne (230a)

Compound **229a** (746 mg, 2.06 mmol) in anhyd CH_2Cl_2 (15 mL) and $BaMnO_4$ (1.05 g, 4.10 mmol) in one portion according to general procedure D affording a crude ketone (589 mg, 80%) as a yellow oil, which was used in the next step without further purification. R_f = 0.7 (hexanes/CH_2Cl_2, 1:5).

CBr_4 (826 mg, 2.45 mmol) in CH_2Cl_2 (16 mL), PPh_3 (1.30 g, 4.96 mmol) and the ketone (589 mg, 1.63 mmol) in CH_2Cl_2 (1 mL) according to general procedure E affording **226a** (210 mg, 25%) as a colorless oil. R_f = 0.7 (hexanes/CH_2Cl_2, 1:1).

IR (cast, $CHCl_3$) 3070, 2958, 2245, 2225, 1589 cm^{-1}; ^1H NMR (300 MHz, $CDCl_3$) δ 7.74–7.69 (m, 4H), 7.46–7.35 (m, 6H), 4.44 (s, 2H), 1.98 (s, 3H), 1.06 (s, 9H); ^{13}C NMR (125 MHz, $CDCl_3$) δ = 135.6, 132.9, 129.8, 127.7, 114.1, 106.6, 93.8, 93.7, 81.9, 76.8, 53.2, 26.7, 19.2, 4.8. EIMS *m/z* 458.9 ([M – *t*–Bu]$^+$, 81); HRMS calcd. for $C_{20}H_{15}OSi^{79}Br^{81}Br$ ([M – *t*–Bu]$^+$) 458.9239, found 458.9253. Anal. calcd. for $C_{24}H_{24}OBr_2Si$: C, 55.83; H, 4.69. Found: C, 55.59; H, 4.76.

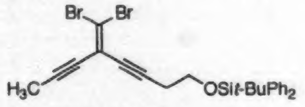

230b

1–(*tert*–Butyldiphenylsilanyloxy)–5–(dibromomethylidene)octa–3,6–diyne (230b)

Compound **229b** (1.09 g, 2.89 mmol) in dry CH_2Cl_2 (30 mL) and $BaMnO_4$ (1.50 g, 5.85 mmol) in one portion according to general procedure D affording a crude ketone as a yellow oil, which was used in the next step without further purification. R_f = 0.4 (hexanes/CH_2Cl_2, 1:1).

CBr_4 (1.90 mg, 5.73 mmol) in CH_2Cl_2 (30 mL) and PPh_3 (3.01 g, 11.5 mmol) and the crude a crude ketone in CH_2Cl_2 (1 mL) according to general procedure E affording **230b** (542 mg, 35%) as a colorless oil. R_f = 0.7 (hexanes/CH_2Cl_2, 1:1).

IR (CH_2Cl_2, cast) 2955, 2919, 2850, 2227(w), 1462 cm^{-1}; ^1H NMR (400 MHz, $CDCl_3$) δ 7.68–7.66 (m, 4H), 7.43–7.35 (m, 6H), 3.80 (t, *J* = 6.8 Hz, 2H), 2.59 (t, *J* = 6.8 Hz, 2H), 1.94 (s, 3H), 1.04 (s, 9H); ^{13}C NMR (100 MHz, $CDCl_3$) δ 135.5, 133.4, 129.6, 127.6, 114.3, 105.4, 94.2, 93.1, 78.8, 77.0, 61.7, 26.7, 23.8, 19.1, 4.6; EIMS *m/z* 472.9 ([M – *t*–Bu]$^+$, 100); HRMS calcd. for $C_{21}H_{17}OSi^{79}Br^{81}Br$ ([M – *t*–Bu]$^+$) 472.9395, found 472.9367.

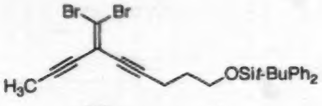

230c

1–(*tert*–Butyldiphenylsilanyloxy)–6–(dibromomethylidene)nona–4,7–diyne (230c)

Compound **229c** (1.29 g, 3.30 mmol) in dry CH_2Cl_2 (30 mL) and $BaMnO_4$ (1.69 g, 6.59 mmol) in one portion according to general procedure D affording a crude ketone as a yellow oil, which was used in the next step without further purification. R_f = 0.8 (CH_2Cl_2).

CBr_4 (2.19 g, 6.60 mmol) in CH_2Cl_2 (30 mL) and PPh_3 (3.46 g, 13.2 mmol) and crude ketone in CH_2Cl_2 (1 mL) according to general procedure E affording **230c** (663 mg, 37%) as a colorless oil. A small quantity of PPh_3 (ca. 5%) could not be separated from **230c**. R_f = 0.6 (hexanes/CH_2Cl_2, 2:1).

IR (CH_2Cl_2, cast) 2930, 2857, 2223, 1428, 1111 cm^{-1}; ^{1}H NMR (400 MHz, $CDCl_3$) δ 7.67–7.64 (m, 4H), 7.43–7.32 (m, 6H), 3.77 (t, *J* = 6.0 Hz, 2H), 2.49 (t, *J* = 6.8 Hz, 2H), 1.82 (app. quint, *J* = 6.4 Hz, 2H), 1.96 (s, 3H), 1.04 (s, 9H); ^{13}C NMR (100 MHz, $CDCl_3$) δ 135.4, 133.7, 129.5, 127.5, 114.4, 105.1, 96.8, 92.9, 78.1, 77.0, 62.2, 30.9, 26.7, 19.1, 16.2, 4.6; EIMS *m/z* 487.0 ([M – *t*–Bu]$^+$, 100); HRMS calcd. for $C_{22}H_{19}OSi^{79}Br^{81}Br$ ([M – *t*–Bu]$^+$) 486.9551, found 486.9553.

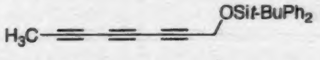

231a

1–(*tert*–Butyldiphenylsilanyloxy)–2,4,6–octatriyne (231a)

Compound **230a** (259 mg, 0.502 mmol) in anhyd hexanes (15 mL) and BuLi (2.5 M in hexanes; 0.24 mL, 0.60 mmol) according to general procedure F yielding **231a** (69.0 mg, 39%) as a colorless oil. $R_f = 0.3$ (hexanes/CH_2Cl_2, 3:1).

IR (cast, $CHCl_3$) 3070, 2958, 2892, 2223, 1472 cm^{-1}. ^1H NMR (400 MHz, $CDCl_3$) δ 7.70–7.67 (m, 4H), 7.46–7.37 (m, 6H), 4.36 (s, 2H), 1.96 (s, 3H), 1.06 (s, 9H); ^{13}C NMR (100 MHz, $CDCl_3$) δ 135.6, 132.6, 130.0, 127.8, 76.6, 74.9, 70.3, 64.8, 63.8, 58.9, 53.1, 26.7, 19.2, 4.5. EIMS *m/z* 356.2 ([M^+], 1) 299.1 ([M – *t*–Bu]$^+$, 96); HRMS calcd. for $C_{24}H_{24}OSi$ (M^+) 356.1596, found 356.1594. Anal. calcd. for $C_{24}H_{24}OSi$: C, 80.85; H, 6.78. Found: C, 80.28; H, 7.01.

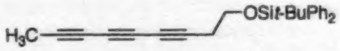

231b

1–(*tert*–Butyldiphenylsilanyloxy)–3,5,7–nonatriyne (231b)

Compound **230b** (488 mg, 0.920 mmol) in dry hexanes (10 mL) and BuLi (2.5 M in hexanes; 0.45 mL, 1.13 mmol) according to general procedure F yielding **231b** (260 mg, 76%) as a colorless oil. $R_f = 0.6$ (hexanes/CH_2Cl_2, 3:1).

IR (microscope) 3071, 2932, 2858, 2222, 1112 cm^{-1}; ^1H NMR (300 MHz, $CDCl_3$) δ 7.67–7.63 (m, 4H), 7.45–7.34 (m, 6H), 3.75 (t, $J = 6.6$, 2H), 2.51 (t, $J = 6.6$ Hz, 2H), 1.93 (s, 3H), 1.04 (s, 9H); ^{13}C NMR (100 MHz, $CDCl_3$) δ 135.4, 133.2, 129.6, 127.6, 75.9, 74.9, 66.7, 64.8, 61.7, 60.5, 59.5, 26.6, 23.4, 19.1, 4.35; EIMS *m/z* 370.2 (M^+, 2), 313.1 ([M – *t*–Bu]$^+$, 69); HRMS calcd. for $C_{25}H_{26}OSi$ ([M – *t*–Bu]$^+$) 370.1753, found 370.1760.

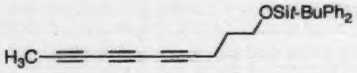

231c

1–(*tert*–Butyldiphenylsilanyloxy)–4,6,8–decatriyne (231c)

Compound **230c** (586 mg, 1.08 mmol) in dry hexanes (10 mL) and BuLi (2.5 M in hexanes; 0.52 mL, 1.30 mmol) according to general procedure F yielding **231c** (342 mg, 82%) as a colorless oil. $R_f = 0.5$ (hexanes/CH_2Cl_2, 3:1).

IR (microscope) 3071, 2956, 2858, 2221, 1472, 1111 cm^{-1}; ^{1}H NMR (400 MHz, $CDCl_3$) δ 7.66–7.63 (m, 4H), 7.44–7.35 (m, 6H), 3.70 (t, $J = 6.0$ Hz, 2H), 2.43 (t, $J = 6.8$ Hz, 2H), 1.75 (tt, $J = 6.8$ Hz, 6.0 Hz, 2H), 1.94 (s, 3H), 1.03 (s, 9H); ^{13}C NMR (100 MHz, $CDCl_3$) δ 135.4, 133.5, 129.5, 127.5, 78.5, 74.7, 65.8, 64.9, 61.9, 60.3, 59.7, 30.8, 26.7, 19.1, 15.8, 4.4; EIMS *m/z* 384.2 (M^+, 1), 314.1 ([M – *t*–Bu]$^+$, 100); HRMS calcd. for $C_{22}H_{19}OSi$ ([M – *t*–Bu]$^+$) 314.1205, found 314.1203.

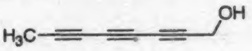

208a

2,4,6–Octatriyn–1–ol (208a)

Compound **231a** (108 mg, 0.302 mmol) in wet THF (15 mL) and TBAF (0.6 mL, 1.0 M in THF, 0.6 mmol) according to general procedure A yielding **208a** (26.9 mg, 75%); as magenta crystals. Mp 89–92 °C (Lit. 93 °C). $R_f = 0.3$ (CH_2Cl_2).

IR (cast, $CHCl_3$) 3243, 2912, 2849, 2220, 1432 cm^{-1}. ^{1}H NMR (400 MHz, $CDCl_3$) δ 4.32 (d, $J = 6.4$, 2H), 1.96 (s, 3H), 1.55 (t, $J = 6.4$ Hz, 1H); ^{13}C NMR (100 MHz, $CDCl_3$) δ 74.4, 71.1, 64.6, 64.4, 58.3, 51.6, 4.5, one signal not observed. HRMS calcd. for C_8H_6O (M^+) 118.0419, found 118.0420.

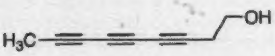

208b

3,5,7–nonatriyn–1–ol (208b)

Compound **231b** (233 mg, 0.629 mmol) in wet THF (10 mL) and TBAF (0.94 mL, 1.0 M in THF, 0.94 mmol) according to general procedure A yielding **208b** (80 mg, 96%) as a white crystalline solid that turned purple when exposed to light. Mp 55–57 °C (Lit. 63.5–64 °C).[3] $R_f = 0.3$ (CH_2Cl_2).

IR (microscope) 3347, 3264, 2933, 2876, 2218, 2036(w), 1055 cm^{-1}; ^{1}H NMR (500 MHz, $CDCl_3$) δ 3.74 (t, J = 6.0 Hz, 2H), 2.54 (t, J = 6.0 Hz, 2H), 1.93 (s, 3H), 1.67 (br s, 1H); ^{13}C NMR (125 MHz, $CDCl_3$) δ 75.4, 75.3, 67.5, 64.8, 61.2, 60.6, 59.3, 23.8, 4.5; HRMS calcd. for C_9H_8O (M^+) 132.0575, found 132.0577. Spectral data were consistent with that reported in the literature.[5,7]

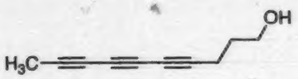

208c

4,6,8–decatriyn–1–ol (208c)

Compound **231c** (318 mg, 0.861 mmol) in wet THF (10 mL) and TBAF (1.3 mL, 1.0 M in THF, 1.3 mmol) according to general procedure A yielding **208c** (125 mg, 99%) as a white crystalline solid. Mp 65–68 °C (Lit. 68–70.5 °C).[4] $R_f = 0.2$ (CH_2Cl_2).

IR (microscope) 3205, 2901, 2221, 1060 cm^{-1}; ^{1}H NMR (500 MHz, $CDCl_3$) δ 3.72 (t, J = 6.0 Hz, 2H), 2.40 (t, 7.0 Hz, 2H), 1.77 (app. quintet, J = 6.5 Hz, 2H), 1.40 (br s, 1H), 1.93 (s, 3H); ^{13}C NMR (125 MHz, $CDCl_3$) δ 78.1, 75.1, 66.1, 64.9, 61.3, 60.7, 59.6, 30.8, 15.9, 4.5; HRMS calcd. for $C_{10}H_{10}O$ (M^+) 146.0732, found 146.0735. (Reported IR data: 3600, 2212, 1056 cm^{-1}).[8]

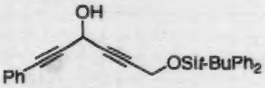

232a

1–(*tert*–Butyldiphenylsilanyloxy)–6–phenylhexa–2,5–diyn–4–ol (232a)

Phenylacetylene (558 mg, 5.46 mmol) in THF (100 mL) at –78 °C was added BuLi (2.5 M in hexanes; 2.2 mL, 5.4 mmol) and aldehyde **223** (1.46 g, 4.52 mmol) according to general procedure C yielding **232a** (1.63 g, 85%), as a light yellow oil. R_f = 0.4 (CH_2Cl_2). IR (cast, $CHCl_3$) 3383, 3070, 3050, 2930, 2231, 1589 cm^{-1}; ^1H NMR (500 MHz, $CDCl_3$) δ 7.72–7.70 (m, 4H), 7.44–7.30 (m, 11H), 5.24 (d, *J* = 7.7 Hz, 1H), 4.38(5) (s, 1H), 4.38(2) (s, 1H), 2.00 (d, *J* = 7.7 Hz, 1H), 1.00 (s, 9H); ^{13}C NMR (125 MHz, $CDCl_3$) δ 135.7(9), 135.7(8), 133.1(3), 133.1(2), 131.9, 129.9(0), 129.8(9), 128.9, 128.4, 127.8, 122.0, 85.9, 84.4, 83.3, 82.3, 52.7, 52.6, 26.7, 19.2; one coincident signal not observed. EIMS *m/z* 367.1 ([M – *t*–Bu]$^+$, 6); HRMS calcd. for $C_{24}H_{19}O_2Si$ ([M – *t*–Bu]$^+$) 367.1155, found 367.1146. Anal. calcd. for $C_{28}H_{28}O_2Si$: C, 79.20; H, 6.65. Found: C, 79.37; H, 6.41.

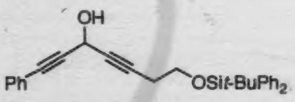

232b

1–(*tert*–Butyldiphenylsilanyloxy)–7–phenylhepta–3,6–diyn–5–ol (232b)

Phenylacetylene (195 mg, 1.91 mmol) in THF (25 mL) at –78 °C was added BuLi (2.5 M in hexanes; 0.78 mL, 2.0 mmol) and aldehyde **223a** (730 mg, 2.17 mmol) according to general procedure C yielding **232b** (645 mg, 77%) as a light yellow oil. R_f = 0.2 (hexanes/CH_2Cl_2, 1:2).

IR ($CHCl_3$, cast) 3402, 3071, 2931, 2857, 2223, 2198, 1622, 1112 cm^{-1}; ^1H NMR (500 MHz, $CDCl_3$) δ 7.70–7.68 (m, 4H), 7.44–7.36 (m, 8 H), 7.32–7.26 (m, 3H), 5.29 (br d, *J* = 2.0 Hz, 1H), 3.80 (t, *J* = 7.0 Hz, 2H), 2.52 (td, *J* = 7.0 Hz, 2.0 Hz, 2H), 2.22 (s, 1H), 1.06 (s, 9H); ^{13}C NMR (125 MHz, $CDCl_3$) δ 135.6, 133.6, 131.9, 129.7, 128.7, 128.2, 127.7, 122.1, 86.5, 84.0, 82.9, 78.5, 62.1, 52.9, 26.8, 22.9, 19.2; EIMS *m/z* 379.1 ([M – *t*–Bu]$^+$, 14); HRMS calcd. for $C_{25}H_{19}O_2Si$ ([M – *t*–Bu]$^+$) 379.1155, found 379.1151.

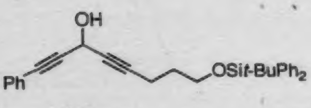

232c

1–(*tert*–Butyldiphenylsilanyloxy)–8–phenylocta–4,7–diyn–6–ol (232c)

Phenylacetylene (140 mg, 1.37 mmol) in THF (15 mL) at –78 °C was added BuLi (2.5 M in hexanes; 0.55 mL, 1.37 mmol) and aldehyde **223b** (536 mg, 1.53 mmol) according to general procedure C yielding **232c** (425 mg, 69%) as a yellow oil. R_f = 0.3 (hexanes/CH_2Cl_2, 1:2).

IR (microscope) 3390, 3071, 2931, 2858, 2286, 2227, 2199, 1598 cm^{-1}; ^1H NMR (500 MHz, $CDCl_3$) δ 7.66–7.63 (m, 4H), 7.45–7.33 (m, 8H), 7.32–7.27 (m, 3H), 5.27 (br s, 1H), 3.73 (t, *J* = 6.0 Hz, 2H), 2.40 (td, *J* = 7.5 Hz, 2.0 Hz, 2H), 2.08 (br s, 1H), 1.77 (tt, *J* = 7.5 Hz, 6.0 Hz, 2H), 1.03 (s, 9H); ^{13}C NMR (125 MHz, $CDCl_3$) δ 135.6, 133.8, 131.8, 129.6, 128.7, 128.3, 127.6, 122.1, 86.6, 85.4, 83.9, 77.6, 62.3, 52.9, 31.2, 26.9, 19.2, 15.3; EIMS *m/z* 395.1 ([M – *t*–Bu]$^+$, 21); HRMS calcd. for $C_{26}H_{23}O_2Si$ ([M – *t*–Bu]$^+$) 395.1467, found 395.1467. Anal. calcd. for $C_{30}H_{33}O_2Si$: C, 79.60; H, 7.13. Found: C, 79.31; H, 7.29.

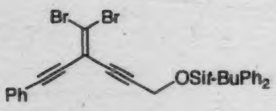

233a

1–(*tert*–Butyldiphenylsilanyloxy)–4–(dibromomethylidene)–6–phenylhexa–2,5–diyne (233a)

Compound **232a** (519 mg, 1.22 mmol) in anhyd CH_2Cl_2 (27 mL) and $BaMnO_4$ (940 mg, 3.67 mmol) in one portion according to general procedure D affording a ketone (459 mg, 89%), as a yellow oil. R_f = 0.4 (hexanes/CH_2Cl_2, 1:1).

IR (cast, $CHCl_3$) 3070, 2958, 2893, 2196, 1596, cm^{-1}; ^1H NMR (500 MHz, $CDCl_3$) δ

7.71–7.69 (m, 4H), 7.59–7.57 (m, 2H), 7.49–7.37 (m, 9H), 4.50 (s, 2H), 1.06 (s, 9H); ^{13}C NMR (100 MHz, $CDCl_3$) δ 160.5, 135.7, 133.4, 132.4, 131.3, 130.1, 128.8, 127.9, 119.5, 91.8, 91.2, 89.1, 85.1, 52.6, 26.7, 19.3. EIMS *m/z* 422.2 (M^+, 2), 365.1 ($[M - t\text{–}Bu]^+$, 100); HRMS calcd. for $C_{28}H_{26}O_2Si$ (M^+) 422.1702, found 422.1698. Anal. alcd. for $C_{28}H_{26}O_2Si$: C, 79.58; H, 6.20. Found: C. 79.28; H, 6.26.

CBr_4 (1.51 g, 4.55 mmol), PPh_3 (2.30 g, 8.78 mmol) and the ketone (1.26 g, 2.97 mmol) in CH_2Cl_2 (5 mL) according to general procedure E affording **233a** (905 mg, 53%, 57% based on recovered starting material), as a light yellow oil. R_f = 0.8 (hexanes/CH_2Cl_2, 1:1).

IR (cast, $CHCl_3$) 3070, 2998, 2958, 2216, 2192, 1471 cm^{-1}; ^{1}H NMR (400 MHz, $CDCl_3$) δ 7.73–7.70 (m, 4H), 7.51–7.47 (m, 2H), 7.43–7.30 (m, 9H), 4.47 (s, 2H), 1.06 (s, 9H); ^{13}C NMR (100 MHz, $CDCl_3$) δ 135.6, 132.9, 131.6, 129.9, 129.2, 128.4, 127.8, 122.1, 113.9, 107.9, 95.7, 94.4, 86.1, 81.5, 53.2, 26.7, 19.2. EIMS *m/z* 520.9 ($[M - t\text{–}Bu]^+$, 27); HRMS calcd. for $C_{25}H_{17}OSi^{79}Br^{81}Br$ ($[M - t\text{–}Bu]^+$) 520.9395, found 520.9385. Anal. calcd. for $C_{29}H_{26}OBr_2Si$: C, 60.22; H, 4.53. Found: C, 59.63; H, 4.39.

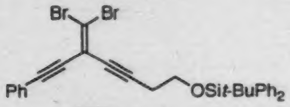

233b

1–(*tert*–Butyldiphenylsilanyloxy)–5–(dibromomethylidene)–7–phenylhexa–3,6–diyne (233b)

Compound **232b** (439 mg, 1.00 mmol) in dry CH_2Cl_2 (10 mL) and $BaMnO_4$ (511 mg, 1.99 mmol) in one portion according to general procedure D affording the intermediate ketone as a yellow oil. R_f = 0.5 (hexanes/CH_2Cl_2, 1:2). The product was carried to the next step.

CBr_4 (663 mg, 2.00 mmol) in CH_2Cl_2 (10 mL), PPh_3 (1.05 g, 4.00 mmol) and the crude ketone in CH_2Cl_2 (5 mL) according to general procedure E affording **233b** (541 mg, 91% two steps) as a light yellow oil. $R_f = 0.4$ (hexanes/CH_2Cl_2, 1:1).

IR ($CHCl_3$, cast) 3071, 2931, 2878, 2205, 1112 cm^{-1}; ^1H NMR (500 MHz, $CDCl_3$) δ 7.70–7.67 (m, 4H), 7.48–7.46 (m, 2H), 7.41–7.28 (m, 9H), 3.84 (t, J = 7.0 Hz, 2H), 2.62 (t, J = 7.0 Hz, 2H), 1.05 (s, 9H); ^{13}C NMR (125 MHz, $CDCl_3$) δ 135.6, 133.5, 131.6, 129.7, 129.1, 128.4, 127.7, 122.2, 114.3, 106.9, 95.2, 95.1, 86.4, 78.4, 61.8, 26.8, 24.0, 19.2; EIMS *m/z* 535.0 ([M – *t*–Bu]$^+$, 100); HRMS calcd. for $C_{26}H_{19}OSi^{79}Br^{81}Br$ ([M – *t*–Bu]$^+$) 534.9551, found 534.9542. Anal. calcd. for $C_{30}H_{28}OBr_2Si$: C, 60.82; H 4.76. Found: C, 60.72; H, 4.81.

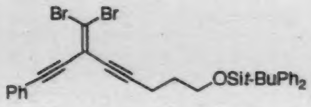

233c

1–(*tert*–Butyldiphenylsilanyloxy)–6–(dibromomethylidene)–8–phenylocta–4,7–diyne (233c)

Compound **232c** (388 mg, 0.857 mmol) in dry CH_2Cl_2 (25 mL) and $BaMnO_4$ (441 mg, 1.72 mmol) in one portion according to general procedure D affording the intermediate ketone (357 mg, 92%) as a yellow oil. $R_f = 0.5$ (hexanes/CH_2Cl_2, 1:2). The crude product was carried on to the next step without further purification.

CBr_4 (526 mg, 1.59 mmol) in CH_2Cl_2 (10 mL), PPh_3 (832 mg, 3.17 mmol) and the ketone (357 g, 0.792 mmol) in CH_2Cl_2 (5 mL) according to general procedure E affording **233c** (361 mg, 75%) as a light yellow oil. $R_f = 0.6$ (hexanes/CH_2Cl_2, 2:1).

IR (microscope) 3070, 2931, 2857, 2221, 1589 cm^{-1}; ^1H NMR (500 MHz, $CDCl_3$) δ 7.66–7.64 (m, 4H), 7.48–7.47 (m, 2H), 7.41–7.29 (m, 9H), 3.78 (t, J = 6.0, 2H), 2.52 (t, J

= 7.0 Hz, 2H), 1.84 (quint, J = 6.5 Hz, 2H), 1.04 (s, 9H); ^{13}C NMR (125 MHz, $CDCl_3$) δ 135.6, 133.8, 131.6, 129.6, 129.0, 128.4, 127.7, 122.3, 114.4, 106.6, 97.7, 95.1, 86.5, 77.8, 62.3, 31.0, 26.9, 19.2, 16.3; EIMS m/z 549.0 ([M – t–Bu]$^+$, 100); HRMS calcd. for $C_{27}H_{21}OSi^{79}Br^{81}Br$ ([M – t–Bu]$^+$) 548.9708, found 548.9711. Anal. calcd. for $C_{31}H_{30}OBr_2Si$: C, 61.39; H, 4.99. Found: C, 61.64; H, 5.07.

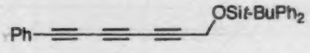

234a

1–(*tert*–Butyldiphenylsilanyloxy)–7–phenyl–2,4,6–heptatriyne (234a)

Compound **233a** (548 mg, 0.948 mmol) in anhyd hexanes (32 mL) and BuLi (2.4 M in hexanes; 0.8 mL, 2.0 mmol) according to general procedure F yielding **234a** (^{1}H NMR of the purified product showed ca. 5% of an impurity that could not be separated chromatographically) and yield **234a** (356 mg, 90% as a yellow oil. R_f = 0.6 (hexanes/CH_2Cl_2, 1:1).

IR (cast, $CHCl_3$) 3071, 2958, 2857, 2191, 1472 cm^{-1}; ^{1}H NMR (400 MHz, $CDCl_3$) δ 7.70–7.67 (m, 4H), 7.52–7.50 (m, 2H), 7.46–7.29 (m, 9H), 4.39 (s, 2H), 1.06 (s, 9H); ^{13}C NMR (100 MHz, $CDCl_3$) δ 135.6, 133.0, 132.6, 130.0, 129.7, 128.5, 127.8, 120.9, 78.4, 76.97, 74.3, 70.1, 66.3, 62.9, 53.2, 26.4, 19.2. EIMS m/z 418.1 (M$^+$, 2), 361.1 ([M – t–Bu]$^+$, 23); HRMS calcd. for $C_{29}H_{26}OSi$ (M$^+$) 418.1753, found 418.1753.

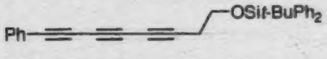

234b

1–(*tert*–Butyldiphenylsilanyloxy)–8–phenyl–3,5,7–octatriyne (234b)

Compound **233b** (589 mg, 0.994 mmol) in dry hexanes (10 mL) and BuLi (2.5 M in hexanes; 0.44 mL, 1.1 mmol) according to general procedure F yielding **234b** (360 mg, 84%) as a yellow oil. R_f = 0.4 (hexanes/CH_2Cl_2, 3:1).

IR ($CHCl_3$, cast) 3071, 2930, 2857, 2215, 1112 cm^{-1}; ^1H NMR (400 MHz, $CDCl_3$) δ 7.67–7.65 (m, 4H), 7.51–7.48 (m, 2H), 7.45–7.28 (m, 9H), 3.78 (t, *J* = 6.8 Hz, 2H), 2.56 (t, *J* = 6.8 Hz, 2H), 1.05 (s, 9H); ^{13}C NMR (100 MHz, $CDCl_3$) δ 135.6, 133.3, 133.0, 129.8, 129.5, 128.4, 127.7, 121.1, 79.6, 75.5, 74.6, 67.2, 66.7, 61.7, 59.8, 26.8, 23.8, 19.2; EIMS *m/z* 432.2 (M^+, 4), 375.1 ($[M - t\text{–}Bu]^+$, 100); HRMS calcd. for $C_{30}H_{28}OSi$ (M^+) 432.1910, found 432.1911. Anal. calcd. for $C_{30}H_{28}OSi$: C, 83.29; H, 6.52. Found: C, 82.94; H, 6.48.

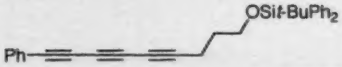

234c

1–(*tert*–Butyldiphenylsilanyloxy)–9–phenyl–4,6,8–nonatriyne (234c)

Compound **233c** (249 mg, 0.411 mmol) in dry hexanes (10 mL) and BuLi (2.5 M in hexanes; 0.18 mL, 0.45 mmol) according to general procedure F yielding **234c** (184 mg, 99%) as a yellow oil. R_f = 0.3 (hexanes/CH_2Cl_2, 3:1).

IR (microscope) 3071, 2931, 2858, 2214, 1111 cm^{-1}; ^1H NMR (500 MHz, $CDCl_3$) δ 7.67–7.64 (m, 4H), 7.52–7.49 (m, 2H), 7.44–7.29 (m, 9H), 3.73 (t, *J* = 6.0 Hz, 2H), 2.50 (t, *J* = 7.0 Hz, 2H), 1.78 (quint, *J* = 6.5 Hz, 2H), 1.05 (s, 9H); ^{13}C NMR (125 MHz, $CDCl_3$) δ 135.6, 133.6, 133.0, 129.7, 129.5, 128.4, 127.7, 121.2, 82.3, 75.4, 74.7, 67.4, 65.9, 62.0, 59.6, 30.9, 26.9, 19.2, 16.2; EIMS *m/z* 446.2 (M^+, 2), 389.1 ($[M - t\text{–}Bu]^+$, 100); HRMS calcd. for $C_{27}H_{21}OSi$ ($[M - t\text{–}Bu]^+$) 389.1362, found 389.1351.

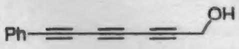

209a

7–Phenyl–2,4,6–heptatriyn–1–ol (209a)

Compound **234a** (77 mg, 0.18 mmol) in wet THF (5 mL) and TBAF (1.0 M, THF; 0.4

mL, 0.4 mmol) according to general procedure A yielding **209a** (31 mg, 96%) as a light yellow oil. Compound **209a** was previously reported to be a solid, but in our hands, all attempts at crystallization have been unsuccessful. $R_f = 0.3$ (hexanes/EtOAc, 4:1).

IR (cast, $CHCl_3$) 3307, 3064, 2928, 2856, 2190, 1490 cm^{-1}; ^{1}H NMR (500 MHz, $CDCl_3$) δ 7.50 (d, $J = 7.5$ Hz, 2H), 7.38 (t, $J = 7.5$ Hz, 1 H), 7.31 (t, $J = 7.5$ Hz, 2H), 4.40 (s, 2H), 1.60 (s, 1 H); ^{13}C NMR (125 MHz, $CDCl_3$) δ 133.1, 129.9, 128.6, 120.8, 77.9, 77.3, 77.1, 71.0, 65.8, 63.5, 51.7. EIMS *m/z* 180.1 (M^+, 2), 126.0 ($[PhC{\equiv}CC{\equiv}CH]^+$, 100); HRMS calcd. for $C_{13}H_8O$ (M^+) 180.0575, found 180.0574.

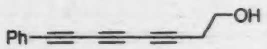

209b

7–Phenyl–3,5,7–octatriyn–1–ol (209b)

Compound **234b** (186 mg, 0.430 mmol) in wet THF (5 mL) and TBAF (1.0 M in THF; 0.86 mL, 0.86 mmol) according to general procedure A yielding **209b** (78 mg, 93%) as a light yellow oil. $R_f = 0.2$ (CH_2Cl_2).

IR (CH_2Cl_2, cast) 3346, 3062, 2952, 2889, 2214, 2191, 1046 cm^{-1}; ^{1}H NMR (300 MHz, $CDCl_3$) δ 7.49 (m, 2H), 7.40–7.26 (m, 3H), 3.77 (t, $J = 6.0$ Hz, 2H), 2.60 (t, $J = 6.0$ Hz, 2H), 1.69 (br s, 1H); ^{13}C NMR (125 MHz, $CDCl_3$) δ 133.0, 129.6, 128.5, 121.0, 78.9, 75.9, 74.4, 67.3, 66.8, 60.6, 60.3, 24.0; EIMS *m/z* 194.1 (M^+, 85), 163.1 ($[PhC{\equiv}CC{\equiv}CC{\equiv}CCH_2]^+$, 100); HRMS calcd. for $C_{14}H_{10}O$ (M^+) 194.0732, found 194.0736.

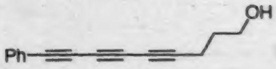

209c

9–Phenyl–4,6,8–nonatriyn–1–ol (209c)

Compound **234c** (184 mg, 0.412 mmol) in wet THF (10 mL) and TBAF (1.0 M in THF; 0.82 mL, 0.82 mmol) according to general procedure A yielding **209c** (73 mg, 85%) as a light yellow oil. R_f = 0.2 (CH_2Cl_2).

IR (microscope) 3204, 3063, 2952, 2880, 2215, 2192, 1059 cm^{-1}; ^1H NMR (300 MHz, $CDCl_3$) δ 7.50–7.45 (m, 2H), 7.38–7.28 (m, 3H), 3.75 (t, J = 6.0 Hz, 2H), 2.47 (t, J = 6.9 Hz, 2H), 1.80 (quint, J = 6.0 Hz, 2H), (OH signal was not observed); ^{13}C NMR (100 MHz, $CDCl_3$) δ 132.9, 129.5, 128.4, 121.1, 81.6, 75.6, 74.5, 67.1, 66.1, 61.2, 59.8, 30.7, 16.1; HRMS calcd. for $C_{15}H_{12}O$ (M^+) 208.0888, found 208.0891.

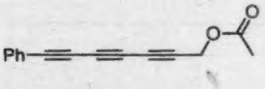

235a

7–Phenylhepta–2,4,6–triynylacetate (235a)

To **209a** (158 mg, 0.877 mmol) in CH_2Cl_2 (10 mL) was added Ac_2O (108 mg, 1.06 mmol), DMAP (50 mg, 0.41 mmol), and Et_3N (0.1 mL). The reaction was stirred at rt for 5 h until TLC analysis showed that acetylation had taken place. Et_2O (10 mL) and sat. aq NH_4Cl (10 mL) were added. The organic phase was separated, washed with sat. aq NaCl (2 × 10 mL), and dried over $MgSO_4$. Solvent removal and purification by column chromatography (hexanes/EtOAc, 4:1) afforded **235a** (158 mg, 81%) as a white solid, decomposed immediately under ambient condition. R_f = 0.5 (hexanes/EtOAc, 4:1).

IR (cast, $CHCl_3$) 3056, 2929, 2192, 1749, 1220 cm^{-1}; ^1H NMR (300 MHz, CD_3CN) δ 7.69 (d, J = 7.5 Hz, 2H), 7.60 (t, J = 7.5 Hz, 1H), 7.51 (t, J = 7.5 Hz, 2H), 4.88 (s, 2H), 2.16 (s, 3H); ^{13}C NMR (100 MHz, CD_3CN) δ 170.8, 134.0, 131.5, 129.8, 120.9, 78.5, 76.3, 74.0, 70.7, 66.2, 63.8, 53.0, 20.7. HRMS (MeOH/toluene, 3:1) calcd. for $C_{15}H_{10}O_2Na$ ($[M + Na]^+$) 245.0573, found, 245.0571.

8.3.2 *Chapter 3*

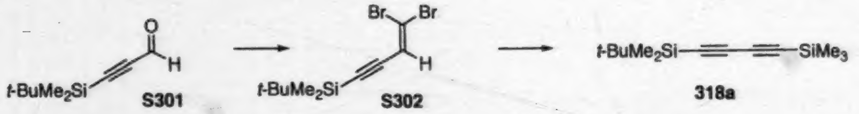

Compound **S302**: CBr_4 (598 mg, 1.80 mmol) and PPh_3 (950 mg, 3.62 mmol) were added to CH_2Cl_2 (10 mL) and allowed to stir for 5 min at rt. The mixture was added to ketone **S301**[9] (152 mg, 0.902 mmol) in CH_2Cl_2 (1 mL). The progress of the reaction was monitored by TLC. Hexanes (10 mL) was added and solvent was reduced to ca. 10 mL. The inhomogeneous mixture was filtered through silica gel and solvent removed *in vacuo*. Column chromatography (silica gel, hexanes) and yielded **S302** (274 mg, 94%) as a colorless oil. $R_f = 0.7$ (hexanes/CH_2Cl_2 3:1).

IR ($CHCl_3$, cast) 2954, 2858, 2170 (w), 2122 (w) cm^{-1}; ^1H NMR (400 MHz, $CDCl_3$) δ 6.56 (s, 1H), 0.94 (s, 9H), 0.13 (s, 6H); ^{13}C NMR (100 MHz, $CDCl_3$) δ 119.6, 103.0, 102.3, 101.2, 25.9, 16.5, –5.01. EIMS *m/z* 310.9 (M^+, 7), 266.9 ($[M - tBu]^+$, 55); HRMS calcd. for $C_{10}H_{16}{}^{79}Br^{81}BrSi$ (M^+) 310.9368, found 310.9371.

Compound **318a**: **S302** (264 mg, 0.814 mmol) in THF (1 mL) was cooled to –78 °C. LDA [reaction between BuLi (2.5 M in hexanes, 98 mL, 2.5 mmol) and *i*–Pr_2NH (0.34 mL, 2.4 mmol) in THF (10 mL) at –78 °C. The mixture was stirred for 30 min] was added over a period of ca. 1 min and stirred for 1 h. Trimethylsilylchloride (0.13g, 1.2 mmol) was added to the mixture above by syringe and the reaction was warmed to rt overnight. The reaction was quenched with satd. aq. NH_4Cl (10 mL) and Et_2O (10 mL), the organic layer separated, washed with satd. aq. NaCl (10 mL), dried over $MgSO_4$, and the solvent removed, and the residue purified by. Column chromatography (silica gel, hexanes) provided **318a** (177 mg, 92%) as a colorless oil. $R_f = 0.5$ (hexanes).

IR ($CHCl_3$, µscope) 2954, 2859, 2069, 2046 (w), 1471 cm^{-1}; ^1H NMR (400 MHz, $CDCl_3$) δ 0.92 (s, 9H), 0.17 (s, 9H), 0.11 (s, 6H); ^{13}C NMR (100 MHz, $CDCl_3$) δ 88.5, 88.1, 85.2, 84.5, 25.9, 16.6, –0.6, –5.0. EIMS *m/z* 236.1 (M^+, 9), 179.1 ($[M - tBu]^+$, 100); HRMS calcd. for $C_{13}H_{24}Si_2$ 236.1417, found 236.1411.

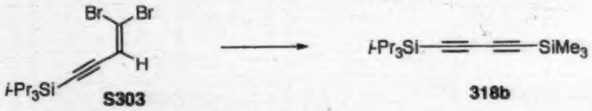

Compound **318b**: **S303**[10] (4.29 mg, 11.7 mmol) in Et_2O (10 mL) was cooled to –78 °C. LDA [reaction between BuLi (2.5 M in hexanes, 14.0 mL, 35.0 mmol) and *i*–Pr_2NH (4.92 mL, 35.1mmol) in Et_2O (70 mL) at –78 °C. The mixture was stirred for 30 min] was added over a period of ca. 1 min and stirred for 1 h. Trimethylsilylchloride (1.9 g, 17 mmol) was added to the mixture above by syringe and the reaction was warmed to rt overnight. The reaction was quenched with satd. aq. NH_4Cl (70 mL) and Et_2O (70 mL), the organic layer separated, washed with satd. aq. NaCl (70 mL), dried over $MgSO_4$, and the solvent removed. Column chromatography (silica gel, hexanes) provided **318b** (3.21 mg, 98%) as a colorless oil. $R_f = 0.7$ (hexanes).

IR (µscope) 2945, 2867, 2066, 1463 cm^{-1}; ^1H NMR (500 MHz, $CDCl_3$) δ 1.06 (s, 21H), 0.18 (s, 9H); ^{13}C NMR (125 MHz, $CDCl_3$) δ 89.7, 88.5, 84.4, 83.1, 18.5, 11.3, –0.4. EIMS *m/z* 278.2 (M^+, 38), 235.1 ($[M - i\text{–}Pr_3]^+$, 100); HRMS calcd. for $C_{16}H_{30}Si_2$ 278.1886, found 278.1885.

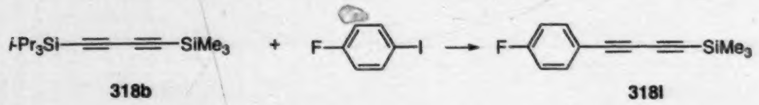

Compound **318i**: to **318b** (889 mg, 3.19 mmol) and K_2CO_3 (0.50 mg, 3.6 mmol) in THF/MeOH (10 mL, 1:1 v/v) was added and stirred until TLC showed the desilylation took place. Et_2O and NH_4Cl (10 mL) were added. The organic phase separated, washed with satd. aq. NaCl (2 x 3 mL), dried ($MgSO_4$) and reduced to 5 mL. To the deprotected alkyne, NEt_3 (25 mL), CuI (10 mg, 0.053 mmol) and $Pd(Ph_3)_4$ (20 mg, 0.017 mmol) and *p*–fluoroiodobenzene (0.64 g, 2.9 mmol) were added. The reaction was stirred and heated at 70 °C overnight. Solvent removal and purification by column chromatography (silica gel, hexanes) afforded **382i** (822 mg, 96%) as a colorless oil. $R_f = 0.6$ (hexanes).

IR (µscope) 2945, 2867, 2207, 2100, 1600 cm^{-1}; ^1H NMR (400 MHz, CDCl3) δ 7.47 (dd, $J = 8.9$ Hz, 5.4 Hz, 2H), 6.99 (app t, $J = 8.8$ Hz, 2H), 1.09 (s, 21H); ^{13}C NMR (100 MHz, $CDCl_3$) δ 162.9 (d, $J = 249.8$ Hz), 134.6 (d, $J = 8.6$ Hz), 117.6 (d, $J = 3.5$ Hz), 115.7 (d, $J = 22.3$ Hz), 89.2, 87.9, 74.4, 18.5, 11.2 (one signal not observed). EIMS *m/z* 300.2 (M^+, 29), 257.1 ($[M - i\text{-Pr}]^+$, 100); HRMS calcd. for $C_{19}H_{25}SiF$ (M^+) 300.1710, found 300.1708. Anal. calcd. for $C_{19}H_{25}SiF$: C, 75.94; H, 8.39. Found: C, 75.81; H, 8.32.

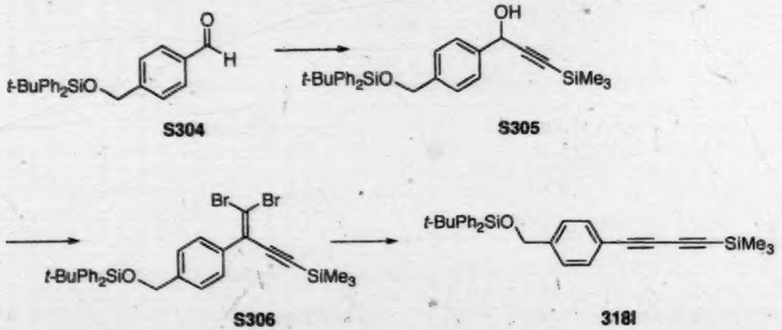

Compound S305: Trimethylsilylacetylene (0.62 mg, 6.3 mmol) in THF (30 mL) was cooled to –78 °C. BuLi (2.5 M in hexanes, 2.3 mL, 5.8 mmol) was slowly added over 1 min and the mixture allowed to stir for 0.5 h. The aldehyde **S304**[11] (1.96 mg, 5.23 mmol) was dissolved in THF (5 mL), and then added to the lithium acetylide mixture. The reaction was warmed to rt, then quenched with satd. aq. NH_4Cl (2 x 30 mL) and Et_2O (30 mL), washed with satd. aq. NaCl (30 mL) dried over $MgSO_4$, and the solvent removed *in vacuo*. Column chromatography (silica gel, CH_2Cl_2) provided **S305** (1.82 g, 74%) as light yellow oil. $R_f = 0.6$ (CH_2Cl_2).

IR ($CHCl_3$, cast) 3358, 2958, 2857, 2173 (w) cm^{-1}; ^1H NMR (400 MHz, CDC13) δ 7.70–7.67 (m, 4H), 7.50 (d, $J = 8.0$ Hz, 2H), 7.44–7.34 (m, 8H), 5.44 (d, $J = 5.2$ Hz, 1H), 4.77 (s, 2H), 2.11 (br s, 1H), 1.09 (s, 9H), 0.20 (s, 9H); ^{13}C NMR (100 MHz, $CDCl_3$) δ 141.3, 138.8, 135.4, 133.3, 129.6, 127.6, 126.6, 126.1, 104.9, 91.4, 65.1, 64.8, 26.7, 19.2, –0.3. ESI MS (MeOH) *m/z* 495.2 ($[M + Na]^+$); HRMS calcd. for $C_{29}H_{36}O_2Si_2Na$ (M^+) 495.2146, found 495.2147.

Compound **S306**: To alcohol **S305** (703 mg, 1.49 mmol) in CH_2Cl_2 (100 mL) at rt was added PCC (640 mg, 2.97 mmol), celite (1 g), and molecular sieves (4 Å, 1 g). The reaction was stirred overnight. The reaction mixture was passed through a plug of silica gel (CH_2Cl_2) to remove chromium waste and the solvent removed *in vacuo* to afford the intermediate ketone as a colorless oil. $R_f = 0.6$ (hexanes/CH_2Cl_2 1:1). The ketone was carried to the next step without further purification.

CBr_4 (987 mg, 2.98 mmol) and PPh_3 (1.56 mg, 5.95 mmol) were added to CH_2Cl_2 (50 mL) and allowed to stir for 5 min at rt. The mixture was added to ketone in CH_2Cl_2 (5 mL). The progress of the reaction was monitored by TLC until the ketone was no longer present. Hexanes (50 mL) was added, the solvent was reduced to ca. 20 mL, the inhomogeneous mixture filtered through silica gel, and solvent removed *in vacuo*.

Column chromatography (silica gel, hexanes) yielded **S306** (223 mg, 24%) as a colorless oil. $R_f = 0.4$ (hexanes/CH_2Cl_2 3:1).

IR ($CHCl_3$, cast) 3071, 2959, 2134 (w) cm^{-1}; ^{1}H NMR (400 MHz, $CDCl_3$) δ 7.69–7.66 (m, 4H), 7.44–7.32 (m, 10H), 4.75 (s, 2H), 1.09 (s, 9H), 0.2 (s, 9H); ^{13}C NMR (100 MHz, $CDCl_3$) δ 141.6, 136.3, 135.6, 133.3, 130.9, 129.7, 128.5, 127.8, 125.7, 104.0, 103.4, 100.0, 65.2, 26.9, 19.3, –0.3. EIMS *m/z* 570.0 ([M – *t*-Bu]$^+$, 64); HRMS calcd. for $C_{26}H_{25}{}^{79}Br^{81}BrOSi$ (M^+) 569.9692, found 569.9692.

Compound **318l**: **S306** (223 mg, 0.356 mmol) in hexanes (5 mL) was cooled to –78 °C. BuLi (2.5 M in hexanes, 0.17 mL, 0.43 mmol) was added over a period of ca. 1 min and the reaction stirred for 1 h. The reaction was quenched with satd. aq. NH_4Cl (5 mL) and Et_2O (5 mL), the organic layer separated, washed with satd. aq. NaCl (5 mL), dried over $MgSO_4$, and the solvent removed. Column chromatography (silica gel, hexanes) provided **318l** (121 mg, 73%) as a colorless oil. $R_f = 0.5$ (hexanes/CH_2Cl_2 3:1).

IR ($CHCl_3$, cast) 3070, 2958, 2857, 2205, 2102 cm^{-1}; ^{1}H NMR (400 MHz, CDCl3) δ 7.65 (d, $J = 8.0$ Hz, 4H), 7.44–7.39 (m, 4H), 7.34–7.33 (m, 4H), 7.28–7.26 (m, 2H), 4.73 (s, 2H), 1.07 (s, 9H), 0.2 (s, 9H); ^{13}C NMR (100 MHz, CDCl3) δ 142.7, 135.5, 133.2, 132.6, 129.8, 127.8, 125.9, 119.7, 90.4, 88.0, 73.8, 65.1, 26.8, 19.3, –0.4, one signal not observed. EIMS *m/z* 466.2 (M^+, 2), 409.1 ([M – *t*-Bu]$^+$, 100); HRMS calcd. for $C_{30}H_{34}OSi_2$ 466.2148, found 466.2156.

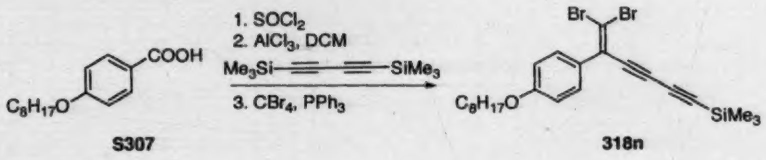

Compound **318n**: To compound **S307** (2.70 g, 10.8 mg) in a flame dried flask fitted with a drying tube was added $SOCl_2$ (2.58 g, 21.6 mmol). The mixture was allowed to stir at rt for 24 h. Excess $SOCl_2$ was removed *in vacuo* using a water aspirator and the remaining acid chloride was diluted with dry CH_2Cl_2 (20 mL). *Bis*–trimethylsilylbutadiyne (2.51g, 12.9 mmol) was added to the mixture and cooled to –20 °C. $AlCl_3$ (2.16 g, 16.2 mmol) was then added and the mixture allowed to warm to rt. The reaction was poured into aqueous acid HCl in ice (10% v:v) and the organic layer was washed with NH_4Cl (2 x 20 mL), NaCl (2 x 20 mL) and dried over $MgSO_4$. Solvent removal *in vacuo* gave the crude ketone which was carried to the next reaction without further characterization.

To this ketone, PPh_3 (8.36 g, 31.9 mmol) and CBr_4 (5 g, 15.6 mmol) in CH_2Cl_2 (40 mL) at 0 °C were added. The reaction was slowly warmed to rt until no more ketone remained. The reaction was diluted with hexanes (40 mL) and filtration through a short plug of silica with hexanes yielded pure **318n** (1.12 mg, 20%) as a white crystalline solid. R_f = 0.6 (hexanes/CH_2Cl_2 3:1).

IR ($CHCl_3$, cast) 2926, 2093 (w), 1506 cm^{-1}; ^1H NMR (400 MHz, $CDCl_3$) δ 7.31 (d, J = 8.8 Hz, 2H), 6.85 (d, J = 8.8 Hz, 2H), 3.94 (t, J = 6.6 Hz, 2H), 1.76 (app quint, J = 7.0 Hz, 2H), 1.45–1.27 (m, 10H), 0.87 (t, J = 6.4 Hz, 3H); ^{13}C NMR (125 MHz, $CDCl_3$) δ 159.5, 129.9, 129.6, 129.1, 114.3, 101.6, 95.1, 87.4, 81.8, 75.2, 68.1, 31.8, 29.3, 29.2, 29.1(9), 26.0, 22.7, 14.1, –0.53. EI HRMS calcd. for $C_{23}H_{30}OSi^{79}Br^{81}Br$ 510.0412, found 510.0410. Anal. calcd. for $C_{23}H_{30}OSi^{79}Br^{81}Br$: C, 54.13; H, 5.92. Found: C, 54.08; H, 5.62.

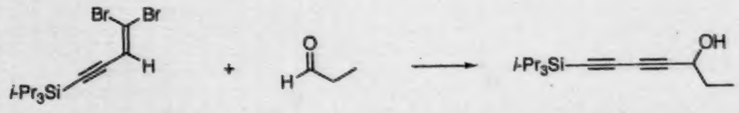

S303 **318g**

Compound **318g**: Compound **S303**[10] (684 mg, 1.87 mmol) in hexanes (10 mL) was cooled to –78 °C. BuLi (2.5 M in hexanes,1.4 mL, 3.5 mmol) at –78 °C was added over a period of ca. 1 min and stirred for 1 h. Propionaldehyde (0.12 mg, 2.1 mmol) was added to the mixture above by syringe and the reaction was warmed to rt overnight. The reaction was quenched with satd. aq. NH$_4$Cl (10 mL) and Et$_2$O (10 mL), the organic layer separated, washed with satd. aq. NaCl (10 mL), dried over MgSO$_4$, and the solvent removed. Column chromatography (silica gel, hexanes) provided **318g** (269 mg, 54%) as yellow oil. R_f = 0.5 (CH$_2$Cl$_2$).

IR (μscope) 3181, 2944, 2867, 2105, 1463 cm^{-1}; ^{1}H NMR (400 MHz, CDCl$_3$) δ 4.36 (dd, *J* = 12.2 Hz, 6.4 Hz, 1H), 1.74 (app quint, *J* = 6.4 Hz, 2H), 1.78 (br d, *J* = 5.6 Hz, 1H), 1.06 (s, 21H), 1.01 (t, *J* = 7.5 Hz, 3H); ^{13}C NMR (100 MHz, CDCl$_3$) δ 88.8, 84.8, 70.3, 64.1, 30.6, 18.5, 11.2, 9.4. EIMS *m/z* 264.2 (M$^+$, 7), 221.1 ([M – *i*–Pr]$^+$, 100); HRMS calcd. for C$_{16}$H$_{28}$OSi (M$^+$) 264.1910, found 264.1911.

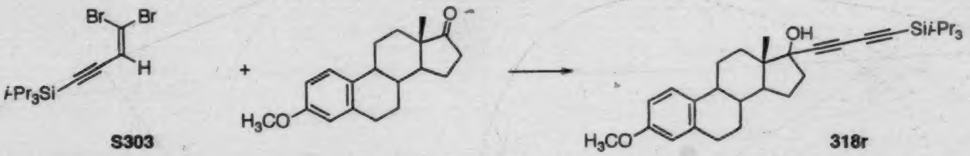

Compound **318r**: Compound **S303**[10] (523 mg, 1.43 mmol) in Et$_2$O (10 mL) was cooled to –78 °C. LDA [reaction between BuLi (2.5 M in hexanes, 1.70 mL, 4.25 mmol) and *i*–Pr$_2$NH (0.60 mL, 76 mmol) in Et$_2$O (10 mL) at –78 °C and the mixture was stirred for 30 min] was added over a period of ca. 1 min and stirred for 1 h. Sterone (0.365 mg, 1.28 mmol) was added to the mixture above by syringe and the reaction was warmed to rt overnight. The reaction was quenched with satd. aq. NH$_4$Cl (10 mL) and Et$_2$O (10 mL), the organic layer separated, washed with satd. aq. NaCl (10 mL), dried over MgSO$_4$, and the solvent removed. Column chromatography (silica gel, hexanes) provided **318r** (584 mg, 73%) as a white crystalline solid. Mp 155–158 °C. R_f = 0.5 (CH_2Cl_2).

IR (µscope) 3402, 2943, 2866, 2216 (w), 2096, 1257 cm^{-1}; ^{1}H NMR (500 MHz, $CDCl_3$) δ 7.20 (d, *J* = 7.2 Hz, 1H), 6.70 (dd, *J* = 2.8, 8.5 Hz, 1H), 6.61 (d, *J* =2.8 Hz, 1H), 3.76 (s, 3H), 2.86–2.81 (m, 2H), 2.40–2.32 (m, 2H), 2.25 (dt, *J* = 4.0, 11.0 Hz, 1H), 2.01 (ddq, *J* = 3.9, 12.0, 13.8 Hz, 1H), 1.94 (t, *J* = 3.0 Hz, 1H), 1.89–1.65 (m, 5H), 1.51–1.34 (m, 4H), 1.08 (s, 21H), 0.86 (s, 3H); ^{13}C NMR (125 MHz, $CDCl_3$) δ 15.5, 137.9, 132.5, 126.4, 113.8, 111.5, 89.1, 85.0, 80.6, 79.8, 71.5, 55.2, 49.8, 48.0, 43.4, 39.5, 39.0, 33.1, 29.8, 27.2, 26.4, 23.0, 18.6, 12.8, 11.3. EIMS *m/z* 490.3 (M$^+$, 10), 447.3 ([M – *i*–Pr]$^+$, 41); HRMS calcd. for $C_{32}H_{46}O_2Si$ (M$^+$) 490.3137, found 490.3130.

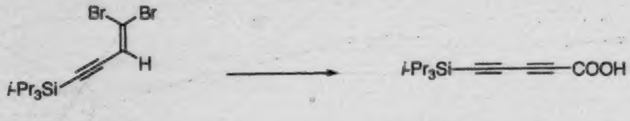

S303 **321**

Compound **321**: Compound **S303**[10] (369 mg, 1.01 mmol) in hexanes (5 mL) was cooled to –78 °C. BuLi (2.5 M in hexanes, 0.85 mL, 2.13 mmol) was added. The mixture was stirred for 1 h. Carbon dioxide generated from dry ice and passed through a drying tube filled with $CaCl_2$ was bubbled into the reaction overnight The reaction was quenched with water (10 mL) and Et_2O (10 mL). The aqueous phase was separated and neutralized with aq. HCl (10%) and Et_2O (10 mL) was added. The organic layer separated, washed with satd. aq. NaCl (10 mL), dried over $MgSO_4$, and the solvent removed to afford **321** (170 mg, 67%) as a light yellow oil.

IR (µscope) 2946, 2868, 2246 (w), 2204, 2105, 1687 cm^{-1}; ^{1}H NMR (500 MHz, $CDCl_3$) δ 1.08 (s, 21H), (COOH signal not observed); ^{13}C NMR (100 MHz, $CDCl_3$) δ 155.2, 94.1, 87.1, 73.6, 18.4, 11.1, (one signal not observed). EIMS *m/z* 250.1 (M^+, 7), 207.1 ($[M - i\text{–Pr}]^+$, 100); HRMS calcd. for $C_{14}H_{22}O_2Si$ (M^+) 250.1389, found 250.1393.

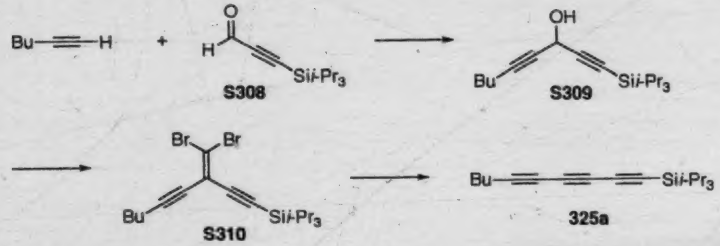

Compound **S309**: 1–Hexayne (872 mg, 10.6 mmol) in THF (100 mL) was cooled to –78 °C. BuLi (2.5 M in hexanes, 4.2 mL, 11 mmol) was slowly added over 1 min and the mixture allowed to stir for 0.5 h. **S308**[10] (1.87 g, 8.89 mmol) was added to the lithium acetylide mixture. The reaction was warmed to rt, quenched with satd. aq. NH_4Cl (100 mL) and Et_2O (100 mL), the organic layer separated, washed with satd. aq. NaCl (100 mL), dried over $MgSO_4$, the solvent removed, and the residue purified by column chromatography (silica gel, CH_2Cl_2/hexanes 1:1) afforded **S309** (2.37 g, 91%) as a colorless oil. $R_f = 0.4$ (CH_2Cl_2/hexanes 1:1).

IR ($CHCl_3$, cast) 3370, 2943, 2866, 2233 (w), 2174 (w), 1464 cm^{-1}; ^1H NMR (500 MHz, $CDCl_3$) δ 5.07 (t, $J = 2.0$ Hz, 1H), 2.21 (dt, $J = 2.0$ Hz, 7.0 Hz, 2H), 2.05 (br s, 1H), 1.48 (app sec, $J = 7.0$ Hz, 2H), 1.41 (app sept, $J = 7.0$ Hz, 2H), 1.06 (s, 21H), 0.89 (t, $J = 7.0$ Hz, 3H); ^{13}C NMR (125 MHz, $CDCl_3$) δ 104.9, 85.4, 85.2, 77.7, 52.8, 30.4, 21.8, 18.5, 18.3, 13.5, 11.1. EIMS *m/z* 292.2 (M^+, 7); HRMS calcd. for $C_{18}H_{32}OSi$ (M^+) 292.2222, found 292.2218. Anal. calcd. for $C_{18}H_{32}OSi$: C, 73.90; H, 11.03. Found: C, 73.63; H, 10.95.

Compound **S310**: To compound **S309** (873 mg, 2.98 mmol) in CH_2Cl_2 (20 mL) at rt was added PCC (1.28 g, 5.94 mmol), celite (1 g), and molecular sieves (4 Å, 1 g). The reaction was stirred overnight. The reaction mixture was passed through a plug of silica gel (CH_2Cl_2) to remove chromium waste and the solvent removed *in vacuo* to afford the intermediate ketone as a colorless oil. R_f = 0.6 (hexanes/CH_2Cl_2 1:1). The ketone was carried to the next step without further purification.

CBr_4 (1.56 g, 4.70 mmol) and PPh_3 (2.46 g, 9.38 mmol) were added to CH_2Cl_2 (25 mL) and allowed to stir for 5 min at rt. The mixture was added to ketone in CH_2Cl_2 (5 mL). TLC analysis was used to monitor the reaction, indicating that dibromoolefination was complete in 1 h. Hexanes (25 mL) was added and solvent was reduced to ca. 20 mL, the inhomogeneous mixture filtered through silica gel and solvent removed *in vacuo*. Column chromatography (silica gel, hexanes) yielded **S310** (786 mg, 59%) as a colorless oil. R_f = 0.8 (hexanes).

IR ($CHCl_3$, cast) 2958, 2866, 2222, 2158 (w), 1463 cm^{-1}; ^1H NMR (500 MHz, $CDCl_3$) δ 2.33 (t, J = 7.0 Hz, 2H), 1.54 (quint, J = 7.0 Hz, 2H), 1.45 (dt, J = 7.0 Hz, 7.5 Hz, 2H), 0.90 (t, J = 7.5 Hz, 3H); ^{13}C NMR (125 MHz, $CDCl_3$) δ 114.9, 106.9, 102.6, 98.6, 98.1, 77.9, 30.1, 21.8, 19.4, 18.6, 13.5, 11.2. EIMS *m/z* 446.0 (M^+, 34), 403.0 ($[M - i\text{-}Pr]^+$, 100); HRMS calcd. for $C_{19}H_{30}{}^{79}Br^{81}BrSi$ (M^+) 446.0463, found 446.0460.

Compound **325a**: Compound **S310** (367 mg, 0.826 mmol) in mixture of toluene (2 mL) and hexanes (8 mL) was cooled to –78 °C. BuLi (2.5 M in hexanes, 0.40 mL, 1.0 mmol). The mixture was warmed to rt. The reaction was quenched with satd. aq. NH_4Cl (10 mL) and Et_2O (10 mL), the organic layer separated, washed with satd. aq. NaCl (10 mL), dried over $MgSO_4$, and the solvent removed. Column chromatography (silica gel, hexanes/CH_2Cl_2 6:1) provided **325** (203 mg, 86%) as a colorless oil. R_f = 0.7 (hexanes/CH_2Cl_2 6:1).

IR ($CHCl_3$, cast) 2959, 2867, 2211, 2166 (w), 2078, 1463 cm^{-1}; ^1H NMR (500 MHz, $CDCl_3$) δ 2.28 (t, *J* = 7.0 Hz, 2H), 1.53–1.48 (m, 3H), 1.40 (app sex, *J* = 7.0 Hz, 2H), 1.06 (s, 21H), 0.89 (t, *J* = 7.0 Hz, 3H); ^{13}C NMR (125 MHz, $CDCl_3$) δ 90.1, 83.0, 80.7, 65.5, 61.5, 60.4, 30.0, 21.9, 19.1, 18.5, 13.5, 11.3. EIMS *m/z* 286.2 (M^+, 24), 243.2 ($[M - i\text{-}Pr]^+$, 100); HRMS calcd. for $C_{19}H_{30}Si$ (M^+) 286.2117, found 286.2114. Anal. calcd. for $C_{19}H_{30}Si$: C, 79.64; H, 10.55. Found: C, 79.59; H, 10.67.

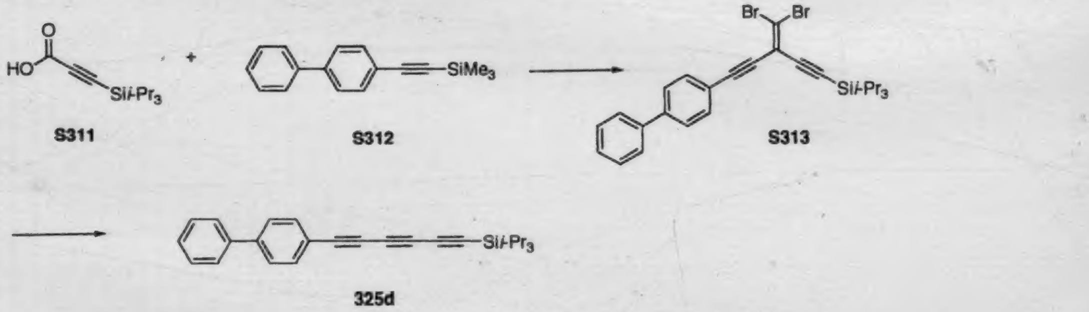

Compound **S312**: $SOCl_2$ (1.6 g, 13 mmol) was added to the **S311**[12] (820 mg, 3.62 mmol) in a dry flask protected from moisture with a drying tube containing $CaCl_2$, and the mixture allowed to stir overnight at rt. The excess $SOCl_2$ was then removed *in vacuo* to provide the acid chloride. CH_2Cl_2 (50 mL) was added and the temperature of the solution was lowered to –20 °C. **S312**[13] (907 mg, 3.62 mmol) and $AlCl_3$ (530 mg, 3.97 mmol) were added and the reaction mixture warmed to rt over 3 h. The reaction was carefully quenched by the addition of the reaction to 10% HCl (50 mL). The organic layer was separated, washed with satd. aq. $NaHCO_3$ (50 mL), NaCl (50 mL), dried over $MgSO_4$, and the solvent removed *in vacuo*. The crude reaction was passed through a plug of silica to remove baseline material afforded crude ketone.

CBr_4 (1.70 g, 5.13 mmol) and PPh_3 (2.68 g, 10.2 mmol) were added to CH_2Cl_2 (25 mL) and allowed to stir for 5 min at rt. The mixture was added to the crude ketone in CH_2Cl_2 (5 mL). The progress of the reaction was monitored by TLC until complete. Hexanes (25 mL) was added and solvent was reduced to ca. 20 mL, the inhomogeneous mixture filtered through silica gel and solvent removed *in vacuo*. Column chromatography (silica gel, hexanes/CH_2Cl_2 6:1) yielded **S313** (1.40 g, 71%) as a colorless oil. $R_f = 0.5$ (hexanes/CH_2Cl_2 6:1).

IR ($CHCl_3$, µscope) 2943, 2865, 2201, 1486 cm^{-1}; ^1H NMR (400 MHz, $CDCl_3$) δ 7.62–7.57 (m, 6H), 7.44 (t, $J = 7.5$ Hz, 2H), 7.26 (t, $J = 7.4$ Hz, 1H), 1.13 (s, 21H); ^{13}C NMR (100 MHz, $CDCl_3$) δ 141.8, 140.1, 132.0, 128.8, 127.7, 127.2, 127.1, 127.0, 126.9, 122.3, 121.0, 114.5, 108.3, 102.0, 99.6, 95.5, 86.8, 18.5, 11.1. EIMS *m/z* 542.0 (M^+, 84); HRMS calcd. for $C_{27}H_{30}{}^{79}Br^{81}BrSi$ (M^+) 542.0463, found 542.0457.

Compound **325d**: **S313** (1.40 g, 2.58 mmol) in hexanes (30 mL) was cooled to –78 °C. BuLi (2.5 M in hexanes, 1.1 mL, 2.8 mmol) were added. The mixture was warmed to rt. The reaction was quenched with satd. aq. NH_4Cl (30 mL) and Et_2O (30 mL), the organic layer separated, washed with satd. aq. NaCl (30 mL), dried over $MgSO_4$, and the solvent removed. Column chromatography (silica gel, hexanes/CH_2Cl_2 6:1) provided **325d** (797 mg, 81%) as brown solid. Mp 103–105 °C. $R_f = 0.6$ (hexanes/CH_2Cl_2 6:1).

IR ($CHCl_3$, µscope) 2957, 2865, 2176, 2071, 1599 cm^{-1}; ^1H NMR (400 MHz, $CDCl_3$) δ 7.58–7.53 (m, 6H), 7.44 (t, $J = 7.5$ Hz, 2H), 7.36 (t, $J = 7.4$ Hz, 1H), 1.09 (s, 21H); ^{13}C

NMR (100 MHz, $CDCl_3$) δ 142.4, 139.8, 133.4, 128.8, 127.9, 127.0, 127.0, 119.5, 89.7, 86.9, 76.4, 75.0, 67.5, 60.6, 18.4, 11.2. EIMS *m/z* 382.2 (M^+, 52), 339.2 ($[M - i\text{–}Pr]^+$, 100); HRMS calcd. for $C_{27}H_{30}Si$ (M^+) 382.2117, found 382.2115.

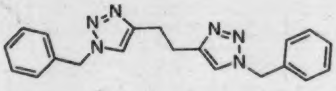

315a

Compound **315a**: Compound **316a** (99.3 mg, 1.27 mmol, in 50% pentane), benzyl azide (362 mg, 2.72 mmol) were used as per the general procedure J and yielded **309a** (268 mg, 61%) as a white powder. Mp 173–175 °C $R_f = 0.3$ (CH_2Cl_2/EtOAc 1:1).

IR ($CHCl_3$, cast) 3112, 3064, 1700 cm^{-1}; ^1H NMR (400 MHz, $CDCl_3$) δ 7.31–7.30 (m, 6H), 7.22–7.16 (m, 4H), 7.11 (s, 2H), 5.39 (s, 4H), 3.03 (s, 4H); ^{13}C NMR (125 MHz, $CDCl_3$) δ 134.8, 129.0, 128.6, 127.9, 54.1, 25.4, (two signals not observed). EIMS *m/z* 344.2 (M^+, 14), 316.2 ($[M - N_2]^+$, 7); HRMS calcd. for $C_{20}H_{20}N_6$ 344.1750, found 344.1741. Anal. calcd. for $C_{20}H_{20}N_6$: C, 69.75; H, 5.85; N, 24.40. Found: C, 69.52; H, 6.10; N, 23.82.

A single crystal of compound **315a** was obtained by slow diffusion of hexanes into a solution of **309a** in CH_2Cl_2 at 4 °C. $C_{20}H_{20}N_6$, M = 344.42, monoclinic group $P2_1/c$ (No. 14), $Dc = 1.301$ g/cm^{-3}, $a = 18.592(2)$ Å, $b = 5.4325(7)$ Å, $c = 8.7921(11)$ Å, $\beta = 89.155(2)^\circ$, $V = 879.01(19)$ Å^3, $Z = 2$, $\mu = 0.082$ mm^{-1}, T = –80 °C. Final $R_1(F) = 0.0474$ (1234 observations $[F_o^2 \geq -2\delta(F_o^2)]$, $\omega R_2(F^2) = 0.1506$ for 118 variables and 1801 data with $F_o^2 \geq -3\delta(F^2)$.

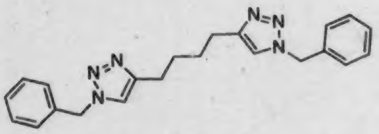

315b

Compound **315b**: Compound **316b** (810 mg, 0.763 mmol), benzyl azide (203 mg, 1.53 mmol) were used as per the general procedure J and yielded **315b** (277 mg, 97%) as a white crystalline solid. Mp 157–160 °C. R_f = 0.3 (CH_2Cl_2/EtOAc 1:1).

IR ($CHCl_3$, cast) cm^{-1}; ^1H NMR (300 MHz, $CDCl_3$) δ 7.21–7.17 (m, 6H), 7.11 (s, 2H), 7.09 (d, *J* = 7.3 Hz, 4H), 5.33 (s, 4H), 2.56 (br s, 4H), 1.59 (br s, 4H); ^{13}C NMR (125 MHz, $CDCl_3$) δ 134.9, 129.0, 128.6, 128.0, 54.1, 28.8, 25.4, (two signals not observed). EIMS *m/z* 372.2 (M^+, 27), 253.1 ($[M - N_2]^+$, 5); HRMS calcd. for $C_{22}H_{24}N_6$ 372.2062, found 372.2064.

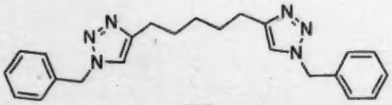

315c

Compound **315c**: Compound **316c** (200 mg, 1.66 mmol), benzyl azide (469 mg, 3.52 mmol) were used as per the general procedure J and yielded **315c** (621 mg, 97%) as a white crystalline solid. Mp 115–118 °C. R_f = 0.5 (CH_2Cl_2: EtOAc 1:1).

IR ($CHCl_3$, cast) 3307, 2930, 2855, 1457 cm^{-1}; ^1H NMR (300 MHz, $CDCl_3$) δ 7.37–7.31 (m, 6H), 7.23–7.20 (m, 4H), 7.16 (s, 2H), 5.46 (s, 4H), 2.65 (t, *J* = 7.6 Hz, 4H), 1.67 (quint, *J* = 7.6 Hz, 4H), 1.41–1.33 (m, 2H); ^{13}C NMR (100 MHz, $CDCl_3$) δ 148.7, 134.9, 129.0, 128.6, 128.0, 120.6, 54.0, 29.0, 28.6, 25.5 EIMS *m/z* 386.2 (M^+, 1); HRMS calcd. for $C_{23}H_{26}N_6$ 386.2219, found 386.2206.

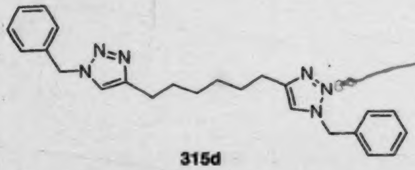

315d

Compound **315d**: Compound **316d** (82.2 mg, 0.612 mmol), benzyl azide (170 mg, 1.28 mmol) were used as per the general procedure J and yielded **315d** (227 mg, 93%) as a light green powder. Mp 148–151 °C. $R_f = 0.4$ (CH_2Cl_2/EtOAc 1:1).

IR ($CHCl_3$, cast) 3061, 2928, 2851, 1467 cm^{-1}; ^1H NMR (300 MHz, $CDCl_3$) δ 7.38–7.31 (m, 6H), 7.23–7.21 (m, 4H), 7.14 (s, 2H), 5.46 (s, 4H), 2.64 (t, J = 7.4 Hz, 4H), 1.59 (br s, 4H), 1.35–1.28 (m, 4H); ^{13}C NMR (125 MHz, $CDCl_3$) δ 148.8, 135.0, 129.0, 128.6, 128.0, 120.5, 54.0, 29.2, 28.8, 25.6. EIMS *m/z* 400.2 (M^+, 22); HRMS calcd. for $C_{24}H_{28}N_6$ 400.2376, found 400.2370.

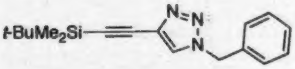

317a

Compound **317a**: Compound **318a** (149 mg, 0.630 mmol), benzyl azide (74.7 mg, 0.461 mmol) were used as per the general procedure J and yielded **317a** (125 mg, 75%) as a colorless oil. $R_f = 0.4$ (CH_2Cl_2).

IR ($CHCl_3$, cast) 2929, 2857, 2171, 1458 cm^{-1}; ^1H NMR (400 MHz, $CDCl_3$) δ 7.51 (s, 1H), 7.37–7.33 (m, 3H), 7.25–7.22 (m, 2H), 5.49 (s, 2H), 0.94 (s, 9H), 0.14 (s, 6H); ^{13}C NMR (100 MHz, $CDCl_3$) δ 134.0, 131.3, 129.1, 128.9, 128.1, 126.1, 97.0, 94.1, 54.2, 26.0, 16.5, –4.9. EIMS *m/z* 297.2 (M^+, 1), 269.2 ($[M - N_2]^+$, 17); HRMS calcd. for $C_{17}H_{23}SiN_3$ 297.1661, found 297.1652. Anal. calcd. for $C_{17}H_{23}SiN_3$: C, 68.64; H, 7.79; N, 14.13. Found: C, 68.37; H, 7.83; N, 13.83.

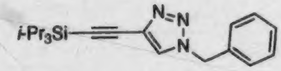

317b

Compound **317b**: Compound **318b** (93.8 mg, 0.337 mmol), benzyl azide (44.8 mg, 0.336 mmol) were used as per the general procedure J and yielded **317b** (77 mg, 67%) as a white solid. Mp 69–71 °C. $R_f = 0.4$ (CH_2Cl_2).

IR (CH_2Cl_2, cast) 2925, 2866, 2171 cm^{-1}; ^1H NMR (400 MHz, $CDCl_3$) δ 7.56 (s, 1H), 7.40–7.35 (m, 3H), 7.28–7.25 (m, 2H), 5.51(s, 2H), 1.11 (s, 21H); ^{13}C NMR (100 MHz, $CDCl_3$) δ 134.0, 129.1, 128.8(4), 128.8(3), 128.1, 126.1, 95.1, 54.2, 18.5, 11.1 (one signal not observed). EIMS *m/z* 339.2 (M^+, 7), 311.2($[M - N_2]^+$, 97), 296.2 ($[M - i\text{-}Pr]^+$, 100); HRMS calcd. for $C_{20}H_{29}SiN_3$ 339.2131, found 339.2121.

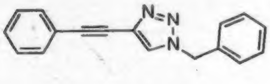

317c

Compound **317c**: Compound **318c**[14] (143 mg, 0.721 mmol), benzyl azide (85.3 mg, 0.641 mmol) were used as per the general procedure J and yielded **317c** (121 mg, 73%) as a white crystalline solid. Mp 105–107 °C. $R_f = 0.3$ (CH_2Cl_2).

IR (CH_2Cl_2, cast) 3122, 2230(w), 1456 cm^{-1}; ^{1}H NMR (400 MHz, $CDCl_3$) δ 7.61 (s, 1H), 7.53–7.50 (m, 2H), 7.39–7.28 (m, 8H), 5.55 (s, 2H); ^{13}C NMR (100 MHz, $CDCl_3$) δ 134.1, 131.6, 131.5, 129.2, 129.0, 128.8, 128.4, 128.1, 125.8, 122.3, 92.6, 78.5, 54.3. EIMS *m/z* 259.1 (M^+, 28), 231.1 ($[M - N_2]^+$, 38); HRMS calcd. for $C_{17}H_{13}N_3$ 259.1110, found 259.1102. Anal. calcd. for $C_{17}H_{13}N_3$: C, 78.74; H, 5.05; N, 16.20. Found: C, 78.71; H, 5.22; N, 16.22.

A single crystal for X–ray crystallography were grown by diffusing hexanes into a solution of **317c** in CH_2Cl_2 at rt. $C_{17}H_{13}N_3$, M = 259.31, monoclinic group $P2_1/n$ (an alternate setting of $P2_1/c$ [No. 14]), $Dc = 1.262$ g cm^{-3}, $a = 5.7277(8)$ Å, $b = 14/2042(18)$ Å, $c = 16.811(2)$ Å, $\beta = 93.6141(18)°$, $V = 1365.0(3)$ Å^3, $Z = 4$, $\mu = 0.077$ mm^{-1}, T = –80 °C. Final $R_1(F) = 0.0409$ (2030 observations $[F_o^2 \geq -2\delta(F_o^2)]$), $\omega R_2(F^2) = 0.1507$ for 181 variables and 2800 data with $F_o^2 \geq -3\delta(F^2)$. CCDC no. 623595.

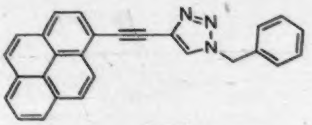

317d

Compound **317d**: Compound **318d** (159 mg, 0.490 mmol), benzyl azide (58.6 mg, 0.440 mmol) were used as per the general procedure J and yielded **317d** (105 mg, 62%) as a yellow powder. Mp 168–171 °C. $R_f = 0.2$ (CH_2Cl_2).

IR (CH_2Cl_2, cast) 3139 (w), 3041(w), 2216 (w), 1456 cm^{-1}; ^1H NMR (500 MHz, $CDCl_3$) δ 8.61 (d, J = 9.1 Hz, 1H), 8.20 (d, J = 7.6 Hz, 1H), 8.18 (d, J = 7.8 Hz, 1H), 8.16 (d, J = 9.5 Hz, 1H), 8.14 (d, J = 9.2 Hz, 1H), 8.09 (d, J = 5.1 Hz, 1H), 8.08 (d, J = 6.0 Hz, 1H), 8.02 (d, J = 9.0 Hz, 1H), 8.01 (t, J = 7.6 Hz, 1H), 7.73 (s, 1H), 7.43–7.38 (m, 3H), 7.323–7.31 (m, 2H), 5.60 (s, 2H); ^{13}C NMR (125 MHz, $CDCl_3$) δ 134.2, 132.0, 131.8, 131.6, 131.2, 131.0, 129.6, 129.3, 129.0, 128.5, 128.4, 128.2, 127.2, 126.3, 125.9, 125.8, 125.7, 125.5, 124.5, 124.4, 124.2, 116.7, 91.9, 83.9, 54.5, (two signals not observed). EIMS *m/z* 383.1 (M^+, 1), 354.1 ($[M - N_2]^+$, 1); HRMS calcd. for $C_{27}H_{16}N_3$ 383.1422, found 383.1417. Anal. calcd. for $C_{27}H_{16}N_3$: C, 84.57; H, 4.47; N, 10.96. Found: C, 84.18; H, 4.56; N, 10.81.

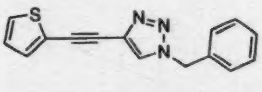

317e

Compound **317e**: Compound **318e**[15] (182 mg, 0.893 mmol), benzyl azide (107 mg, 0.800 mmol) were used as per the general procedure J and yielded **317e** (150 mg, 71%) as a white crystalline solid. Mp 86–88 °C. $R_f = 0.35$ (CH_2Cl_2).

IR (CH_2Cl_2, cast) 3129, 2953, 2220 (w), 1457 (w) cm^{-1}; ^1H NMR (300 MHz, $CDCl_3$) δ 7.60 (s, 1H), 7.39–7.36 (m, 3H), 7.31–7.26 (m, 4H), 6.99 (dd, J = 3.7, 5.1 Hz, 1H), 5.54

(s, 2H); ^{13}C NMR (125 MHz, APT, $CDCl_3$) δ 134.0, 132.7, 131.2, 129.2, 129.0, 128.2, 128.0, 127.1, 125.9, 122.2, 86.0, 82.1, 54.4, (two signals not observed). EIMS *m/z* 265.1 (M^+, 14), 237.1 ($[M - N_2]^+$, 14); HRMS calcd. for $C_{15}H_{11}N_3S$ 265.0674, found 265.0675. Anal. calcd. for $C_{15}H_{11}N_3S$: C, 67.90; H, 4.18; N, 15.84. Found: C, 67.64; H, 4.25; N, 15.37.

A single crystal of compound **317e** was obtained from slow evaporation of solution of compound **317e** in CH_2Cl_2 at rt. $C_{15}H_{11}N_3S$, M = 265.33, monoclinic group $P2_1/n$ (an alternate setting of $P2_1/c$ [No. 14]), $Dc = 1.343$ g/cm^{-3}, $a = 9.9330(10)$ Å, $b = 5.7873(6)$ Å, $c = 23.287(2)$ Å, $\beta = 101.4178(14)^\circ$, $V = 1312.2(2)$ Å^3, $Z = 4$, $\mu = 0.235$ mm^{-1}, T = –80 °C. Final $R_1(F) = 0.0456$ (2254 observations $[F_o^2 \geq -2\delta(F_o^2)]$), $\omega R_2(F^2) = 0.1209$ for 179 variables and 2672 data with $F_o^2 \geq -3\delta(F_o^2)$.

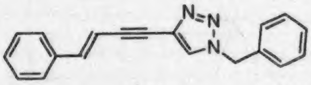

317f

Compound **317f**: Compound **318f** (107 mg, 0.476 mmol), benzyl azide (56.5 mg, 0.424 mmol) were used as per the general procedure J and yielded **317f** (83 mg, 69%) as a yellow solid. Mp 113–115 °C. $R_f = 0.3$ (CH_2Cl_2).

IR (CH_2Cl_2, cast) 3126, 2434 (w), 2360 (w), 1454 cm^{-1}; ^{1}H NMR (400 MHz, $CDCl_3$) δ 7.53 (s, 1H), 7.40–7.25 (m, 10H),5.52 (s, 2H); ^{13}C NMR (125 MHz, $CDCl_3$) δ 142.3, 136.0, 134.1, 131.6, 129.2, 129.0, 128.9, 128.7, 128.1, 126.4, 125.6, 107.1, 92.1, 80.5, 54.4, (two signals not observed). EIMS *m/z* 285.1 (M^+, 15), 257.1 ($[M - N_2]^+$, 28); HRMS calcd. for $C_{19}H_{15}N_3$ 285.1266, found 285.1266. Anal. calcd. for $C_{19}H_{15}N_3$: C, 79.98; H, 5.30; N, 14.73. Found: C, 79.55; H, 5.32; N, 14.52.

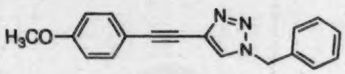

317g

Compound **317g**: Compound **318g**[15] (144 mg, 0.631 mmol), benzyl azide (74.7 mg, 0.561 mmol) were used as per the general procedure J and yielded **317g** (134 mg, 83%) as a white crystalline solid. Mp 159–162 °C. $R_f = 0.3$ (CH_2Cl_2).

IR ($CHCl_3$, cast) 3130, 2962, 2836, 2228 (w), 1504 cm^{-1}; ^1H NMR (400 MHz, $CDCl_3$) δ 7.47 (s, 1H), 7.36–7.26 (m, 5H), 7.19–7.16 (m, 2H), 6.75 (d, $J = 9.0$ Hz, 2H), 5.44 (s, 2H), 3.71 (s, 3H); ^{13}C NMR (100 MHz, $CDCl_3$) δ 159.9, 134.1, 133.0, 131.7, 129.1, 128.8, 128.0, 125.3, 114.3, 113.9, 92.5, 77.0, one signal not observed. EIMS m/z 289.1 (M^+, 33), 261.1 ($[M - N_2]^+$, 17); HRMS calcd. for $C_{18}H_{15}ON_3$ 289.1215, found 289.1218. Anal. calcd. for $C_{18}H_{15}ON_3$: C, 74.72; H, 5.23; N, 14.52. Found: C, 74.54; H, 5.37; N, 14.03.

A single crystal of compound **317g** grown by diffusing hexanes into CH_2Cl_2 at rt. $C_{18}H_{15}N_3O$, M = 289.33, monoclinic group $P2_1$ [No. 14], $Dc = 1.296$ g/cm^3, a = 9.1938(9) Å, b = 5.6198(6) Å, c = 14.7114(14) Å, β = 102.6687(14)°, V = 741.59(13) Å^3, $Z = 2$, $\mu = 0.083$ mm^{-1}, T = –80 °C. Final $R_1(F) = 0.0303$ (2779 observations $[F_o^2 \geq -2\delta(F_o^2)]$), $\omega R_2(F^2) = 0.0792$ for 199 variables and 3025 data with $F_o^2 \geq -3\delta(F_o^2)$. CCDC no. 623596.

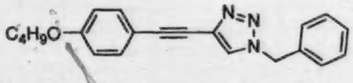

317h

Compound **317h**: Compound **318h**[15] (69 mg, 0.27 mmol), benzyl azide (301 mg, 0.224 mmol) were used as per the general procedure J and yielded **317h** (61 mg, 82%) as a white crystalline solid. Mp 117–119 °C. $R_f = 0.3$ (CH_2Cl_2).

IR ($CHCl_3$, cast) 2958, 2229 (w), 1453 cm^{-1}; ^1H NMR (500 MHz, $CDCl_3$) δ 7.55 (s, 1H), 7.41 (d, *J* = 89 Hz, 2H), 7.7.39–7.34 (m, 3H), 7.26 (dd, *J* = 2.0, 7.1 Hz, 2H), 6.82 (d, *J* = 8.9 Hz, 2H), 5.52 (s, 2H), 3.94 (t, *J* = 6.6 Hz, 2H), 1.74 (app quint, *J* = 7.0 Hz, 2H), 1.47 (sex, *J* = 7.4 Hz, 2H), 0.95 (t, *J* = 7.4 Hz, 3H); ^{13}C NMR (125 MHz, $CDCl_3$) δ 159.6, 134.2, 133.1, 131.8, 129.2, 128.9, 128.1, 125.4, 114.6, 114.1, 92.7, 67.8, 54.3, 31.2, 19.2, 13.8. EIMS *m/z* 331.2 (M^+, 41); HRMS calcd. for $C_{21}H_{21}ON_3$ 331.1685, found 331.1686. Anal. calcd. for $C_{21}H_{21}ON_3$: C, 76.11; H, 6.39; N, 12.68. Found: C, 75.89; H, 6.44; N, 12.55.

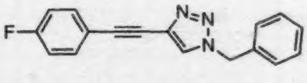

317i

Compound **317i**: Compound **318i** (562 mg, 1.87 mmol), benzyl azide (192 mg, 1.44 mmol) were used as per the general procedure J and yielded **317i** (287 mg, 72%) as a white crystalline solid. Mp 108–110 °C. R_f = 0.3 (CH_2Cl_2).

IR (μscope) 3120, one alkyne peak was not observed, 1503 cm^{-1}; ^1H NMR (500 MHz, $CDCl_3$) δ 7.60 (s, 1H), 7.48–7.45 (m, 2H), 7.36–7.34 (m, 3H), 7.27–7.25 (m, 2H), 7.02–6.98 (m, 2H), 5.52 (s, 2H); ^{13}C NMR (125 MHz, $CDCl_3$) δ 163.7 (d, *J* = 249.9 Hz), 134.1, 133.6 (d, *J* = 8.3 Hz), 131.3, 129.2, 129.0, 128.1, 125.9, 118.4 (d, *J* = 3.4 Hz), 115.7 (s, *J* = 21.9 Hz), 91.5, 78.3, 54.3. EIMS *m/z* 277.1 (M^+, 6), 249.1 ($[M – N_2]^+$, 17); HRMS calcd. for $C_{17}H_{12}N_3F$ 277.1015, found 277.1008. Anal. calcd. for $C_{17}H_{12}N_3F$: C, 73.63; H, 4.36; N, 15.15. Found: C, 73.49; H, 4.34; N, 14.92.

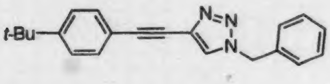

317j

Compound **317j**: Compound **318j**[14] (153 mg, 0.601 mmol), benzyl azide (64.0 mg, 0.481 mmol) were used as per the general procedure J and yielded **317j** (113 mg, 74%) as a white crystalline solid. Mp 153–155 °C. $R_f = 0.4$ (CH_2Cl_2).

IR ($CHCl_3$, cast) 3135, 2962, 2868, 2229 (w), 1457 cm^{-1}; ^{1}H NMR (400 MHz, $CDCl_3$) δ 7.50 (s, 1H), 7.36 (d, J = 8.8 Hz, 2H), 7.33–7.25 (m, 5H), 7.21–7.18 (m, 2H), 5.46 (s, 2H), 1.22 (s, 9H); ^{13}C NMR (100 MHz, $CDCl_3$) δ 152.1, 134.1, 131.7, 131.3, 129.2, 129.0, 128.2, 125.6, 125.4, 119.2, 92.8, 77.8, 54.4, 34.8, 31.1. EIMS *m/z* 315.2 (M^+, 10), 287.2 ($[M - N_2]^+$, 11); HRMS calcd. for $C_{21}H_{21}N_3$ 315.1736, found 315.1730. Anal. calcd. for $C_{21}H_{21}N_3$: C, 79.97; H, 6.71; N, 13.32. Found: C, 79.79; H, 6.87; N, 13.13.

A single crystal was obtained from slow evaporation of a solution of compound **317j** in a solution of $CHCl_3$ at 4 °C. $C_{21}H_{21}N_3$, M = 315.41, monoclinic group $P2_1$ [No. 4], Dc = 1.221 g/cm^{-3}, $a = 5.7566(11)$ Å, $b = 7{,}9092(15)$ Å, $c = 18.846(4)$ Å, $\beta = 90.312(3)^\circ$, V = 858.1(3) Å^3, $Z = 2$, $\mu = 0.073$ mm^{-1}, T = –80 °C. Final $R_1(F) = 0.0532$ (2805 observations $[F_o^2 \geq -2\delta(F_o^2)]$), $\omega R_2(F^2) = 0.1431$ for 325 variables and 3498 data with $F_o^2 \geq -3\delta(F_o^2)$.

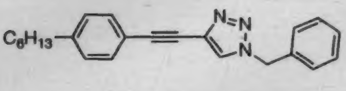

317k

Compound **317k**: Compound **318k**[14] (126 mg, 0.445 mmol), benzyl azide (53.3 mg, 0.400 mmol) were used as per the general procedure J and yielded **317k** (99.7 mg, 73%) as a white solid. Mp 84–86 °C. $R_f = 0.4$ (CH_2Cl_2).

IR ($CHCl_3$, cast) 3099, 2923, 1453, (one alkyne peak not observed) cm^{-1}; ^{1}H NMR (500 MHz, $CDCl_3$) δ 7.56 (s, 1H), 7.40 (d, J = 8.2 Hz, 2H), 7.39–7.32 (m, 3H), 7.26 (dd, J = 2.0, 7.0 Hz, 2H), 7.12 (d, J = 8.1 Hz, 2H), 5.53 (s, 2H), 2.58 (t, J = 7.7 Hz, 2H), 1.58 (app quint, J = 7.2 Hz, 2H), 1.28 (s, 6H), 0.86 (t, J = 6.6, 3H); ^{13}C NMR (125 MHz, $CDCl_3$) δ

144.0, 134.1, 131.7, 131.5, 129.2, 129.0, 128.5, 128.2, 125.6, 119.4, 92.9, 77.8, 54.4, 35.9, 31.7, 31.1, 28.9, 22.6. EIS *m/z* HRMS calcd. for $C_{23}H_{25}N_3$ 344.2121, found 344.2122 (M + H) Anal. calcd. for $C_{23}H_{25}N_3$: C, 80.43; H, 7.34; N, 12.23. Found: C, 80.23; H, 7.39; N, 12.07.

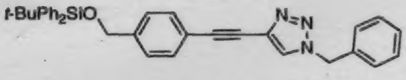

317l

Compound **317l**: Compound **318l** (115 mg, 0.246 mmol), benzyl azide (33.0 mg, 0.248 mmol) were used as per the general procedure J and yielded **317l** (93 mg, 71%) as a white crystalline solid. Mp 134–136 °C. $R_f = 0.4$ (CH_2Cl_2).

IR ($CHCl_3$, cast) 2958, 2892, 2857, 2230 (w) cm^{-1}; ^1H NMR (300 MHz, $CDCl_3$) δ 7.64–7.60 (m, 4H), 7.54 (s, 1H), 7.44–7.23 (m, 15H), 5.50 (s, 2H), 4.71 (s, 2H), 1.04 (s, 9H); ^{13}C NMR (100 MHz, $CDCl_3$) δ 142.0, 135.5, 134.1, 133.3, 131.5, 129.7, 129.2, 129.0, 128.1, 127.7, 125.9, 125.7, 120.7, 92.7, 78.0, 65.2, 54.4, 32.1, 26.8, 19.3. EIMS *m/z* 470.2 ($[M - t\text{–}Bu]^+$, 54); HRMS calcd. for $C_{30}H_{24}SiON_3$ 470.1689, found 470.1689. Anal. calcd. for $C_{34}H_{33}OSiN_3$: C, 77.38; H, 6.30; N, 7.96. Found: C, 77.39; H, 6.57; N, 7.92.

A single crystal was obtained from slow evaporation from a solution of compound **317l** in $CHCl_3$ at 4 °C. $C_{34}H_{33}N_3OSi$, M = 527.72, monoclinic group C_c (No. 9), $Dc = 1.169$ g/cm^{-3}, $a = 45.300(8)$ Å, $b = 10.1710(17)$ Å, $c = 13.213(2)$ Å, $\beta = 99.865(5)^\circ$, $V = 5998.0(17)$ Å^3, $Z = 8$, $\mu = 0.108\ mm^{-1}$, T = –80 °C. Final $R_1(F) = 0.0436$ (5665 observations $[F_o^2 \geq -2\delta(F_o^2)]$), $\omega R_2(F^2) = 0.0956$ for 704 variables and 8809 data with $F_o^2 \geq -3\delta(F_o^2)$.

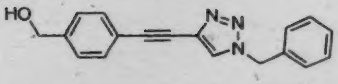

317m

Compound **317m**: Compound **318m** (129 mg, 0.276 mmol), benzyl azide (36.2 mg, 0.272 mmol) were used as per the general procedure J and yielded **317m** (69 mg, 86%) as a white crystalline solid. Mp 125–127 °C. R_f = 0.4 (CH_2Cl_2).

IR ($CHCl_3$, cast) 3191, 3121, 2203 (w), 1452 cm^{-1}; ^{1}H NMR (300 MHz, CDC13) δ 7.58 (s, 1H), 7.48 (d, *J* = 8.2 Hz, 2H), 7.40–7.25 (m, 7H), 5.53 (s, 2H), 4.69 (s, 2H), 1.80 (br s, 1H); ^{13}C NMR (100 MHz, CDC13) δ 141.5, 134.0, 131.7, 129.1, 128.9, 128.1, 126.7, 125.7, 121.4, 92.3, 78.4, 64.8, 54.3. ESMS *m/z* HRMS calcd. for $C_{18}H_{15}ON_3$ 290.1288, found 290.1288.

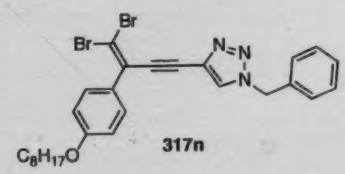

317n

Compound **317n**: Compound **318n** (257 mg, 0.504 mmol), benzyl azide (59.7 mg, 0.448 mmol) were used as per the general procedure J and yielded **317n** (167 mg, 65%) as a yellow solid. Mp 42–44 °C. R_f = 0.4 (CH_2Cl_2).

IR ($CHCl_3$, cast) 2927, 2855, 2219 (w), 1457 cm^{-1}; ^{1}H NMR (400 MHz, $CDCl_3$) δ 7.56 (s, 1H), 7.39–7.33 (m, 5H), 7.25–7.22 (m, 2H), 6.85 (d, *J* = 8.8 Hz, 2H), 5.49 (s, 2H), 3.93 (t, *J* = 6.6 Hz, 2H), 1.76 (app quint, *J* = 7.0 Hz, 2H), 1.47–1.38 (m, 2H), 1.32–1.27 (m, 8H), 0.87 (t, *J* = 6.8 Hz, 3H); ^{13}C NMR (100 MHz, $CDCl_3$) δ 159.3, 133.9, 130.8, 129.9, 129.8(9), 129.3, 129.1, 128.9, 128.1, 126.1, 114.2, 99.1, 91.8, 86.1, 68.0, 54.3, 31.7, 29.2, 29.1, 29.1(0), 25.9, 22.6, 14.0, (one signal not observed). EIMS *m/z* 571.1 (M^+, 15), 464.1 ($[M - N_2]^+$, 79); HRMS calcd. for $C_{27}H_{29}ON_3{}^{79}Br^{81}Br$ 571.0657, found

571.0660. Anal. calcd. for $C_{27}H_{29}ON_3Br_2$: C, 56.76; H, 5.12; N, 7.35. Found: C, 56.83; H, 5.38; N, 7.08.

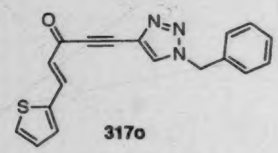
317o

Compound **317o**: Compound **318o** (120 mg, 0.464 mmol), benzyl azide (53.3 mg, 0.400 mmol) were used as per the general procedure J and yielded **317o** (66 mg, 5%) as a brown oil. $R_f = 0.6$ (CH_2Cl_2/EtOAc 9:1).

IR ($CHCl_3$, cast) 2916 (w), 2219, 1613 cm^{-1}; ^{1}H NMR (300 MHz, $CDCl_3$) δ 8.03 (d, J = 15.8 Hz, 1H), 7.77 (s, 1H), 7.47 (d, J = 5.1 Hz, 1H), 7.41–7.36 (m, 3H), 7.29–7.26 (m, 3H), 7.09 (dd, J = 5.0, 3.7 Hz, 1H), 6.63 (d, J = 15.8 Hz, 1H), 5.56 (s, 2H); ^{13}C NMR (125 MHz, $CDCl_3$) δ 176.8, 141.2, 139.3, 133.6, 132.9, 130.5, 129.4, 129.2, 129.0, 128.8, 128.6, 128.2, 126.9, 89.9, 80.3, 54.6. ES HRMS calcd. for $C_{18}H_{13}OSN_3Na$ ([M + Na)$^+$] 342.0672, found 342.0674.

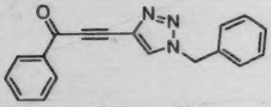
317p

Compound **317p**: Compound **318p**[16] (33.7 mg, 0.149 mmol), benzyl azide (26.0 mg, 0.200 mmol) were used as per the general procedure J and yielded **317p** (28.9 mg, 68%) as a light yellow crystalline solid. Mp 100–103 °C. $R_f = 0.2$ (CH_2Cl_2).

IR ($CHCl_3$, cast) 3135(w), 2209, 1639 cm^{-1}; ^{1}H NMR (300 MHz, $CDCl_3$) δ 8.20 (d, J = 7.0 Hz, 2H), 7.81 (s, 1H), 7.61 (t, J = 7.4 Hz, 1H), 7.49 (t, J = 7.6 Hz, 2H), 7.41–7.36 (m, 3H), 7.31–7.27 (m, 2H), 5.57 (s, 2H); ^{13}C NMR (100 MHz, $CDCl_3$) δ 177.5, 136.3, 134.4, 133.5, 129.7, 129.4, 129.3, 129.0, 128.9, 128.7, 128.3, 90.3, 82.1, 54.6. EIMS *m/z*

287.1 (M$^+$, 1), 259.1 ([M – N_2]$^+$, 3); HRMS calcd. for $C_{18}H_{13}ON_3$ 287.1059, found 287.1059. Anal. calcd. for $C_{18}H_{13}ON_3$: C, 75.25; H, 4.56; N, 14.63. Found: C, 75.00; H, 4.60; N, 14.34.

A single crystal of compound **317p** was obtained from a slow diffusion of hexanes into a solution of compound **317p** in hexanes/CH_2Cl_2 at rt. $C_{18}H_{13}N_3O$, M = 287.31, triclinic group $P\bar{1}$ (No. 2), Dc = 1.292 g/cm^{-3}, a = 7.8486(8) Å, b = 8.8827(9) Å, c = 12.1321(13) Å, α = 70.6508 (19)°, β = 79.5467(19)°, γ = 68.0695(19)°, V = 738.68(13) Å^3, Z = 2, μ = 0.083 mm^{-1}, T = –80 °C. Final $R_1(F)$ = 0.0428 (1724 observations [$F_o^2 \geq -2\delta(F_o^2)$]), $\omega R_2(F^2)$ = 0.1208 for 199 variables and 2608 data with $F_o^2 \geq -3\delta(F_o^2)$

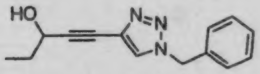

317q

Compound **317q**: Compound **318q** (92.6 mg, 0.350 mmol), benzyl azide (37.3 mg, 0.280 mmol) were used as per the general procedure J and yielded **317q** (31 mg, 46%) as light yellow solid. Mp 44–46 °C. R_f = 0.2 (CH_2Cl_2/EtOAc 6:1).

IR ($CHCl_3$, μscope) 3360, 3138, 2967, 2932, 2240 (w) cm^{-1}; ^{1}H NMR (300 MHz, $CDCl_3$) δ 7.50 (s, 1H), 7.38–7.33 (m, 3H), 7.26–7.22 (m, 2H), 5.49 (s, 2H), 4.50 (t, J = 6.4 Hz, 1H), 2.12 (br s, 1H), 1.78 (qd, J = 7.4 Hz, 6.4 Hz, 2H), 1.02 (t, J = 7.4 Hz, 3H); ^{13}C NMR (100 MHz, $CDCl_3$) δ 134.0, 130.8, 129.2, 129.0, 128.1, 125.9, 93.8, 74.2, 64.0, 54.3, 30.6, 9.5. EIMS m/z 241.1 (M$^+$, 7); HRMS calcd. for $C_{14}H_{15}ON_3$ 241.1215, found 241.1220. Anal. calcd. for $C_{14}H_{15}ON_3$: C, 69.69; H, 6.27; N, 17.41. Found: C, 69.57; H, 6.29; N, 17.08.

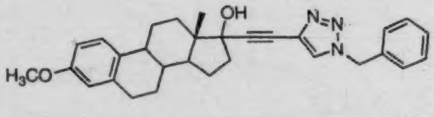

317r

Compound **317r**: Compound **318r** (127 mg, 0.258 mmol), benzyl azide (30.9 mg, 0.232 mmol) were used as per the general procedure J and yielded **317r** (81.6 mg, 75%) as a white solid. Mp 173–175 °C. $R_f = 0.6$ (CH_2Cl_2/EtOAc 3:1).

IR ($CHCl_3$, μscope) 3378, 2933, 2237 (w), 1455 cm^{-1}; ^{1}H NMR (400 MHz, $CDCl_3$) δ 7.53 (s, 1H), 7.37–7.33 (m, 3H), 7.25–7.23 (m, 2H), 7.17 (d, *J* = 8.6 Hz, 1H), 6.69 (dd, *J* = 2.7, 8.6 Hz, 1H), 6.61 (d, 2.7 Hz, 1H), 2.82–2.81 (m, 2H), 2.48 (br s, 1H), 2.40 (qd, *J* = 5.4, 13.8 Hz, 1H), 2.33 (dq, *J* = 13.5, 2.9 Hz, 1H), 2.20 (dt, *J* = 4.0, 11.5 Hz, 1H), 2.06 (ddd, *J* = 3.2, 12.4, 16.8, 1H), 1.92 (dt, *J* = 4.1, 12.9 Hz, 1H), 1.85 (dquint, *J* = 2.7, 12.3 Hz, 1H), 1.79–1.75 (m, 2H), 1.71 (dd, *J* = 7.5, 12.2, 1H), 1.53–1.29 (m, 4H); ^{13}C NMR (100 MHz, $CDCl_3$) δ 157.3, 137.9, 134.0, 132.5, 131.0, 129.1, 128.9, 128.1, 126.3, 125.8, 113.7, 111.4, 96.4, 80.3, 75.3, 55.1, 54.2, 49.6, 47.5, 43.3, 39.4, 38.8, 33.0, 29.8, 27.1, 26.4, 22.9, 12.8. EIMS *m/z* 467.3 (M$^+$, 10); HRMS calcd. for $C_{30}H_{33}O_2N_3$ 467.2573, found 467.2578. Anal. calcd. for $C_{30}H_{33}O_2N_3$: C, 77.06; H, 7.11; N, 8.99. Found: C, 76.90; H, 7.19; N, 8.78.

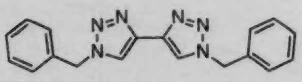

319

Compound **319**: Compound **215** (169 mg, 0.675 mmol), benzyl azide (89.5 mg, 0.672 mmol) were used as per the general procedure J and yielded **319** (86 mg, 41%) as a white powder. Mp 224–227 °C.

IR ($CHCl_3$, cast) 3075, 1458 cm^{-1}; ^{1}H NMR (300 MHz, $CDCl_3$) δ 7.98 (s, 2H), 7.38–7.33 (m, 6H), 7.29– 7.26 (m, 4H), 5.54 (s, 4H); ^{13}C NMR (100 MHz, $CDCl_3$) δ 134.3, 129.2, 128.9, 128.2, 54.5, (two signals not observed). ES HRMS calcd. for $C_{18}H_{17}N_6$ ([M + H]) 317.1509, found 317.1509.

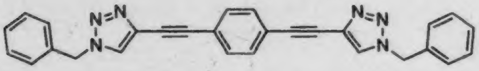

320

Compound **320**: Compound **323**[17] (188 mg, 0.591 mmol), benzyl azide (170 mg, 0.160 mmol) were used as per the general procedure J and yielded **320** (206 mg, 79%) as an orange insoluble powder. Mp > 200 °C. R_f could not be obtained.

IR ($CHCl_3$, cast) 3036, 2924, 2853, 1958, 1814, 1479 cm^{-1}; ^1H NMR (500 MHz, CD_2Cl_2) δ 7.69 (s, 2H), 7.51 (s, 4H), 7.40–7.38 (m, 6H), 7.30 (d, $J = 7.5$ Hz, 4H), 5.55 (s, 4H); ^{13}C NMR could not be obtained due to its low solubility. EIMS *m/z* 440.2 (M^+, 7), 384.2 ($[M - N_4]^+$, 7); HRMS calcd. for $C_{28}H_{20}N_6$ 440.1750, found 440.1743.

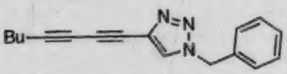

324a

Compound **324a**: Compound **325a** (96.5 mg, 0.337 mmol), benzyl azide (40.5 mg, 0.304 mmol) were used as per the general procedure J and yielded **324a** (64.0 mg, 80%) as a colorless oil. $R_f = 0.4$ (CH_2Cl_2).

IR ($CHCl_3$, cast) 3139, 2958, 2872, 2246 cm^{-1}; ^1H NMR (400 MHz, $CDCl_3$) δ 7.53 (s, 1H), 7.37–7.33 (m, 3H), 7.25–7.22 (m, 2H), 5.49 (s, 2H), 2.32 (t, $J = 7.0$ Hz, 2H), 1.56–1.48 (m, 2H), 1.46–1.36 (m, 2H), 0.89 (t, $J = 7.3$ Hz, 3H); ^{13}C NMR (100 MHz, $CDCl_3$) δ 133.9, 130.6, 129.2, 129.0, 128.1, 127.0, 86.0, 78.0, 64.6, 63.5, 54.4, 30.1, 21.9, 19.2, 13.5. EIMS *m/z* 263.1 (M^+, 4), 235.1 ($[M - N_2]^+$, 12); HRMS calcd. for $C_{17}H_{17}N_3$ 263.1422, found 263.1419.

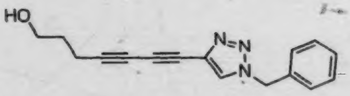

324b

Compound **324b**: Compound **325b**[18] (123 mg, 0.233 mmol), benzyl azide (0.266 mg, 0.200 mmol) were used as per the general procedure J and yielded **324b** (24.8 mg, 47%) as a white crystalline solid. Mp 70–73 °C. R_f = 0.5 (CH_2Cl_2/EtOAc 2:1).

IR ($CHCl_3$, μscope) 3380, 3140, 2951, 2246, 2162(w) cm^{-1}; ^1H NMR (300 MHz, $CDCl_3$) δ 7.53 (s, 1H), 7.37–7.34 (m, 3H), 7.26–7.22 (m, 2H), 5.50 (s, 2H), 3.74 (t, J = 6.1 Hz, 2H), 2.47 (t, J = 7.0 Hz, 2H), 1.80 (tt, J = 7.0 Hz, 6.1 Hz, 2H), 1.54 (br s, 1H); ^{13}C NMR (125 MHz, $CDCl_3$) δ 134.8, 130.5, 129.2, 129.0, 128.1, 127.1, 85.0, 77.8, 65.0, 63.8, 61.3, 54.4, 30.8, 16.1. EIMS m/z 265.1 (M^+, 4); HRMS calcd. for $C_{16}H_{15}ON_3$ 265.1215, found 265.1209.

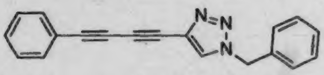

324c

Compound **324c**: Compound **325c**[19] (171 mg, 0.769 mmol), benzyl azide (74.7 mg, 0.561 mmol) were used as per the general procedure J and yielded **324c** (0.108 mg, 68%) as a light yellow crystalline solid. Mp 114–116 °C. R_f = 0.5 (CH_2Cl_2).

IR ($CHCl_3$, μscope) 3140, 3034, 2225(w), 2157 cm^{-1}; ^1H NMR (300 MHz, $CDCl_3$) δ 7.30(s, 1H), 7.22–7.18 (m, 2H), 7.09–6.94 (m, 8H), 5.22 (s, 2H); ^{13}C NMR (100 MHz, $CDCl_3$) δ 133.8, 132.6, 130.4, 129.5, 129.3, 129.1, 128.4, 128.2, 127.3, 121.3, 82.5, 77.4, 73.3, 70.3, 54.4. EIMS m/z 283.1 (M^+, 10), 255.1 ($[M - N_2]^+$, 39); HRMS calcd. for $C_{19}H_{13}N_3$ 283.1110, found 283.1110. Anal. calcd. for $C_{19}H_{13}N_3$: C, 80.54; H, 4.62; N, 14.83. Found: C, 80.40; H, 4.76; N, 14.51.

A single crystal of compound **324c** were grown by diffusing hexanes into CH_2Cl_2 at rt. $C_{19}H_{13}N_3$, M = 283.32, triclinic group $P\bar{1}$ (No. 2), $Dc = 1.260$ g/cm^{-3}, $a = 6.3632(8)$ Å, $b = 7.9519(9)$ Å, $c = 15.1874(18)$ Å, $\alpha = 102.3564(18)^\circ$, $\beta = 95.3363(18)^\circ$, $\gamma = 91.0645(18)^\circ$, $V = 746.84(15)$ Å^3, $Z = 2$, $\mu = 0.076$ mm^{-1}, T = –80 °C. Final $R_1(F) = 0.436$ (2130 observations $[F_o^2 \geq -2\delta(F_o^2)]$), $\omega R_2(F^2) = 0.1274$ for 199 variables and 3013 data with $F_o^2 \geq -3\delta(F_o^2)$. CCDC no. 623597.

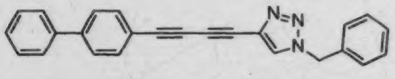

324d

Compound **324d**: Compound **325d** (87.3 mg, 0.228 mmol), benzyl azide (21.4 mg, 0.161 mmol) were used as per the general procedure J and yielded **324d** (36.3 mg, 63%) as a brown crystalline solid. Mp 172–175 °C. $R_f = 0.4$ (CH_2Cl_2).

IR ($CHCl_3$, cast) 3112, 2223 (w), 2158 (w) cm^{-1}; ^{1}H NMR (400 MHz, $CDCl_3$) δ 7.56 (s, 1H), 7.54–7.49 (m, 6H), 7.38 (t, $J = 7.5$ Hz, 2H), 7.34–728 (m, 4H), 7.23 –7.20 (m, 2H), 5.48 (s, 2H); ^{13}C NMR (100 MHz, $CDCl_3$) δ 142.1, 139.9, 133.7, 132.9, 130.4, 129.2, 129.0, 128.8, 128.1, 127.8, 127.2, 127.0, 126.9, 120.0, 82.4, 77.4, 73.8, 70.5, 54.3. EIMS *m/z* 359.1 (M^+, 14), 331.1 ($[M - N_2]^+$, 57); HRMS calcd. for $C_{25}H_{17}N_3$ 359.1422, found 359.1427.

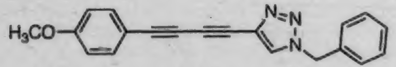

324e

Compound **324e**: Compound **325e**[16] (123 mg, 0.487 mmol), benzyl azide (0.0427 mg, 0.321 mmol) were used as per the general procedure J and yielded **324e** (0.83.4 mg, 83%) as a yellow crystalline solid. Mp 161–163 °C. $R_f = 0.4$ (CH_2Cl_2).

IR ($CHCl_3$, μscope) 3116, 2222 (w), 2154 (w), 1604 cm^{-1}; ^{1}H NMR (300 MHz, $CDCl_3$) δ 7.58 (s, 1H), 7.44 (d, J = 8.0 Hz, 2H), 7.40–7.35 (m, 3H), 7.27–7.24 (m, 3H), 6.83 (d, J = 9.0 Hz, 2H), 3.80 (s, 3H); ^{13}C NMR (100 MHz, $CDCl_3$) δ 160.5, 134.2, 133.8, 130.5, 129.2, 129.0, 128.1, 127.0, 114.1, 113.1, 82.7, 77.6, 72.1, 69.7, 55.3, 54.3. EIMS *m/z* 313.1 (M^+, 27), 285.1 ($[M - N_2]^+$, 45); HRMS calcd. for $C_{20}H_{15}ON_3$ 313.1215, found 313.1212. Anal. calcd. for $C_{20}H_{15}ON_3$: C, 76.66; H, 4.82; N, 13.41. Found: C, 76.27; H, 4.88; N, 13.00.

A single crystal of compound **324e** was obtained from slow evaporation of a solution of compound **324e** in $CDCl_3$ at 4 °C. $C_{20}H_{15}N_3O$, M = 313.35, monoclinic group $P2_1$ (No. 4), Dc = 1.281 g/cm^{-3}, a = 10.7789(10) Å, b = 5.6104(5) Å, c = 14.1828(13) Å, β = 108.6532(13)°, V = 812.64(13) Å^3, Z = 2, μ = 0.081 mm^{-1}, T = –80 °C. Final $R_1(F)$ = 0.0306 (3069 observations [$F_o^2 \geq -2\delta(F_o^2)$]), $\omega R_2(F^2)$ = 0.0817 for 218 variables and 3302 data with $F_o^2 \geq -3\delta(F_o^2)$.

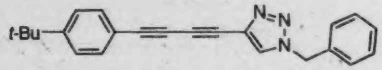

324f

Compound 324f: Compound **325f**[19] (155 mg, 0.555 mmol), benzyl azide (0.0534 mg, 0.401 mmol) were used as per the general procedure J and yielded **324f** (99.5 mg, 73%) as a yellow crystalline solid. Mp 170–173 °C. R_f = 0.4 (CH_2Cl_2).

IR ($CHCl_3$, μscope) 3142, 2924, 2224 (w) cm^{-1}; ^{1}H NMR (500 MHz, $CDCl_3$) δ 7.54 (s, 1H), 7.39 (t, J = 8.4 Hz, 2H), 7.33–7.28 (m, 5H), 7.22–7.20 (m, 2H), 5.48 (s, 2H), 1.25 (s, 9H); ^{13}C NMR (125 MHz, $CDCl_3$) δ 153.0, 133.9, 132.4, 130.6, 129.3, 129.1, 128.2, 127.2, 125.5, 118.2, 82.8, 77.7, 72.7, 69.9, 54.4, 34.9, 31.1. EIMS *m/z* 339.2 (M^+, 30), 311.2 ($[M - N_2]^+$, 79); HRMS calcd. for $C_{23}H_{21}N_3$ 339.1736, found 339.1743.

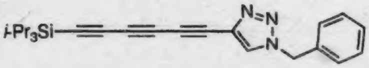

326a

Compound **326a**: Compound **327a**[10] (171 mg, 0.524 mmol), benzyl azide (0.0550 mL, 0.440 mmol) were used as per the general procedure J and yielded **326a** (68.7 mg, 40%) as a colorless oil. $R_f = 0.5$ (CH_2Cl_2).

IR ($CHCl_3$, cast) 3139, 2945, 2866, 2207, 2077, 1497 cm^{-1}; ^{1}H NMR (400 MHz, $CDCl_3$) δ 7.65 (s, 1H), 7.39–7.37 (m, 3H), 7.28–7.26 (m, 2H), 5.53 (s, 2H), 1.09 (s, 21H); ^{13}C NMR (100 MHz, $CDCl_3$) δ 133.6, 129.6, 129.2, 129.0, 128.2, 128.1, 89.3, 87.6, 77.8, 68.2, 65.2, 59.7, 54.4, 18.4, 11.2. EIMS *m/z* 359.2 ($[M - N_2]^+$, 100); HRMS calcd. for $C_{24}H_{29}NSi$ (M^+) 359.2069, found 359.2078.

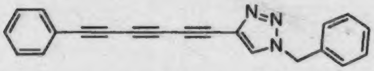

326b

Compound **326b**: Compound **327b**[19] (157 mg, 0.637 mmol), benzyl azide (74.7 mg, 0.561 mmol) were used as per the general procedure J and yielded **326b** (42.7 mg, 25%) as a yellow crystalline solid. Mp 133–135 °C. $R_f = 0.5$ (CH_2Cl_2).

IR ($CHCl_3$, cast) 3141, 2919, 2201 cm^{-1}; ^{1}H NMR (400 MHz, $CDCl_3$) δ 7.62 (s, 1H), 7.51 (d, $J = 6.9$ Hz, 2H), 7.40–7.36 (m, 4H), 7.31 (t, $J = 7.2$ Hz, 2H), 7.27–7.24 (m, 2H), 5.52 (s, 2H); ^{13}C NMR (100 MHz, $CDCl_3$) δ 133.6, 132.9, 129.8, 129.7, 129.2, 129.0, 128.4, 128.1, 120.5, 79.2, 77.9, 74.0, 67.5, 67.3, 65.6, 54.4. EIMS *m/z* 307.1 (M^+, 8), 279.1 ($[M - N_2]^+$, 67); HRMS calcd. for $C_{21}H_{13}N_3$ 307.1110, found 307.1113.

A single crystal of compound **326b** was obtained from a slow evaporation of compound **326b** in CH_2Cl_2 at 0 °C. $C_{21}H_{13}N_3$, M = 307.34, orthorohombic group *Pca*2$_1$ (No. 29), *D*c = 1.263 g/cm^{-3}, $a = 10.8926(10)$ Å, $b = 20.0670(19)$ Å, $c = 7.3933(7)$ Å, $V = 616.0(3)$ Å^3,

$Z = 4$, $\mu = 0.076$ mm^{-1}, T = –80 °C. Final $R_1(F) = 0.0332$ (1621 observations $[F_o^2 \geq -2\delta(F_o^2)]$), $\omega R_2(F^2) = 0.1070$ for 217 variables and 1796 data with $F_o^2 \geq -3\delta(F_o^2)$.

Trapping Diynone 317p with BnN_3 from *Chrysanthemum coronarium*

Fresh roots (50.8 g) and aerial and flower parts (527.6 g) were ground separately. To the roots were added Et_2O (500 mL), hexanes (500 mL), benzene (50 mL) and H_2O (500 mL). The reaction mixture was stirred at rt for 10 h. The organic phase was separated whereas the aqueous phase was extracted with Et_2O (3 x 200 mL). Two organic solutions were combined and washed with satd. aq. NH_4Cl (2 x 200 mL), satd. aq. NaCl (2 x 200 mL), and dried over $MgSO_4$. The resulting solution was filtered.

To the aerial and flower parts were added to Et_2O (1000 mL), hexanes (1000 mL), benzene (20 mL) and H_2O (1000 mL). The reaction mixture was stirred at rt for 10 h. The organic phase was separated whereas the aqueous phase was extracted with Et_2O (3 x 300 mL). Two organic solutions were combined and washed with satd. aq. NH_4Cl (2 x 300 mL), satd. aq. NaCl (2 x 300 mL), and dried over $MgSO_4$. The resulting solution was filtered.

The two organic solutions (the root extract and the aerial and flower extract) were combined and added to DMF (10 mL). The mixture was concentrated to ca. 8–10 mL. To the resulting solution was added DMF (5 mL), ascorbic acid (0.1 g), $CuSO_4 \cdot 5H_2O$ (0.1 g), BnN_3 (1.6 m L) and H_2O (5 mL) in sequence. This was allowed to stir at rt for 12 h, followed by an aqueous workup, solvent removal, and purification via column chromatography (solvent, silica gel). Fractions were spotted against synthetic **317p**.

Fractions containing compounds with similar R_f to that of compound **317p** were collected.

8.3.3 Chapter 4

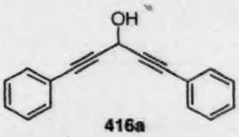
416a

Compound **416a**: Phenylacetylene (0.93 g, 9.1 mmol) in THF (46 mL) at –78 °C and BuLi (2.5 M in hexanes, 3.5 mL, 8.8 mmol) were used as per the general procedure C and yielded **416a** (1.69 g, 80%) as a colorless oil. Spectral data are consistent with those reported previously.[20]

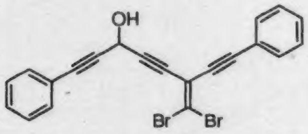
416b

Compound **416b**: terminal alkyne **415b** (2.17 g, 7.00 mmol), LDA [BuLi (2.5 M in hexanes, 4.2 mL, 11 mmol) and diisopropylamine (1.5 mL, 11 mmol) were used as per the general procedure I] and ketone **414** used as per the general procedure C and yielded **416b** (1.11 g, 36%). Compound **416b** was not fully characterized because the desired product could not be obtained pure. This alcohol was carried to the next reaction.

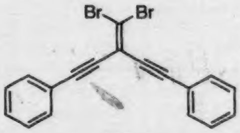
417a

Compound **417a** was synthesized by Diederich; See: Diederich, F.; Philp, D.; Seiler, S. *J. Chem. Soc., Chem. Commun.* **1994**, 205–208.

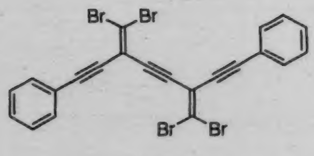

417b

Compound **417b**: Alcohol **416b** (1.11 g, 2.52 mmol) in CH_2Cl_2 (25 mL) and $BaMnO_4$ (1.29 g, 5.04 mmol) were used as per the general procedure D and yielded the desired ketone R_f = 0.7 (hexanes/CH_2Cl_2 1:1). This ketone was carried to the next reaction without further characterization.

CBr_4 (1.26 g, 3.80 mmol), PPh_3 (1.99 g, 7.59 mmol) in CH_2Cl_2 (25 mL) and the ketone above) were used as per the general procedure E and yielded **417b** (0.98 g, 65%) as a yellow crystalline solid. Mp 126–129 °C. R_f = 0.5 (hexanes/CH_2Cl_2 3:1).

IR (CH_2Cl_2, cast) 2055 (w), 2203, 1487 cm^{-1}; ^1H NMR (500 MHz, $CDCl_3$) δ 7.52 (d, J = 8.0 Hz, 4H), 7.39–7.31 (m, 6H); ^{13}C NMR (125 MHz, $CDCl_3$) δ 131.7, 129.3, 128.5, 122.0, 113.8, 109.6, 96.5, 91.4, 85.3. EIMS *m/z* 593.7 (M^+, 58); HRMS calcd. for $C_{22}H_{10}{}^{79}Br_2{}^{81}Br_2$ (M^+) 593.7475, found 593.7474.

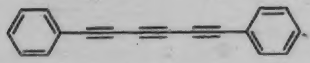

409

Compound **409**: **417a** (1.30 g, 3.36 mmol) in toluene (3 mL) at –78 °C and BuLi (2.5 M in hexanes, 1.6 mL, 4.0 mmol) were used as per the general procedure E and yielded **409** (601 mg, 79%) as white crystalline solid. Spectral data were consistent with those reported previously.[3]

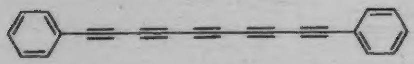

411

Compound **411**: Compound **417b** (897 mg, 1.51 mmol) in toluene (25 mL) at –78 °C and

BuLi (2.5 M in hexanes, 1.8 mL, 4.5 mmol) were used as per the general procedure E and yielded **411** (207 mg, 50%) as yellow crystalline solid. DSC shows a decomposition at 172 °C. Spectral data were consistent with those reported previously.[3]

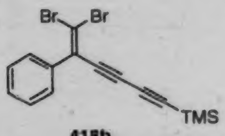

418b

Compound **418b**: Benzoyl chloride (0.36 mg, 2.57 mmol) in CH_2Cl_2 (25 mL), bis(trimethylsilyl)butadiyne (500 mg, 2.57 mmol) at –20 °C and $AlCl_3$ (**511** mg, 3.85 mmol) were used as per the general procedure G and afford the intermediate ketone which was used without further characterization.

CBr_4 (1.71 g, 5.16 mmol), PPh_3 (2.70 g, 10.3 mmol) in CH_2Cl_2 (50 mL) at 0 °C and the ketone above were used as per the general procedure E and afford **418b** (753 mg, 77%) as an off–white solid. Mp 85–87 °C. R_f = 0.7 (hexanes/CH_2Cl_2 6:1).

IR ($CHCl_3$, cast) 2959, 2195, 2094, 1251 cm^{-1}; ^{1}H NMR (400 MHz, $CDCl_3$) δ 7.38–7.33 (m, 5H), 0.18 (s, 9H); ^{13}C NMR (125 MHz, $CDCl_3$) δ 137.2, 130.0, 128.8, 128.51, 128.49, 102.7, 95.4, 87.3, 82.2, 74.9, –0.6; HRMS calcd. for $C_{15}H_{14}{}^{79}Br^{81}BrSi$ (M^+) 381.9211, found 381.9212. Anal. calcd. for $C_{15}H_{14}Br_2Si$: C, 47.14; H, 3.69. Found: C, 47.00; H, 3.30.

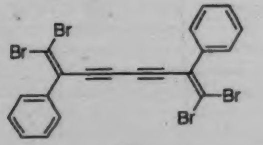

419a

Compound **419a**: Terminal alkyne (397 mg, 1.39 mmol), CuCl (15 mg, 0.15 mmol) in CH_2Cl_2 (10 mL) and TMEDA (1 mL) were used as per the general procedure A and afforded **419a** (382 mg, 97%) as a white crystalline solid. Mp 158–160 °C. R_f = 0.4

(Hexanes/CH_2Cl_2 6:1).

IR (CH_2Cl_2, cast) 3075 (w), 1955 (w), 1533 cm^{-1}; ^{1}H NMR (300 MHz, $CDCl_3$) δ 7.38–7.34 (m, 10H); ^{13}C NMR (125 MHz, $CDCl_3$) δ 137.0, 130.1, 128.9, 128.6, 128.5, 103.0, 83.6, 81.4. EIMS *m/z* 569.7 (M^+, 4), 250.1 ($[M - 4Br]^+$, 100); HRMS calcd. for $C_{20}H_{10}{}^{79}Br_2{}^{81}Br_2$ (M^+) 569.7475, found 569.7481. Anal. calcd. for $c_{20}H_{10}Br_4$; C, 42.15; H, 1.77. Found: C, 42.35; H, 1.81.

Compound **419b** was reported and named as **601a** in Chapter 6.

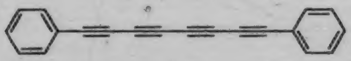

410

Compound **410**: **419a** (336 mg, 0.590 mmol) in toluene (6 mL) at –78 °C and BuLi (2.5 M in hexanes, 0.52 mL, 1.3 mmol) were used as per the general procedure E and afforded **410** (78.9 mg, 53%) as a yellow crystalline solid. DSC was measured. The spectral data were consistent with those reported.[19]

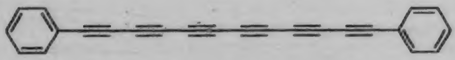

412a

Compound **412a**: Compound **419b** (81.6 mg, 0.132 mmol) in toluene (3 mL) at 0 °C and BuLi (2.5 M in hexanes, 0.12 mL, 0.3 mmol) were used as per general procedure E. A small amount of compound **412a** was detected on TLC.

Compounds **420a,b 421a,b**, **412a** and **413** were synthesized previously.[19]

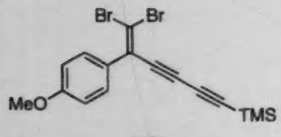

422b

Compound **422b**: To 3–methoxylbenzoic acid (2.00 g, 13.2 mmol) was added $SOCl_2$ (2.35 g, 19.7 mmol) and the reaction was stirred at rt overnight affording the acid chloride as per general procedure G. To the acid chloride in CH_2Cl_2 (130 mL), bis(trimethylsilyl)butadiyne (2.60 g, 13.4 mmol) at –20 °C and $AlCl_3$ (2.63 g, 19.7 mmol) were used as per general procedure E yielding ketone ($R_f = 0.3$, hexanes/CH_2Cl_2 1:1) that was carried on without further purification.

CBr_4 (15.9 g, 47.9 mmol), PPh_3 (25.1 g, 95.7 mmol), Et_3N (1.67 mL) in CH_2Cl_2 (260 mL) at 0 °C and the ketone above were used per as per general procedure E yielding **422b** (1.75 g, 33%) as an off–white solid. Mp 72–74 °C. $R_f = 0.6$ (hexanes/CH_2Cl_2 1:1). IR ($CHCl_3$, cast) 3002, 2958, 2194, 2092, 1606, 1575 cm^{-1}; ^{1}H NMR (125 MHz, $CDCl_3$) δ 7.33 (d, $J = 9.0$ Hz, 2H), 6.87 (d, $J = 9.0$ Hz, 2H), 3.80 (s, 3H), 0.19 (s, 9H); ^{13}C NMR (125 MHz, $CDCl_3$) δ 159.9, 129.9, 129.6, 129.4, 113.8, 101.8, 95.2, 87,4, 81.9, 75.1, 55.3, –0.5; HRMS calcd. for $C_{16}H_{16}O^{79}Br^{81}BrSi$ (M^+) 411.9317, found 411.9314. Anal. calcd. for $C_{16}H_{16}OBr_2Si$: C, 46.62; H, 3.91. Found: C, 46.74; H, 3.69.

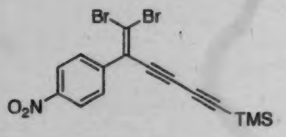

422e

Compound **422e**: 4–Nitrobenzoyl chloride (2.45 g, 13.2 mmol), bis(trimethylsilyl)butadiyne (2.30 g, 11.8 mmol) in CH_2Cl_2 (100 mL) at –20 °C and $AlCl_3$ (2.4 g, 18.0 mmol) were used as per general procedure D, affording the intermediate ketone (3.38 g, 94%) as a yellow oil. This intermediate was carried onto the next reaction without further characterization.

CBr_4 (3.15 g, 9.50 mmol), PPh_3 (5.00 g, 19.1 mmol) in CH_2Cl_2 (100 mL) at 0 °C and the ketone above were used as the general procedure E, yielding **422e** (2.54 g, 75%) as a cream colored powder. Mp 80–83 °C. $R_f = 0.6$ (hexanes/CH_2Cl_2 1:1).

IR ($CHCl_3$, cast film) 2960 (w), 2096 (w), 1595, 1523 cm^{-1}; ^1H NMR (300 MHz, $CDCl_3$) δ 8.22 (d, $J = 2.0$ Hz, 2H), 7.58 (d, $J = 2.0$ Hz, 2H); ^{13}C NMR (125 MHz, $CDCl_3$, APT) δ 147.7, 143.4, 129.7, 128.1, 123.9, 123.8, 104.8, 96.7, 86.8, 73.8. EIMS *m/z* 424.9 (M^+, 28), 411.9 ($[M - CH_3]^+$, 100); HRMS calcd. for $C_{15}H_{13}O_2Si^{79}Br_2$ (M^+) 424.9082, found 424.9085. Anal. calcd. for $C_{15}H_{13}O_2SiBr_2$: C, 42.18; H, 3.07; N, 3.28. Found: C, 42.30; H, 2.81; N, 3.16.

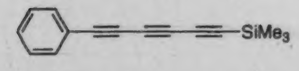

423a

Compound **423a**: Compound **422a** (124 mg, 0.311 mmol) in hexanes (8 mL) at –78 °C and BuLi (2.5 M in hexanes, 0.14 mL, 0.35 mmol) were used as per general procedure F, yielding **423a** (70.1 mg, 97%) as a yellow oil. $R_f = 0.5$ (hexanes).

IR ($CHCl_3$, cast) 2958, 2174, 2076, 1594, 1251 cm^{-1}; ^1H NMR (500 MHz, $CDCl_3$) δ 7.50 (d, $J = 7.5$ Hz, 2H), 7.36 (t, $J = 7.5$ Hz, 1H), 7.31 (t, $J = 7.5$ Hz, 2H), 0.21 (s, 9H); ^{13}C NMR (125 MHz, $CDCl_3$) δ 133.1, 129.7, 128.5, 120.8, 89.0, 88.0, 76.9, 74.3, 66.8, 61.6, –0.5; EIMS *m/z* 222.1 (M^+, 45), 207.1 ($[M - CH_3]^+$, 100); HRMS calcd. for $C_{15}H_{14}Si$ (M^+) 222.0865, found 222.0867.

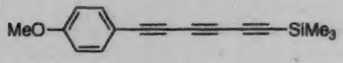

423b

Compound **423b**: Compound **422b** (1.74 g, 4.22 mmol) in hexanes (100 mL) at –78 °C and BuLi (2.5 M in hexanes, 2.53 mL, 6.33 mmol) were used as per general procedure F, yielding **423b** (1.06 g, 99%) as an off–white crystalline solid. Mp 76–78 °C. $R_f = 0.7$ (hexanes/CH_2Cl_2 2:1).

IR ($CHCl_3$, cast) 3017, 2963, 2178, 2073, 1602, 1508, 1254 cm^{-1}; ^1H NMR (500 MHz, $CDCl_3$) δ 7.44 (d, J = 9.0 Hz, 2H), 6.82 (d, J = 9.0 Hz, 2H), 3.80 (s, 3H), 0.20 (s, 9H); ^{13}C NMR (125 MHz, $CDCl_3$) δ 160.8, 134.8, 114.2, 112.6, 88.6, 88.2, 76.7, 73.3, 66.4, 62.0, 55.4, –0.5; EIMS *m/z* 252.1 (M^+, 64), 237.1 ($[M - CH_3]^+$, 100); HRMS calcd. for $C_{16}H_{16}OSi$ (M^+) 252.0971, found 253.0946. Anal. calcd. for $C_{16}H_{16}OSi$: C, 76.14; H, 6.39. Found: C, 75.96; H, 6.28.

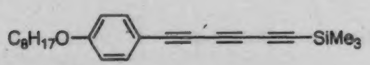

423c

Compound **423c**: Compound **422c** (1.02 g, 2.00 mmol) in hexanes (40 mL) at –78 °C and BuLi (2.5 M in hexanes, 0.9 mL, 2.3 mmol) were used as per general procedure F, yielding **423c** (639 mg, 94%) as a white solid; Mp 71–73 °C. $R_f = 0.6$ (hexanes/CH_2Cl_2 4:1).

IR (CH_3Cl, cast) 2926, 2855, 2178, 2073, 1600 cm^{-1}; ^1H NMR (500 MHz, $CDCl_3$) δ 7.42 (d, J = 9.0 Hz, 2H), 6.80 (d, J = 9.0 Hz, 2H), 3.94 (t, J = 6.5 Hz, 3H), 1.75 (app quint, J = 6.5 Hz, 2H), 1.46–1.40 (m, 4H), 1.34–1.26 (m, 6H), 0.87 (t, J = 7.0 Hz, 3H), 0.20 (s, 9H); ^{13}C NMR (100 MHz, $CDCl_3$) δ 160.4, 134.8, 114.7, 112.2, 88.5, 88.2, 73.2, 68.2, 66.4, 62.0, 31.8, 29.3, 29.2, 29.1, 26.0, 22.6, 14.1, –0.48. EIMS 350.2 (M^+, 86), 238.1 ($[M - C_8H_{16}]^+$, 100); HRMS calcd. $C_{23}H_{30}OSi$ (M^+) 350.2066, found 350.2066. Anal. calcd. for $C_{23}H_{30}OSi$: C, 78.80; H, 8.63. Found: C, 78.81; H, 8.80.

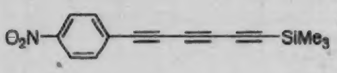

423e

Compound **423e**: Compound **422c** (1.17 g, 2.73 mmol) in hexanes (100 mL) at 0 °C and BuLi (2.5 M in hexanes, 1.3 mL, 3.3 mmol) were used as per general procedure F. After the addition of BuLi into the reaction, the solution turned black instantly. The resulting product was isolated; however, it could not be identified.

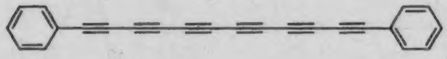

412a

Compound **412a**: Compound **423a** (14.9 mg, 0.067 mmol) in THF/MeOH (3 mL, 1:1 v/v) and K_2CO_3 (9.3 mg, 0.067 mmol) were used as per general procedure A, affording the terminal triyne. CuCl (6.6 mg, 0.067 mmol) in CH_2Cl_2 (3 mL), TMEDA (0.03 mL) and oxygen passed through the solution for 10 min to give a blue–green color were used as general procedure G, yielding **412a** (6.7 mg, 67%) as an orange crystalline solid that was sparingly soluble in organic solvents. Mp 133 °C (dec., DSC). $R_f = 0.5$ (hexanes); UV–vis (THF) λ_{max} (ε) 301 (128,000), 312 (129,000), 319 (135,000), 337 (155,000), 354 (80,6000), 394 (18,500), 426 (16,400), 465 (8,000) nm; IR (CH_2Cl_2, cast) 2174, 2159 cm^{-1}; ^{1}H NMR (300 MHz, $CDCl_3$) δ 7.55 (d, $J = 7.5$ Hz, 4H), 7.44 (t, J 7.5 Hz, 2H), 7.35 (t, $J = 7.5$ Hz, 4H); ^{13}C NMR (75.5 MHz, $CDCl_3$, APT) δ 133.5, 130.4, 128.7, 120.2, 77.5, 74.3, 67.3, 64.6, 63.6, 62.6; HRMS calcd. for $C_{24}H_{10}$ (M$^+$) 298.0783, found 298.0776.

Single crystals were grown from slow diffusion of hexanes into a hexanes/CH_2Cl_2. $C_{24}H_{10}$, M = 298.32, monoclinic space group $P2_1/n$ (an alternate setting of $P2_1/c$ No. 14), $D_c = 1.194$ g cm^{-3}, $a = 7.7266(9)$ Å, $b = 12.4682(14)$ Å, $c = 17.2826(19)$ Å, $\beta = 94.797(2)$ Å, $\gamma = 102.0395(19)$ Å, $V = 1659.1(3)$ Å^3, $Z = 4$, $\mu = 0.068$ (mm^{-1}), T = –80

°C. Final $R_1(F) = 0.0534$, $wR^2(F^2) = 0.1305$ for 217 variables and 3404 data with $F_o^2 \geq -3\sigma(F^2)$ (1612 $[F_o^2 \geq -2\sigma(F_o^2)]$. CCDC no. 249138.

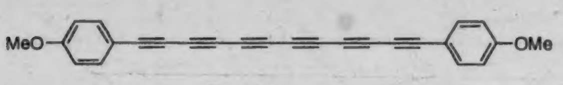

412b

Compound **412b**: Compound **423b** (101 mg, 0.400 mmol) in THF/MeOH (4 mL, 1:1 v/v) and K_2CO_3 (55 mg, 0.40 mmol) were used as per general procedure A, affording the terminal triyne. CuCl (39.6 mg, 0.400 mmol) in CH_2Cl_2 (20 mL), TMEDA (0.2 mL) and oxygen were used as per general procedure G, yielding **412b** (50.2 mg, 70%) as an organe crystalline solid that was sparingly soluble in organic solvents. Mp 150 °C (dec., DSC). $R_f = 0.3$ (hexanes/CH_2Cl_2 2:1). UV–vis (THF) λ_{max} (ε) 289 (77,300), 305 (92,100), 328 (111,000), 351 (164,000), 378 (99,100), 403 (34,500), 437 (27,000), 476 (13,300) nm. IR ($CHCl_3$, cast) 2972, 2171, 1598, 1510, 1442, 823 cm^{-1}; ^{1}H NMR (400 MHz, $CDCl_3$) δ 7.47 (db, $J = 9.0$ Hz, 4H), 6.83 (d, $J = 9.0$ Hz, 4H), 3.81 (s, 6H); ^{13}C NMR (100 MHz, $CDCl_3$) δ 161.2, 135.3, 114.4, 112.1, 77.9, 76.7, 73.6, 67.2, 64.6, 63.2, 55.5; HRMS calcd. for $C_{26}H_{14}O_2$ (M^+) 358.0994, found 358.0990.

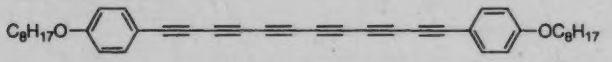

412c

Compound **412c**: Compound **423c** (639 mg, 1.82 mmol) in THF (20 mL) and TBAF (1.0 M in THF, 1.8 mL, 1.82 mmol) were used as per general procedure A, yielding the terminal triyne. CuCl (0.1 g, 6.6 mg, 0.067 mmol) in CH_2Cl_2 (10 mL), TMEDA (0.03 mL) and oxygen passed through the solution for 10 min to giva a blue–green color were used as per general procedure G, yielding **412c** (255 mg, 50%) as an orange powder. Mp 133.4 °C and endotherm 132.0 °C (DSC). $R_f = 0.3$ (hexanes/CH_2Cl_2 5:1). UV–vis (THF)

λ_{max} (ε) 305 (64,000), 329(73,000), 352 (103,000), 380 (63,000), 404 (25,000), 438 (18,000), 477 (8,500). IR (CH_2Cl_2, cast) 2919, 2168, 2152, 1600 cm^{-1}; ^1H NMR (400 MHz, $CDCl_3$) δ 7.45 (d, *J* = 8.8 Hz, 2H), 6.81 (d, *J* = 8.8 Hz, 2H), 3.95 (t, *J* = 6.6 Hz, 2H), 1.76 (quint, *J* = 7.2 Hz, 2H), 1.46–1.38 (m, 2H), 1.34–1.25 (m, 10H), 0.87 (t, *J* = 7.2 Hz, 3H); ^{13}C NMR (100 MHz, $CDCl_3$) δ 160.9, 135.2, 114.9, 111.5, 78.0, 73.5, 68.3, 67.1, 64.6, 63.8, 62.9, 31.8, 29.3, 29.2, 29.1, 26.0, 22.6, 14.1. Maldi MS (Dithranol) *m/z* 554 (M^+).

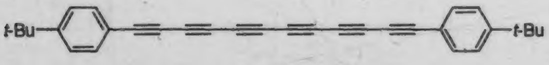

412d

Compound **412d**: Compound **423d**[15] ((210 mg, 0.754 mmol) in THF/MeOH (10 mL, 1:1 v/v) and K_2CO_3 (104 mg, 0.754 mmol) were used as per general procedure A, affording the terminal triyne. CuCl (75 mg, 0.757 mmol) in CH_2Cl_2 (40 mL), TMEDA (3 mL) and oxygen passed through the solution for 10 min to give a blue–green color were used as per general procedure G, yielding **412d** (120 mg, 78%) as an orange crystalline solid that was sparingly soluble in organic solvents. Mp 150 °C (dec., DSC). R_f = 0.5 (hexanes). UV–vis (THF) λ_{max} (ε) 287 (82,400), 302 (127,000), 321 (148,000), 342 (206,000), 364 (101,000), 398 (25,800), 430 (22,500), 469 (10,900) nm. IR ($CHCl_3$, cast) 2959, 2899, 2173, 2159, 1563, 850 cm^{-1}; ^1H NMR (400 MHz, $CDCl_3$) δ 7.46 (d, *J* = 8.7 Hz, 4H), 7.34 (d, *J* = 8.7 Hz, 4H), 1.29 (s, 9H); ^{13}C NMR (100 MHz, $CDCl_3$, APT) δ 154.1, 133.3, 125.7, 116.9, 77.9, 73.9, 67.0, 64.5, 63.6, 62.7, 35.0, 31.0; EIMS *m/z* 410.2 (M^+, 84), 395.2 ($[M - CH_3]^+$, 46); HRMS calcd. for $C_{32}H_{26}$ (M^+) 410.2035, found 410.2057.

Single crystals were grown from slow diffusion of hexanes into a CH_2Cl_2. $C_{32}H_{26}$, M = 410.53, triclinic space group $P\bar{1}$ (No. 2), D_c = 1.136 g cm^{-3}, *a* = 8.2179(9) Å, *b* =

16.7512(18) Å, c = 17.8407(19) Å, β = 91.395(2) Å, γ = 102.0395(19) Å, V = 2400.9(4) Å^3, Z = 4, μ = 0.064 (mm^{-1}), T = –80 °C. Final $R_1(F)$ = 0.0703, $wR^2(F^2)$ = 0.2027 for 577 variables and 9710 data with $F_o^2 \geq -3\sigma(F^2)$ (4752 [$F_o^2 \geq -2\sigma(F_o^2)$)]. CCDC no. 249139.

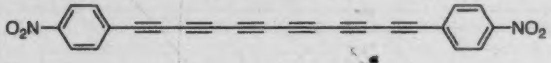

412e

Compound **412e**: Compound **426c** (211 mg, 0.599 mmol) in THF (5 mL) at rt and TBAF (1.0 M in THF, 1.0 mL, 1.0 mmol) were used as per general procedure A. Upon work–up, a intractable product was resulted and could not be identified.

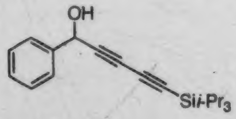

428a

Compound **428a**: Compound **425**[10] (316 mg, 0.863 mmol), LDA [BuLi (2.5 M in hexanes, 1.0 mL, 2.6 mmol) and diisopropylamine (0.36 mL, 2.59 mmol) in THF (10 mL) were used as per general procedure J] and benzaldehyde (78.2 mg, 0.737 mmol) were used as per general procedure C, yielding **428a** (84.7 mg, 37%) as a brown oil. R_f = 0.5 (CH_2Cl_2).

IR ($CHCl_3$, μscope) 3350 (br), 2944, 2866, 2105, 1457 cm^{-1}; ^{1}H NMR (400 MHz, $CDCl_3$) δ 7.50 (d, J = 7.1 Hz, 2H), 7.40–7.30 (m, 3H), 5.50 (s, 1H), 2.33 (s, 1H), 0.08 (s, 21H); ^{13}C NMR (100 MHz, $CDCl_3$) δ 139.5, 128.7, 128.6, 126.6, 88.7, 85.8, 75.6, 71.8, 64.9, 18.4, 11.1. EIMS m/z 312.2 (M$^+$, 15), 269.1 ([M – *i*–Pr], 18); HRMS calcd. for $C_{20}H_{28}SiO$ (M$^+$) 312.1910, found 312.1911.

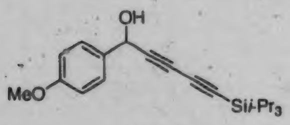

428b

Compound **428b**: Compound **425**[10] (315 mg, 0.863 mmol), LDA [BuLi (2.5 M in hexanes, 1.0 mL, 2.6 mmol) and diisopropylamine (0.36 mL, 2.6 mmol) in THF (10 mL) were used as per general procedure G] and anisaldehyde (98.5 mg, 0.723 mmol) were used as per general procedure C, yielding **428b** (38.4 mg, 16%) as a brown oil. R_f = 0.4 (CH_2Cl_2).

IR ($CHCl_3$, cast) 3371 (br), 2944, 2866, 2104, 1512 cm^{-1}; ^1H NMR (400 MHz, $CDCl_3$) δ 7.42 (d, J = 8.7 Hz, 2H), 6.89 (d, J = 8.7 Hz, 2H), 5.45 (d, J = 5.4 Hz, 1H), 3.80 (s, 3H), 2.18 (d, J = 5.7 Hz, 1H), 1.07 (s, 21H); ^{13}C NMR (100 MHz, $CDCl_3$) δ 159.8, 131.8, 128.0, 114.0, 88.7, 85.7, 75.8, 71.6, 64.6, 55.2, 18.4, 11.1. EIMS *m/z* 342.2 (M^+, 14), 299.1 ($[M - i\text{–}Pr]^+$, 100); HRMS calcd. for $C_{21}H_{30}SiO_2$ (M^+) 342.2015, found 342.2019.

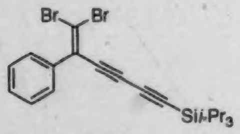

430a

Compound **430a**: Compound **428a** (587 mg, 5.54 mmol) in CH_2Cl_2 (20 mL), PCC (1.50 g, 6.96 mmol), celite (0.5 g) and molecular sieves (0.5 g) were used as per general procedure D, affording the intermediate ketone that was carried on to the next step without further purification.

CBr_4 (670 mg, 2.02 mmol), PPh_3 (1.06 g, 4.04 mmol) in CH_2Cl_2 (10 mL) at 0 °C and ketone above were used as per general procedure E, yielding **430a** (413 mg, 37%) as a colorless oil. R_f = 0.8 (hexanes/CH_2Cl_2 3:1).

IR (CH_3Cl, cast) 2943, 2865, 2091, 1490 cm^{-1}; ^1H NMR (300 MHz, $CDCl_3$) δ 7.40–7.34 (m, 5H), 1.07 (s, 21H); ^{13}C NMR (125 MHz, $CDCl_3$) δ 137.4, 130.1, 128.8, 128.5, 102.6, 92.9, 89.0, 82.6, 73.7, 18.5, 11.3 (one signal not observed). EIMS 466.0 (M^+, 42), 423.0 ($[M - i\text{–}Pr]^+$, 100); HRMS calcd. $C_{21}H_{26}OSi^{79}Br^{81}Br$ (M^+) 466.0150, found 466.0161.

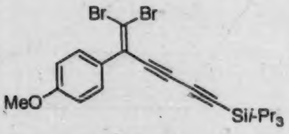

430b

Compound **430b**: Compound **428b**(768 mg, 5.64 mmol), PCC (1.50 g, 6.96 mmol) in CH_2Cl_2 (10 mL), celite (0.7 g) and molecular sieves (0.7 g) were used as per general procedure D, affording the intermediate ketone that was carried on to the next step without further purification.

CBr_4 (860 mg, 2.59 mmol), PPh_3 (1.36 g, 5.19 mmol) in CH_2Cl_2 (10 mL) at 0 °C and ketone were used as per general procedure E, yielding **430b** (520 mg, 19%) as a colorless oil. $R_f = 0.5$ (hexanes/CH_2Cl_2 3:1).

IR (CH_3Cl, cast) 2943, 2865, 2088, 1606, 1505 cm^{-1}; ^1H NMR (500 MHz, $CDCl_3$) δ 7.34 (d, $J = 9.0$ Hz, 2H), 6.88 (d, $J = 9.0$ Hz, 2H), 3.80 (s, 3H), 1.07 (s, 21H); ^{13}C NMR (125 MHz, $CDCl_3$) δ 159.9, 129.9, 129.6, 113.9, 101.7, 92.6, 89.1, 82:473.9, 55.3, 18.5, 11.3, (one signal not observed). EIMS 496.0 (M^+, 74), 453.0 ($[M - i\text{–}Pr]^+$, 100); HRMS calcd. $C_{22}H_{28}OSi^{79}Br^{81}Br$ (M^+) 496.0256, found 496.0254.

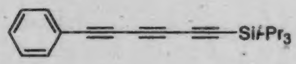

424a

Compound **424a**: Compound **430b** (0.377 g, 0.804 mmol) in hexanes (12 mL) at –78 °C and BuLi (1.6 M in hexanes, 0.56 mL, 0.90 mmol) were used as per general procedure F, affording **424a** (247 mg, 100%) as a yellow oil. $R_f = 0.6$ (hexanes). UV–vis (THF) λ_{max} (ε) 284 (14,000), 301 (24,000), 322 (32,000), 345 (23,000). IR (CH_3Cl, cast) 2944, 2865, 2175, 2074 cm^{-1}; ^1H NMR (500 MHz, $CDCl_3$) δ 7.50 (d, $J = 7.5$ Hz, 2H), 7.37 (t, $J = 7.5$ Hz, 1H), 7.30 (t, $J = 7.5$ Hz, 2H), 1.08 (s, 21); ^{13}C NMR (125 MHz, $CDCl_3$) δ 133.1, 129.7, 128.5, 120.9, 89.7, 86.7, 76.5, 74.4, 67.3, 60.6, 18.5, 11.3 EIMS 306.2 (M^+, 53), 263.1 ($[M - i\text{–}Pr]^+$, 100); HRMS calcd. $C_{21}H_{26}OSi$ (M^+) 306.1804, found 306.1803.

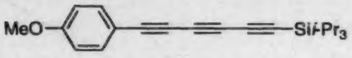

424b

Compound **424b**: Compound **430b** (473 mg, 0.952 mmol) in hexanes (10 mL) at –78 °C and BuLi (1.6 M in hexanes, 0.65 mL, 1.0 mmol) were used as per general procedure E, yielding **424b** (297 mg, 93%) as a light green–yellow crystalline solid. Mp 67–70 °C. R_f = 0.6 (hexanes/CH_2Cl_2 3:1). UV–vis (THF) λ_{max} (ε) 309 (27,000), 329 (37,000), 353 (27,000). IR (CH_3Cl, cast) 2943, 2865, 2177, 2070, 1601 cm^{-1}; ^1H NMR (300 MHz, $CDCl_3$) δ 7.44 (d, J = 9.0 Hz, 2H), 6.82 (d, J = 9.0 Hz, 2H), 3.80 (s, 3H), 1.07 (s, 21); ^{13}C NMR (125 MHz, $CDCl_3$) δ 160.8, 134.8, 114.2, 112.7, 89.9, 86.3, 76.9, 73.4, 66.9, 61.0, 55.4, 18.5, 11.3. EIMS 336.2 (M^+, 82), 293.1 ($[M - i\text{–}Pr]^+$, 100); HRMS calcd. $C_{22}H_{28}OSi$ (M^+) 336.1910, found 336.1906. Anal. calcd. for $C_{22}H_{28}OSi$: C, 78.51; H, 8.39. Found: C, 78.13; H, 8.91.

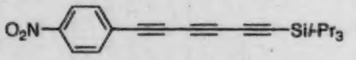

424c

Compound **424c**: Compound **425** (243 mg, 0.665 mmol) in toluene (5 mL) at –20 °C and BuLi (2.5 M in hexanes, 0.87 mL, 2.2 mmol) were used as per general procedure E. $ZnCl_2$ (1.0 M in THF, 1.3 mL, 1.3 mmol) was added to the reaction mixture above, followed by the addition of **429**[21] (0.18 mg, 1.22 mmol) were used as per general procedure M, yielding **424c** (150 mg, 64%) as a yellow crystalline solid. Mp 112–115 °C. R_f = 0.4 (hexanes/CH_2Cl_2 3:1). UV–vis (THF) λ_{max} (ε) 315 (16,000), 337 (25,000), 361 (22,000). IR (CH_3Cl, cast) 2956, 2921, 2850, 1462, (alkynyl signal was not observed) cm^{-1}; ^{1}H NMR (400 MHz, $CDCl_3$) δ 7.21 (d, J = 8.8 Hz, 2H), 7.66 (d, J = 8.8 Hz, 2H), 1.14 (s, 21); ^{13}C NMR (125 MHz, $CDCl_3$) δ 147.7, 133.8, 127.9, 123.7, 89.2, 89.0, 79.2, 73.8, 69.8, 59.6, 18.5, 11.3. EIMS 351.2 (M$^+$, 26), 308.1 ([M – *i*–Pr]$^+$, 100); HRMS calcd. $C_{21}H_{25}O_2NSi$ (M$^+$) 351.1655, found 351.1656. Anal. calcd. for $C_{21}H_{25}O_2NSi$: C, 71.75; H, 7.17; N, 3.98. Found: C, 71.35; H, 7.08; N, 3.87.

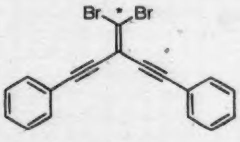

435

Compound **435**: CBr_4 (541 mg, 1.63 mmol), $^{13}CBr_4$ (109 mg, 0.315 mmol), PPh_3 (171 mg, 0.653 mmol, first portion; 853 mg, 3.26 mmol, second portion) in CH_2Cl_2 (8 mL) and **434**[20] (188 mg, 0.814 mmol) were used as per general procedure M, yielding **435** (250 mg, 79%). Spectral data were consistent with those reported previously for the unlabelled analogue.[22]

^{13}C NMR (100 MHz, $CDCl_3$) δ131.6, 129.1, 128.3, 122.0, 114.1 (pseudo–t, ^1J = 96 Hz), 107.6 (C*), 95.7, 85.9.

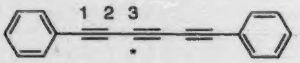

431

Compound **431**: Compound **435** (244 mg, 0.633 mmol) in toluene (4 mL), hexanes (4 mL) at –78 °C were used as per general procedure F, yielding **431** (89 mg, 62%). Spectral data were consistent with those of **409**, except for the C≡C coupling.

^{13}C NMR (100 MHz, $CDCl_3$) δ 132.9, 129.6, 128.4, 120.9, 78.5 (C1, pseudo–t, ^2J = 20 Hz), 74.4 (C2, pseudo–tt, ^1J = 164 Hz), 66.4 (C3, pseudo–t, ^1J = 164 Hz, ^2J = 20 Hz).

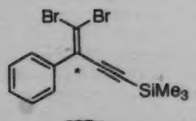

437a

Compound **437a**: benzoic acid (100% enrichment, 125 mg, 1.01 mmol) in CH_2Cl_2 (1 mL) and thionylchloride (24 mg, 2.06 mmol) were stirred overnight. Bis(trimethylsilyl)acetylene (173 mg, 1.02 mmol) in CH_2Cl_2 (5 mL) at –20 °C and $AlCl_3$ (162 mg, 1.21 mmol) were used as per general procedure G, affording the intermediate ketone that was carried on to the next step without further purification.

CBr_4 (0.371 mg, 1,12 mmol), PPh_3 (584 mg, 2.33 mmol) in CH_2Cl_2 (5 mL) at 0 °C and the ketone above were used as per procedure B, yielding **437a** (128 mg, 35%). Spectral data were consistent with those reported previously for the unlabelled analogue.[15]

^{13}C NMR (100 MHz, $CDCl_3$) δ 131.0 (C*), 128.6, 128.5, 128.2, –0.39, the two alkyne and one vinyl signals were not observed due to low signal to noise.

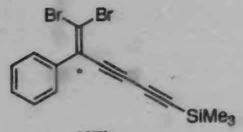

437b

Compound **437b**: benzoic acid (100% enrichment, 184 mg, 1.49 mmol) in CH_2Cl_2 (1 mL) and thionylchloride (49 mg, 4.1 mL) were stirred overnight. Bis(trimethylsilyl)butadiyne (290 mg, 1.49 mmol) in CH_2Cl_2 (14 mL) at –20 °C and $AlCl_3$ (239 mg, 1.79 mmol) were used as per general procedure G, affording the intermediate ketone that was carried on to the next step without further purification.

CBr_4 (744 mg, 2.24 mmol), PPh_3 (1.17 mg, 4.47 mmol) in CH_2Cl_2 (14 mL) at 0 °C and the ketone above were used as per procedure B, yielding **437b** (190 mg, 33%). Spectral data were consistent with those of **418b**.

^{13}C NMR (100 MHz, CDCl$_3$) δ 130.0 (m), 129.9 (s), 128.7, 128.0, 128.4, 102.6 (d, ^{1}J = 91 Hz), 95.3, 87.2 (d, ^{3}J = 4 Hz), 81.5 (d, ^{2}J = 13 Hz), 74.8 (d, ^{1}J = 97 Hz), –0.66.

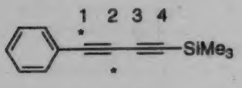

438a

Compound **438a**: Compound **437a** (126 mg, 0.352 mmol) in hexanes (8 mL) at –78 °C and BuLi (2.5 M in hexanes, 0.16 mL, 0.40 mmol) were used as per general procedure F, yielding **438a** as a mixture of the two possible isotopomers (54.1 mg, 78%). Spectral data were consistent with those reported previously for the unlabelled analogue.[15]

^{13}C NMR (100 MHz, CDCl$_3$) δ 132.7 (d, J = 2 Hz), 129.3, 128.4 (d, J = 3 Hz), 122.0 (dd, ^{1}J= 14, ^{1}J = 91 Hz), 90.6 (C4, d, ^{2}J= 14 Hz), 88.4 (C3, dd, ^{1}J = 150, $^{2}J_{C\text{–}C}$ = 18 Hz), 77.3 (C1, dd, ^{2}J = 91, ^{1}J = 196 Hz), 74.3 (C2, dd, ^{2}J = 141, ^{1}J = 202 Hz), –0.39.

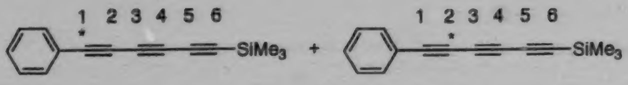

438a

Compound **438a**: Compound **437b** (190 mg, 0.498 mmol) in hexanes (15 mL) at –78 °C and BuLi (2.5 M in hexanes, 0.24 mL, 0.60 mmol) were used as per general procedure F, yielding **438a** as a mixture of the two possible isotopomers (86.7 mg, 78%). Spectral data were consistent with those of **423a**.

^{13}C NMR (100 MHz, CDCl$_3$) δ 133.1 (d, J = 2 Hz,) 129.8 (s), 128.5 (d, J = 6 Hz), 120.8 (dd, J = 14, 92 Hz), 89.0 (dd, J = 3, 5 Hz), 88.1 (dd, J = 3, 6 Hz), 74.2 (C2, m), 66.8 (dd, J = 16, 21 Hz), 61.5 (C1, dd, ^{1}J = 163, ^{2}J = 19 Hz), –0.51.

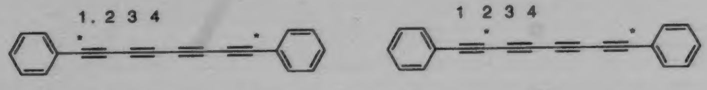

432

Compound **432**: Compound **438a** (54.1 mg, 0.273 mmol) in THF/MeOH (3 mL, v/v 1:1) and K_2CO_3 (50 mg, 0.36 mmol) were used as per general procedure A, yielding the terminal diyne.

CuCl (50 mg, 0.50 mmol) in CH_2Cl_2 (5 mL), TMEDA (0.1 mL) and the terminal diyne above were used as per general procedure B, yielding **432** as a mixture of the three possible isotopomers (35.7, 52%). Spectral data were consistent with those of **410**.

^{13}C NMR (100 MHz, $CDCl_3$, irradiation at C1, 77.7 ppm) δ 133.1, 129.9, 128.5, 120.4 (d, J = 13 Hz), 74.4 (C2, intense carbon enrichment), 67.0 (m), 63.5 (C3, d, J = 158 Hz).

^{13}C NMR (100 MHz, $CDCl_3$, irradiation at C2, 74.4 ppm) δ 133.1, 129.9, 128.5 (d, J = 6 Hz), 120.4 (d, J = 86 Hz), 67.0 (m), 63.5 (C3, d, ^4J = 5 Hz, has larger coupling constants then those of 67.0 ppm, assigned as C3).

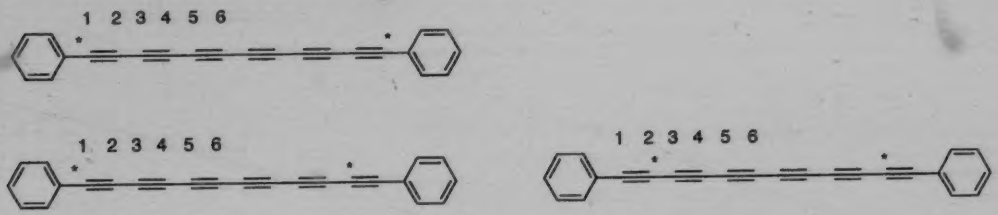

433

Compound **433**: Compound **438b** (8.6 mg, 38.7 mmol) in THF/MeOH (3 mL, v/v 1:1) and K_2CO_3 (8 mg, 0.06 mmol) were used as per general procedure A, yielding the terminal triyne.

CuCl (8 mg, 0.08 mmol) in CH_2Cl_2 (3 mL), TMEDA (0.1 mL) and the terminal triyne above were used as per general procedure B, yielding **433** as a mixture of the three possible isotopomers (5.0 mg, 87%). Spectral data were consistent with those of **412**.

^{13}C NMR (125 MHz, $CDCl_3$) δ 123.9, 122.0, 121.0, 120.1 (dd, $J = 14, 91$ Hz), 77.5 (C1, dd, m), 74.3 (C2, m), 67.2 (C4, d, $^2J = 20$, $^3J = 5$ Hz), 64.6 (C6), 63.6 (C5, d, $^3J = 5$ Hz), 62.5 (C3, dd, $^1J = 159$, $^2J = 19$ Hz).

8.3.4 Chapter 5

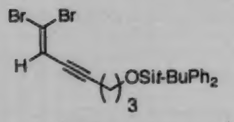

S501

Compound **S501**: CBr_4 (1.17 g, 3.35 mmol), PPh_3 (1.86 g, 7.10 mmol) in CH_2Cl_2 (10 mL) and aldehyde **219b**[18] (628 mg, 1.77 mmol) were used as per general procedure D, yielding **S501** (683 mg, 76%) as a colorless oil. $R_f = 0.5$ (hexanes/CH_2Cl_2 3:1).

IR ($CHCl_3$, cast) 3071, 2931, 2858, 2219 (w) cm^{-1}; ^1H NMR (300 MHz, $CDCl_3$) δ 7.67–7.62 (m, 4H), 7.43–7.33 (m, 6H), 6.47 (t, $J = 2.3$ Hz, 1H), 3.75 (t, $J = 6.0$ Hz, 2H), 2.46 (dt, $J = 2.3, 7.0$ Hz, 2H), 1.79 (app. quint, 6.0 Hz, 2H), 1.03 (s, 9H); ^{13}C NMR (100 MHz, $CDCl_3$) δ 135.5, 133.8, 129.6, 127.6, 120.0, 100.0, 100.2, 98.9, 77.9, 62.2, 31.1, 26.8, 19.2, 16.3. EIMS *m/z* 448.9 ([M – *t*–Bu]$^+$, 100); HRMS calcd. for $C_{19}H_{17}SiO^{79}Br^{81}Br$ (M – *t*–Bu)$^+$ 448.93945, found 448.9387.

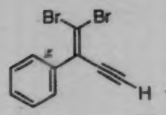

506a

Compound **506a.** Dibromoolefin **517a**[23] (7.00 g, 19.5 mmol) was dissolved in THF/MeOH (50 mL, v/v 1:1), and K_2CO_3 (0.10 g, 0.75 mmol) were used as per general procedure A, The solution was passed through a short silica gel column to afford **506a** (5.21 g, 93%) as a white solid. Mp 39–42 °C. $R_f = 0.6$ (hexanes/CH_2Cl_2 3:1).

IR ($CHCl_3$, cast) 3290 cm^{-1}; ^1H NMR (400 MHz, $CDCl_3$) δ 7.44–7.40 (m, 2H), 7.39–7.34 (m, 3H), 3.59 (s, 1H); ^{13}C NMR (100 MHz, $CDCl_3$) δ 137.7, 130.1, 128.7, 128.5, 128.4, 100.8, 85.8, 82.7. EIMS *m/z* 285.9 (M$^+$, 49), 126.0 ([M – 2Br]$^+$, 100); HRMS calcd. for

$C_{10}H_6Br_2$ 285.8816, found 285.8816. Anal. calcd. for $C_{10}H_6Br_2$: C, 42.00; H, 2.11. Found: C, 41.80; H, 1.95.

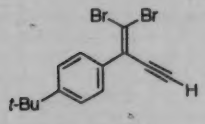

506b

Compound **506b**: Compound **517b**[15] (3.10 g, 7.48 mmol), K_2CO_3 (0.50 g, 0.38 mmol) were used as per the general procedure A and yielding **506b** (2.48 g, 97%) as a light pink powder. Mp 71–73 °C. $R_f = 0.7$ (hexanes/CH_2Cl_2 6:1).

IR ($CHCl_3$, cast) 3275, 2969, 1920 (w), 1118 cm^{-1}; ^{1}H NMR (400 MHz, $CDCl_3$) δ 7.37 (s, 4H), 3.57 (s, 1H), 1.31 (s, 9H); ^{13}C NMR (100 MHz, CDCl3) δ 151.8, 134.5, 129.9, 128.1, 125.2, 100.0, 85.4, 82.8, 34.6, 31.1. EIMS *m/z* 345.0 (M^+, 6); HRMS calcd. for $C_{14}H_{17}{}^{79}Br^{81}Br$ 344.9677, found 344.9682. Anal. calcd. for $C_{14}H_{17}Br_2$: C 49.16; H 4.13. Found: C 49.14, H 4.20.

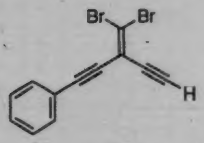

506c

Compound **506c**: Compound **517c**[24] (1.9 g, 5.0 mmol) was dissolved in THF/MeOH (40 mL, v/v 1:1), and pulverized K_2CO_3 (0.10 g, 0.75 mmol) were used as per general procedure A. The solution was passed through a short silica gel column to afford **506c** (1.2 g, 77%) as a pale yellow oil. As the neat oil **506c** slowly discolored, **506c** is best stored in a solution of hexanes, under refrigeration, unless used immediately. $R_f = 0.5$ (hexanes/CH_2Cl_2 4:1).

IR ($CHCl_3$, cast) 3293, 2226, 2189, 2108 cm^{-1}; ^{1}H NMR (400 MHz, $CDCl_3$) δ 7.52–7.49 (m, 2H), 7.34–7.30 (m, 3H), 3.50 (s, 1H); ^{13}C NMR (100 MHz, CDCl3) δ 131.6, 129.3, 128.4, 121.9, 113.4, 109.5, 96.2, 85.8, 83.9, 79.7. EIMS *m/z* 309.9 (M^+, 95), 150.0 ($[C_{12}H_6]^+$, 100); HRMS calcd. for $C_{12}H_6{}^{79}Br^{81}Br$ 309.8816, found 309.8809. Anal. calcd. for $C_{12}H_6Br_2$: C 46.50; H 1.95. Found: C 46.74, H 1.97.

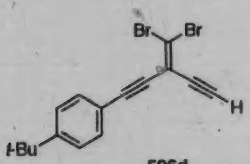

506d

Compound **506d**: Compound **517d**[23] (0.65 g, 1.5 mmol) was dissolved in THF/MeOH (15 mL, v/v 1:1), and pulverized K_2CO_3 (0.073 g, 0.52 mmol) were used as per general procedure A. The solution was passed through a short silica gel column to afford **506d** (0.51 g, 93%) as a pale yellow solid. Mp 82–83 °C. $R_f = 0.6$ (hexanes/CH_2Cl_2 4:1). IR ($CHCl_3$, cast) 3294, 2228, 2193, 2108 cm^{-1}; ^1H NMR (400 MHz, $CDCl_3$) δ 1.30 (s, 9H), 3.50 (s, 1H), 7.35 (d, $J = 8.0$ H, 2H), 7.44 (d, $J = 8.0$, 2H); ^{13}C NMR (100 MHz, CDCl3) δ 31.1, 34.9, 79.8, 83.8, 85.3, 96.6, 109.1, 113.5, 118.9, 125.5, 131.4, 152.8. EIMS *m/z* 365.9 (M^+, 44), 350.9 ($[M - CH_3]^+$, 100); HRMS calcd. for $C_{16}H_{14}{}^{79}Br^{81}Br$ 365.9442, found 365.9439. Anal. calcd. for $C_{16}H_{14}Br_2$: C, 52.49; H, 3.85. Found: C, 52.39; H, 3.95.

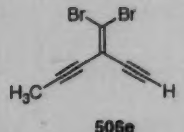

506e

Compound **506e**: Compound **506e**[25] (861 mg, 2.69 mmol) was dissolved in THF/MeOH (10 mL, v/v 1:1), and pulverized K_2CO_3 (0.10 g, 0.75 mmol) were used as per general procedue A. The solution was passed through a short silica gel column to afford **506e** (516 mg, 77%) as a pale yellow oil. As the neat oil **506e** slowly discolored, **506e** is best stored in a solution of hexanes under refrigeration, unless used immediately. R_f = 0.5 (hexanes).

IR ($CHCl_3$, cast) 3291, 2915, 2284, 2225, 2103 cm^{-1}; ^{1}H NMR (500 MHz, $CDCl_3$) δ 3.43 (s, 1H), 1.98 (s, 3H); ^{13}C NMR (125 MHz, $CDCl_3$) δ 113.6, 108.2, 94.3, 83.2, 80.2, 76.6, 4.8. HRMS calcd. for $C_7H_4{}^{79}Br^{81}Br$ 247.8659, found 247.8665.

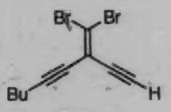

506f

Compound **506f**: Compound **517f**[17] (109 mg, 0.304 mmol) was dissolved in THF/MeOH (5 mL, v/v 1:1) and K_2CO_3 (0.10 g, 0.75 mmol) were used as per the general procedure A to afford **506f** (66.9 mg, 76%) as a colorless oil. R_f = 0.4 (hexanes).

IR ($CHCl_3$, cast) 3295, 2957, 2872, 2223, 2105, 1106 cm^{-1}; ^{1}H NMR (500 MHz, $CDCl_3$) δ 3.42 (s, 1H), 2.33 (t, 7.0Hz, 2H), 1.58–1.52 (m, 2H), 1.47–1.41 (m, 2H), 0.91 (t, 7.5Hz, 3H); ^{13}C NMR (125 MHz, CDCl3) δ 113.6, 108.1, 98.8, 83.1, 80.2, 77.5, 30.1, 21.9, 19.4, 13.5. EIMS *m/z* 289.9 (M$^+$, 78); HRMS calcd. for $C_{10}H_{10}{}^{79}Br^{81}Br$ 289.9129, found 289.9126.

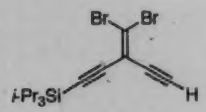

506g

Compound **506g:** Compound **517g**[26] (183 mg, 0.398 mmol) was dissolved in THF/MeOH (10 mL), and pulverized K_2CO_3 (0.10 g, 0.75 mmol) were used as per general procedure A. The solution was passed through a short silica gel column to afford **506e** (112 mg, 72%) as a pale yellow oil. As the neat oil **506g** slowly discolored, **506g** is best stored in a solution of hexanes, under refrigeration, unless used immediately. R_f = 0.5 (hexanes).

IR ($CHCl_3$, cast) 3302, 2943, 2890, 2180, 2135 cm^{-1}; ^{1}H NMR (500 MHz, $CDCl_3$) δ 3.44 (s, 1H), 1.09 (s, 21H); ^{13}C NMR (125 MHz, $CDCl_3$) δ 113.8, 110.4, 101.7, 100.3, 83.7, 79.8, 18.6, 11.1. EIMS *m/z* 390.0 (M^+, 20), 346.9 ($[M - i\text{-}Pr]^+$, 100); HRMS calcd. for $C_{15}H_{22}Si^{79}Br^{81}Br$ 389.9837, found 389.9826.

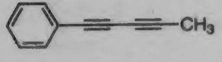

508a

Compound **508a**: Compound **506a** (358 mg, 1.25 mmol), BuLi (1.6 M in hexanes, 1.7 mL, 2.7 mmol), and methyl iodide (27 mg, 1.9 mmol) were used as per the general procedure K and yielded **508a** (117 mg, 67%) as a yellow oil. $R_f = 0.4$ (hexanes).

IR ($CHCl_3$, cast) 3055, 2912, 2250, 1595, 1490 cm^{-1}; ^{1}H NMR (400 MHz, $CDCl_3$) δ 7.46 (td, *J* = 6.4, 1.6 Hz, 2H), 7.32–7.26 (m, 3H), 2.00 (s, 3H); ^{13}C NMR (100 MHz, $CDCl_3$) δ 132.5, 128.8, 128.3, 122.1, 80.3, 74.4, 74.1, 64.3, 4.6; HRMS calcd. for $C_{11}H_8$ 140.0626, found 140.0621.

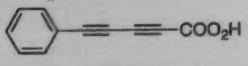

508b

Compound **508b**: Compound **506a** (168 mg, 0.86 mmol), BuLi (1.6 M in hexanes, 0.81 mL, 1.3 mmol) were used as per the general procedure K. CO_2, generated from dry ice, was passed through a drying tube filled with $CaCl_2$ and then was bubbled through the reaction mixture via syringe. After quenching the mixture with 10% aq. HCl, it was basicified by using a 10% aq. NaOH. The aqueous layer was separated and neutralized with 10% aq. HCl and Et_2O (5 mL). The mixture was reduced to dryness and yielded **508b** (64 mg, 64%) as a brown solid. Mp 125–128 °C (Lit. 144 °C).

IR ($CHCl_3$, cast) 2926, 2226, 1621 cm^{-1}; ^{1}H NMR (500 MHz, $CDCl_3$) δ 7.55 (d, *J* = 7.5 Hz, 2H), 7.44 (t, *J* = 7.5 Hz, 1H), 7.35 (t, *J* = 7.5 Hz, 2H), OH signal was not observed;

^{13}C NMR (125 MHz, $CDCl_3$) δ 156.4, 133.2, 130.7, 128.7, 119.7, 85.0, 73.8, 71.9, 70.8; EIMS *m/z* 170.0 (M^+, 18), 126.0 ($[C_{10}H_6]^+$,100); HRMS calcd. for $C_{11}H_6O_2$ 170.0368, found 170.0370. Spectra are consistent with those reported.

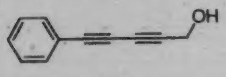
508c

Compound **508c**:[27] Compound **506a** (203 mg, 0.709 mmol), BuLi (2.5 M in hexanes, 0.62 mL, 1.6 mmol), and paraformaldehyde (641 mg, 2.13 mmol) were used as per the general procedure K and yielded **508c** (64.1 mg, 58%) as a yellow oil. R_f = 0.2 (CH_2Cl_2). IR ($CHCl_3$, cast) 3181, 3061, 2914, 2243 cm^{-1}; ^{1}H NMR (300 MHz, $CDCl_3$) δ 7.50–7.46 (m, 2H), 7.38–7.27 (m, 3H), 4.40 (br d, *J* = 5.1, 2H), 1.52 (br s, 1H); ^{13}C NMR (100 MHz, $CDCl_3$) δ 132.6, 129.3, 128.4, 121.4, 80.5, 78.6, 73.2, 70.4, 51.6. HRMS calcd. for $C_{11}H_8O$ 156.0575, found 156.0574.

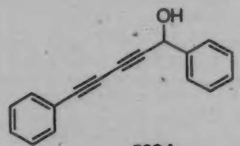
508d

Compound **508d**: Compound **506a** (167 mg, 0.586 mmol), BuLi (2.5 M in hexanes, 0.52 mL, 1.3 mmol), and benzaldehyde (73 mg, 0.69 mmol) were used as per the general procedure K and yielded **508d** (94.7 mg, 70%) as an orange solid. R_f = 0.5 (CH_2Cl_2/hexanes 2:1). Mp 75–78 °C.

IR ($CHCl_3$, cast) 3319, 3032, 2242 cm^{-1}; ^{1}H NMR (400 MHz, $CDCl_3$) δ 7.55 (d, *J* = 6.8 Hz, 2H), 7.49 (dt, *J* = 6.8, 2.0 Hz, 2H), 7.42–7.29 (m, 6H), 5.58 (d, *J* = 6.0 Hz, 1H), 2.35 (d, *J* = 6.0 Hz, 1H); ^{13}C NMR (100 MHz, $CDCl_3$) δ 139.7, 132.6, 129.4, 128.8, 128.7, 128.4, 126.7, 121.3, 81.6, 79.4, 73.2, 71.3, 65.2. HRMS calcd. for $C_{17}H_{12}O$ 232.0888, found 232.0888.

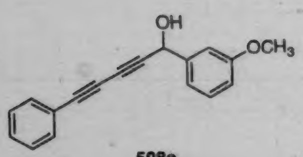

508e

Compound **508e**: Compound **506a** (175 mg, 0.611 mmol), BuLi (2.5 M in hexanes, 0.54 mL, 1.4 mmol), and *m*–methoxylbenzaldehyde (92 mg, 0.67 mmol) were used as per the general procedure K and yielded **508e** (116 mg, 72%) as a yellow solid. Mp 28–31 °C. R_f = 0.6 (CH_2Cl_2).

IR ($CHCl_3$, cast) 3375, 2241, 2210, 1262 cm^{-1}; ^1H NMR (300 MHz, $CDCl_3$) δ 7.52–7.48 (m, 2H), 7.41–7.29 (m, 4H), 7.15–7.10 (m, 2H), 6.90 (d, J = 2.7Hz, 1H), 5.57 (d, J = 6.5 Hz, 1H), 3.82 (s, 3H), 2.51 (d, J = 6.5, 1H); ^{13}C NMR (125 MHz, $CDCl_3$) δ 159.9, 141.2, 132.6, 129.8, 129.4, 128.4, 121.4, 118.9, 114.4, 112.1, 81.6, 79.4, 73.2, 71.3, 65.1, 55.4. HRMS calcd. for $C_{18}H_{14}O_2$ 262.0994, found 262.0996. Anal. calcd. for $C_{18}H_{14}O_2$: C, 82.42; H, 5.38. Found: C, 82.33; H, 5.29.

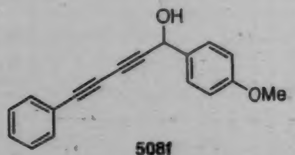

508f

Compound **508f**: Compound **506a** (172 mg, 0.600 mmol), BuLi (2.5 M in hexanes, 0.52 mL, 1.3 mmol), and *p*–methoxybenzaldehyde (90 mg, 0.7 mmol) were used as per the general procedure K and yielded **508f** (114 mg, 72%) as a yellow solid. Mp 67–69 °C. R_f = 0.4 (CH_2Cl_2).

IR ($CHCl_3$, cast) 3395, 2241, 2211, 1250 cm^{-1}; ^1H NMR (400 MHz, $CDCl_3$) δ 7.50–7.35 (m, J = 6.8 Hz, 4H), 7.37–7.28 (m, 3H), 6.91 (dt, J = 8.8, 2.5 Hz, 2H), 5.53 (d, J = 6.0 Hz, 1H), 3.80 (s, 3H), 2.16 (d, J = 6.0 Hz, 1H); ^{13}C NMR (100 MHz, $CDCl_3$) δ 159.9, 132.6, 132.1, 129.4, 128.4, 128.2, 121.4, 114.1, 81.9, 79.4, 73.2, 71.1, 64.8, 55.4. HRMS calcd. for $C_{18}H_{14}O_2$ 262.0994, found 262.1004.

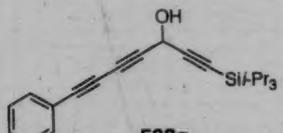

508g

Compound **508g**: Compound **506a** (185 mg, 0.646 mmol), BuLi (2.5 M in hexanes, 0.57 mL, 1.4 mmol), and aldehyde[10] (140 mg, 0.665 mmol) were used as per the general procedure K and yielded **508g** (159 mg, 75%) as a yellow oil. R_f = 0.3 (hexanes/CH_2Cl_2 4:3).

IR ($CHCl_3$, cast) 3219, 2243, 2208, 1034 cm^{-1}; ^{1}H NMR (400 MHz, $CDCl_3$) δ 7.49 (dd, *J* = 6.8, 1.6 Hz, 2H), 7.36–7.31 (m, 3H), 5.24 (d, *J* = 6.0 Hz, 1H), 2.29 (d, *J* = 6.8 Hz, 1H), 1.08 (s, 21H); ^{13}C NMR (100 MHz, $CDCl_3$) δ 132.6, 129.5, 128.4, 121.2, 102.6, 87.3, 79.5, 78.7, 73.0, 69.0, 53.2, 18.5, 11.1. EIMS *m/z* 336.2 (M$^+$, 36), 293.1 ([M – *i*–Pr]$^+$, 43). HRMS calcd. for $C_{22}H_{28}OSi$ (M$^+$) 336.1910, found 336.1909.

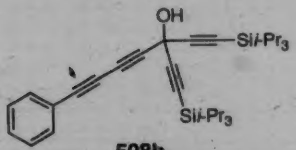

508h

Compound **508h**: Compound **506a** (181 mg, 0.636 mmol), BuLi (2.5 M in hexanes, 0.53 mL, 1.3 mmol), and ketone[28] (219 mg, 0.56 mmol) were used as per the general procedure K and yielded **508h** (275 mg, 95%) as a yellow oil. R_f = 0.3 (hexanes/CH_2Cl_2 3:1).

IR ($CHCl_3$, cast) 3447, 2892, 2232 cm^{-1}; ^{1}H NMR (300 MHz, $CDCl_3$) δ 7.50 (dd, *J* = 6.6, 3.3 Hz, 2H), 7.40–7.28 (m, 3H), 2.79 (s, 1H), 1.08 (s, 42H), (OH peak was not observed); ^{13}C NMR (100 MHz, $CDCl_3$) δ 132.7, 129.6, 128.4, 121.2, 103.0, 85.6, 80.4, 78.6, 73.0, 67.3, 54.9, 18.5, 11.1. EIMS *m/z* 473.3 ([M – *i*–Pr]$^+$, 23), 347.2 ([$C_{20}H_{35}OSi$]$^+$, 48); HRMS calcd. for $C_{33}H_{48}OSi_2$ 473.2696, found 473.2696.

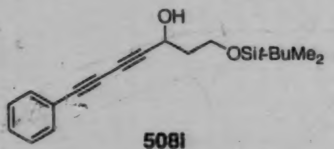

508i

Compound **508i**: Compound **506a** (516 mg, 1.78 mmol), BuLi (1.6 M in hexanes, 2.4 mL, 3.8 mmol), and aldehyde[29] (311 mg, 1.73 mmol) were used as per the general procedure K and yielded **508i** (307 mg, 57%) as a yellow oil. R_f = 0.5 (hexanes/EtOAc 4:1).

IR (CHCl$_3$, cast) 3405, 3063, 2242 cm^{-1}; ^{1}H NMR (300 MHz, CDCl$_3$) δ 7.49–7.45 (m, 2H), 7.37–7.26 (m, 3H), 4.73 (dt, *J* = 6.3, 4.2, 1H), 4.05 (ddd, *J* = 9.9, 8.4, 3.9 Hz, 1H), 3.84 (ddd, *J* = 10.5, 5.4, 4.2 Hz, 1H), 3.59 (d, *J* = 6.3 Hz, 1H), 2.10–2.00 (m, 1H), 1.94–1.94–1.84 (m, 1H), 0.90 (s, 9H), 0.10 (s, 3H), 0.08 (s, 3H); ^{13}C NMR (125 MHz, CDCl$_3$) δ 132.5, 129.2, 128.4, 121.6, 83.1, 78.3, 73.4, 69.6, 62.3, 60.9, 38.4, 25.9, 18.2, –5.5. EIMS *m/z* 257.1 ([M – *t*–Bu]$^+$, 24), 105.0 ([$C_3H_9O_2Si$]$^+$, 100); HRMS calcd. for $C_{15}H_{17}O_2Si$ (M$^+$) 257.0998, found 257.0995. Anal. calcd. for $C_{19}H_{26}O_2Si$: C, 72.56; H, 8.33. Found: C, 72.20; H, 8.43.

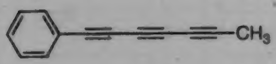

509a

Compound **509a**: Compound **506c** (479 mg, 1.54 mmol), BuLi (2.5 M in hexanes, 1.3 mL, 3.4 mmol), and methyliodide (318 mg, 2.31 mmol) were used as per the general procedure K and yielded **509a** (164 mg, 65%) as a light brown crystalline solid. Spectral data were consistent with those reported.[30]

Single crystals of compound **509a** were grown from a concentrated solution of $CHCl_3$ at 4 °C. Formula: $C_{13}H_8$, $M = 164.19$, monoclinic space group $P2_1/n$ (an alternate setting of $P2_1/c$ [No. 2]), $Dc = 1.158$ g cm^{-3}, $a = 6.1920(8)$, $b = 7.7938(11)$, $c = 19.640(3)$ Å, $\beta = 96.640(2)$, $V = 941.5(2)$ Å^3, $Z = 4$, $\mu = 0.066$ mm^{-1}. Final $R(F) = 0.0400$, $wR2(F^2) = 0.1163$ for 119 variables and 1925 data with $F_o^2 \geq -3\sigma(F_o^2)$ (1415 observations [$F_o^2 \geq 2\sigma(F_o^2)$]).

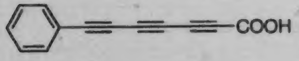

509b

Compound **509b**:[31] Compound **506c** (358 mg, 1.16 mmol), BuLi (2.5 M in hexanes, 1.0 mL, 2.5 mmol) were reacted as per the general procedure K. CO_2, generated from dry ice, was passed through a drying tube filled with $CaCl_2$ and then was bubbled through the reaction mixture via syringe. After quenching the mixture with 10% aq. HCl, it was basicified by using a 10% aq. NaOH. The aqueous layer was separated and neutralized with 10% aq. HCl and Et_2O (5 mL). The mixture was reduced to dryness yielding **509b** (146 mg, 65%) as a brown solid. DSC analysis showed an exothermic peak at 112 °C (dec.).

IR ($CHCl_3$, cast) 2927, 2206, 2182 cm^{-1}; ^1H NMR (400 MHz, $CDCl_3$) δ 7.55–7.53 (m, 2H), 7.43 (dt, $J = 7.4$, 1.6 Hz, 1H), 7.34 (dt, $J = 7.2$, 1.2 Hz, 2H); ^{13}C NMR (125 MHz, $CDCl_3$) δ 155.3, 133.4, 130.6, 128.7, 119.7, 80.7, 73.8, 73.4, 69.7, 67.3, 64.1. HRMS calcd. for $C_{13}H_6O_2$ (M^+) 194.0368, found 194.0370.

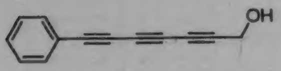

509c

Compound **509c**: Compound **506c** (534 mg, 1.72 mmol), BuLi (1.6 M in hexanes, 2.4 mL, 3.8 mmol), and paraformaldehyde (101 mg, 3.33 mmol) were used as per the general procedure K and yielded **509c** (224 mg, 72%) as a yellow oil. Spectral data were consistent with those reported.[32]

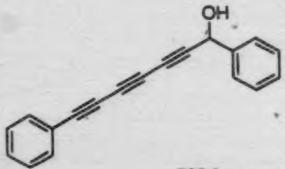

509d

Compound **509d**: Compound **506c** (219 mg, 0.705 mmol), BuLi (2.5 M in hexanes, 0.62 mL, 1.5 mmol), and benzaldehyde (82 mg, 0.77 mmol) were used as per the general procedure K and yielded **509d** (98 mg, 54%) as a yellow oil. R_f = 0.4 (CH_2Cl_2).

IR ($CHCl_3$, cast) 3362, 3063, 2957, 2191 cm^{-1}; ^1H NMR (400 MHz, $CDCl_3$) δ 7.56–7.52 (m, 4H), 7.44–7.32 (m, 6H), 5.57 (s, 1H), 2.28 (br s, 1H); ^{13}C NMR (100 MHz, $CDCl_3$) δ 139.2, 133.0, 129.8, 128.85, 128.84, 128.5, 126.7, 120.7, 78.9, 77.7, 74.1, 71.7, 65.7, 65.2, 64.3. EIMS *m/z* 256.1 (M^+, 88), 226.1 ($[C_{18}H_{10}]^+$, 100); HRMS calcd. for $C_{19}H_{12}O$ (M^+) 256.0888, found 256.0883.

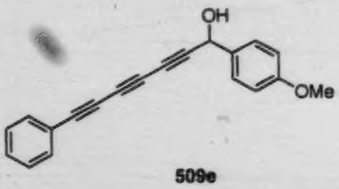

509e

Compound **509e**: Compound **506c** (256 mg, 0.824 mmol), BuLi (2.5 M in hexanes, 0.73 mL, 1.8 mmol), and *p*–anisaldehyde (120 mg, 0.904 mmol) were used as per the general procedure K and yielded **509e** (128 mg, 54%) as a yellow solid. Mp 53–55 °C. R_f = 0.3 (CH_2Cl_2).

IR ($CHCl_3$, cast) 3383, 2837, 2191, 1611, 1512 cm^{-1}; ^{1}H NMR (300 MHz, $CDCl_3$) δ 7.54–7.30 (m, 7H), 6.92 (d, *J* = 9.0 Hz, 2H), 5.51 (d, *J* = 6.0 Hz, 1H), 3.83 (s, 3H), 2.15 (d, *J* = 6.0 Hz, 1H); ^{13}C NMR (125 MHz, $CDCl_3$) δ 160.0, 133.0, 131.6, 129.8, 128.5, 128.2, 120.7, 114.2, 79.2, 77.6, 74.1, 71.4, 65.8, 64.8, 64.2, 55.4; HRMS calcd. for $C_{20}H_{14}O_2$ (M^+) 286.0994, found 286.1002.

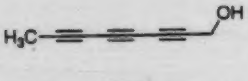

509f

Compound **509f**: Compound **506e** (574 mg, 2.07 mmol), BuLi (2.5 M in hexanes, 1.8 mL, 4.5 mmol), and paraformaldehyde (187 mg, 6.22 mmol) were used as per the general procedure K and yielded **509f** (146 mg, 59%) as a magenta crystalline solid. Spectral data were consistent with those reported.[32]

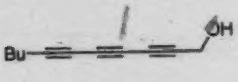

509g

Compound **509g**: Compound **506f** (220 mg, 0.763 mmol), BuLi (2.5 M in hexanes, 0.67 mL, 1.7 mmol), and paraformaldehyde (300 mg, 10 mmol) were used as per the general procedure K and yielded **509g** (67.2 mg, 55%) as a yellow oil. $R_f = 0.3$ (CH_2Cl_2).

IR ($CHCl_3$, cast) 3185, 2959, 2873, 2218, 1465 cm^{-1}; ^{1}H NMR (400 MHz, $CDCl_3$) δ 4.32 (s, 2H), 2.29 (t, *J* = 7.0 Hz, 2H), 1.45–1.35 (m, 2H), 0.89 (t, *J* = 7.2 Hz, 3H); ^{13}C NMR (100 MHz, $CDCl_3$) δ 81.5, 74.6, 71.1, 65.3, 64.3, 58.9, 51.6, 30.0, 21.9, 19.1, 13.4; HRMS calcd. for $C_{11}H_{12}O$ (M^+) 160.0888, found 160.0892.

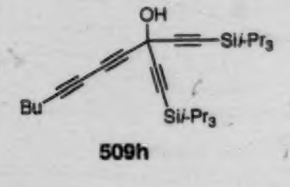

509h

Compound **509h**: Compound **506e** (273 mg, 0.947 mmol) was dissolved in toluene (2 mL) and this solution diluted with hexanes (10 mL) at –20 °C BuLi (2.5 M in hexanes, 0.83 mL, 2.1 mmol), and 1,5–Bis(triisopropyl–silanyl)penta–1,4–diyn–3–one[28] (321 mg, 0.822 mmol) were used as per general procedure K, gave compound **509h** as a brown oil; yield: 370 mg (82%). $R_f = 0.44$ (hexanes/CH_2Cl_2 6:1).

IR ($CHCl_3$, cast) 3435 (w), 2943 (vs), 2866 (vs), 2219 (m), 2155 (w), 1463 (m) cm^{-1}.

^1H NMR (500 MHz, $CDCl_3$) 2.75 (br s, 1H), 2.30 (t, $J = 7.0$ Hz, 2H), 1.54–1.48 (m, 2H), 1.44–1.36 (m, 2H), 1.06 (s, 42H), 0.89 (t, $J = 7.0$ Hz, 3H).

^{13}C NMR (125 MHz, $CDCl_3$) 102.7, 85.9, 82.3, 72.6, 67.8, 66.1, 65.3, 58.6, 54.8, 29.9, 21.9, 19.1, 18.5, 13.4, 11.1; EIMS *m/z* 477.3 ($[M - i\text{–}Pr]^+$, 17); HRMS *m/z* ($[M - i\text{–}Pr]^+$) calcd for $C_{30}H_{45}OSi_2$: 477.3009; found: 477.3019.

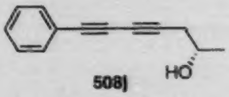

508j

Compound **508j**: Compound **506a** (201 mg, 0.703 mmol), BuLi (2.5 in hexanes, 0.62 mL, 1.6 mmol) and (*S*)–(–)–propylene oxide (Aldrich, 49 mg, 0.06 mL, 0.84 mmol) were used as per the general procedure K and yielded (–)–**508j** (45 mg, 30%) as a yellow oil. $R_f = 0.2$ (hexanes). $[\alpha]^{20}_D$ –9.3 (c 1.31, MeOH).

IR ($CHCl_3$) 3356, 3055, 2971, 2230 cm^{-1}; ^1H NMR (400 MHz, $CDCl_3$) δ 7.50 (dd, $J =$ 8.0, 1.3 Hz, 2H), 7.35–7.26 (m, 3H), 4.04–3.99 (m, 1H), 2.55 (A part of ABX, $J = 17.2$, 5.6 Hz, 1H), 2.52 (B part of ABX, $J = 17.2$, 5.6 Hz, 1H), 1.87 (bd, $J = 4.0$ Hz, 1H), 1.29 (d, $J = 6.4$ Hz, 3H); ^{13}C NMR (100 MHz, $CDCl_3$) δ 1[illegible]2.5, 129.0, 128.4, 121.8, 80.7, 75.4, 74.0, 67.4, 66.4, 30.2, 22.6. EIMS *m/z* 184.1 (M^+, 32), 347.2 ($[C_{11}H_8]^+$, 100);

HRMS cacld. for $C_{13}H_{12}O$ (M^+) 184.0888, found 184.0887. Spectral data were consistent with that reported for the (+)–enantiomer reported.[33]

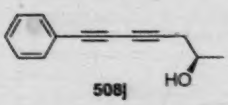
508j

Compound **508j**: Compound **506a** (237 mg, 0.830 mmol), BuLi (2.5 M in hexanes, 0.73 mL, 1.8 mmol) and *R*–(+)–propylene oxide (mg, 0.05 mL, 0.71 mmol) were used as per the general procedure K and yielded (+)–**508j** (27 mg, 20%) as a yellow oil. R_f = 0.2 (hexanes). $[\alpha]^{20}_{D}$ +6 (c 0.55, MeOH). Spectra were consistent with compound **508j**.[33]

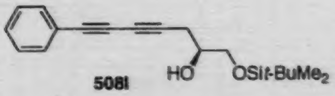
508l

Compound **508l**: Compound **506a** (213 mg, 0.746 mmol) was dissolved in toluene (2 mL), followed by the addition of hexanes (10 mL), BuLi (2.5 M in hexanes, 0.66 mL, 1.7 mmol), and (*R*)–(+)–glycidyl ether (Aldrich, 0.13 g, 0.14 mL, 0.68 mmol, dissolved in 2 mL of Et_2O) and HMPA (0.3 mL) were used as per the general procedure K and yielded **508l** (47 mg, 22%) as a light brown oil. R_f = 0.25 (hexanes/CH_2Cl_2 1:1). $[\alpha]^{20}_{D}$ –7.3 (c 0.24, MeOH).

IR ($CHCl_3$, cast) 3429, 3063, 2929, 2247 cm^{-1}; ^1H NMR (300 MHz, $CDCl_3$) δ 7.46 (dd, *J* = 8.0, 1.3 Hz, 2H), 7.34–7.26 (m, 3H), 3.87–3.82 (m, 1H), 3.72 (dd, *J* = 10.0, 4.0 Hz, 1H), 3.63 (dd, *J* =10.0, 5.6 Hz, 1H), 2.60 (A part of ABM, *J* = 17.6 Hz, 1H), 2.57 (B part of ABM, *J* = 17.6 Hz, 1H), 2.47 (d, *J* = 5.6 Hz, 1H), 0.90 (s, 9H), 0.08(7) (s, 3H), 0.85 (s, 3H); ^{13}C NMR (125 MHz, $CDCl_3$) δ 132.5, 128.9, 128.3, 121.9, 80.3, 75.3, 74.1, 70.1, 66.0, 65.6, 25.8, 24.4, 18.2, –5.40, –5.42. EIMS *m/z* 314.2 (M^+. 1). 257/1 ([M – *t*–Bu]$^+$, 45), 141.1 ($[C_{11}H_9]^+$, 100); HRMS calcd. for $C_{19}H_{26}O_2Si$ (M^+) 314.1702, found 314.1700. Anal. calcd. for $C_{19}H_{26}O_2Si$: C, 72.56; H, 8.33. Found: C, 72.06; H, 8.33.

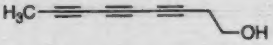

509l

Compound **509j**: Compound **506e** (451 mg, 1.82 mmol), BuLi (2.5 M in hexanes, 1.6 mL, 4.0 mmol), and THF (4 mL) was added into the mixture instead of Et_2O. To the reaction above, mixture of oxirane (2 mL, 40 mmol) in NH_3 (5 mL) at –20 °C was transferred via a canula. The reaction was warmed to rt overnight. Quenching was followed the general procedure K described above yielding **509j** (140 mg, 58%) as a white crystal turned purple exposed to light. Spectra were consistent with those of **204** in Chapter 2.

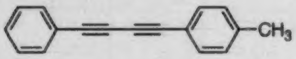

511a

Compound **511a**:[34] Compound **506a** (286 mg, 0.998 mmol), BuLi (2.5 M in hexanes, 0.90 mL, 2.3 mmol), $ZnCl_2$ (0.5 M in THF, 2.4 mL, 1.2 mmol), *p*–tolyl iodide (260 mg, 1.19 mmol), and $Pd(PPh_3)_4$ (57 mg, 0.049 mmol) were used as per the general procedure L and yielded **511a** (195 mg, 90%) as a white solid.

^{1}H NMR (400 MHz, $CDCl_3$) δ 7.53–7.51 (m, 2H), 7.42 (d, J = 8.0 Hz, 2H), 7.36–7.30 (m, 3H), 7.14 (d, J = 8.0 Hz, 2H), 2.36 (s, 3H); ^{13}C NMR (100 MHz, $CDCl_3$) δ 139.6, 132.5, 132.4, 129.2, 129.1, 128.4, 121.9, 118.7, 81.9, 81.2, 74.1, 73.3, 21.6.

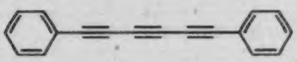

511b

Compound **511b**: Compound **506a** (150 mg, 0.484 mmol), BuLi (2.5 M in hexanes, 0.45 mL, 1.1 mmol), $ZnCl_2$ (0.5 M in THF, 1.2 mL, 0.60 mmol), phenyl iodide (121 mg, 0.593

mmol), and $Pd(PPh_3)_4$ (27.7 mg, 0.024 mmol) were used as per the general procedure L and yielded **511b** (76.1 mg, 0.337 mmol, 70%) as a white solid. Spectral data were consistent with those reported.[3]

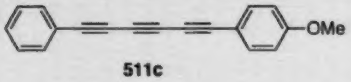

511c

Compound **511c**: Compound **506c** (309 mg, 0.996 mmol), BuLi (2.5 M in hexanes, 0.90 mL, 2.3 mmol), $ZnCl_2$ (0.5 M in THF, 2.4 mL, 1.2 mmol), *p*–iodoanisole (255 mg, 1.09 mmol), and $Pd(PPh_3)_4$ (56 mg, 0.049 mmol) were used as per the general procedure L and yielded **511c** (203 mg, 0.793 mmol, 80%) as an orange solid. Mp 120–121 °C. $R_f = 0.6$ (hexanes/CH_2Cl_2 3:2).

IR ($CHCl_3$, cast) 2194, 2174 cm^{-1}; ^1H NMR (400 MHz, $CDCl_3$) δ 3.84 (s, 3H), 6.87 (d, $J = 8.8$ Hz, 2H), 7.34–7.40 (m, 3H), 7.50 (d, $J = 8.8$ Hz, 2H), 7.54 (d, $J = 8.0$ Hz, 2H); ^{13}C NMR (100 MHz, $CDCl_3$) δ 55.3, 66.0, 66.8, 73.4, 74.6, 78.3, 79.0, 112.8, 114.2, 121.1, 128.5, 129.6, 132.9, 134.7, 160.8. HRMS calcd. for $C_{19}H_{12}O$ (M^+) 256.0888, found 256.0882. Anal. calcd. for $C_{19}H_{12}O$: C, 89.04; H, 4.72. Found: C, 89.05; H, 4.69.

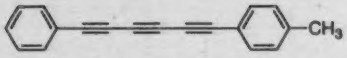

511d

Compound **511d**: Compound **506c** (312 mg, 1.01 mmol), BuLi (2.5 M in hexanes, 1.0 mL, 2.5 mmol), $ZnCl_2$ (0.5 M in THF, 2.5 mL, 1.3 mmol), *p*–iodotoluene (234 mg, 1.07 mmol), and $Pd(PPh_3)_4$ (58 mg, 0.051 mmol) were used as per the general procedure L and yielded **511d** (195 mg, 0.812 mmol, 70%) as a white solid. Mp 111–112 °C. $R_f = 0.6$ (hexanes/CH_2Cl_2 3:1).

IR ($CHCl_3$, cast) 3081, 3018, 2247, 2195 cm^{-1}; ^1H NMR (400 MHz, $CDCl_3$) δ 2.38 (s, 3H), 7.12 (d, $J = 8.0$ Hz, 2H), 7.32–7.40 (m, 3H), 7.42 (d, $J = 8.0$ Hz, 2H), 7.52 (d, $J =$

8.0 Hz, 2H); ^{13}C NMR (100 MHz, $CDCl_3$) δ 21.7, 66.2, 66.7, 73.9, 74.5, 78.4, 79.0, 117.8, 121.1, 128.5, 129.3, 129.6, 132.9 (2x), 140.2. HRMS calcd. for $C_{19}H_{12}$ (M^+) 240.0939, found 240.0934. Anal. calcd. for $C_{19}H_{12}$: C, 94.97; H, 5.05. Found: C, 95.05; H, 5.08.

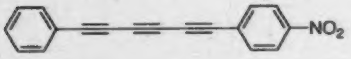

511e

Compound **511e**: Compound **506c** (233 mg, 0.752 mmol), BuLi (2.5 M in hexanes, 0.70 mL, 1.8 mmol), $ZnCl_2$ (0.5 M in THF, 1.7 mL, 0.85 mmol), *p*–iodonitrobenzene (222 mg, 0.891 mmol), and $Pd(PPh_3)_4$ (40 mg, 0.035 mmol) were used as per the general procedure L and yielded **511e** (171 mg, 0.631 mmol, 84%) as a yellow solid. Mp 205 °C (dec.). R_f = 0.3 (hexanes/CH_2Cl_2 7:3).

IR ($CHCl_3$, cast) 3103, 3066, 2190, 2174 cm^{-1}; ^{1}H NMR (400 MHz, $CDCl_3$) δ 7.34–7.42 (m, 3H), 7.53 (t, J = 7.2 Hz, 2H), 7.66 (d, J = 8.8 Hz, 2H), 8.19 (d, J = 8.8 Hz, 2H); ^{13}C NMR (100 MHz, $CDCl_3$) δ 65.5, 69.2, 74.1, 75.9, 79.3, 80.2, 120.6, 123.8, 128.1, 128.6, 130.2, 133.1, 133.7, 147.8. HRMS calcd. for $C_{18}H_9NO_2$ (M^+) 271.0633, found 271.0635.

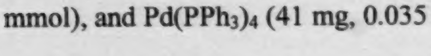

511f

Compound **511f**: Compound **506d** (250 mg, 0.683 mmol), BuLi (1.6 M in hexanes, 1.0 mL, 1.6 mmol), $ZnCl_2$ (0.5 M in THF, 1.5 mL, 0.75 mmol), iodotoluene (150 mg, 0.688 mmol), and $Pd(PPh_3)_4$ (41 mg, 0.035 mmol) were used as per the general procedure L and yielded **511f** (123 mg, 0.414 mmol, 60%) as a pale yellow solid. Mp 175 °C (dec.). R_f = 0.6 (hexanes/CH_2Cl_2 4:1).

IR ($CHCl_3$, cast) 3084, 3038, 2962, 2248, 2193 cm^{-1}; ^{1}H NMR (400 MHz, $CDCl_3$) δ 1.30 (s, 9H), 2.35 (s, 3H), 7.12 (d, J = 7.6 Hz, 2H), 7.34 (d, J = 7.6 Hz, 2H), 7.41 (d, J = 8.4

Hz, 2H), 7.45 (d, J = 8.4 Hz, 2H); ^{13}C NMR (100 MHz, $CDCl_3$) δ 21.7, 31.1, 35.0, 66.3, 66.4, 74.0 (2x), 78.8, 78.9, 117.9 (2x), 125.5, 129.3, 132.8, 132.9, 140.1, 153.2. EIMS *m/z* 296.2 (M^+, 86), 281.1 ($[M - CH_3]^+$, 100]); HRMS calcd. for $C_{23}H_{20}$ (M^+) 296.1565, found 296.1553. Anal. calcd. for $C_{23}H_{20}$: C, 93.20; H, 6.80. Found: C, 92.91; H, 6.91.

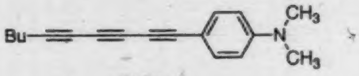

511g

Compound **511g**: Compound **506f** (259 mg, 0.899 mmol), BuLi (2.5 M in hexanes, 0.79 mL, 2.0 mmol), $ZnCl_2$ (0.5 M in THF, 2.2 mL, 1.1 mmol), *4*–iodo–*N,N*–dimethylaniline (202 mg, 0.818 mmol) and $Pd(PPh_3)_4$ (60 mg, 0.052 mmol) mmol were used as per the general procedure L and yield **511g** (53 mg, 24%) as a yellow solid. Mp 148–150 °C; R_f = 0.45 (hexanes/CH_2Cl_2 2:1).

IR (μscope) 3774, 2965, 2820, 2209, 2176, 2095, 1891 cm^{-1}; ^{1}H NMR (400 MHz, $CDCl_3$) δ 7.36 (d, J = 8.8 Hz, 2H), 6.56 (d, J = 8.8 Hz, 2H), 1.56–1.49 (m, 2H), 1.45–1.36 (m, 2H), 2.97 (s, 6H), 2.31 (t, J = 7.2 Hz, 2), 0.90 (t, J = 7.2 Hz, 3H); ^{13}C NMR (100 MHz, $CDCl_3$) δ 150.7, 134.3, 111.6, 107.1, 82.1, 73.1, 66.8, 65.9, 60.4, 40.1, 30.2, 21.9, 19.3, 13.5; HRMS calcd. for $C_{18}H_{19}N$ (M^+) 249.1518, found 249.1519. Anal. calcd. for $C_{18}H_{19}N$: C, 86.70; H, 7.68; N, 5.62. Found: C, 86.84; H, 7.94; N, 5.63.

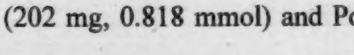

511h

Compound **511h**: Compound **506g** (390 mg, 1.00 mmol), BuLi (1.6 M in hexanes, 1.5 mL, 2.4 mmol), $ZnCl_2$ (0.5 M in THF, 2.5 mL, 1.3 mmol), *p*–iodotoluene (220 mg, 1.01 mmol), and $Pd(PPh_3)_4$ (57 mg, 0.049 mmol) were used as per the general procedure L and yielded **511h** (221 mg, 69%) as a white solid. Mp 69 °C. R_f = 0.7 (hexanes/CH_2Cl_2 4:1).

IR ($CHCl_3$, cast) 2891, 2178, 2072 cm^{-1}; ^1H NMR (400 MHz, $CDCl_3$) δ 1.11 (s, 21H), 2.37 (s, 3H), 7.14 (d, *J* = 8.4 H, 2H), 7.41 (d, *J* = 8.4 H, 2H); ^{13}C NMR (100 MHz, $CDCl_3$) δ 11.3, 18.5, 21.6, 60.8, 67.0, 73.8, 76.9, 86.4, 89.9, 117.7, 129.3, 133.0, 140.2. EIMS *m/z* 320.2 (M^+, 34), 277.1 ($[M - i\text{–}Pr]^+$, 100); HRMS calcd. for $C_{22}H_{28}Si$ (M^+) 320.1960, found 320.1958. Anal. calcd. for $C_{22}H_{28}Si$: C, 82.43; H, 8.80. Found: C, 82.60; H, 8.83.

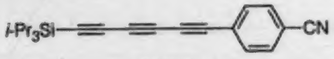

511l

Compound **511i**: Compound **506g** (632 mg, 1.62 mmol), BuLi (2.5 M in hexanes, 1.40 mL, 3.5 mmol), $ZnCl_2$ (0.5 M in THF, 4.9 mL, 12.3 mmol), *4*–iodo–benzonitrile (370 mg, 1.62 mmol) and $Pd(PPh_3)_4$ (60 mg, 0.052 mmol) mmol were used as per the general L procedure and yield **511i** (419 mg, 78%) as a brown crystalline solid. Mp 94–96 °C; R_f = 0.5 (hexanes/CH_2Cl_2 1:1).

IR (μscope) 2944, 2866, 2228, 2073, 1600 cm^{-1}; ^1H NMR (500 MHz, $CDCl_3$) δ 7.58 (obs q, *J* = 8.5 Hz, 4H), 1.08 (s, 21H); ^{13}C NMR (125 MHz, $CDCl_3$) δ 132.4, 132.1, 125.9, 118.1, 112.9, 89.3, 88.7, 78.4, 74.1, 69.4, 59.6, 18.5, 11.3; EIMS *m/z* 318.2 (M^+, 23), 288.1 ($[M - i\text{–}Pr]^+$, 100); HRMS calcd. for $C_{22}H_{25}SiN$ (M^+) 318.1756, found 318. 1755

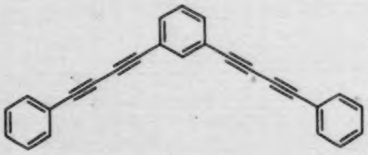

511j

Compound **511j**: Compound **506a** (215 mg, 0.752 mmol), BuLi (2.5 M in hexanes, 0.66 mL, 1.7 mmol), $ZnCl_2$ (0.5 M in THF, 1.8 mL, 0.9 mmol), 1,3–diiodobenzene (110 mg, 320 mmol) and $Pd(PPh_3)_4$ (60 mg, 0.052 mmol) mmol were used as per the general procedure L and yield **511j** (71.1 mg, 64%) as a yellow solid. Mp 115–117 °C. $R_f = 0.3$ (hexanes/CH_2Cl_2 6:1).

IR (μscope) 3062, 2220, 1589 cm^{-1}; ^1H NMR (500 MHz, $CDCl_3$) δ 7.65–7.64(6) (m, 1H), 7.54–7.48 (m, 7H), 7.39–7.29 (m, 8H); ^{13}C NMR (125 MHz, $CDCl_3$) δ 136.1, 133.0, 132.6, 129.4, 128.7, 128.5, 122.5, 121.6, 82.1, 80.2, 74.8, 73.7; HRMS calcd. for $C_{26}H_{14}$ (M^+) 313.1096, found 313.1099.

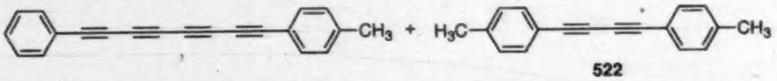

521

522

Compounds **521 and 522**: Compound **506c** (310 mg, 1.00 mmol), BuLi (1.6 M in hexanes, 1.5 mL, 2.1 mmol), $ZnCl_2$ (0.5 M in THF, 2.5 mL, 1.3 mmol), 1–iodo–2–phenylethyne (251 mg, 1.15 mmol), and $Pd(PPh_3)_4$ (53.5 mg, 0.046 mmol) were used as per the general procedure L and yielded **521** (90.0 mg, 34%) as a yellow solid homocoupling product **522** (50.7 mg, 24%).

Compound 521. Mp 93–94 °C. $R_f = 0.6$ (hexanes/CH_2Cl_2 4:1).

IR ($CHCl_3$, cast) 2200, 2130 cm^{-1}; ^1H NMR (400 MHz, $CDCl_3$) δ 2.36 (s, 3H), 7.13 (d, J = 7.9 Hz, 2H), 7.32 (t, J = 7.2 Hz, 2H), 7.39 (t, J = 7.2 Hz, 1H), 7.42 (d, J = 8.0 Hz, 2H), 7.52 (d, J = 8.0 Hz, 2H); ^{13}C NMR (100 MHz, $CDCl_3$) δ 21.7, 63.5, 63.9, 66.9, 67.3, 73.9, 74.5, 77.6, 78.1, 117.3, 120.6, 128.5, 129.4, 130.0, 133.2 (2x), 140.6. HRMS calcd. for $C_{21}H_{12}$ (M^+) 264.0939, found 264.0936. Anal. calcd. for $C_{21}H_{12}$: C, 95.42; H, 4.58. Found: C, 95.66; H, 4.62.

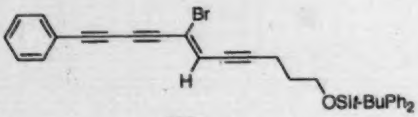

525

Compound **525**: To **506a** (151 mg, 0.528 mmol) dissolved in toluene (10 mL) at –40 °C was added BuLi (2.5 M in hexanes, 0.46 mL, 1.2 mmol) dropwise. The mixture was warmed to 0 °C for 5 min, and then cooled to –10 °C. $ZnCl_2$ (0.5 M in THF, 1.16 mL, 0.56 mmol) was added and the mixture stirred for 1 h. To the mixture, **S501** (240 mg, 0.474 mmol), $Pd(PPh_3)$ (61 mg, 0.053 mmol), Et_3N (0.08 mL, 0.58 mmol) were added and the reaction was heated to 65 °C and maintained at this temperature for 2 days, yielding **525** (145 mg, 55%) as a colorless oil. $R_f = 0.4$ (hexanes/CH_2Cl_2 3:1).

IR ($CHCl_3$, cast) 3070 (w), 2930, 2857, 2214, 1442 cm^{-1}; ^1H NMR (500 MHz, $CDCl_3$) δ 7.66 (d, $J = 7.9$ Hz, 4H), 7.49 (d, $J = 8.4$ Hz, 2H), 7.43–7.32 (m, 9H), 6.43 (t, $J = 2.3$ Hz, 1H), 3.78 (t, $J = 6.0$ Hz, 2H), 2.57 (dt, $J = 2.3$, 6.9 Hz, 2H), 1.82 (quint, 6.4 Hz, 2H), 1.05 (s, 9H); ^{13}C NMR (125 MHz, $CDCl_3$) δ 135.6, 133.8, 132.6, 129.8, 129.6, 128.5, 127.7, 122.2, 121.1, 108.4, 105.5, 86.4, 79.4, 78.8, 78.7, 73.0, 62.2, 31.2, 26.9, 19.3, 16.8. ESI MS calcd. for $C_{33}H_{31}OSiBrNa$ $(M + Na)^+$ 573.1220, found 573.1216.

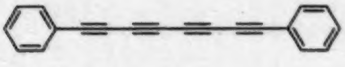

513a

Compound **513a**: Compound **506a** (175 mg, 0.617 mmol), BuLi (2.5 M in hexanes, 0.54 mL, 1.4 mmol), CuBr (88 mg, 0.61 mmol) and TMEDA (2 mL, 13 mmol) were used as per the general procedure M and yielded **513a** (54 mg, 69%) as a yellow oil. $R_f = 0.6$ (hexanes/CH_2Cl_2 6:1).

IR ($CHCl_3$, cast) 3061(w), 2202, 1442 cm^{-1}; ^1H NMR (400 MHz, $CDCl_3$) δ 7.52 (d, 7.2 Hz, 4H), 7.39 (t, 7.4 Hz, 3H), 7.32 (t, 7.2Hz, 4H); ^{13}C NMR (100 MHz, $CDCl_3$) δ 133.2, 130.0, 128.5, 120.5, 77.7, 74.4, 67.2, 63.7. HRMS calcd. for $C_{20}H_{10}$ (M^+) 250.0783, found 250.0783. Spectral data were consistent with those of **410** in Chapter 4.

Single crystals were grown from slow evaporation of a $CHCl_3$ at –4 °C. $C_{20}H_{10}$, M = 250.28, monoclinic space group *P*2$_1$/*n* (an alternate setting of *P*2$_1$/*c* [No. 14]), D_c = 1.211 g cm^{-3}, *a* = 10.7824(12) Å, *b* = 3.9194(5) Å, *c* = 16.901(2) Å, β = 106.0485(17) Å, *V* = 686.39(14) Å^3, *Z* = 2, μ = 0.069 (mm^{-1}), T = –80 °C. Final $R_1(F)$ = 0.0322, $wR^2(F^2)$ = 0.1041 for 92 variables and 4905 data with $F_o^2 \geq -3\sigma(F^2)$ (1.047 [$F_o^2 \geq -3\sigma(F_o^2)$]

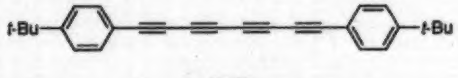

513b

Compound **513b**: Compound **506a** (245 mg, 0.717 mmol), BuLi (2.5 M in hexanes, 0.63 mL, 1.6 mmol), CuBr (100 mg, 0.697 mmol) and TMEDA (2 mL, 13 mmol) were used as per the general procedure M and yielded **513b** (121 mg, 93%) as a crystalline solid. Mp >210 °C; R_f = 0.6 (hexanes/CH_2Cl_2 6:1).

IR ($CHCl_3$, cast) 2945, 2867, 2202, 2134, 2070, 1919, 1599 cm^{-1}; ^{1}H NMR (400 MHz, $CDCl_3$) δ 7.46 (d, *J* = 8.6 Hz, 4H), 7.34 (d, *J* = 8.6 Hz, 4H), 1.29 (s, 18H); ^{13}C NMR (100 MHz, $CDCl_3$) δ 153.5, 132.9, 125.5, 117.3, 77.9, 73.9, 66.9, 63.6, 34.9, 30.9; EIMS *m/z* 362.2 (M$^+$, 99), 347.2 ([M – CH_3]$^+$, 100) HRMS calcd. for $C_{28}H_{26}$ (M$^+$) 362.2035, found 362.2036.

Single crystals were grown from slow evaporation of a $CHCl_3$ at –4 °C. $C_{28}H_{26}$, M = 362.49, monoclinic space group *I2/a* (a nonstandard setting of *C2/c* [No. 60]), D_c = 1.076 g cm^{-3}, *a* = 23.638(2) Å, *b* = 9.4832(9) Å, *c* = 21.160(2) Å, β = 109.3298(19) Å, *V* = 4476.1(8) Å^3, *Z* = 8, μ = 0.060 (mm^{-1}), T = –80 °C. Final $R_1(F)$ = 0.0322 $wR^2(F^2)$ = 0.1778 for 280 variables and 4582 data with $F_o^2 \geq -3\sigma(F^2)$ (2111 [$F_o^2 \geq -2\sigma(F_o^2)$]

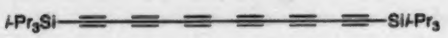

513c

Compound **513c**:[10] Compound **506g** (301 mg, 0.771 mmol), BuLi (2.5 M in hexanes, 0.68 mL, 1.70 mmol), CuBr (110 mg, 0.767 mmol) and TMEDA (2 mL, 13 mmol) were used as per the general procedure M and yielded **513c** (121 mg, 68%) as a colorless oil. $R_f = 0.9$ (hexanes).

IR ($CHCl_3$, cast) 2945, 2867, 2159(w), 2031(w), 1462 cm^{-1}; ^1H NMR (400 MHz, CD_2Cl_2) δ 1.10 (s, 42H); ^{13}C NMR (100 MHz, $CDCl_3$) δ 89.5, 88.0, 63.0, 62.8, 62.5, 61.2, 18.6, 11.7; EIMS *m/z* 458.3 (M^+, 31), 415.2 ($[M - i\text{-}Pr]^+$, 100) HRMS calcd. for $C_{30}H_{42}Si_2$ (M^+) 458.2825, found 458.2826.

The synthesis of compounds **515a–f** was done by Dr. Yasuhiro Morisaka as part of our collaboration on this project, and details have been reported.[23]

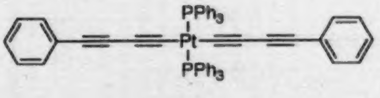

516a

Compound **516a**: Compound **506a** (0.212 g, 0.747 mmol) in toluene (10.0 mL), BuLi (2.5 M in hexanes, 0.66 mL, 1.65 mmol), CuI (0.18 g, 0.945 mmol), *cis*–$PtCl_2(PPh_3)_2$ (0.290 g, 0.367 mmol) were used as per the general procedure O and purified by column chromatography (silica gel, hexanes/CH_2Cl_2 1:1) afforded **516a** (0.312 g, 91%) as an off–white solid.

IR (μscope) 3076, 2182, 2064, 1593, 1434 cm^{-1}; ^1H NMR (500 MHz, CD_2Cl_2) δ 7.78–7.73 (m, 12H), 7.50–7.45 (m, 18H); ^{13}C NMR (100 MHz, CD_2Cl_2) δ 135.3 (psuedo–t, $^2J_{C\text{-}P} = 6$ Hz), 132.3, 131.1 (psuedo–t, $^1J_{C\text{-}P} = 30$ Hz), 130.8, 128.5 (psuedo–t, $^3J_{C\text{-}P} = 5$ Hz), 127.7, 124.3, 110.5, 95.4, 78.4, 71.7, (one coincident signal and $^1J_{C\text{-}Pt}$ coupling for alkynyl carbons not observed due to low S/N because of insolubility); ^{31}P NMR (162 MHz, CD_2Cl_2) δ 19.2 (psuedo–t, J_{P-Pt} = 2570 Hz); MALDI MS (CH_2Cl_2) HRMS calcd. for $C_{56}H_{40}P_2Pt$ (M^+) 969.2253, found 969.2258.

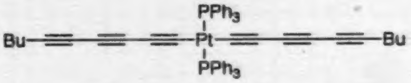

$$\mathrm{Bu{-}C{\equiv}C{-}C{\equiv}C{-}C{\equiv}C{-}\underset{PPh_3}{\overset{PPh_3}{Pt}}{-}C{\equiv}C{-}C{\equiv}C{-}C{\equiv}C{-}Bu}$$

516b

Compound **516b**. Compound **506f** (0.152 g, 0.525 mmol) in toluene (10.0 mL), BuLi (1.6 M in hexanes, 0.72 mL, 1.15 mmol), CuI (0.119 g, 0.599 mmol), *cis*–$PtCl_2(PPh_3)_2$ (0.208 g, 0.263 mmol) were used as per the general procedure O and recrystalized from CH_2Cl_2 by the addition of hexanes to give **516b** as a light yellow powder (0.210 g, 82%). Mp ca. 200 °C (dec.). R_f = 0.3 (hexanes/CH_2Cl_2 2:1).

IR (μscope) 3076, 2955, 2930, 2143, 2041 cm^{-1}; ^{1}H NMR (500 MHz, CD_2Cl_2) δ 7.68–7.64 (m, 12H), 7.50–7.41 (m, 18H), 2.18 (t, J = 7.0, 4H), 1.45–1.39 (m, 4H), 1.36–1.29 (m, 4H), 0.85 (t, J = 7.2 Hz, 6H); ^{13}C NMR (125 MHz, CD_2Cl_2) δ 135.2 (psuedo–t, $^2J_{C-P}$ = 6 Hz), 131.3, 130.5 (t, ^1J = 30 Hz), 128.5 (psuedo–t, $^3J_{C-P}$ = 5 Hz), 105.2 (pseudo–t, $^2J_{C-P}$ = 15 Hz), 95.4 ($^2J_{C-Pt}$ = 265 Hz), 78.1, 66.7, 63.7, 57.2, 30.8, 22.3, 19.5, 13.7; ^{31}P NMR (162 MHz, CD_2Cl_2) δ 19.1 (psuedo–t, $^1J_{P-Pt}$ = 2540 Hz). MALDI MS (CH_2Cl_2) 977.4 for $C_{56}H_{48}P_2Pt$ (M^+).

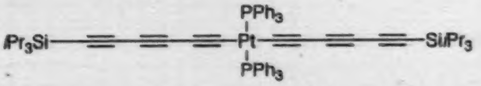

$$\mathrm{\mathit{i}Pr_3Si{-}C{\equiv}C{-}C{\equiv}C{-}C{\equiv}C{-}\underset{PPh_3}{\overset{PPh_3}{Pt}}{-}C{\equiv}C{-}C{\equiv}C{-}C{\equiv}C{-}Si\mathit{i}Pr_3}$$

516c

Compound **516c**: Compound **506g** (0.196 g, 0.503 mmol), BuLi (2.5 M in hexanes, 0.45 mL, 1.12 mmol), CuI (0.125 g, 0.656 mmol), *cis*–$PtCl_2(PPh_3)_2$ (0.199 g, 0.252 mmol) were used as per the general procedure O and recrystalized from MeOH to give **516c** as a white powder (0.219 g, 74%). Mp ca. 240 °C (dec.). R_f = 0.5 (hexanes/CH_2Cl_2 1:1).

IR (μscope) 3060, 2945, 2865, 2150, 2019 cm^{-1}; ^{1}H NMR (400 MHz, CD_2Cl_2) δ 7.67–7.61 (m, 12H), 7.45–7.37 (m, 18H), 1.03–100 (m, 42H); ^{13}C NMR (100 MHz, CD_2Cl_2) δ 135.0 (psuedo–t, $^2J_{C\text{–}P}$ = 6.3 Hz), 131.1, 130.1 (t, $^1J_{C\text{–}P}$ = 30 Hz), 128.3 (psuedo–t, $^3J_{C\text{–}P}$ = 5 Hz), 107.5 (pseudo–t, $^2J_{C\text{–}P}$ = 15 Hz), 94.9, 91.5, 80.8, 64.6, 57.4, 18.5, 11.5; ^{31}P NMR (162 MHz, CD_2Cl_2) δ 19.3 (psuedo–t, $^1J_{P\text{–}Pt}$ = 2525 Hz). ESMS ($C_{66}H_{72}Si_2P_2PtAg$) *m/z* 1284 ([M+Ag]$^+$); ES HRMS *m/z* calcd. for $C_{66}H_{72}Si_2P_2PtAg$ 1284.3341 found 1284.3341.

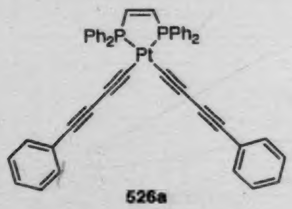

526a

Compound **526a**: Compound **516a** (29.0 mmg, 0.0299 mmol), dppe (12.0 mg, 0.030 mmol) in CH_2Cl_2 (5 mL) were used as per the general procedure P, yielding **526a** (24.1 mg, 96%) as a white solid. Mp 145 °C. R_f = 0.3 (hexanes/CH_2Cl_2 1:2)

IR (CH_2Cl_2, cast) 3055 (w), 2185, 2067 cm^{-1}; ^{1}H NMR (500 MHz, CD_2Cl_2) δ 7.79–7.75 (m, 8H), 7.55–7.50 (m, 13H), 7.43–7.41 (m, 5H), 7.27–7.26 (m, 6H); ^{13}C NMR (125 MHz, CD_2Cl_2) δ 146.7 (pseudo–dd, $^1J_{C\text{–}P}$ = 46 Hz, $^2J_{C\text{–}P}$ = 25 Hz), 133.8–133.6 (m), 132.7 (s), 132.2 (s), 129.6, 129.6–129.5 (m), 128.6 (s), 128.1 (s), 124.1 (s), 103.7 (dd, $^2J_{C\text{–}P}$ = 148.1 Hz for *trans*, $^2J_{C\text{–}P}$ = 16 Hz for *cis*), 93.2 (pseudo–td, $^2J_{C\text{–}Pt}$ = 143 Hz, $^3J_{C\text{–}P}$ = 37 Hz), 77.9 (s), 72,7 (s); ^{31}P NMR (162 MHz, CD_2Cl_2) δ 53.5 (pseudo–t, $J_{P\text{–}Pt}$ = 2298 Hz); MALDI MS (CH_2Cl_2) HRMS calcd. for $C_{46}H_{32}P_2PtNa$ ([M + Na]$^+$) 864.1519, found 864.1520.

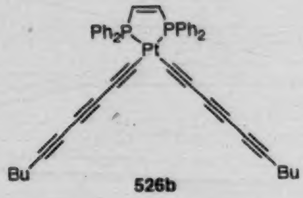

526b

Compound **526b**: Compound **516b** (19.0 mmg, 0.0194 mmol), dppe (7.6 mg, 0.0192 mmol) in CH_2Cl_2 (2.5 mL) were used as per the general procedure P, yielding **526b** (10.6 mg, 65%) as a light yellow solid. Mp 93–95 °C. $R_f = 0.3$ (hexanes/CH_2Cl_2 1:1)

IR (CH_2Cl_2, cast) 3056, 2931, 2146, 2044 cm^{-1}; ^{1}H NMR (400 MHz, CD_2Cl_2) δ 7.70–7.63 (m, 8H), 7.50–7.40 (m, 14H), 2.18 (t, $J = 7.0$ Hz, 4H), 1.45–1.25 (m, 8H), 0.85 (t, $J = 7.3$ Hz, 6H); ^{13}C NMR (125 MHz, CD_2Cl_2) δ 146.9 (pseudo–dd, $^1J_{C\text{–}P} = 50$ Hz, $^2J_{C\text{–}P} = 25$ Hz), 133.7–133.5 (m), 132.3 (s), 129.6–129.5 (m), 129.3, 128.8 (t, $J = 12$ Hz), 98.9 (dd, $^2J_{C\text{–}P} = 148$ Hz for *trans*, $^2J_{C\text{–}P} = 16$ Hz for *cis*), 93.7 (pseudo–td, $^2J_{C\text{–}Pt} = 160$ Hz, $^3J_{C\text{–}P} = 35$ Hz), 78.9 (s), 66.6 (s), 63.3 (pseudo–t, $^3J_{C\text{–}Pt} = 40$ Hz), 58.3 (s), 30.8, 22.3, 19.5, 13.7; ^{31}P NMR (162 MHz, CD_2Cl_2) δ 53.7 (pseudo–t, $J_{P\text{–}Pt} = 2294$ Hz); MALDI MS (CH_2Cl_2) 849.2 (M$^+$).

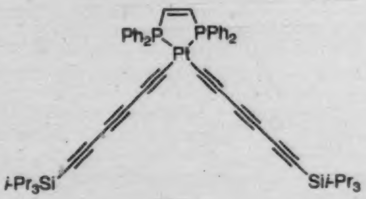

526c

Compound **526c**: Compound **516c** (23.7 mmg, 0.0201 mmol), dppe (7.11 mg, 0.0181 mmol) in CH_2Cl_2 (5 mL) were used as per the general procedure P, yielding **526c** (18.4 mg, 97%) as a white solid. Mp ca. 240 °C (dec.). $R_f = 0.2$ (hexanes/CH_2Cl_2 2:1)

IR (CH_2Cl_2, cast) 3054, 2185, 2067, 1436 cm^{-1}; ^{1}H NMR (400 MHz, CD_2Cl_2) δ 7.72–7.66 (m, 8H), 7.57–7.39 (m, 14H), 1.07 (s, 42H); ^{13}C NMR (100 MHz, CD_2Cl_2) δ 146.4

(pseudo–dd, ${}^{1}J_{C\text{–}P} = 50$ Hz, ${}^{2}J_{C\text{–}P} = 25$ Hz), 133.6–133.3 (m), 132.2 (s), 129–129.3 (m), 128.7 (dt, ${}^{2}J_{C\text{–}P} = 60.0$ Hz, ${}^{2}J_{C\text{–}P} = 24$ Hz), 100.9 (dd, ${}^{2}J_{C\text{–}P} = 147$ Hz for *trans*, ${}^{2}J_{C\text{–}P} = 15$ Hz for *cis*), 93.1 (pseudo–dt, ${}^{2}J_{C\text{–}Pt} = 156$ Hz, ${}^{3}J_{C\text{–}P} = 34$ Hz), 91.4, 81.6, 64.2, 58.2, 18.5, 11.6; ^{31}P NMR (162 MHz, CD_2Cl_2) δ 53.9 (pseudo–t, $J_{P\text{–}Pt} = 2294$); MALDI MS (CH_2Cl_2) HRMS calcd. for $C_{56}H_{64}Si_2P_2PtNa$ ($[M + Na]^+$) 1072.3562, found 1572.3564.

8.3.5 Chapter 6

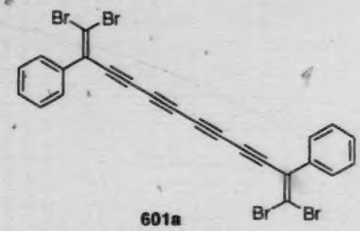

601a

Compound **601a**: Compound **603a** (62.5 mg, 0.164 mmol) was used as per the general procedure M and yielded **601a** (38.0 mg, 75%) as a yellow crystalline solid. Mp 185 °C (dec.). $R_f = 0.5$ (hexanes/CH_2Cl_2 7:1). UV–vis (THF) λ_{max} (ε) 359 (27,600), 386 (30,600), 419 (19,500).

IR ($CHCl_3$, cast) 2192 (w), 1488 cm^{-1}; ^1H NMR (500 MHz, $CDCl_3$) δ 7.36 (s, 10H); ^{13}C NMR (100 MHz, $CDCl_3$) δ 136.6, 129.5, 129.1, 128.6, 128.5, 105.3, 82.0, 76.5, 71.0, 65.0. EIMS *m/z* 617.7 (M^+, 80), 298.1 ($[M - 4Br]^+$, 100); HRMS calcd. for $C_{24}H_{10}{}^{79}Br_2{}^{81}Br_2$ 617.7475, found 617.7488. Anal. calcd. For $C_{24}H_{10}Br_4$: C 46.66; H 1.63. Found: C 46.35; H 1.46.

Single crystals were grown from slow diffusion of hexanes into a solution of hexanes/CH_2Cl_2 at –4 °C. $C_{24}H_{10}Br_4$, M = 617.96, triclinic space group $P\bar{1}$ (No. 2), D_c = 1.916 g cm^{-3}, $a = 9.4512(7)$ Å, $b = 10.1187(7)$ Å, $c = 11.6133(8)$ Å, $\alpha = 96.0941(13)°$, $\beta = 92.5663(13)°$, $\gamma = 103.4569(13)°$, $V = 1071.25(13)$ $Å^3$, $Z = 2$, $\mu = 7.521$ (mm^{-1}), T = –80 °C. Final $R_1(F) = 0.0368$, $wR^2(F^2) = 0.0930$ for 253 variables and 4356 data with $F_o^2 \geq -3\sigma(F^2)$ (3413 [$F_o^2 \geq -2\sigma(F_o^2)$]).

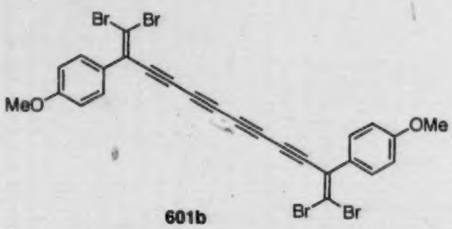

601b

Compound **601b**: Compound **603b** (582 g, 1.46 mmol) was used as per the general procedure M and yielded **601b** (223 g, 63%) as a yellow–green powder. Mp 168–170 °C. $R_f = 0.4$ (hexanes/CH_2Cl_2 3:1). UV–vis (THF) λ_{max} (ε) 360 (26,900), 388 (27,800), 420 (18,300).

IR ($CHCl_3$, cast) 3341 (br), 2924, 2190, 1505 cm^{-1}; ^{1}H NMR (300 MHz, $CDCl_3$) δ 7.32 (d, $J = 9.0$ Hz, 4H), 6.88 (d, $J = 9.0$ Hz, 4H), 3.81 (s, 6H); ^{13}C NMR (100 MHz, $CDCl_3$) δ 159.9, 129.8, 129.0, 128.6, 113.9, 104.1, 81.5, 70.7, 64.8, 55.2, (one signal not observed). EIMS *m/z* HRMS calcd. for $C_{26}H_{14}{}^{79}Br_2{}^{81}Br_2O_2$ 677.7686, found 677.7697. Anal. calcd. For $C_{26}H_{14}Br_4O_2$: C 46.06; H 2.08. Found: C 45.87; H 1.93.

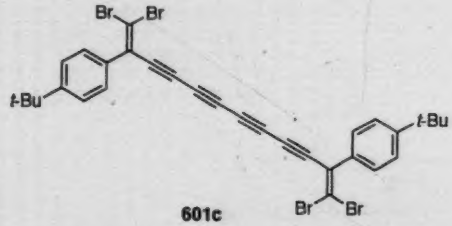

601c

Compound **601c**: Compound **603c** (401 mg, 0.914 mmol) was used as per the general procedure M and yielded **601c** (265 mg, 80%) as a yellow crystalline solid. Mp >230 °C (dec.). $R_f = 0.5$ (hexanes/CH_2Cl_2 7:1). UV–vis (THF) λ_{max} (ε) 359 (25,200), 387 (27,600), 419 (17,500).

IR ($CHCl_3$, cast) 2963, 2182, 1531 cm^{-1}; ^{1}H NMR (300 MHz, $CDCl_3$) δ 7.38 (d, $J = 8.7$ Hz, 4H), 8.7 (d, $J = 8.7$ Hz, 4H), 1.30 (s, 18H); ^{13}C NMR (100 MHz, $CDCl_3$) δ 152.3, 133.5, 129.4, 128.2, 125.6, 104.6, 81.8, 70.9, 65.0, 34.9, 31.3, (one signal not observed). EIMS *m/z* 729.9 (M^+, 30); HRMS calcd. for $C_{32}H_{26}{}^{79}Br_2{}^{81}Br_2$ 729.8727, found 729.8750. Anal. calcd. For $C_{32}H_{26}Br_4$: C 52.64; H 3.59. Found: C 52.05; H 3.45.

Single crystals were grown from slow from slow diffusion of hexanes into a solution of hexanes/CH_2Cl_2 at –4 °C. $C_{32}H_{26}Br_4$, M = 730.17, triclinic space group $P\bar{1}$ (No. 2), D_c = 1.697 g cm^{-3}, a = 5.8968(7) Å, b = 11.1037(14) Å, c = 11.9247(15) Å, α = 69.2510(18)°, β = 78.1507(18)°, γ = 86.0880(19)°, V = 714.58(15) Å^3, Z = 1, μ = 5.601b (mm^{-1}), T = –80 °C. Final $R_1(F) = 0.0342$, $wR^2(F^2) = 0.0905$ for 163 variables and 2911 data with $F_o^2 \geq -3\sigma(F^2)$ (2418 $[F_o^2 \geq -2\sigma(F_o^2)]$.

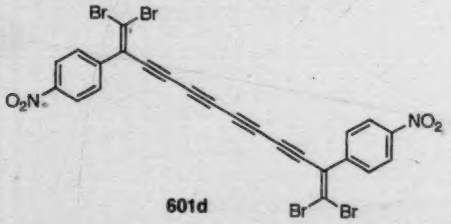

601d

Compound **601d**: Compound **603d** (1.10 g, 2.58 mmol) was used as per the general procedure M and yielded **603d** (469 g, 51%) as a yellow crystalline solid. Mp > 190 °C (dec.). R_f = 0.4 (hexanes/CH_2Cl_2 1:1). UV–vis (THF) λ_{max} (ε) 359 (29,200), 387 (31,700), 419 (19,900).

IR ($CHCl_3$, cast) 2188 (w), 2114 (w), 1517, 1346 cm^{-1}; ^1H NMR (400 MHz, $CDCl_3$) δ 8.34 (d, J = 9.2 Hz, 4H), 8.8 (d, J = 9.2 Hz, 4H); ^{13}C NMR (100 MHz, $CDCl_3$) δ 147.8, 142.5, 129.6, 127.4, 123.8, 107.5, 82.6, 75.4, 71.2, 64.8. EIMS *m/z* 707.7 (M^+, 23), 388.0 ($[M - 4Br]^+$, 6); HRMS calcd. for $C_{24}H_8{}^{79}Br_2{}^{81}Br_2N_2O_4$ 707.7177, found 707.7217. Anal. calcd. For $C_{24}H_8Br_4N_2O_4$: C 40.72; H 1.14; N 3.96. Found: C 40.94; H 1.10; N 3.80.

Single crystals were grown from slow evaporation of a $CDCl_3$ solution at –4 °C. $C_{24}H_8Br_4N_2O_4$, M = 707.96, orthorhombic space group *Pbcn* (No. 60), $D_c = 1.970$ g cm^{-3}, $a = 7.5156(7)$ Å, $b = 14.8934(14)$ Å, $c = 21.315(2)$ Å, $V = 287.3(4)$ Å^3, $Z = 4$, $\mu = 6.777$ (mm^{-1}), T = –80 °C. Final $R_1(F) = 0.0309$, $wR^2(F^2) = 0.0825$ for 154 variables and 2461 data with $F_o^2 \geq -3\sigma(F^2)$ (1968 $[F_o^2 \geq -2\sigma(F_o^2)]$

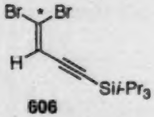

606

Compound **606**:[10] $^{13}CBr_4$ (287 mg, 0.865 mmol), CBr_4 (718 mg, 2.16 mmol), PPh_3 (1.14 mg, 4.33 mmol) in CH_2Cl_2 (15 mL) and **605** (501 mg, 3.38 mmol) were used as per the general procedure E, yielding **606** (17.4 mg, 81%).

^{1}H NMR (500 MHz, $CDCl_3$) δ 6.59 (d, J = 1.5 Hz, 1H), 1.08 (s, 21H); ^{13}C NMR (125 MHz, $CDCl_3$) δ 120.0 (d, ^1J = 88 Hz), 102.9 (C*, pseudo–t, ^1J = 88 Hz), 102.5 (s), 100.8 (d, ^3J = 25 Hz), 18.6, 11.1.

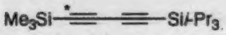

607

Compound **607**: **606** (638 mg, 1.74 mmol) in Et_2O (1 mL), LDA [BuLi (2.5 M in hexanes, 2.1 mL, 5.3 mmol), diisopropylamine (0.73 mL, 0.53 mg, 5.23 mmol) and Et_2O (17 mL) were used per the general procedure I] at –78 °C and stirred for 2 h. To this mixture, Me_3SiCl (0.33 mL, 0.28 mg, 2.61 mmol) dropwise. The reaction was allowed to warm to rt overnight, yielding **607** (**312** mg, 67%) as a colorless oil. R_f = 0.67 (hexanes).

^{1}H NMR (400 MHz, $CDCl_3$) δ 1.06 (s, 21H), 0.18 (s, 9H); ^{13}C NMR (100 MHz, $CDCl_3$) δ 102.9, 84.5 (C*), 65.5, 18.5, 11.3, –0.43.

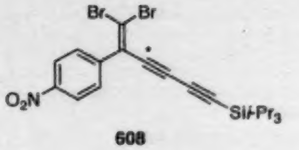

608

Compound **608**: **602d** (239 mg, 1.29 mmol), **607** (321 mg, 1.15 mmol) in CH_2Cl_2 (12 mL) and $AlCl_3$ (230 mg, 1.72 mmol) were used as per the general procedure G, affording the intermediate ketone that was carried on to the next step without further purification. CBr_4 (764 mg, 2.30 mmol), PPh_3 (1.21 mg, 4.61 mmol) in CH_2Cl_2 (12 mL) were used as per the general procedure E and the addition of Et_3N to the mixture of CBr_4 and PPh_3 before mixing with the ketone, yielding **608** (206 mg, 35%) as a colorless oil. R_f = 0.5 (hexanes/CH_2Cl_2 2:1).

^{13}C NMR (125 MHz, $CDCl_3$) δ 147.7, 143.5, 129.7, 128.3 (pseudo–t, ^1J = 50 Hz), 123.8, 104.5, 94.3, 88.7, 88.5 (pseudo–t, ^2J = 9.0 Hz), 83.6 (pseudo–t, ^1J = 101 Hz), 72.8–72.3 (m), 18.5, 11.2.

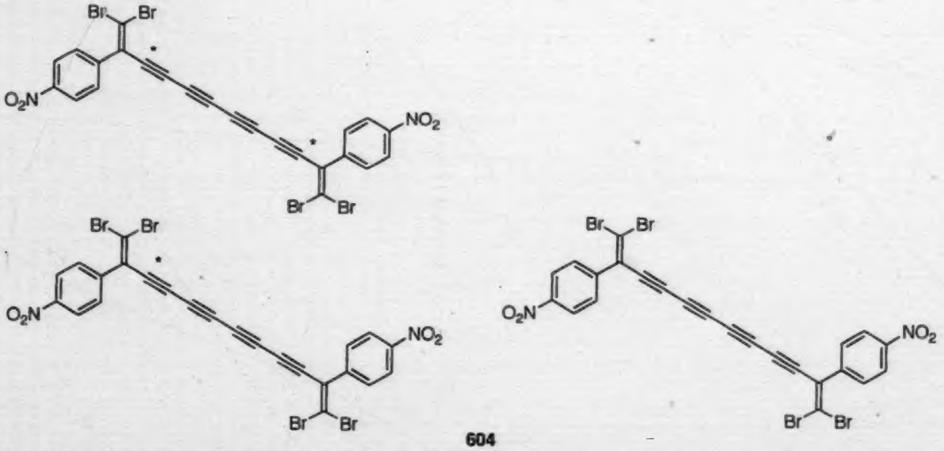

604

Compound **604**: **608** (206 mg, 0.403 mmol) in THF (6 mL) was added TBAF (1.0 M in THF, 0.52 mL, 0.52 mmol) as per the general procedure H, affording the terminal diyne in CH_2Cl_2 (6 mL). To the diyne above, CuCl (20 mg, 0.20 mmol), TMEDA (0.1 mL) and oxygen, yielding **604** as a mixture of three isotopomers (59.7 mg, 42%). Spectral data were consistent with those of **601d**.

^{1}H NMR (400 MHz, $CDCl_3$) δ 8.24 (d, $J = 9.0$ Hz, 4H), 7.6 (d, $J = 9.0$ Hz, 4H); ^{13}C NMR (125 MHz, $CDCl_3$) δ 147.9, 142.7, 129.7, 127.6 (pseudo–t, $^{1}J = 50$ Hz), 124.0, 107.6, 82.7 (pseudo–t, $^{1}J = 187$ Hz), 75.6 (C*), 71.4 (d, $^{2}J = 32$ Hz), 64.9.

8.4 References and Notes

(1) Morrison, C. F.; Burnell, D. J. *Tetrahedron Lett.* **2001**, *42*, 7367–7369.

(2) Livingston, R.; Cox, L. R.; Odermatt, S.; Diederich, F. O. *Helv. Chim. Acta* **2002**, *85*, 3052–3077.

(3) Rubin, Y.; Lin, S. S.; Knobler, C. B.; Anthony, J.; Boldi, A. M.; Diederich, F. *J. Am. Chem. Soc.* **1991**, *113*, 6943–6949.

(4) Nacro, K.; Baltas, M.; Gorrichon, L. *Tetrahedron* **1999**, *55*, 14013–14030.

(5) Tokimoto, K.; Fujita, T.; Takeda, Y.; Takaishi, Y. *Proc. Jpn. Acad.* **1987**, *63*, 277–280.

(6) Bohlmann, F.; Herbst, P.; Gleinig, H. *Chem. Ber.* **1961**, *94*, 948–957.

(7) Higham, C. A.; Jones, E. R. H.; Keeping, J. W.; Thaller, V. *J. Chem. Soc., Perkin Trans. 1* **1974**, 1991–1994.

(8) Bew, R. E.; Chapman, J. R.; Jones, E. R. H.; Lowe, B. E.; Lowe, G. *J. Chem. Soc.* **1966**, 129–135.

(9) Guanti, G.; Banfi, L.; Narisano, E. *Gazzetta Chimica Italiana* **1989**, *119*, 527–532.

(10) Eisler, S.; Slepkov, A. D.; Elliott, E.; Luu, T.; McDonald, R.; Hegmann, F. A.; Tykwinski, R. R. *J. Am. Chem. Soc.* **2005**, *127*, 2666–2676.

(11) Zhang, S. H.; Xu, L.; Trudell, M. L. *Synthesis* **2005**, 1757–1760.

(12) Wipf, P.; Graham, T. H. *Org. Biomol. Chem.* **2005**, *3*, 31–35.

(13) Takahashi, S.; Kuroyama, Y.; Sonogashira, K.; Hagihara, N. *Synthesis* **1980**, 627–630.

(14) Eastmond, R.; Walton, D. R. M. *Tetrahedron* **1972**, *28*, 4591–4599.

(15) Shi Shun, A. L. K.; Chernick, E. T.; Eisler, S.; Tykwinski, R. R. *J. Org. Chem.* **2003**, *68*, 1339–1347.

(16) Ford, M. F.; Walton, D. R. M. *Synthesis* **1973**, 47–48.

(17) Eisler, S.; Chahal, N.; McDonald, R.; Tykwinski, R. R. *Chem.–Eur. J.* **2003**, *9*, 2542–2550.

(18) Luu, T.; Tykwinski, R. R. *J. Org. Chem.* **2006**, *71*, 8982–8985.

(19) Luu, T.; Elliott, E.; Slepkov, A. D.; Eisler, S.; McDonald, R.; Hegmann, F. A.; Tykwinski, R. R. *Org. Lett.* **2005**, *7*, 51–54.

(20) Wadsworth, D. H.; Geer, S. M.; Detty, M. R. *J. Org. Chem.* **1987**, *52*, 3662–3668.

(21) Abe, H.; Suzuki, H. *Bull. Chem. Soc. Jpn* **1999**, *72*, 787–798.

(22) Diederich, F.; Philp, D.; Seiler, P. *J. Chem. Soc., Chem. Commun.* **1994**, 205–208.

(23) Morisaki, Y.; Luu, T.; Tykwinski, R. R. *Org. Lett.* **2006**, *8*, 689–692.

(24) Eisler, S.; Tykwinski, R. R. *J. Am. Chem. Soc.* **2000**, *122*, 10736–10737.

(25) Mukai, C.; Miyakoshi, N.; Hanaoka, M. *J. Org. Chem.* **2001**, *66*, 5875–5880.

(26) Anthony, J.; Boldi, A. M.; Rubin, Y.; Hobi, M.; Gramlich, V.; Knobler, C. B.; Seiler, P.; Diederich, F. *Helv. Chim. Acta* **1995**, *78*, 13–45.

(27) Lee, H. J.; Shim, S. C. *J. Chem. Soc., Chem. Commun.* **1993**, 1420–1422.

(28) Lange, T.; vanLoon, J. D.; Tykwinski, R. R.; Schreiber, M.; Diederich, F. *Synthesis* **1996**, 537–550.

(29) Vijn, R. J.; Hiemstra, H.; Kok, J. J.; Knotter, M.; Speckamp, W. N. *Tetrahedron* **1987**, *43*, 5019–5030.

(30) Shi Shun, A. L. K.; Tykwinski, R. R. *J. Org. Chem.* **2003**, *68*, 6810–6813.

(31) Bohlmann, F.; Queck, I.; Sucrow, W. *Chem. Ber.* **1964**, *97*, 2586–2597.

(32) Luu, T.; Shi, W.; Lowary, T. L.; Tykwinski, R. R. *Synthesis* **2005**, 3167–3178.

(33) Chang, M.–H.; Wang, G.–J.; Kuo, Y.–H.; Lee, C.–K. *J. Chin. Chem. Soc.* **2000**, *47*, 1131–1136.

(34) Fiandanese, V.; Bottalico, D.; Marchese, G.; Punzi, A. *Tetrahedron Lett.* **2003**, *44*, 9087–9090.

Appendix A Selective ^{1}H/^{13}C NMR Spectra

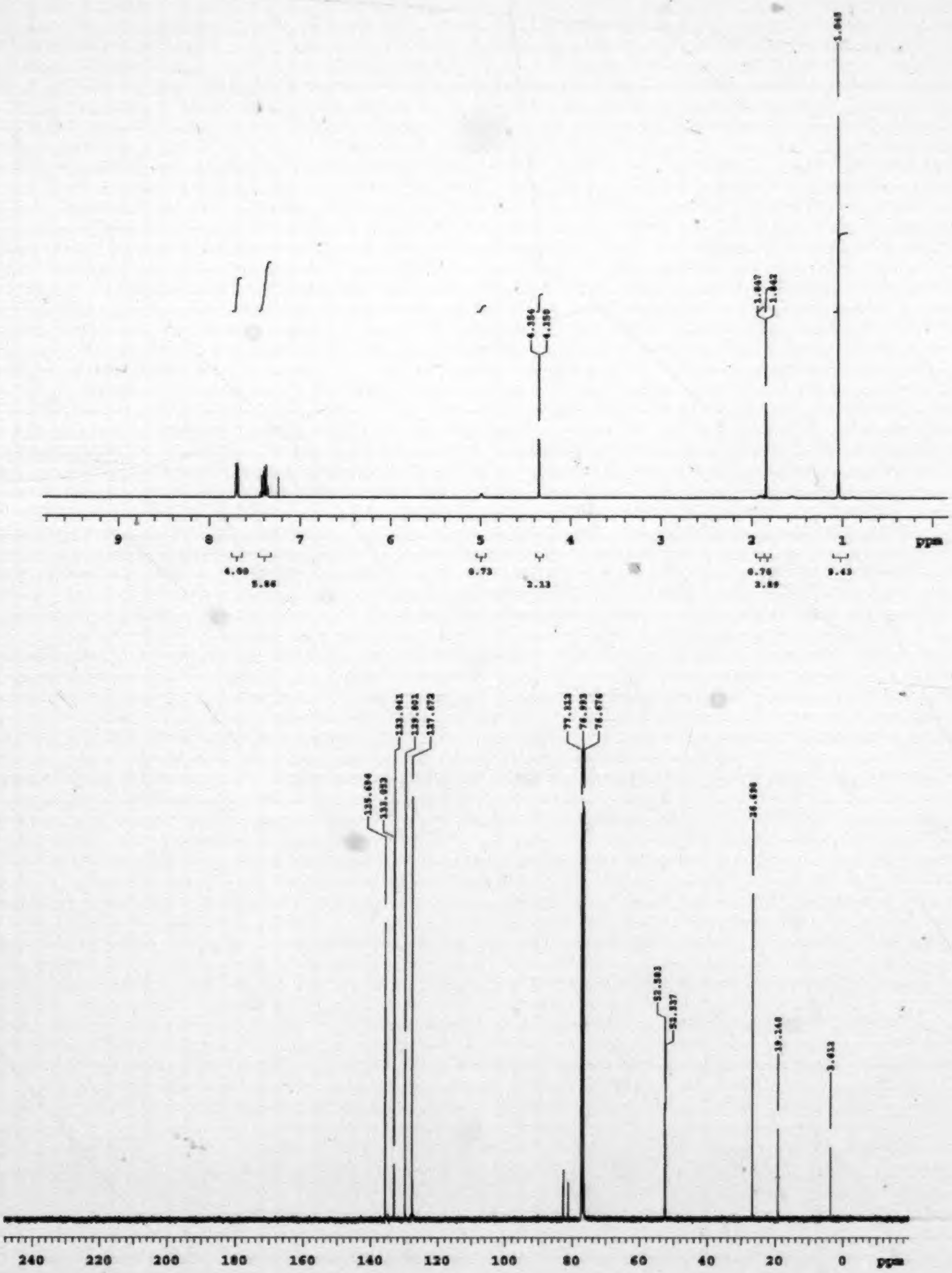

Figure A.1 ^{1}H and ^{13}C NMR spectra of **229a**

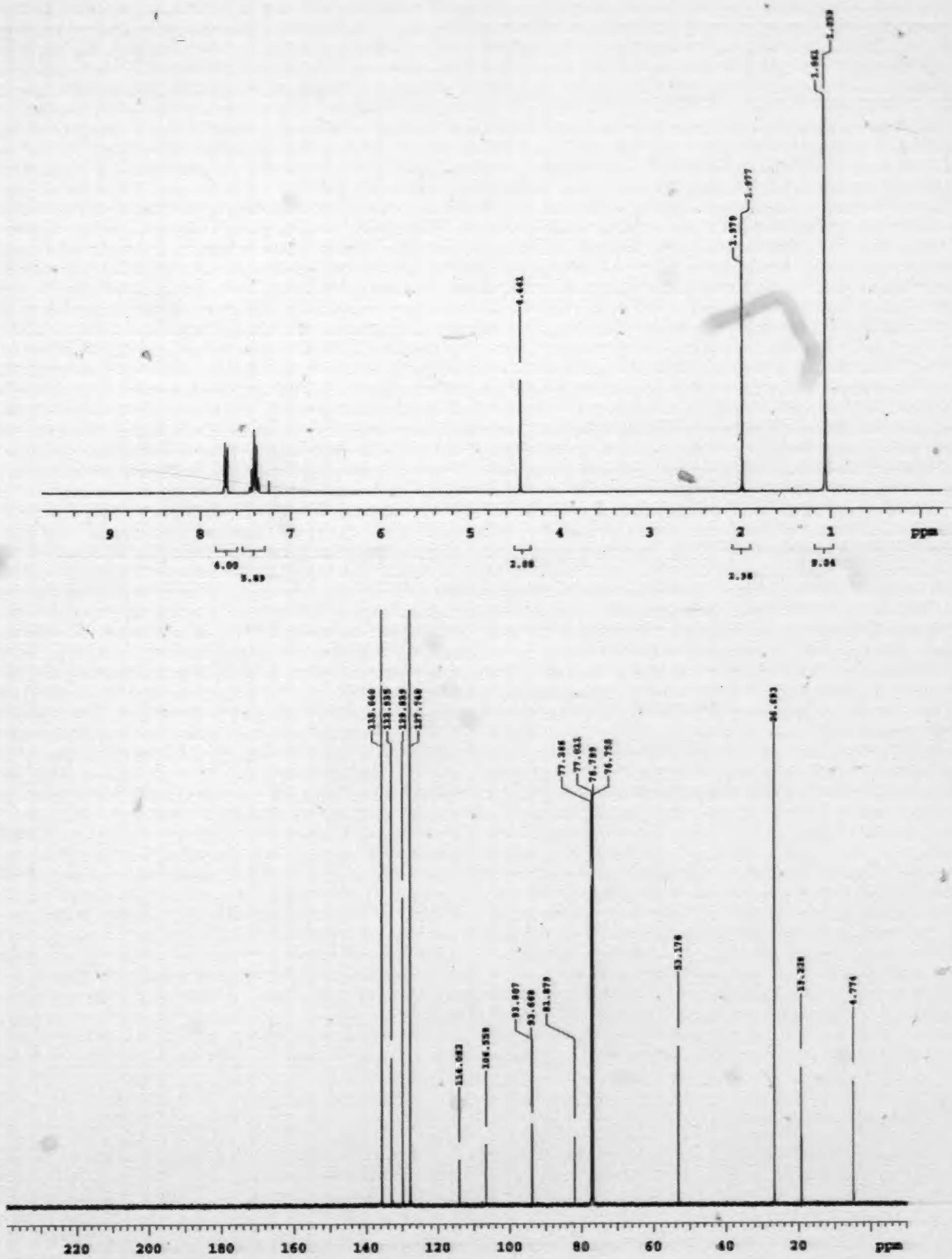

Figure A.2 ^{1}H and ^{13}C NMR spectra of **230a**

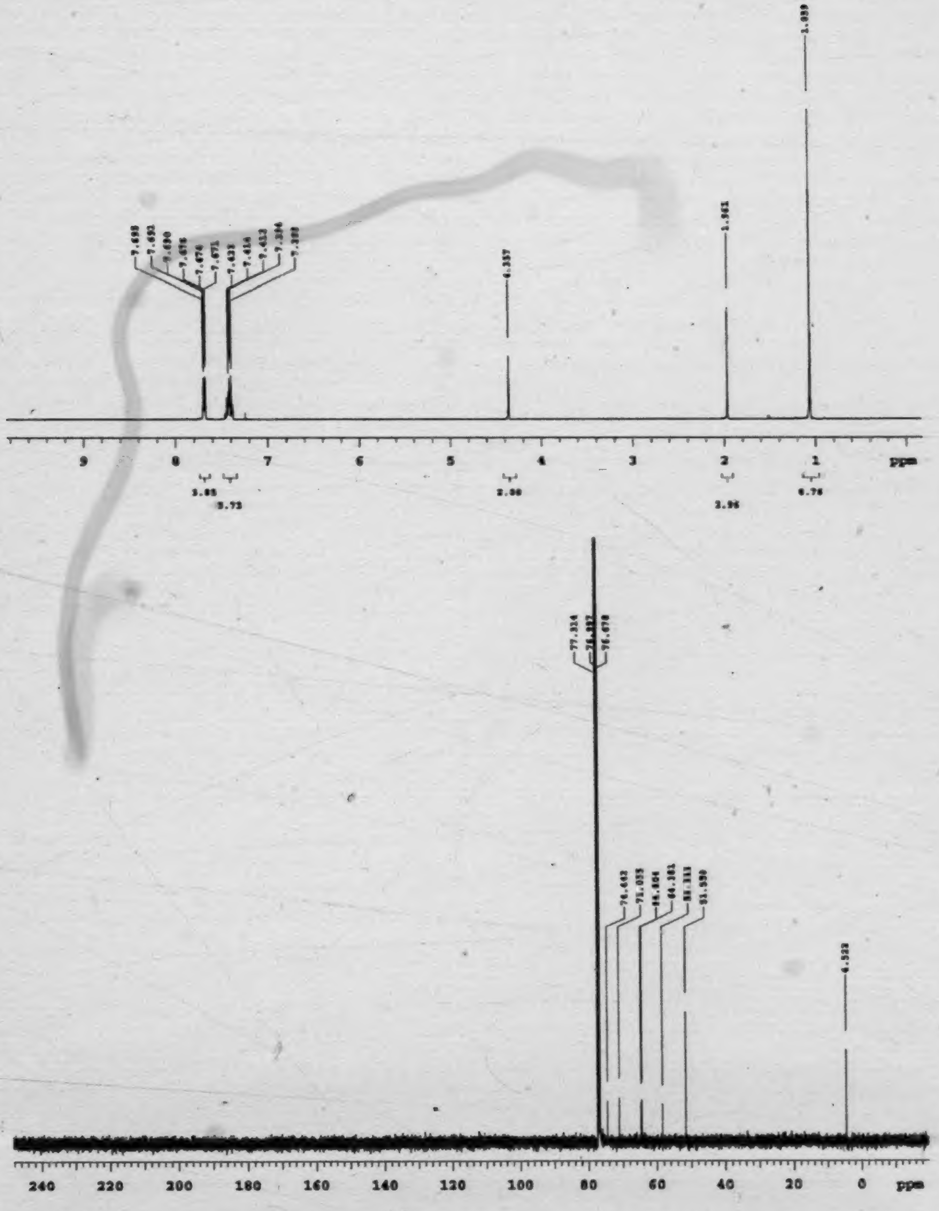

Figure A.3 ^{1}H and ^{13}C NMR spectra of **231a**

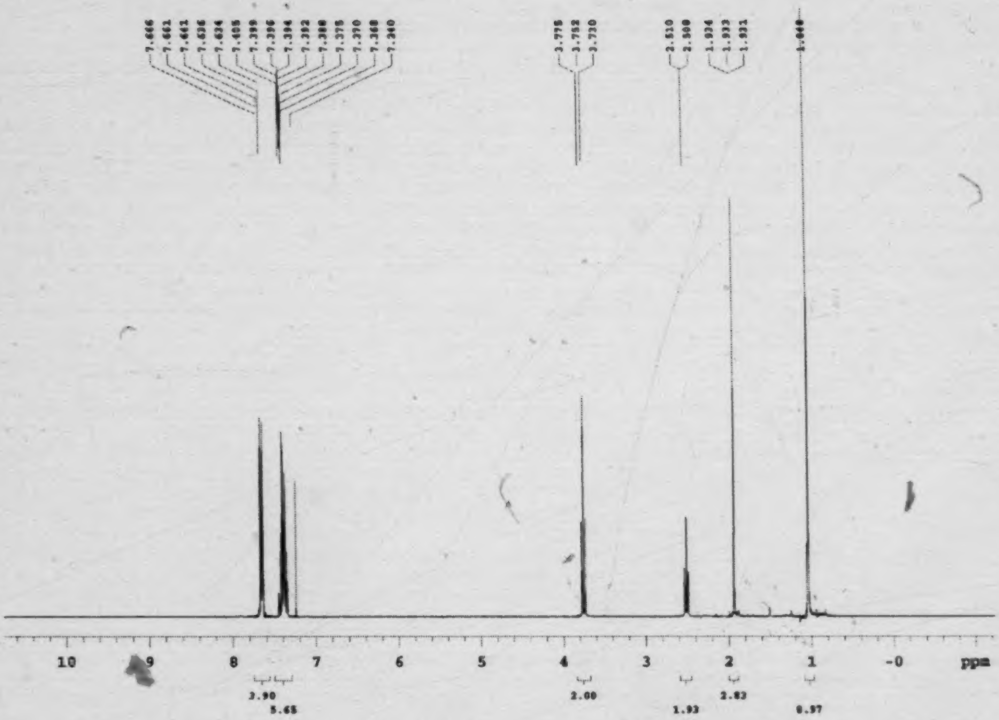

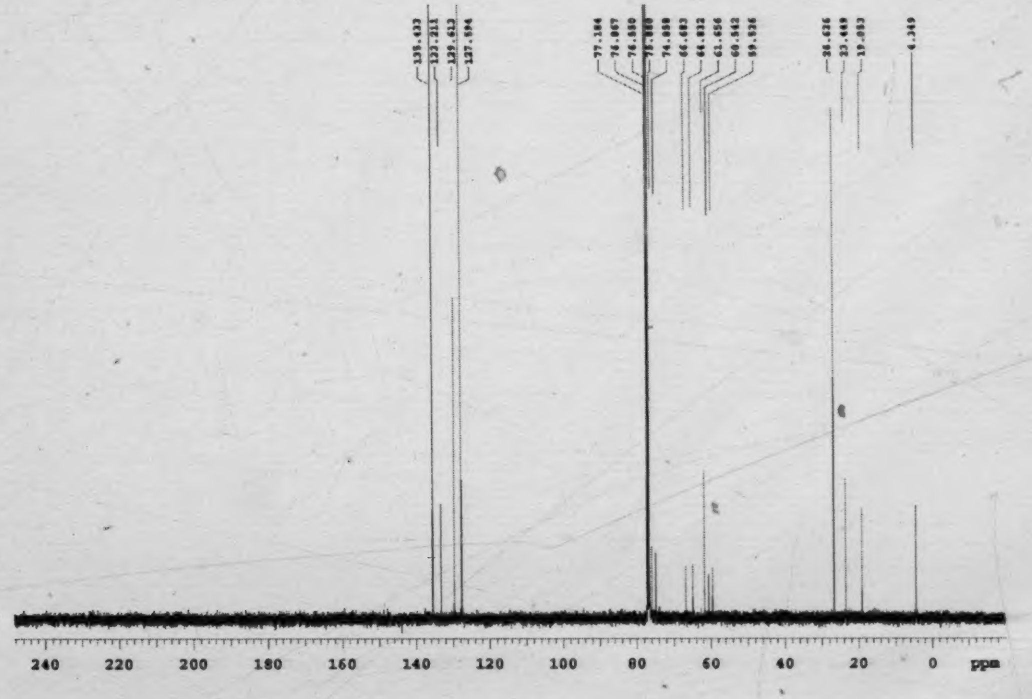

Figure A.4 ^{1}H and ^{13}C NMR spectra of **231b**

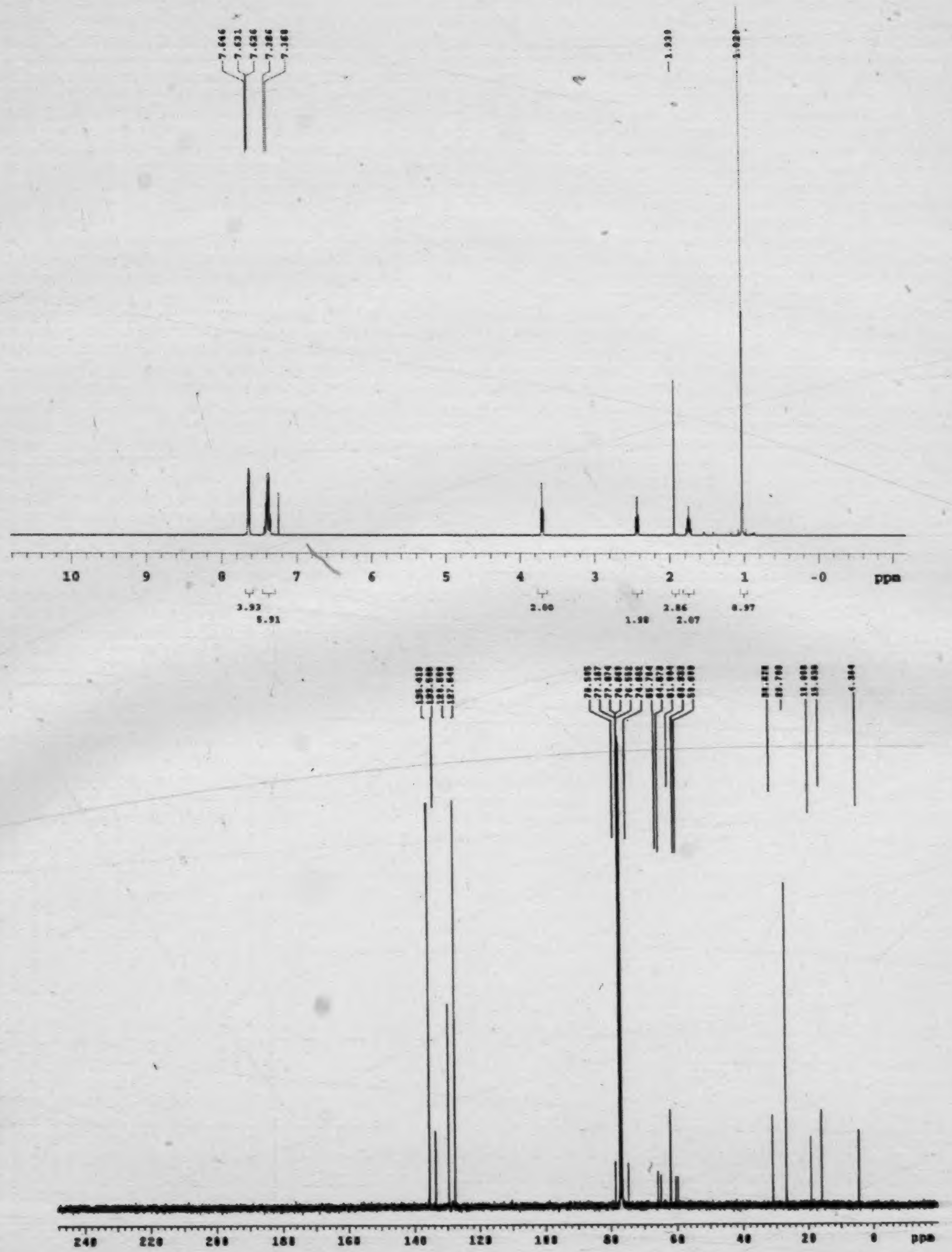

Figure A.5 ^{1}H and ^{13}C NMR spectra of **231c**

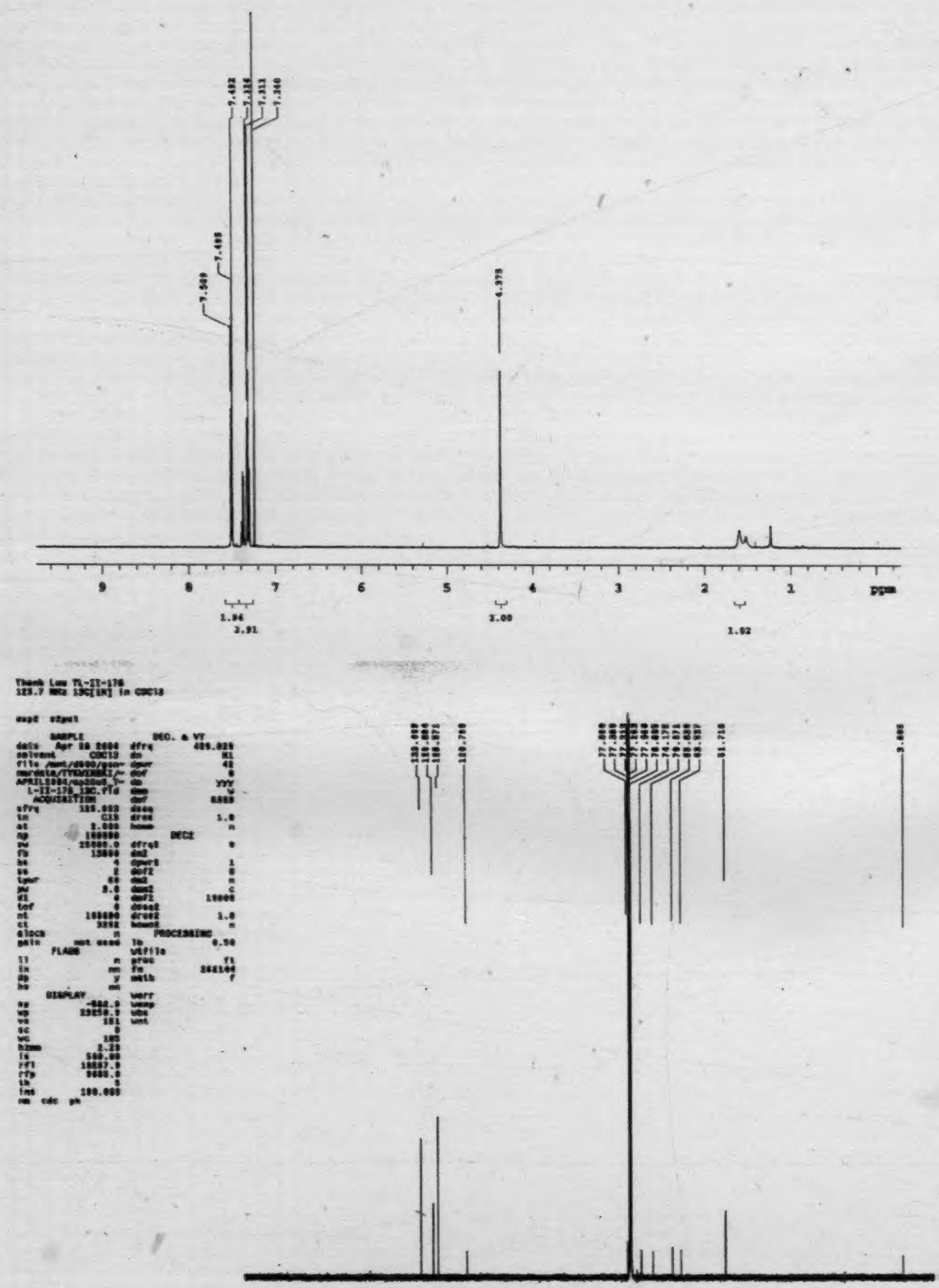

Figure A.6 ^{1}H and ^{13}C NMR spectra of **209a**

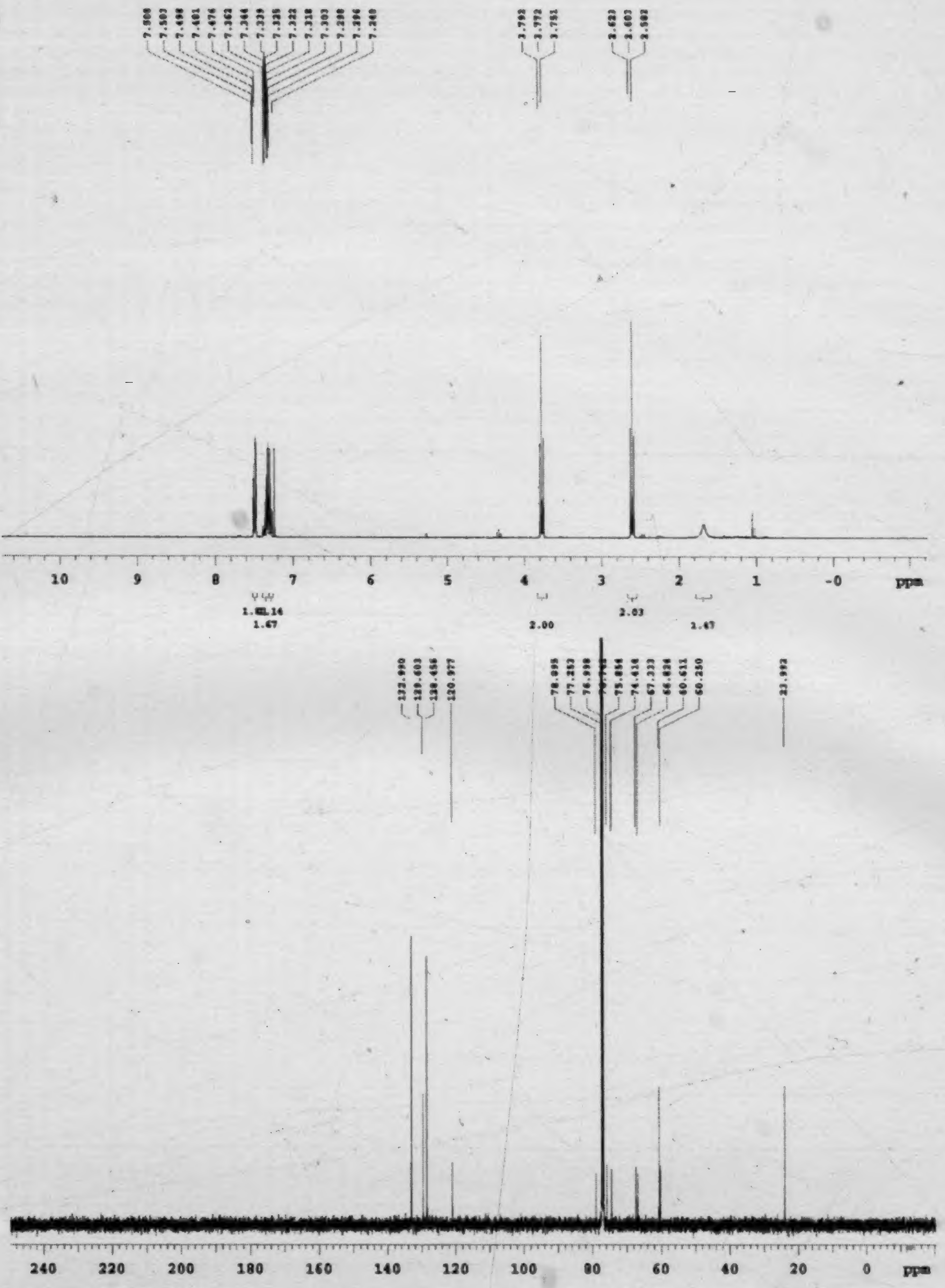

Figure A.7 ^{1}H and ^{13}C NMR spectra of **209b**

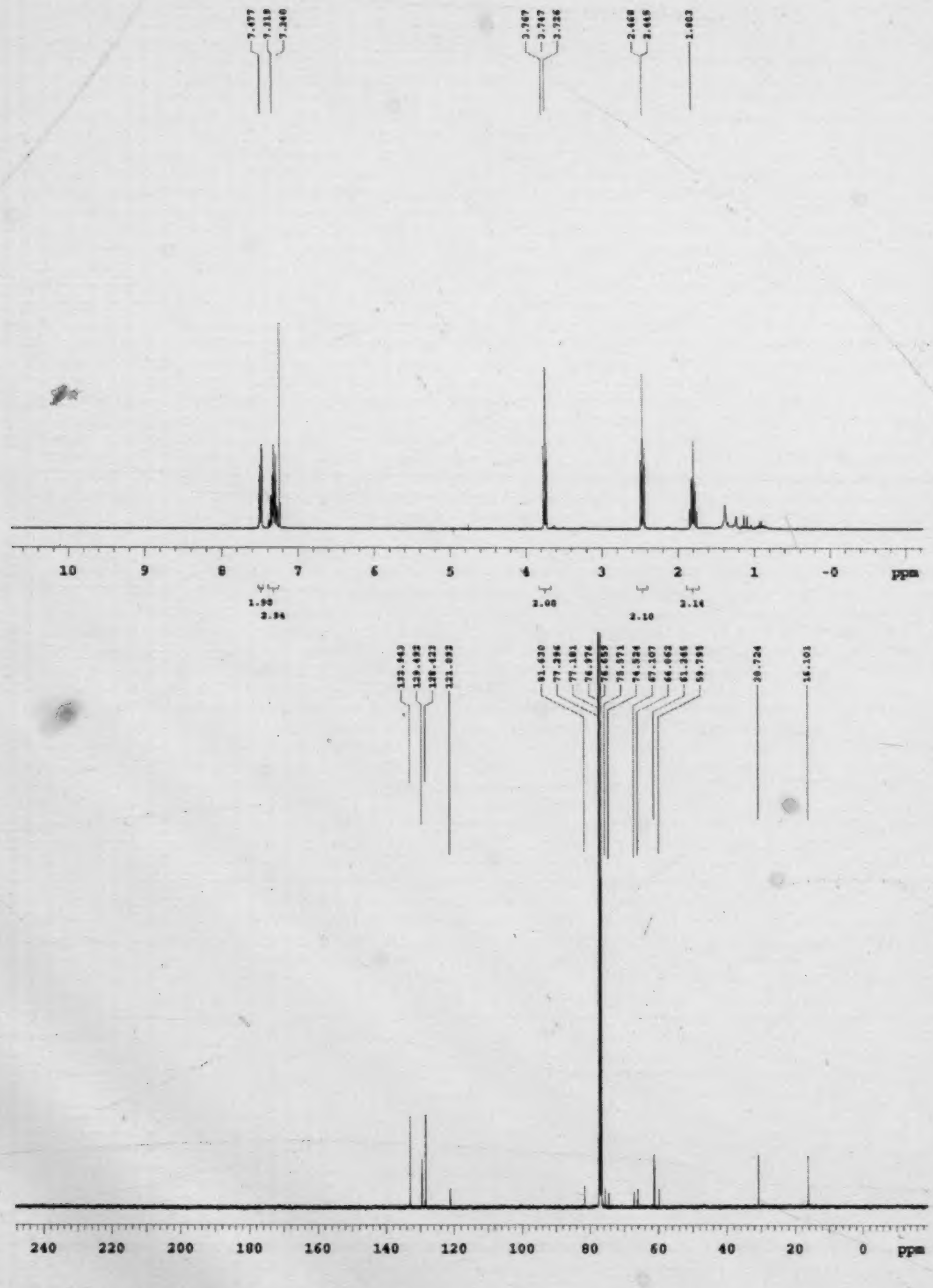

Figure A.8 ${}^{1}H$ and ${}^{13}C$ NMR spectra of **209c**

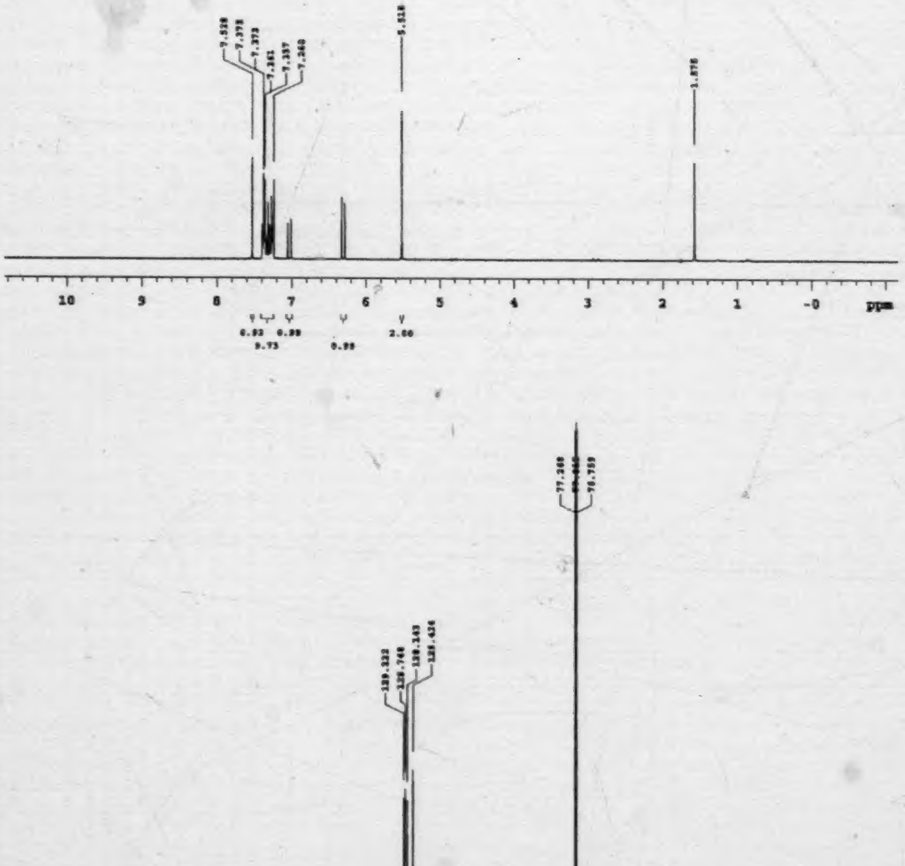

Figure A.9 ^{1}H and ^{13}C NMR spectra of **317f**

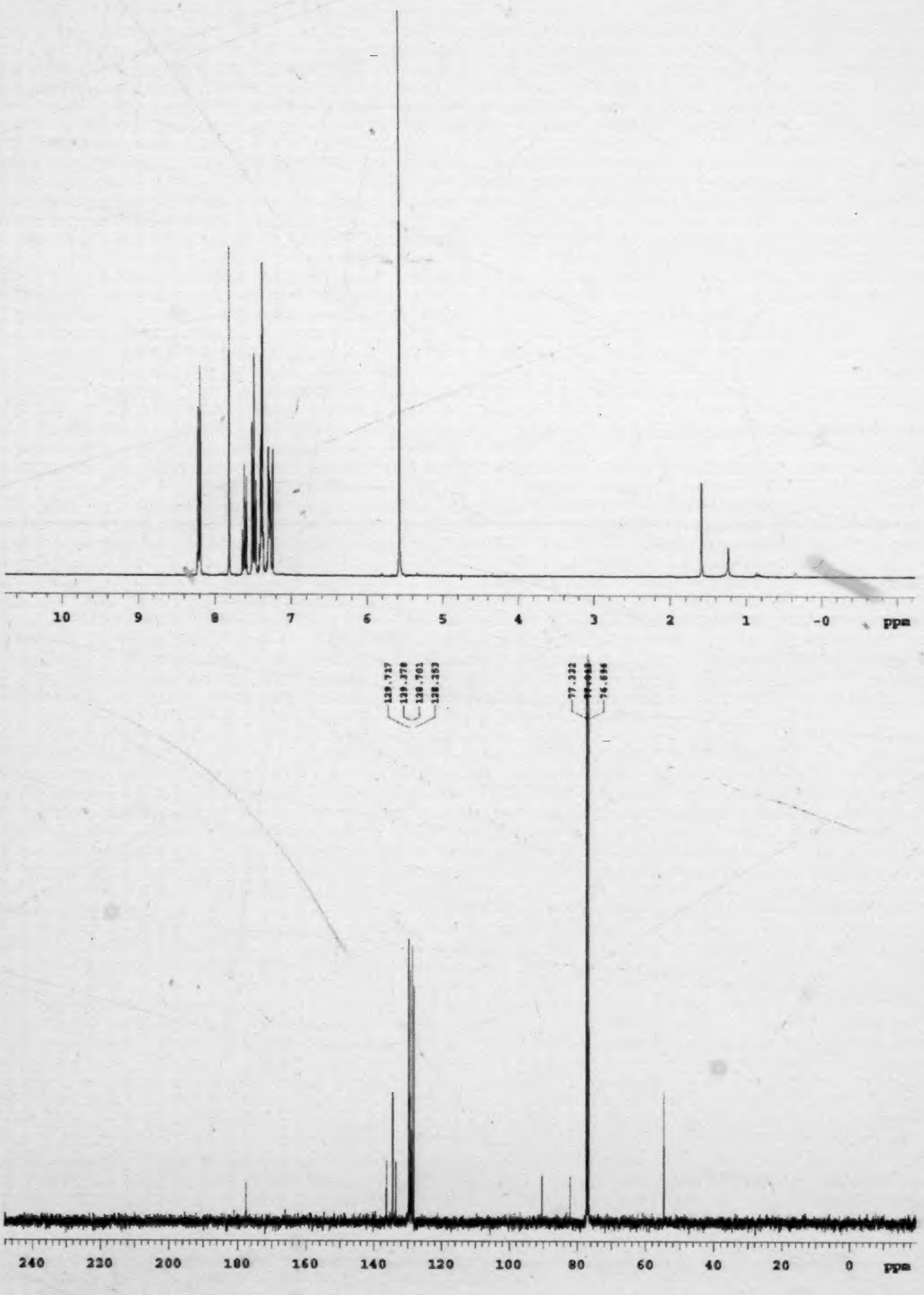

Figure A.10 ^{1}H and ^{13}C NMR spectra of **317p**

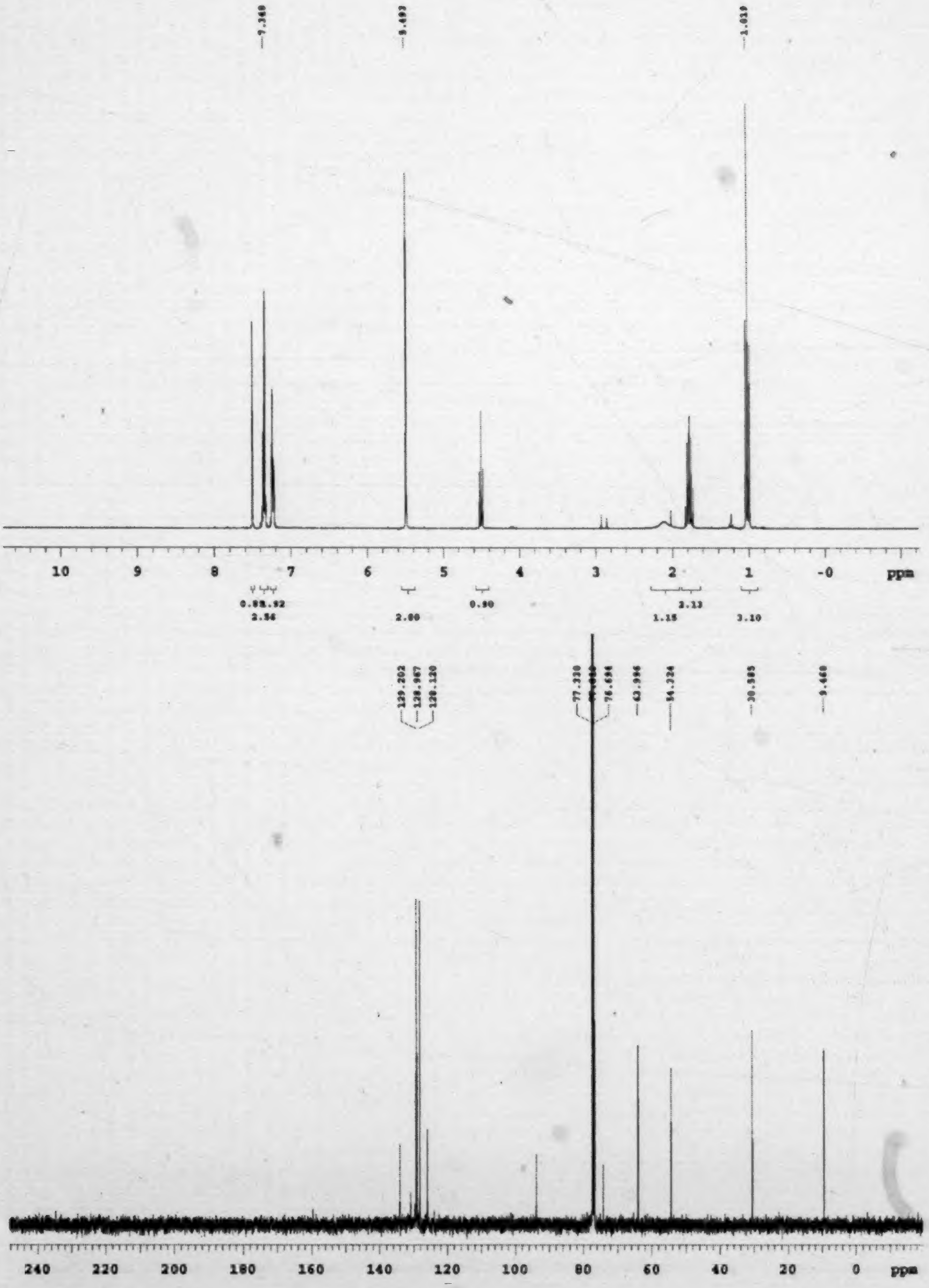

Figure A.11 ^{1}H and ^{13}C NMR spectra of **317q**

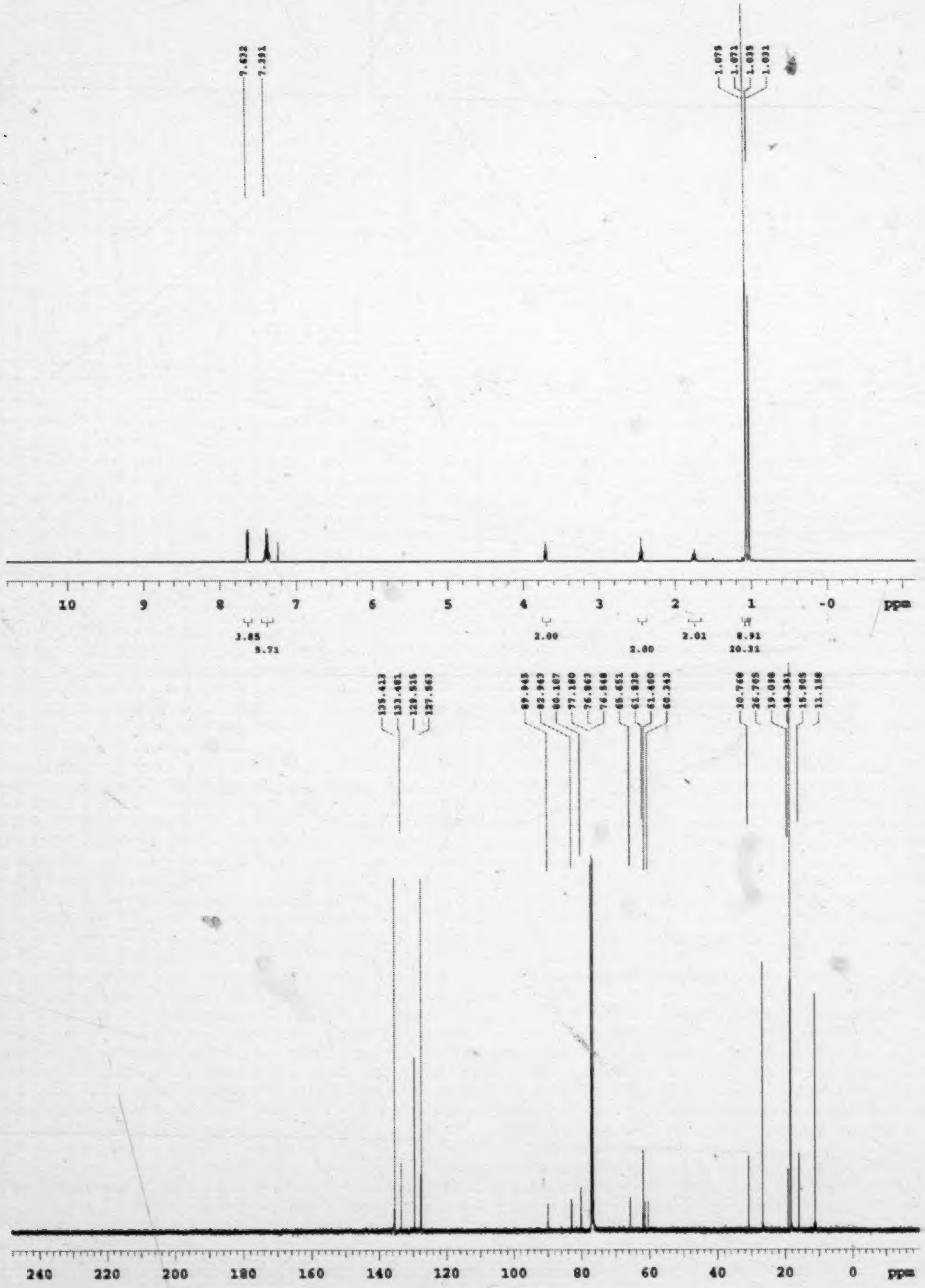

Figure A.12 ^{1}H and ^{13}C NMR spectra of **325b**

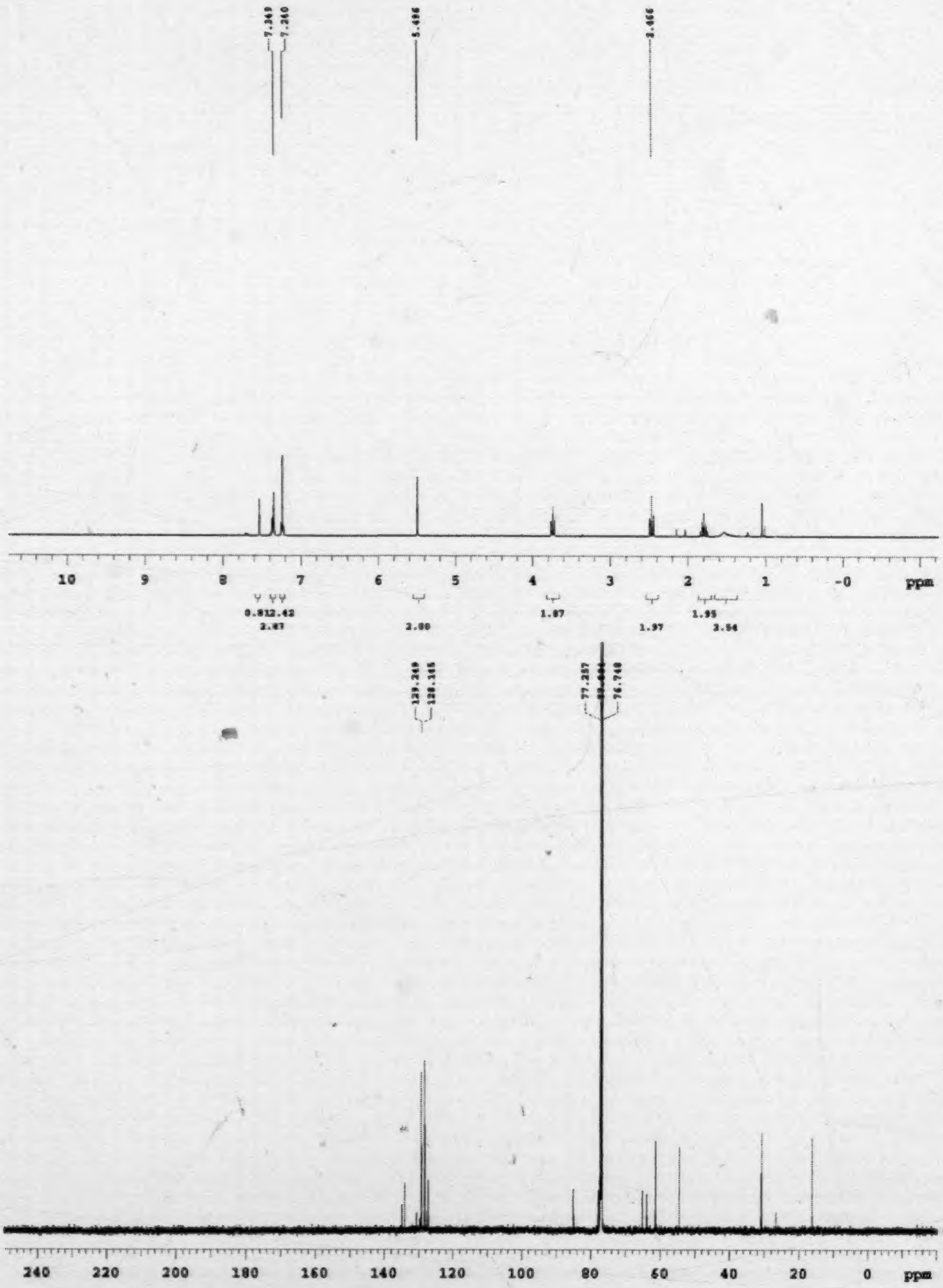

Figure A.13 ^{1}H and ^{13}C NMR spectra of **325b'**

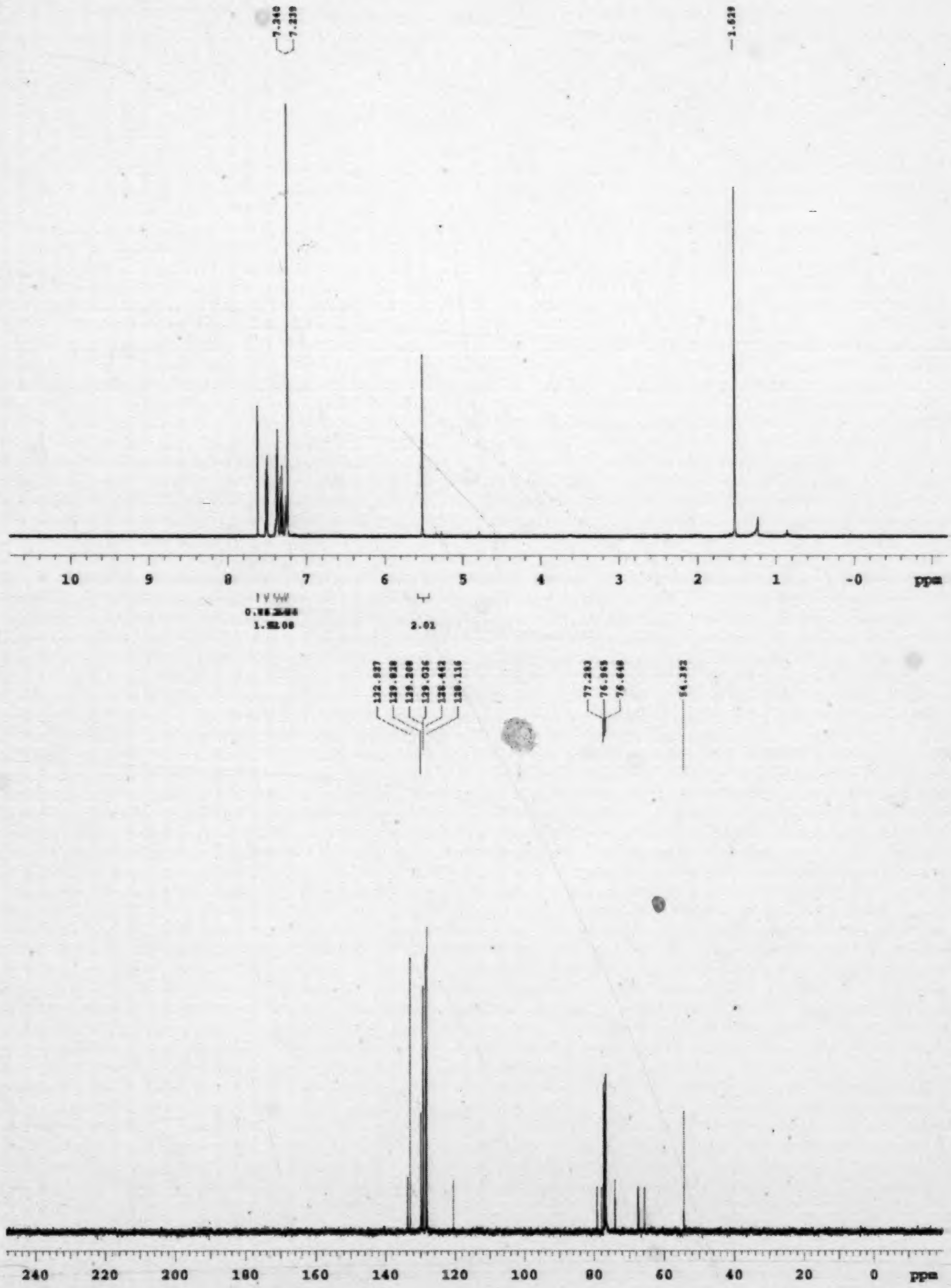

Figure A.14 ^{1}H and ^{13}C NMR spectra of **326b**

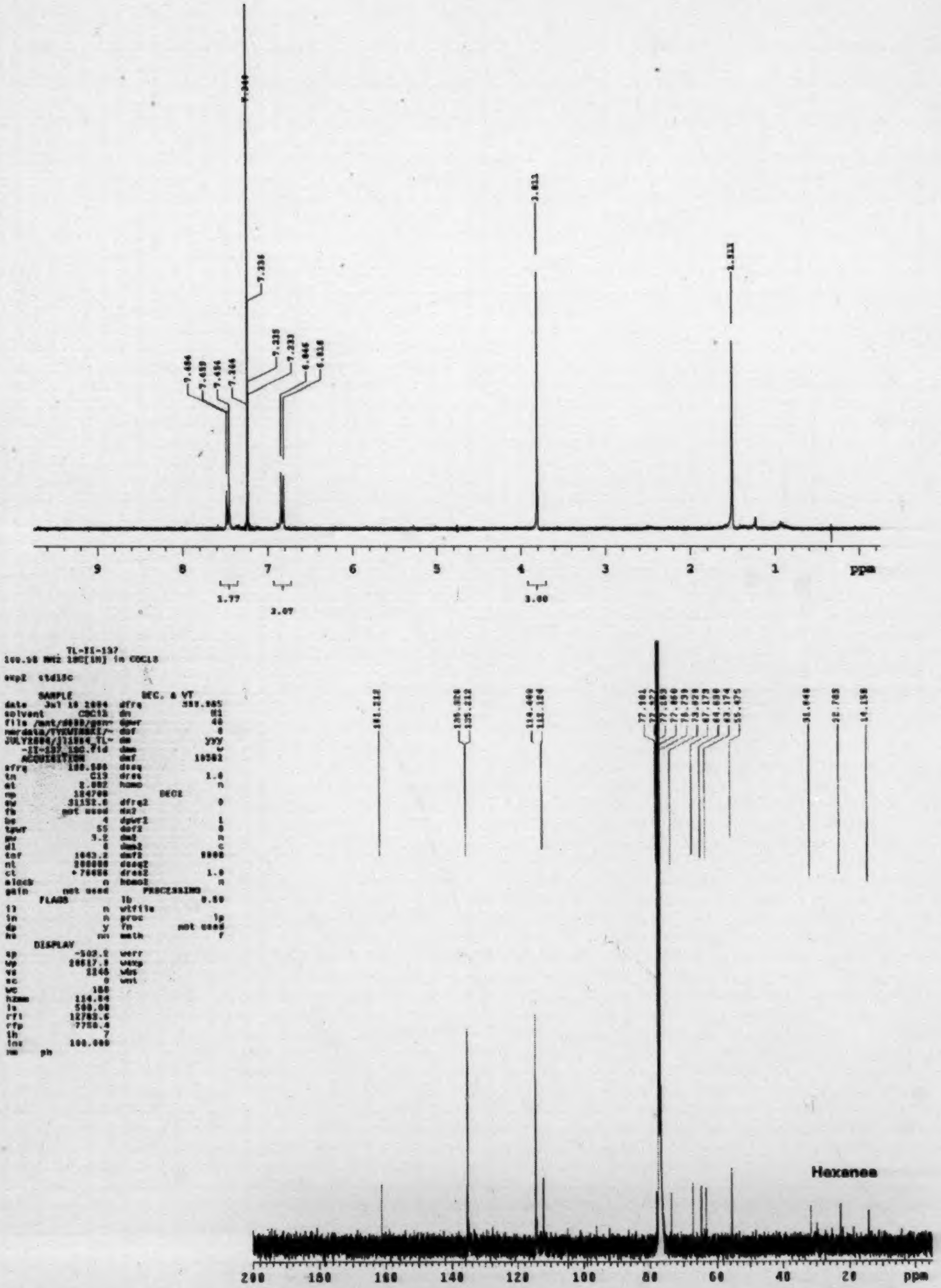

Figure A.15 ^{1}H and ^{13}C NMR spectra of **412b**

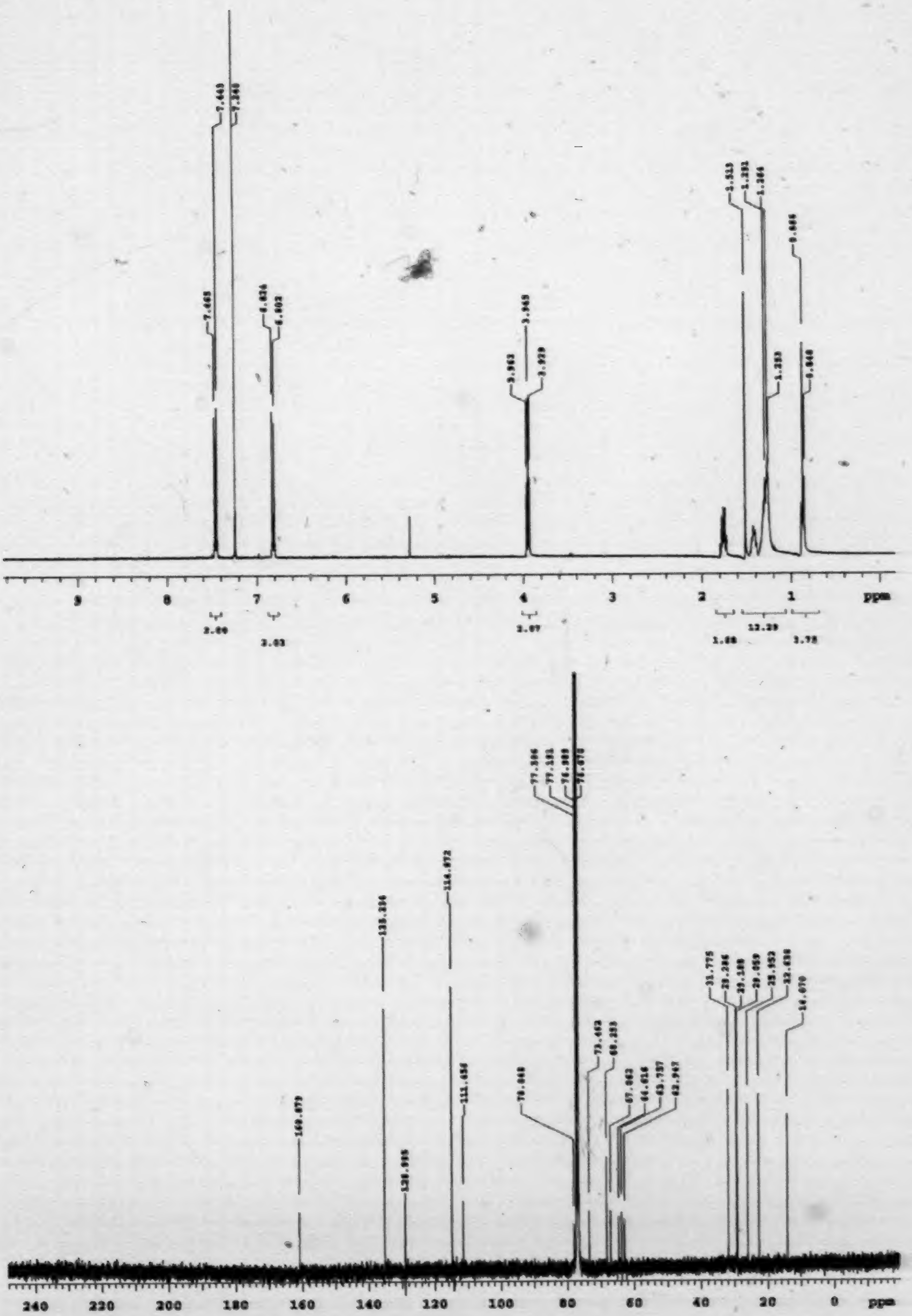

Figure A.16 ^{1}H and ^{13}C NMR spectra of **412c**

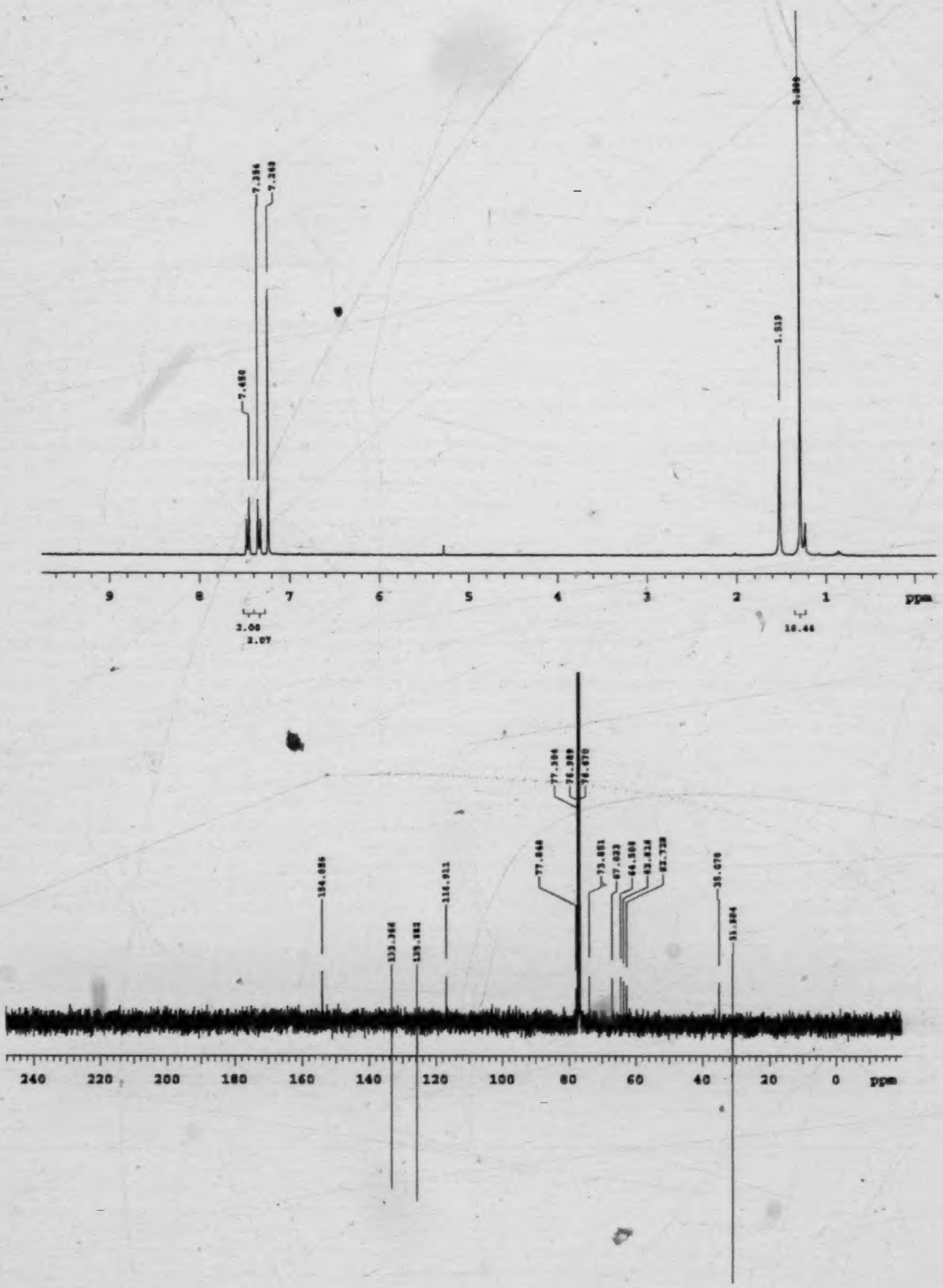

Figure A.17 ^{1}H and ^{13}C NMR spectra of **412d**

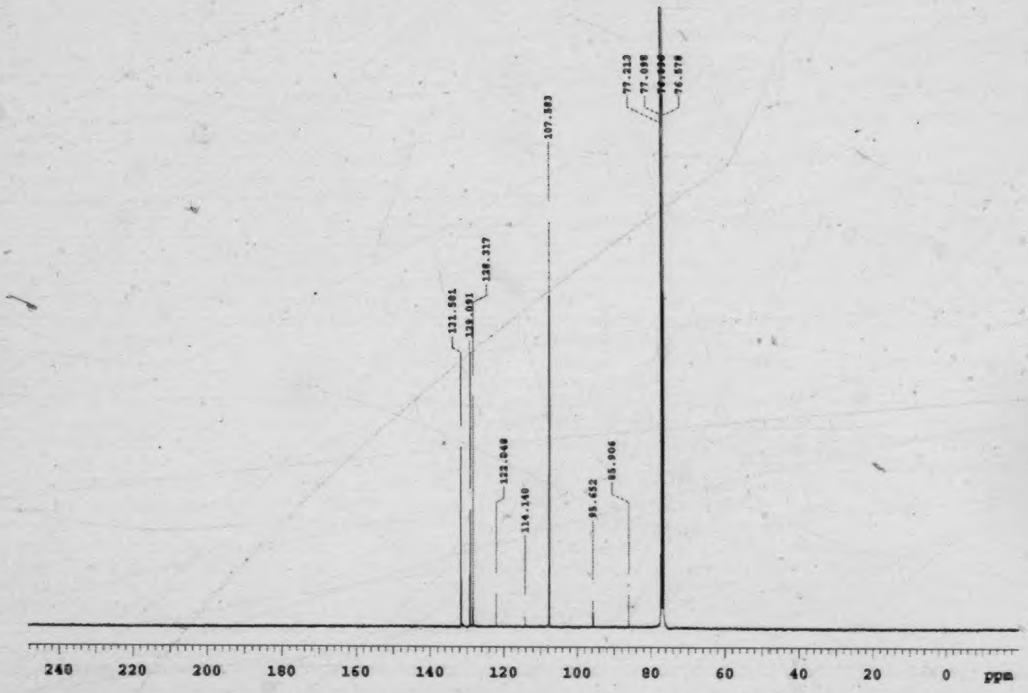

Figure A.18 ^{1}H and ^{13}C NMR spectra of **435**

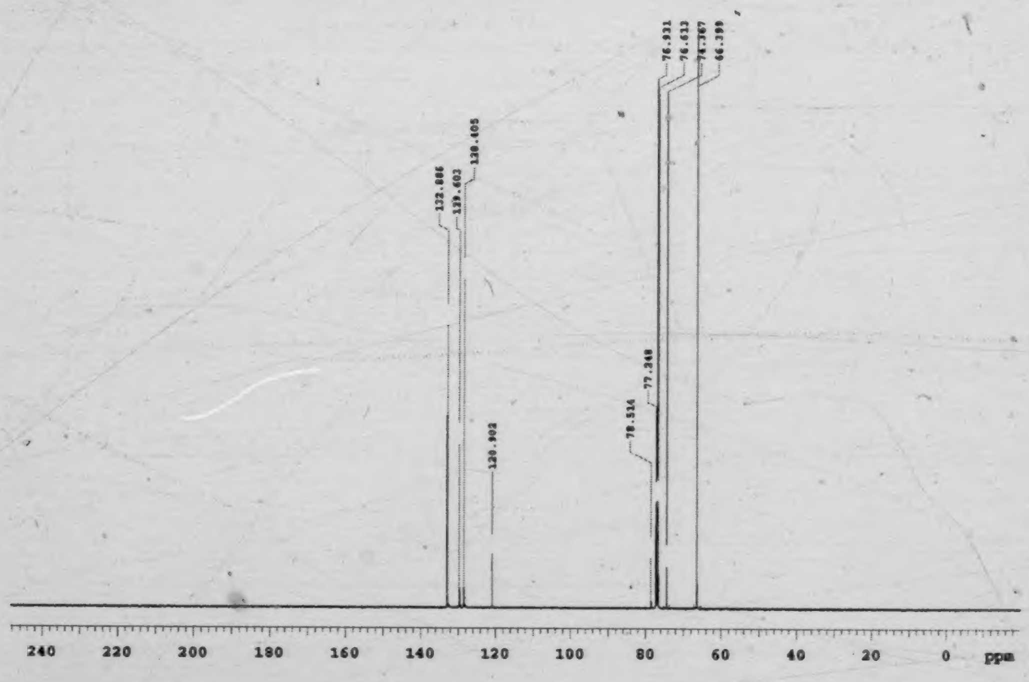

Figure A.19 ^{1}H and ^{13}C NMR spectra of **431**

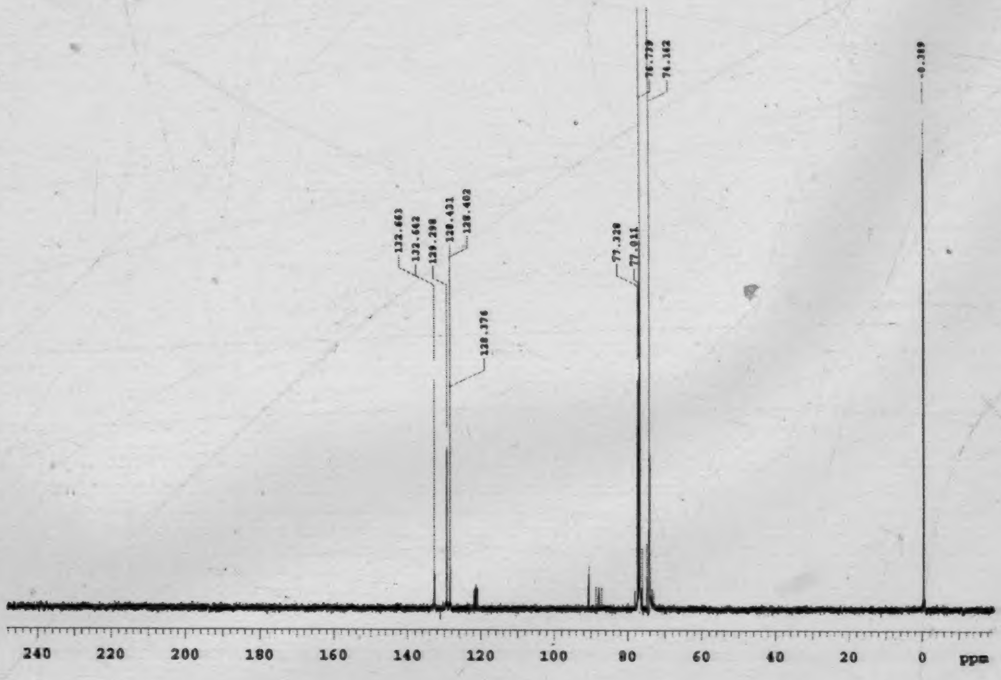

Figure A.20 ^{1}H and ^{13}C NMR spectra of **438a**

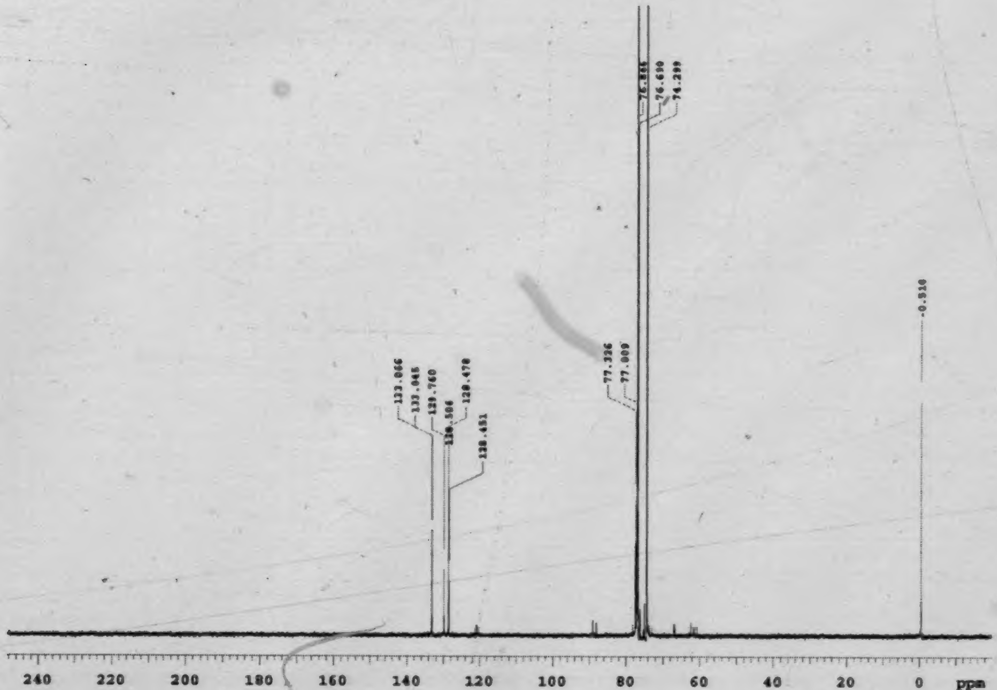

Figure A.21 ^{1}H and ^{13}C NMR spectra of **438b**

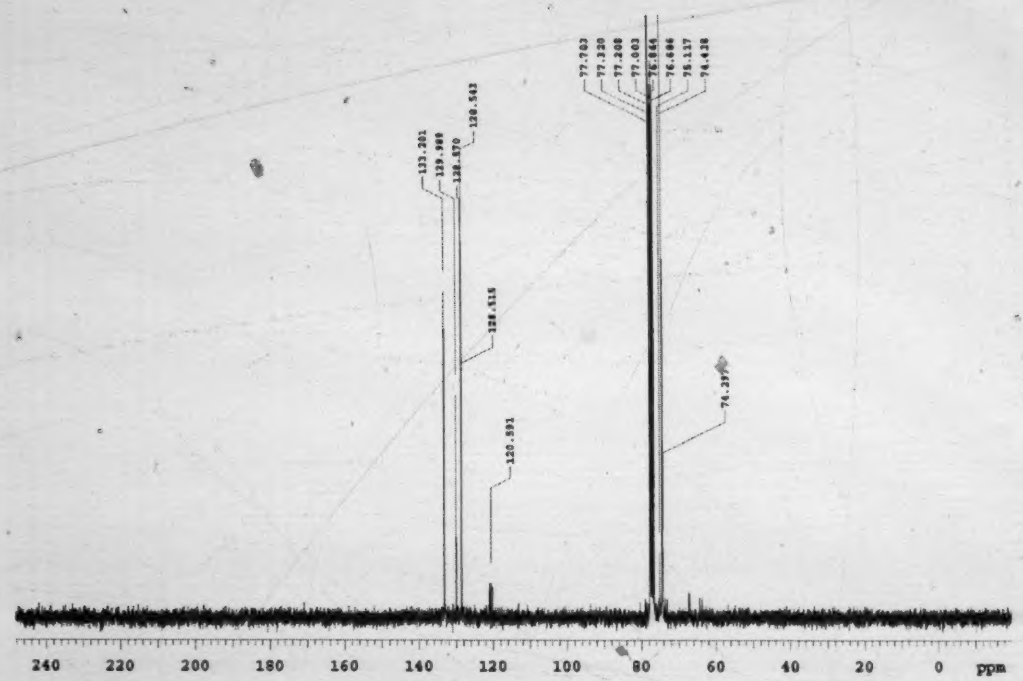

Figure A.22 ^{1}H and ^{13}C NMR spectra of **432**

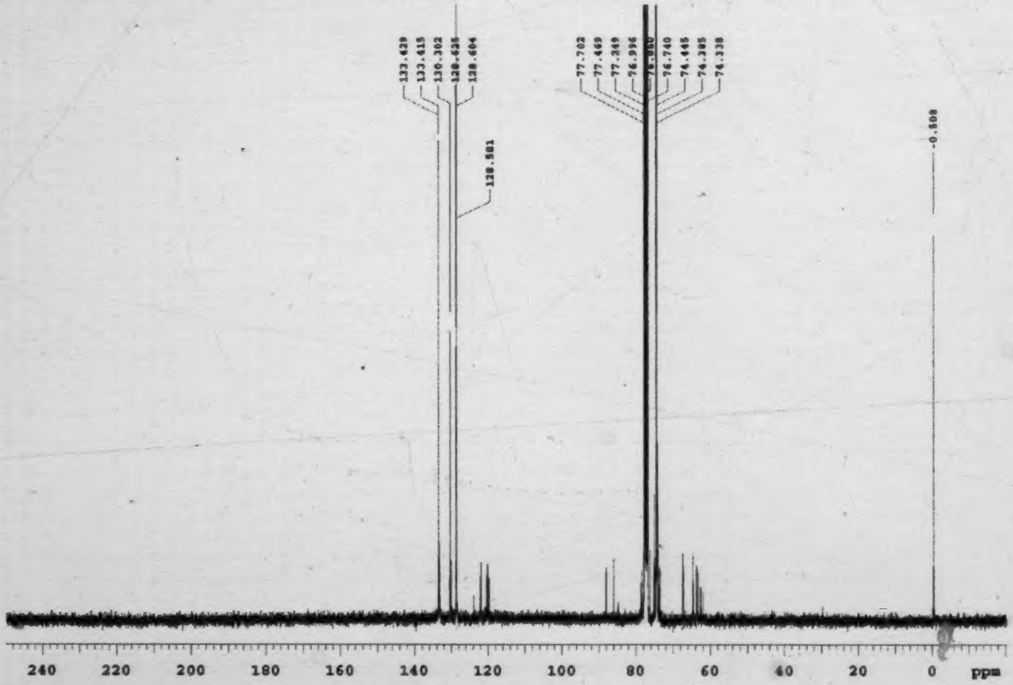

Figure A.23 ^{1}H and ^{13}C NMR spectra of **433**

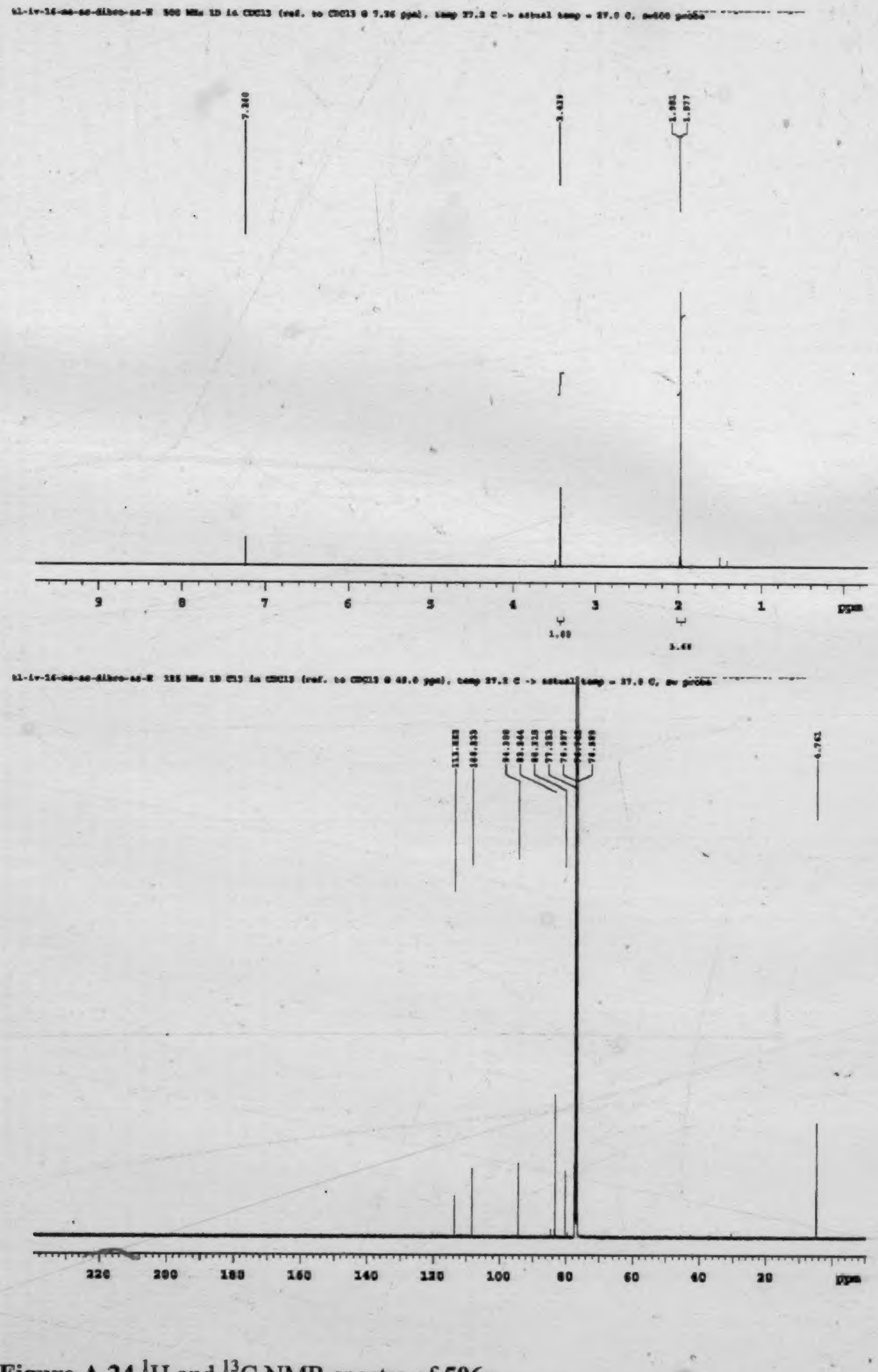

Figure A.24 ^{1}H and ^{13}C NMR spectra of **506e**

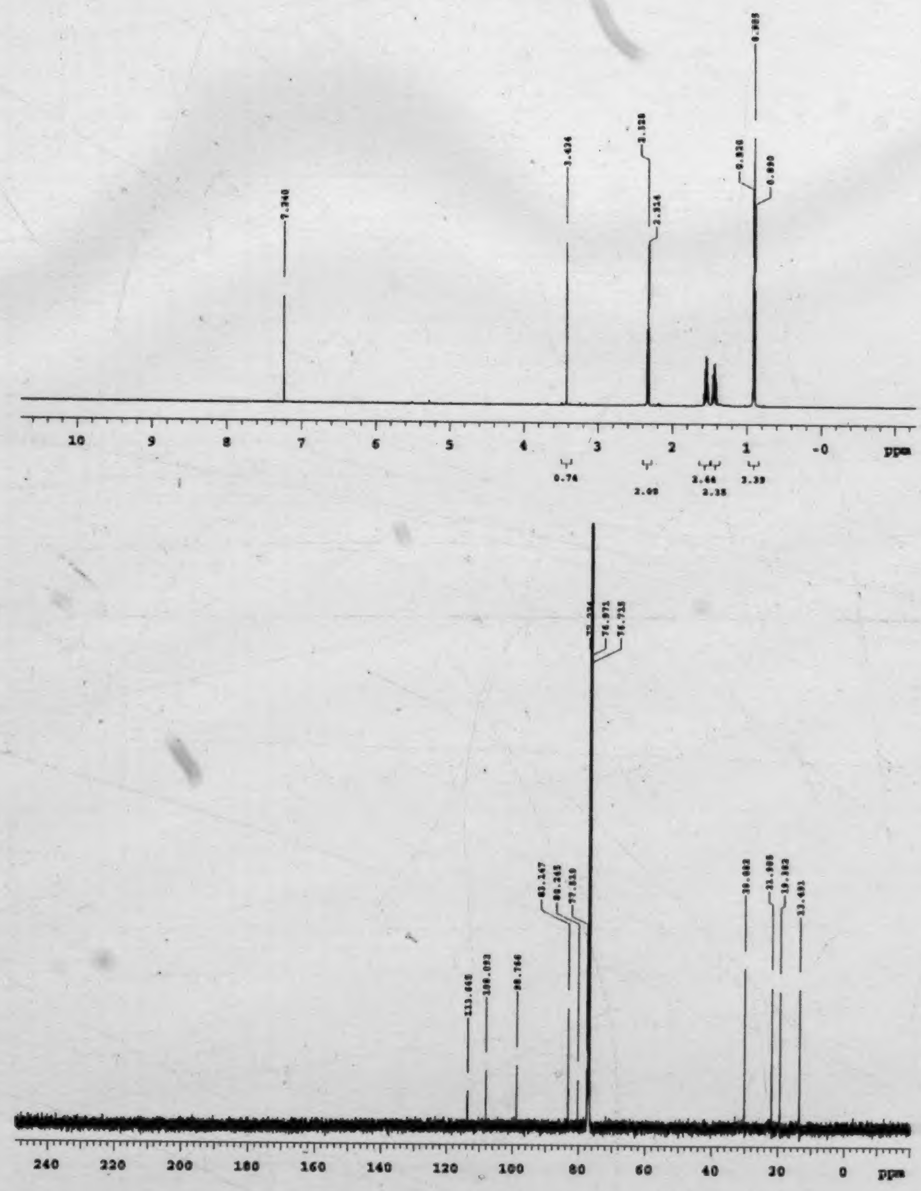

Figure A.25 ^{1}H and ^{13}C NMR spectra of **506f**

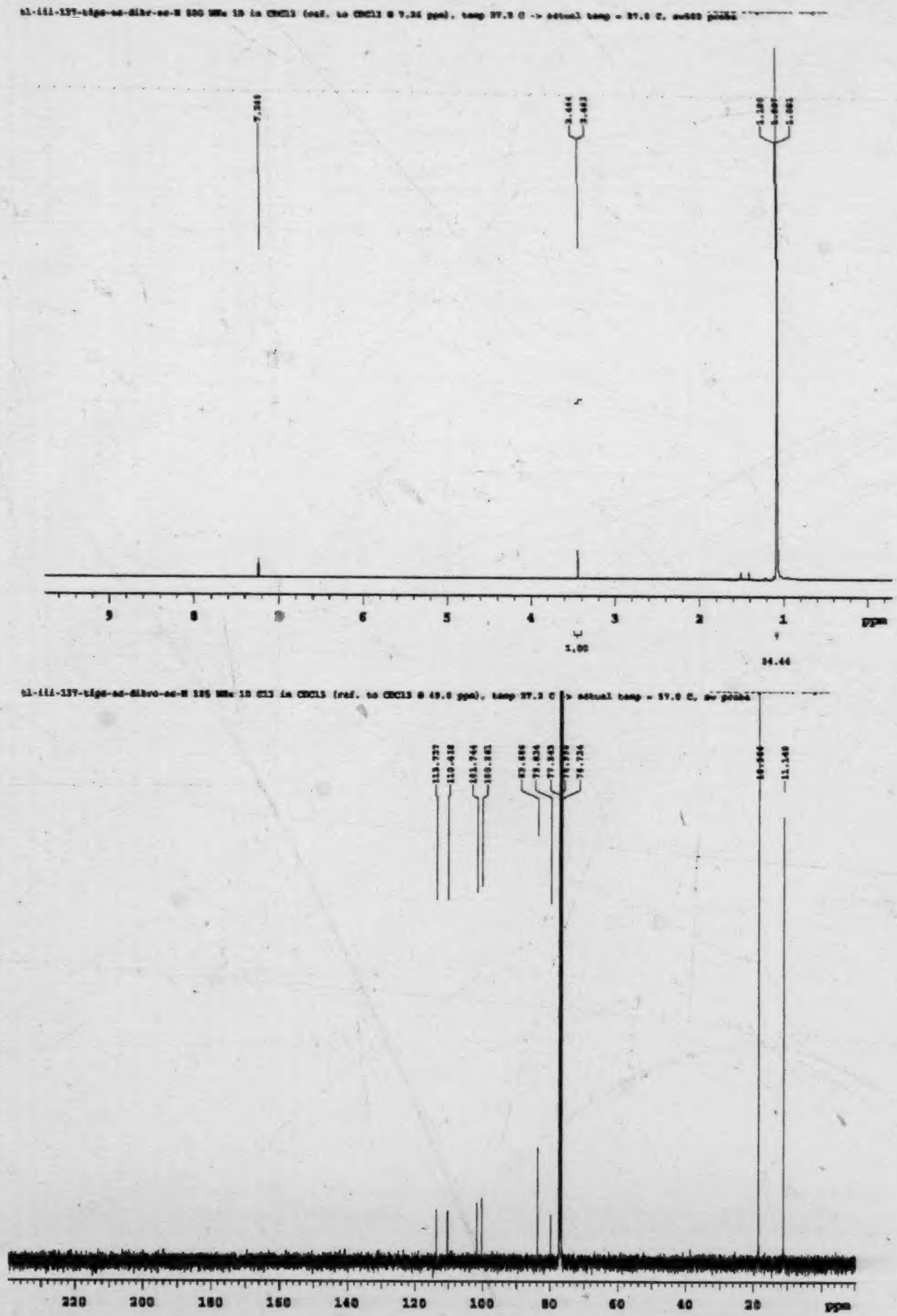

Figure A.26 ^1H and ^{13}C NMR spectra of **506g**

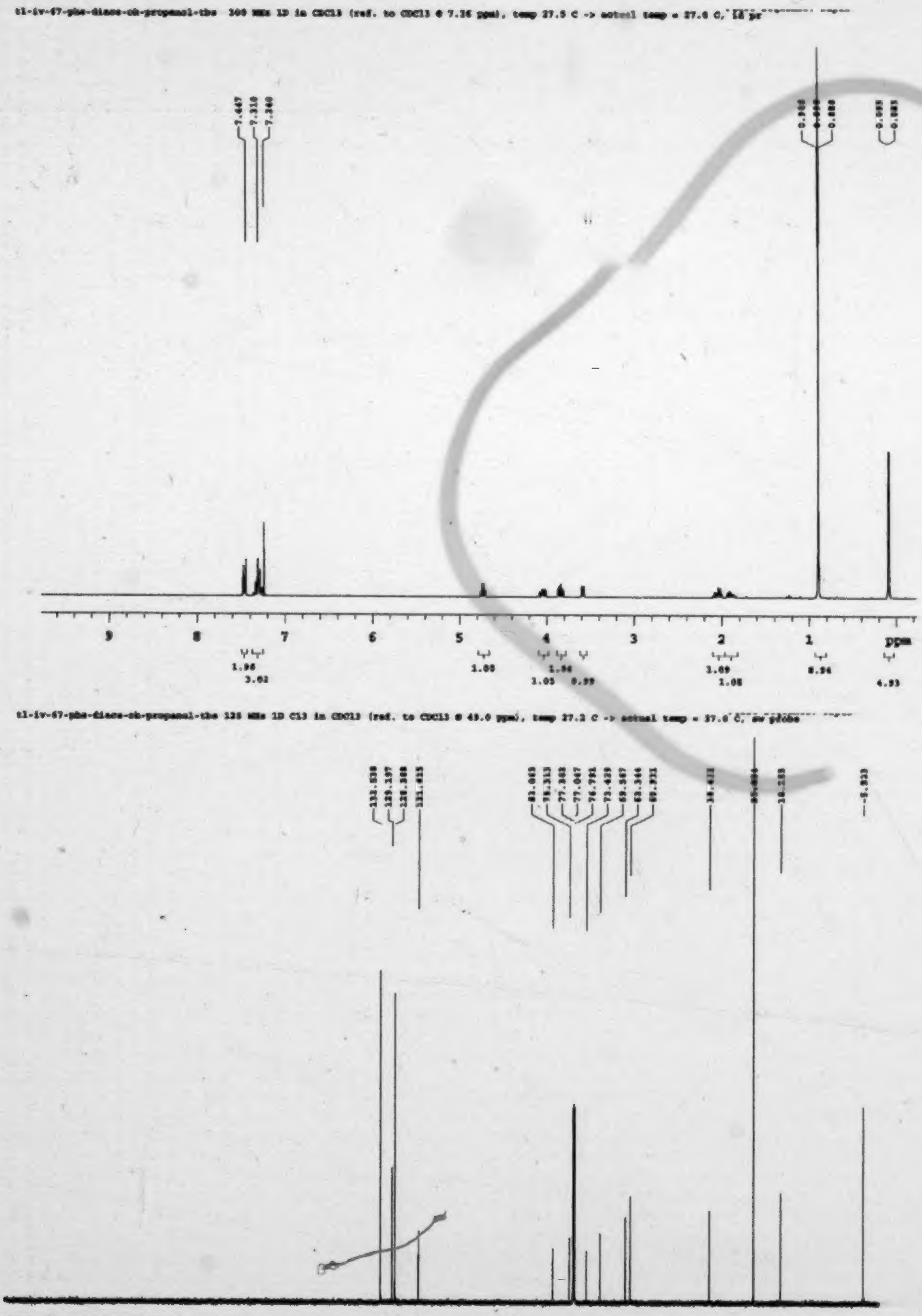

Figure A.27 ^{1}H and ^{13}C NMR spectra of **508i**

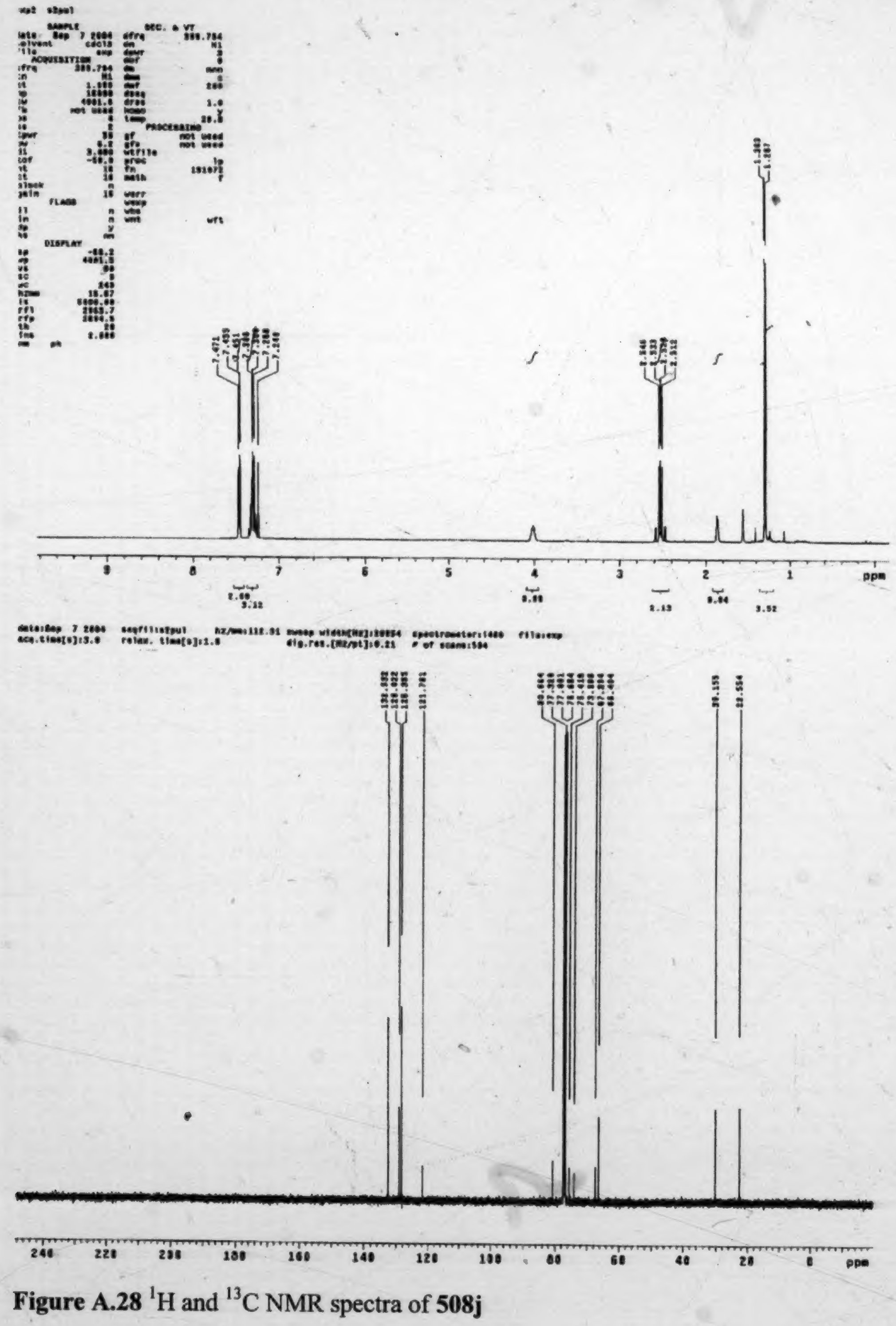

Figure A.28 ^{1}H and ^{13}C NMR spectra of **508j**

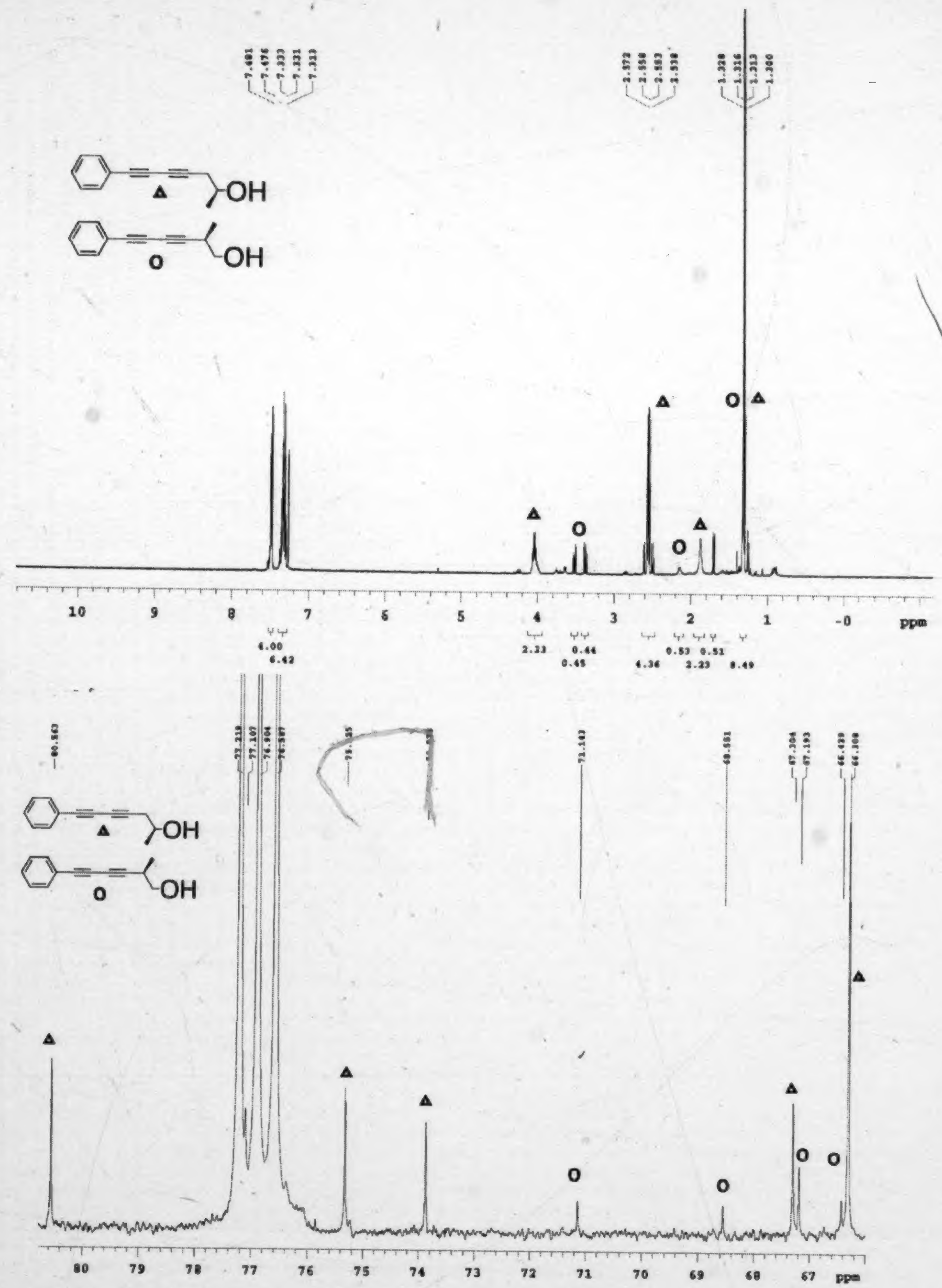

Figure A.29 ^{1}H and ^{13}C NMR spectra of mixtures of **508j/508k**

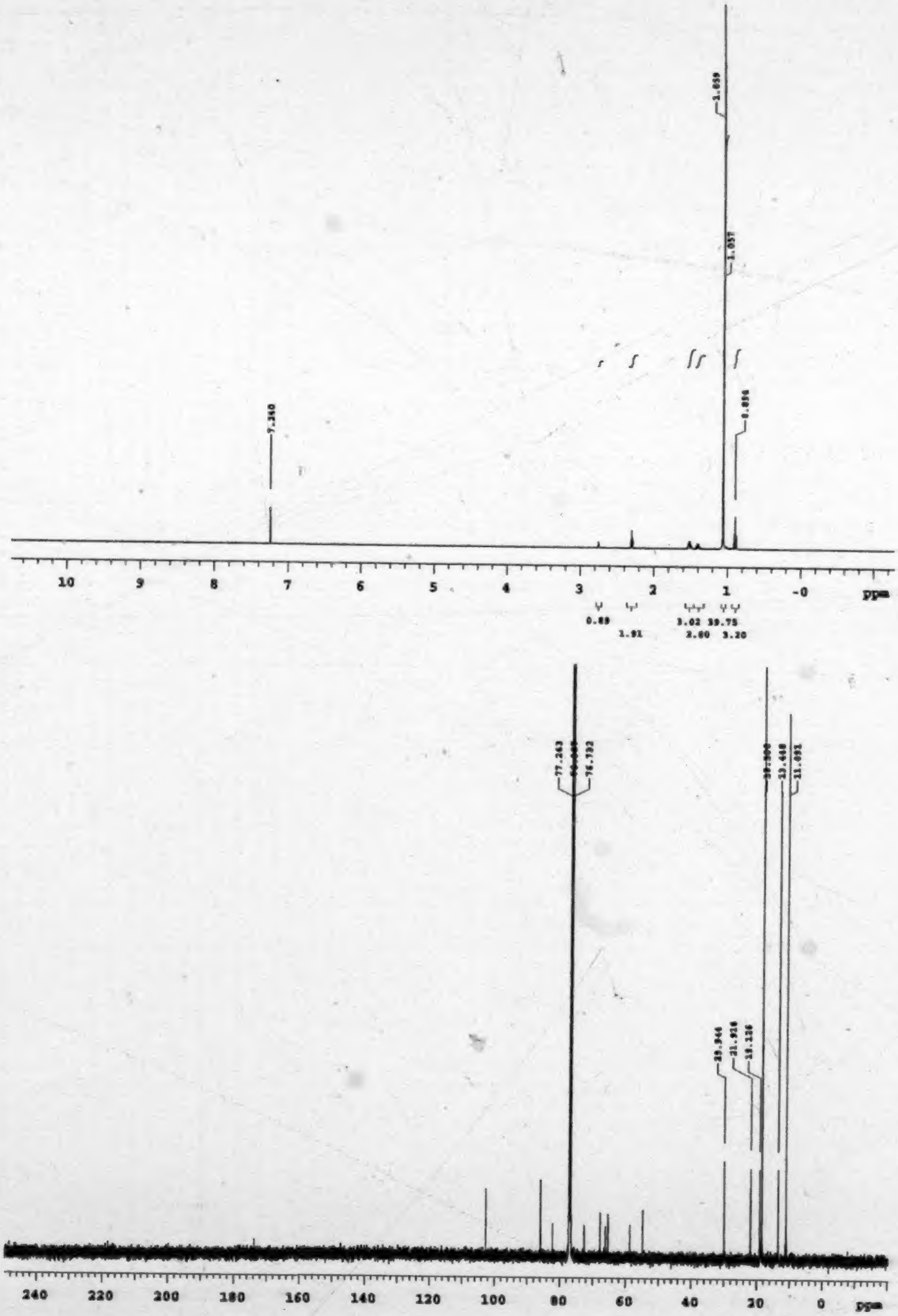

Figure A.30 ^{1}H and ^{13}C NMR spectra of **509h**

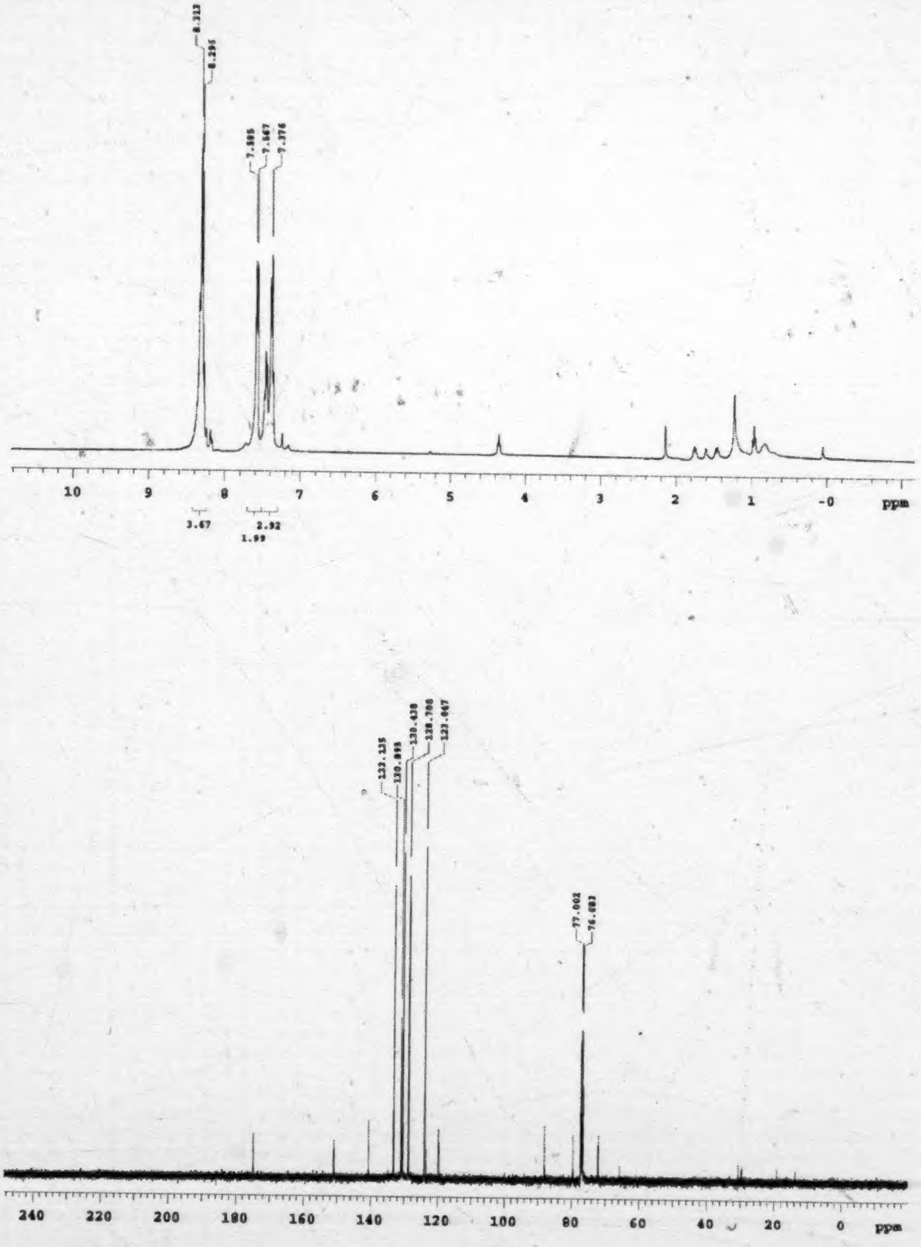

Figure A.31 ^1H and ^{13}C NMR spectra of **515d**

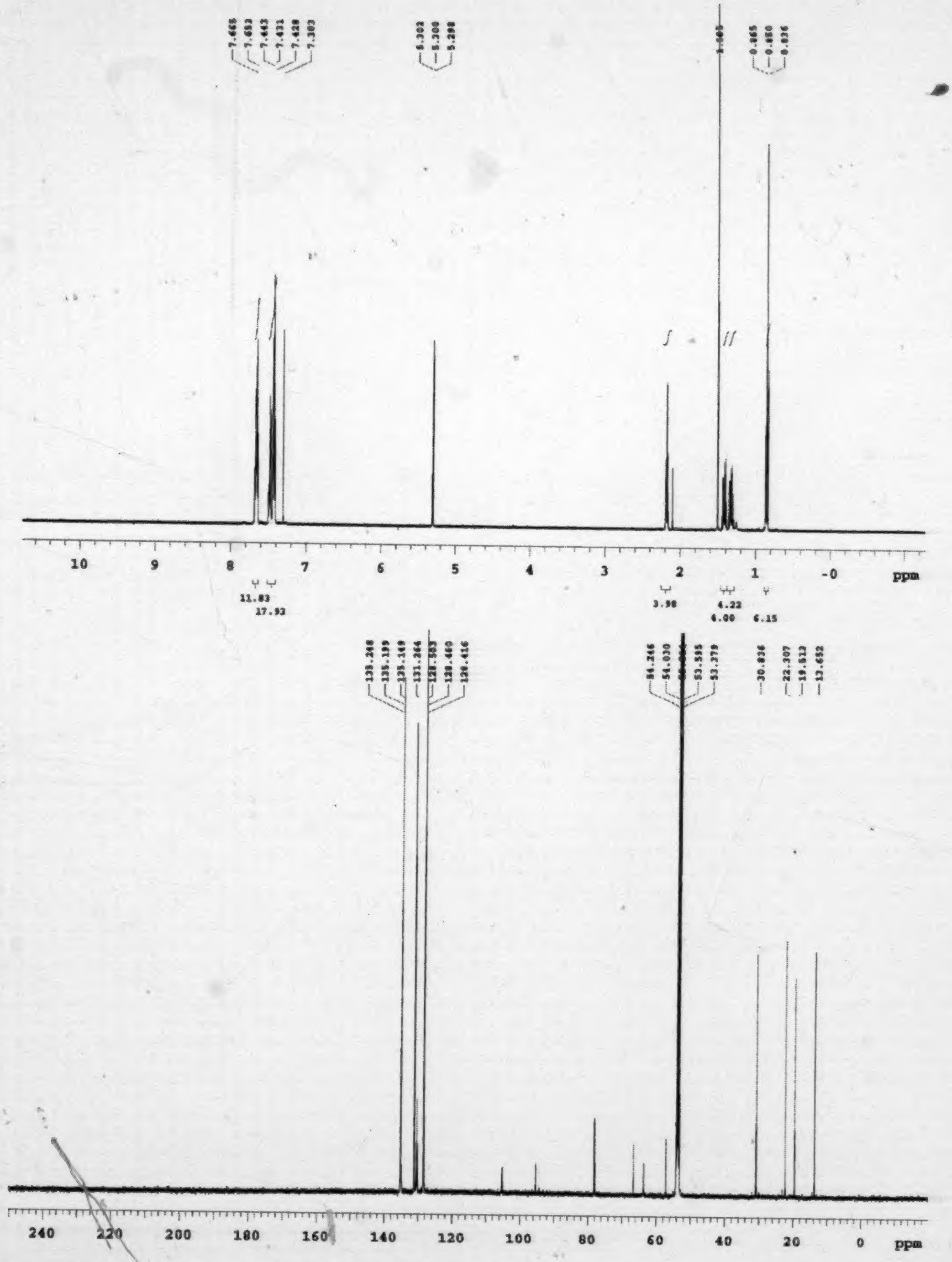

Figure A.32 ^{1}H and ^{13}C NMR spectra of **516b**

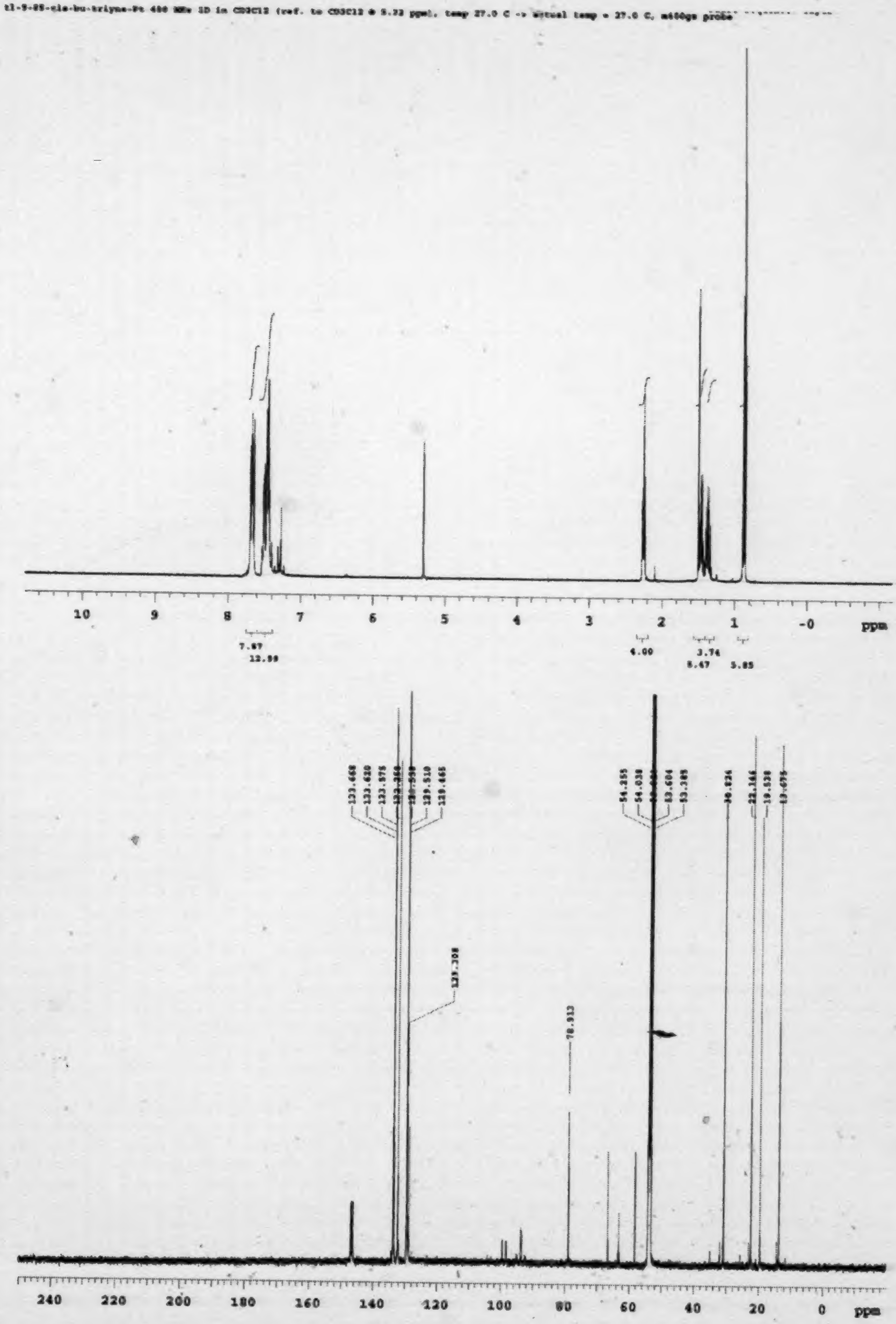

Figure A.33 ^{1}H and ^{13}C NMR spectra of **526b**